Human metapneumovirus in Singapore : epidemiology, fusion-attachment protein interaction and virus-like particle assembly

Loo, Liat Hui

2012

Loo, L. H. (2012). Human metapneumovirus in Singapore : epidemiology, fusion-attachment protein interaction and virus-like particle assembly. Doctoral thesis, Nanyang Technological University, Singapore.

https://hdl.handle.net/10356/53649

https://doi.org/10.32657/10356/53649

Human Metapneumovirus in Singapore: Epidemiology, Fusion-Attachment Protein Interaction and Virus-like Particle Assembly.

LOO LIAT HUI

School of Biological Sciences, College of Science.

A thesis submitted to the Nanyang Technological University, Singapore, in partial fulfillment of the requirements for the degree of Doctor of Philosophy.

2012

ACKNOWLEDGEMENTS

Firstly, I would like to express my gratitude to my project supervisor, Associate Professor Richard J. Sugrue for his willingness to impart his knowledge and skills and his guidance throughout my course of study. I also want to thank the National Medical Research Council for providing the funds for the research grant (NMRC/0956/2005) which covered the most of the project costs. I am also very grateful to my Head of Department (Pathology and Laboratory Medicine), Dr Nancy Tee for the strong support she gave me during my entire study period. I would also like to thank the management of KK Women's and Children's Hospital for generously allowing me the opportunity and time-off to pursue my studies and the National Medical Research Council-Lee Foundation for sponsoring my tuition fees. Next, I would also like to thank Dr Tan Boon Huan for her instruction, help and valuable advice especially in the initial stages of my project and for providing guidance. Thanks also go to Dr Raymond Lin for providing the initial motivation for my studies and Associate Professor Evelyn Koay for her timely words of encouragement. Not forgetting the help and support from all the friends at NTU (including Raihan, Laxmi, Patricia, Chen Hui, Eileen, Debbie, Dawn, Richard, Fu Yi, Li Liang, Nadine, Li Ying, Anu, Gaya, Timothy, Kit Wei, Ley Moy, Eddie, Liwei, Regina), DSO (Pui San, Pei Jun, Elizabeth, Ka Wei, Shirley, Li Fang), KKH (Min Hwee, Han Yang, Zhen Hao, Beng Lee, Zhi Yong, Qi Mei, Xiao Tian, Shida, Kathy, Sharhana, Fahmi, Kenneth, Yuen Ming) and many others whom I may have omitted unintentionally. Thanks also go to the staff at JEOL Asia Pte Ltd for their technical assistance and Geoffrey Toms for his kind gift of antibodies and virus strains.

Finally, I would like to say a big "thank you" to my wife, Valerie, who has been my pillar of strength and my best friend. Thanks also go to my children Matthew, Judith, Naomi and Samuel for putting up with my long hours away and the rest of my family for their patience and understanding. Last, but not the least, I thank God for giving me this once-in-a-lifetime experience.

TABLE OF CONTENTS

LIST OF FIGURES

LIST OF TABLES

ABBREVIATIONS

6-FAM	6-carboxyfluorescein
6HB	6 helical bundle
AcMNPV	*Autographa californica* multiply-enveloped polyhedrosis virus
ALL	acute lymphocytic leukaemia
ALTB	acute laryngotracheobronchitis
APV	avian pneumovirus
BCoV	bovine coronavirus
BHQ1	Black Hole Quencher 1
bRSV	bovine respiratory syncytial virus
BSA	bovine serum albumin
BV	budded virus
CLD	chronic lung disease
CPE	cytopathic effect
Ct	cycle threshold
DMSO	dimethyl sulphoxide
DNA	deoxyribonucleic acid
DSP	dithiobis[succinimidylpropionate]
DTT	dithiothreitol
EDTA	ethylenediamine tetraacetic acid
ELISA	enzyme-linked immunosorbant assay
Endo H	endoglycosidase H
ER	endoplasmic reticulum
F (protein)	fusion protein
FBS	fetal bovine serum
FESEM	field emission scanning electron microscope
FITC	fluorescein isothiocynate
G (protein)	attachment (glyco) protein
Gal	galactose
GalNAc	N-acetylgalactosamine
Glc	glucose
GlcNAc	N-acetylglucosamine
GV	granulosis virus
HBoV	human bocavirus
HCoV	human coronavirus
HFMD	hand, foot and mouth disease
HMPV	human metapneumovirus
HN (protein)	haemagglutinin-neuraminidase protein
HRA/B	heptad repeat A/B
hRSV	human respiratory syncytial virus
HRV	human rhinovirus
IFA	immunofluorescence assay
IRB	Institutional Review Board (Ethics)
KKH	Kandang Kerbau Women's and Children's Hospital
L (protein)	large polymerase subunit protein
LB	Luria-Bertani
LRTI	lower respiratory tract infection
M (protein)	matrix protein
M2 (protein)	M(atrix)2 protein
Man	mannose
MDA-5	melanoma differentiation associated gene 5
MNPV	multiply-enveloped polyhedrosis virus
MOI	multiplicity of infection
mRNA	messenger ribonucleic acid

MVA-T7	modified vaccinia virus, Ankara strain
N (protein)	nucleoprotein
NDV	Newcastle disease virus
NiV	Nipah virus
NNP	neonatal pyrexia
NP-40	nonyl phenoxypolyethoxylethanol
NPV	nuclear polyhedrosis virus
NS1 (protein)	non-structural protein 1
NTU	Nanyang Technological University
ODV	occlusion derived virions
OV	occluded virus
P (protein)	phosphoprotein
PBS	phosphate buffered saline
PCR	polymerase chain reaction
PEDV	porcine epidemic diarrhea virus
PH (protein)	polyhedron
PIV3/5	parainfluenza virus 3/5
PMSF	phenylmethylsulphonyl fluoride
PNGase F	peptide N-glycosidase F
PVM	pneumonia virus of mice
RAP-PCR	random priming-polymerase chain reaction
RIG-1	retinoic acid inducible gene 1
RIPA	radioimmunoprecipitation assay
RNA	ribonucleic acid
RNP	ribonucleoparticle
RT-PCR	reverse transcription-polymerase chain reaction
SARS	severe acute respiratory syndrome
SCID	severe combined immunodeficiency disease
SDS	sodium dodecyl sulphate
SDS-PAGE	sodium dodecyl sulphate-polyacrylamide gel electrophoresis
SH (protein)	small hydrophobic protein
siRNA	small interfering ribonucleic acid
SNPV	singly-enveloped nuclear polyhedrosis virus
STAT1	signal transducers and activators of transcription type 1
SV5	simian virus 5, also known as parainfluenza 5
TBE	Tris-borate-EDTA
TGEV	transmissible gastroenteritis virus
TMPRSS2	transmembrane protease, serine 2
TRTV	turkey rhinotracheitis virus
URTI	upper respiratory tract infection
VLP	virus-like particle

SUMMARY

Human metapneumovirus was discovered in 2001. At the same time, it was also revealed that this virus had been circulating in the human population for at least 50 years. In the years that followed, an increasing number of research groups began to publish work on various aspects of HMPV. One of the main concerns was that this virus was detected in a significant proportion of children below the age of 3 years and caused respiratory symptoms very similar to its nearest related human pathogen: human respiratory syncytial virus. Before this study, there had been no large scale study on the prevalence of HMPV in Singapore. There was also no existing data on the presence of HBoV, HCoV and HRV in hospitalized children in Singapore. We screened five hundred clincial nasopharyngeal samples and found that these four respiratory viruses are present in significant proportions. This discovery will hopefully lead to more research interest in the area of respiratory pathogens in children.

There is currently no vaccine available against HMPV. Just like other Paramyxoviruses, the fusion and attachment proteins were already known to provide the basis of virus infection. By characterizing the fusion and attachment proteins in HMPV, we confirmed that there was some form of interaction between the two proteins. This information would be useful for initiating further studies which can elucidate the detailed mechanism of this interaction which may lead to the development of antiviral strategies against this pathogen.

One of the new advances in vaccine technology involves the use of virus-like particles as immunogens. We successfully produced virus-like particles of HMPV in both mammalian and insect cell lines. Of the two cell lines, the insect cells have the greater potential for mass production of virus-like particles which can be tested as candidate vaccines.

Chapter 1 Introduction

1.1 Discovery of an unknown virus

The first study on the human metapneumovirus (HMPV) was published in June 2001 by Dutch scientists van den Hoogen and co-workers (van den Hoogen et al., 2001). They reported the presence of a new paramyxovirus isolated from nasopharyngeal aspirates of children. Prior to this study, the only known metapneumovirus was isolated from turkeys and known as turkey rhinotracheitis virus (TRTV). TRTV was subsequently renamed avian pneumovirus (APV). Nasopharyngeal aspirates obtained from 28 children were inoculated into a variety of cell types and after 14 days incubation, virus morphology was analysed by electron microscopy. The viral RNA was extracted from the cell culture supernatants, reverse transcribed and then amplified using primers designed from the genes of known paramyxoviruses. In addition, random priming polymerase chain reaction (RAP-PCR) was used to amplify fragments of the unknown viral gene which were then sequenced and compared with available data at that time. By aligning the new virus gene sequences with human and bovine respiratory syncytial virus (hRSV and bRSV), and APV subtypes A to D, it was initially proposed that the virus be classified as a new member of the genus metapneumovirus (Fig 1.1). After examining retrospective clinical samples, the researchers found seropositive cases dating back to 1958. Clearly HMPV cannot be considered a new species of respiratory virus but a newly discovered one. This pioneering work led the way in the field of HMPV research and generated increased interest in the search for more undiscovered respiratory viruses. Soon after this work was published, the same researchers published another article in 2002 detailing the genomic analysis of their first HMPV isolate 00-1 (also known as NL-1-00) (van den Hoogen et al., 2002). This added weight to their proposal to classify HMPV as a member of the Metapneumovirus genus. Two more publications were released in quick succession from Australia (Nissen et al., 2002) and Canada (Peret et al., 2002). Although these two studies were

based on a small number of HMPV isolates (3 and 11 respectively), this formed the beginnings of the three leading research groups that would later spearhead HMPV research.

1.2 Classification of HMPV

Human metapneumovirus is classified under the family Paramyxoviridae, sub-family Pneumovirinae, genus Metapneumovirus and species Human metapneumovirus (International Committee on Taxonomy of Viruses. et al., 2006). Another sub-family Paramyxovirinae contains well known human pathogens like human parainfluenza viruses types 1, 2, 3 and 4; measles virus, mumps virus and Nipah virus. The human virus most related to HMPV is hRSV belonging to the neighbouring genus Pneumovirus (Fig 1.1).

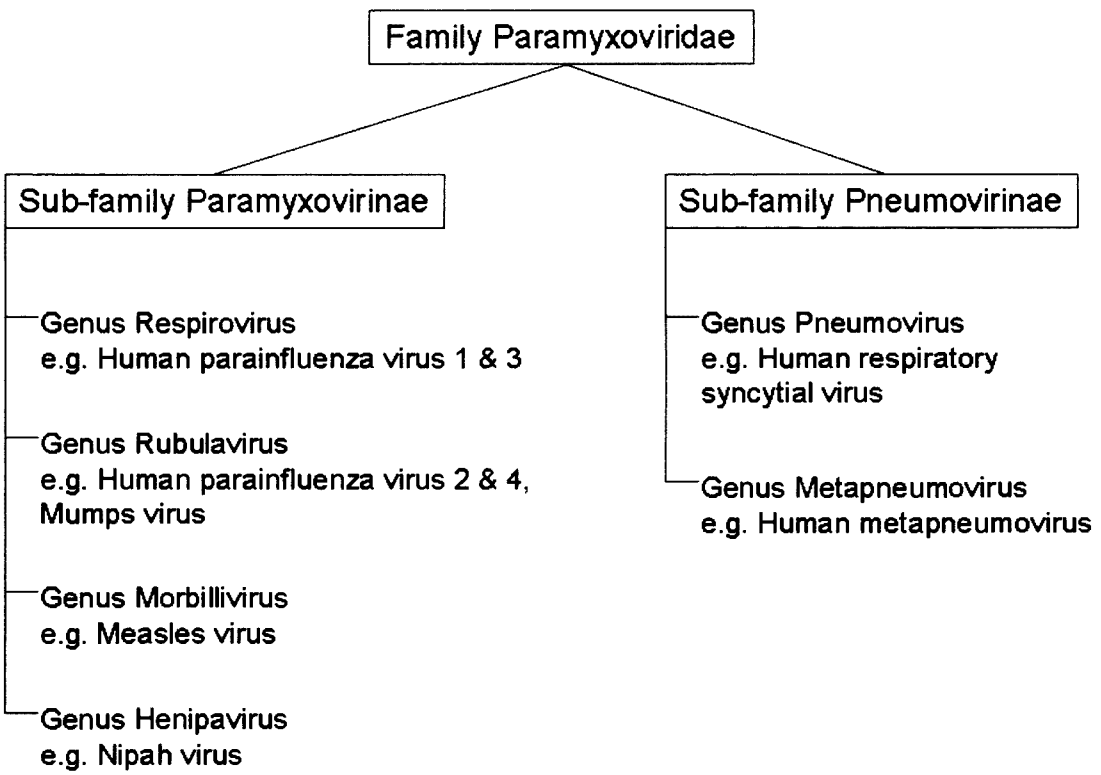

Figure 1.1. Classification of the Paramyxoviridae family. Subfamilies Paramyxovirinae and Pneumovirinae are shown with their respective genera of viruses and examples of known human pathogens. Viruses not infecting humans are omitted from this figure.

All members of the Paramyxovirus family are characterized by having i) an envelope derived from the host cell, ii) a non-segmented genome (in contrast to the

Orthomyxoviruses which have segmented genomes), iii) a fusion protein that is activated under neutral pH conditions, and iv) negative sense genomic RNA. Within the genus Metapneumovirus, there is also a group of avian pneumoviruses (APV) consisting of types A, B, C and D which are closely related to HMPV (Njenga et al., 2003). This relationship has been further demonstrated by the cross-reaction of antibodies to the nucleoprotein of HMPV and APV (Alvarez et al., 2004a). A comparison between the genome of APVc and HMPV is shown in Fig 1.2. A study by van den Hoogen (van den Hoogen et al., 2002) aligned the genes of HMPV proteins with other Paramyxoviruses to show their similarities (Table 1.1). It can be seen that while the sizes of N, P and M proteins are very close among the Pneumovirinae subfamily, the F, M2-1, M2-2 and L proteins are closer in size among the Metapneumovirus genera. Not surprisingly, there is a lot more heterogeneity between the sizes of the G and SH proteins which probably hints at their role in antigenic variation.

	N[a]	P	M	F	M2-1	M2-2	SH	G	L
HMPV	394	294	254	539	187	71	183	236	2005
APV A	391	278	254	538	186	73	174	391	2004
APV B	391	279	254	538	186	73	**175**	414	**2004**
APV C	394	294	254	537	184	71	**175**	**252**	**2005**
APV D	—[b]	—[b]	—[b]	—[b]	—[b]	—[b]	—[b]	389	—[b]
hRSV A	391	241	256	574	194	90	64	298	2165
hRSV B	391	241	256	574	195	90	65	299	2166
bRSV	391	241	256	574	186	90	81	257	2162
PVM	393	295	257	537	176	98	92	396	**2040**
Others[c]	418–542	225–709	335–393	539–565	—[d]	—[d]	—[d]	—[d]	2183–2262

Table 1.1. Comparison of protein sizes of HMPV strain NL-1-00 with other Paramyxoviruses modified from (van den Hoogen et al., 2002). (a) Sizes are based on the number of amino acid residues per protein. (b) Sequences for some virus proteins were not available at the time of publication. (c) The group of "Others" included parainfluenza virus 2 & 3, Sendai virus, measles virus, Nipah virus and Newcastle disease virus. (d) These ORFs are absent in viruses of the "Others" group. HMPV-human metapneumovirus, APV-avian pneumovirus A to D, hRSV-human respiratory syncytial virus, PVM-pneumonia virus of mice.

In terms of evolutionary relationship, APVc has been found to be closer to HMPV than the other avian pneumovirus types (Lwamba et al., 2005; van den Hoogen et al., 2002).

APVc emerged in the United States in the late 1990s (Seal, 2000). One study, comparing the SH, G and L genes of HMPV and APVc (Toquin et al., 2003), found that between the two viruses, the amino acid similarities were 26.9%, 20.6% and 73.6% respectively. An earlier comparison made by Dutch scientists also arrived at a similar conclusion (Table 1.2) when they calculated that the N, P, M, F, M2-1, M2-2 and L proteins of APVc had the highest identity with HMPV compared to other paramyxoviruses. Thus, it has been estimated that HMPV and APVc shared a common ancestor as recently as 200 years ago (de Graaf et al., 2008).

	N[a]	P	M	F	M2-1	M2-2	L
APV A	69	55	78	67	72	26	64
APV B	69	51	76	67	71	27	62-63
APV C	88	68	87	81	84	56	80
hRSV A	41	24	38	33	36	18	44
hRSV B	41	23	37	33	35	19	44
bRSV	41	22	38	34	35	13	44
PVM	45	26	37	38	34	12	50
Others[c]	7-11	4-9	7-10	10-18	–[b]	–[b]	13-15

Table 1.2. Comparison of amino acid identity of HMPV strain NL-1-00 with other Paramyxoviruses modified from (van den Hoogen et al., 2002). (a) Values for G and SH proteins were not calculated due to difficulties in alignment with other known sequences. (b) These ORFs are absent in the viruses of the "Others" group. (c) The group of "Others" included parainfluenza virus 2 & 3, Sendai virus, measles virus, Nipah virus and Newcastle disease virus. HMPV-human metapneumovirus, APV-avian pneumovirus A to D, hRSV-human respiratory syncytial virus, bRSV-bovine respiratory syncytial virus, PVM-pneumonia virus of mice. The dotted rectangle highlights the proteins with highest identity to HMPV proteins.

Based on the genetic sequencing of HMPV isolates, early studies divided HMPV into two main genogroups A and B (Bastien et al., 2003a; Biacchesi et al., 2003; Boivin et al., 2002; Peiris et al., 2003; Peret et al., 2002). This conclusion was drawn by aligning the HMPV gene sequences: N (Bastien et al., 2003a; Ishiguro et al., 2004; Peret et al., 2002), P (Bastien et al., 2003a; Ishiguro et al., 2004; Peret et al., 2002), M (Bastien et al., 2003a; Ishiguro et al., 2004), F (Bastien et al., 2003a; Boivin et al., 2002; Ishiguro et al., 2004; Peiris et al., 2003; Peret et al., 2002), M2-1/2 (Ishiguro et al., 2004), SH (Ishiguro et al., 2004), G (Ishiguro et al., 2004; Peret et al., 2004) and L (Peiris et al.,

2003). In 2004, phylogenetic studies on HMPV proposed that the classification of HMPV could be further subdivided into A1 and A2, B1 and B2 subgenogroups (van den Hoogen et al., 2004). One of the most thorough phylogenetic studies on the HMPV genes was conducted by Ishiguro (Ishiguro et al., 2004). They sequenced all the genes (except the L gene) from seven HMPV clinical isolates and aligned the sequences with known HMPV strains. They found that the SH and G genes and their resultant proteins were the most variable both in terms of length and molecular mass respectively (Table 1.3). All the other genes from N to M2-2 were of consistent length.

HMPV Genogroup	N		P		M		F		M2-1		M2-2		SH		G	
	nt (aa)	MM	nt (aa)	MM	nt (aa)	MM	nt (aa)	MM	nt (aa)	MM	nt (aa)	MM	nt (aa)	MM	nt (aa)	MM
A1	1,185 (394)	43.5	885 (294)	32.5	765 (254)	27.6	1,620 (539)	58.5	564 (187)	21.2	216 (71)	8.2	552 (183)	20.9	711 (236)	25.8
A2	1,185 (394)	43.5	885 (294)	32.7	765 (254)	27.6	1,620 (539)	58.5	564 (187)	21.2	216 (71)	8.2	540 (179)	20.6	660 (219)	23.7
B1	1,185 (394)	43.6	885 (294)	32.5	765 (254)	27.6	1,620 (539)	58.5	564 (187)	21.2	216 (71)	8.2	534 (177)	20.4	696 (231)	25.4
B2	1,185 (394)	43.6	885 (294)	32.5	765 (254)	27.6	1,620 (539)	58.4	564 (187)	21.2	216 (71)	8.2	534 (177)	20.4	711 (236)	25.5

Table 1.3. Lengths and molecular masses of HMPV genes and predicted proteins modified from (Ishiguro et al., 2004). Representative strains from each of the four HMPV genogroups (A1, A2, B1, B2) are shown. nt-nucleotide length in bases, aa-protein length in amino acid residues (in brackets), MM-molecular mass in kDa.

Taking the sequence data one step further, Ishiguro and colleagues compared the amino acid sequences within the four subgenogroups. The results of these can be seen in Table 1.4. The identity levels of the nucleic acid and amino acid sequences within the groups A and B are 90% or higher. The only exception is the G protein which has a nucleic acid identity of about 80% and amino acid identity of about 70%. Generally the sequences of strains within the same group are highly conserved. However, when comparing sequences between group A and group B strains, it becomes obvious that there is significantly more variation. Even then, most of the

structural proteins like N, P, M, F, M2-1 and M2-2 are at least 80% similar which could mean some form of evolutionary selective pressure has kept the sequences fairly conserved. Once again, there are exceptions like the SH and G nucleic acid (58-67%), amino acid (33-58%) sequences and the F nucleic acid (60%) sequences, which are markedly different between the two groups. Despite the differences at the identity level, the phylogenetic trees, constructed using each set of gene sequences, are still able to classify the strains into the two groups and 4 subgroups. This demonstrates that the subgroup classification of HMPV is stable and independent of genes utilised.

Protein	% Nucleotide sequence identity within group[a]		% Nucleotide sequence identity between groups[a]	% Amino acid sequence identity within group[a]		% Amino acid sequence identity between groups[a]
	Group A	Group B		Group A	Group B	
N	94-100 (96)	95-99 (96)	86-87 (86)	99-100 (99)	98-100 (99)	95-96 (96)
P	92-100 (95)	98-99 (95)	80-82 (81)	94-99 (97)	95-99 (97)	84-86 (85)
M	94-99 (97)	95-99 (96)	84-86 (85)	98-100 (99)	99-100 (99)	96-97 (97)
F	85-100 (92)	81-98 (87)	55-61 (60)	98-99 (98)	98-99 (98)	93-94 (94)
M2-1	94-99 (97)	94-99 (96)	86-87 (86)	96-100 (98)	97-100 (98)	94-95 (95)
M2-2	95-100 (97)	95-100 (97)	85-87 (86)	95-100 (97)	97-100 (98)	88-90 (90)
SH	90-99 (94)	88-98 (91)	66-69 (67)	83-99 (92)	81-98 (88)	54-60 (58)
G	75-99 (82)	78-97 (85)	56-60 (58)	61-99 (78)	63-96 (75)	31-35 (33)

Table 1.4. Comparing the level of identity between HMPV genogroup A and B based on their nucleotide and amino acid sequences from Ishiguro et.al.(Ishiguro et al., 2004). (a) number values include calculated averages (in brackets) depending on the number of strains in each genogroup.

In 2006, Huck and colleagues from Germany proposed a further subdivision of the A2 subgroup into A2a and A2b (Huck et al., 2006a). This was based on the F and N gene sequences obtained from 287 clinical specimens. The alignment results they produced showed a clearly demarcated split within the A2 subgroup. Even though this new proposed subdivision is scientifically sound, few publications by other authors have attempted to adopt the A2a and A2b nomenclature.

1.3 Genome organization

The first genome analysis of HMPV was completed by the Dutch in 2002 (van den Hoogen et al., 2002). The genome of HMPV consists of eight genes arranged in a tandem order (Fig 1.2) which codes for 9 proteins spanning a length of approximately 13,300 bases. The 3' end of the genome contains a short leader sequence of about 50 bases and the 5' end contains a similar trailer sequence of about (150)100 bases. In between the open reading frames for each gene, there are short non-coding sequences which contain the information for synthesis of the 5' cap and 3' poly-adenylated tail of the corresponding mRNA. The M2 gene contains two overlapping open reading frames and codes the proteins M2-1 and M2-2.

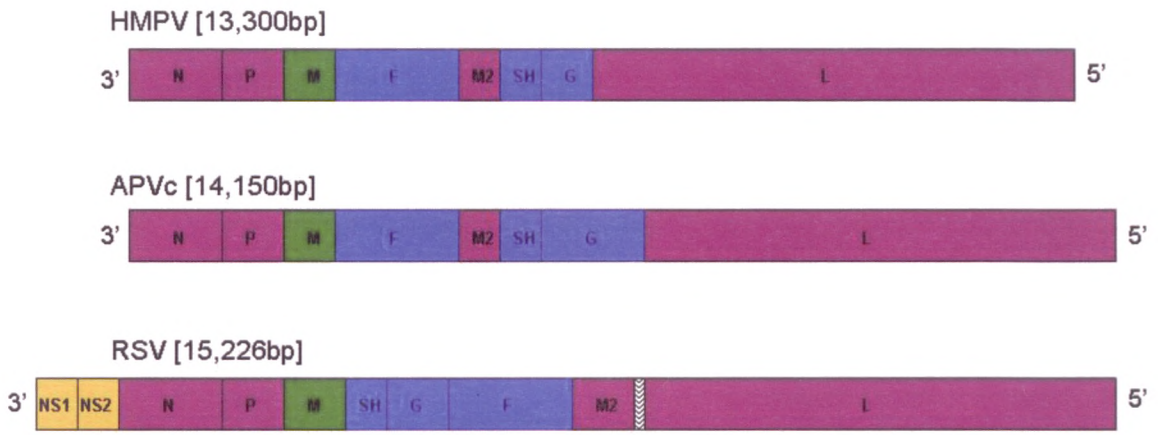

Figure 1.2. Gene organization of human metapneumovirus from (Sugrue et al., 2008). Genome is compared to that of avian pneumovirus C (APVc) and human respiratory syncytial virus (hRSV). Genes encoding non-structural proteins are yellow, polymerase-associated proteins are purple, envelope glycoproteins are blue and matrix protein gene is green. There is an overlap of the reading frames of the M2 and L genes of hRSV (grey shaded area). Gene sizes are approximately to scale.

Although the HMPV genome is very similar to hRSV, one of the most significant differences is the absence of the NS1 and NS2 genes at the 3' end. In addition, HMPV has a different arrangement of the F-M2 and SH-G pair of genes compared to hRSV. The reading frames for the hRSV M2 and L genes overlap across approximately 60 bases. These are some of the reasons for HMPV being classified under the genus Metapneumovirus instead of Pneumovirus. However, it is interesting to note that

among the Pneumoviruses, PVM does not have the M2 and L gene overlap (Easton et al., 2004). HMPV shares the same gene arrangement with that of avian pneumovirus type C (APVc) (Fig 1.2) (i.e. N-P-M-F-M2-SH-G-L).

(**N**)ucleoprotein gene has a length of 1185 bases coding for a protein of 394 amino acids and molecular weight of 43 kDa. The N protein is part of the ribonucleoparticle (RNP) complex and binds to the viral genomic RNA. This association protects the RNA from host nuclease action. In other paramyxoviruses like Sendai virus (Egelman et al., 1989), one N protein is usually associated with 6 nucleotides. However, this number might vary by 1 to 2 nucleotides between the other paramyxoviruses. The N protein in hRSV can aggregate to form multimeric structures (Murphy et al., 2003) in solution and can serve as an initiation point for the assembly of the virus nucleocapsid. The N terminal of the hRSV N protein has also been shown to interact with the P protein (Garcia-Barreno et al., 1996) during virus replication. The N protein has also been found in the soluble form in hRSV infected cells (Garcia-Barreno et al., 1996). The spacer region between the N and P gene is 24 bases in length.

(**P**)hosphoprotein gene has a length of 885 bases coding for a protein of 294 amino acids and molecular weight of 33 kDa. The P protein is also part of the RNP complex and is associated with both N and L proteins (Horikami et al., 1992). In Sendai virus (Tarbouriech et al., 2000), the P protein exists as a tetrameric form. The spacer region between the P and M gene is 33 bases in length.

(**M**)atrix gene has a length of 765 bases coding for a protein of 254 amino acids and molecular weight of 28 kDa. The M protein provides a supporting structure for the virus particle and is located below the virus envelope. Association between the M protein and the surface glycoproteins of Sendai virus was demonstrated by Sanderson (Sanderson et al., 1993; Sanderson et al., 1994). This provided the basis of virus

budding at the host cell surface. HMPV M proteins are likely to have a similar function. The spacer region between M and F is 123 bases in length.

(**F**)usion protein gene has a length of 1620 bases coding for a protein of 539 amino acids and a predicted molecular weight of 56 kDa. The F protein is a type I transmembrane protein and is expressed as a precursor molecule which can be cleaved by a trypsin-like protease to produce a mature form needed for virus-cell fusion (Schowalter et al., 2006b). A mutant strain of HMPV (Schickli et al., 2005) which had a serine-proline substitution at residue position 101 within the PRQSR trypsin cleavage motif was studied. The strain was able to replicate without trypsin but did not show any change in tissue tropism in hamsters. The F proteins in HMPV have been shown to possess an integrin binding site which could be used as a motif for cell attachment and subsequent entry (Cseke et al., 2009). Paramyxovirus F proteins fall under the class I category of fusion proteins. The spacer region between F and M2 is 27-38 bases in length.

M2 (**M2-1** and **M2-2**) protein gene has lengths of 564 and 216 bases coding for proteins of 187 (21 kDa) and 71 (8 kDa) amino acids, respectively. The M2-1 protein is thought to be a transcriptional factor. In hRSV, the M2-1 protein is associated with the RNP and its presence in the host cell allows transcription of the entire genome of hRSV by anti-termination (Fearns and Collins, 1999). The HMPV M2-2 protein has been shown to affect virus replication by controlling the mutation rate of the viral RNA polymerase (Buchholz et al., 2005; Schickli et al., 2008). A recent work (Kitagawa et al., 2010) showed that the presence of M2-2 proteins in HMPV infected cells strongly inhibited the transcription and replication processes of the virus. They found that M2-2 immunoprecipitated with L protein, suggesting that this interaction could be the point of regulation for M2-2. The spacer region between M2 and SH is 31 bases in length.

Small hydrophobic (**SH**) protein gene has a length of 540 bases coding for a protein of 179 amino acids and predicted molecular weight of 20 kDa. The SH protein is most likely to be a transmembrane protein similar to that in hRSV. Biacchesi and co-workers made SH protein-deleted HMPV mutants but could not demonstrate any impairment of viral reproduction when these mutant viruses were used to challenge hamsters (Biacchesi et al., 2004) and African green monkeys (Biacchesi et al., 2005). Thus they concluded that SH protein-deleted HMPV cannot be used as a potential vaccine candidate. The actual role of HMPV SH protein is yet to be determined although in related viruses like hRSV, SH protein has been shown to be associated with F and G proteins in the viral envelope (Feldman et al., 2001) and play a role in cell fusion (Heminway et al., 1994). Bao (Bao et al., 2008a) found that cell cultures and mice infected with SH-deleted HMPV mutants had higher levels of expression of nuclear factor kappa B (NF-κB) dependent genes like (interleukin) IL-6 and IL-8 thereby enhancing proinflammatory processes. The spacer region between SH and G is 212 bases in length.

(**G**)lycoprotein gene has a length of about 660 bases coding for a protein of 219 amino acids and a predicted molecular mass of 24 kDa. The G protein is a type II transmembrane protein and is thought to play a role in attachment to the host cells (Liu et al., 2007). In HMPV, as in hRSV, the G protein expressed on the cell surface is highly glycosylated. This will be discussed in chapter 4. Both N-linked and O-linked glycans are formed on the G protein causing in the apparent increase in protein size due to large numbers of O-linked glycan chains. Previous studies have found the G protein migrating in the 90-100 kDa range (Liu et al., 2007). Biacchesi (Biacchesi et al., 2005; Biacchesi et al., 2004) found that deleting the G protein from HMPV did not inhibit its replication *in vitro* or *in vivo*. However, G-deleted mutants constructed (Bao et al., 2008b) were found to produce higher levels of interferons and NF-κB related genes. They further proved that G protein inhibits the transcription of RIG-1, a known viral RNA sensor in cells (Hornung et al., 2006; Kawai and Akira, 2008; Pichlmair et al.,

2006) by binding to RIG-1. A difference between hRSV G and HMPV G is that the latter does not exist in the secreted form (Roberts et al., 1994). The spacer region between G and L is 189-242 bases.

Large (**L**) subunit of the RNA-dependent RNA polymerase gene has a length of 6018 bases coding for a protein of 2005 amino acids and molecular mass of 230 kDa. The L protein, together with N and P proteins form the RNP which is characteristic of paramyxoviruses (Garcia-Barreno et al., 1996). The L protein is the primary protein involved in transcription of viral mRNA as well as 5' capping and 3' poly-adenylation. It is responsible for replication of the virus genome (both negative and positive strands). Among paramyxoviruses, the L proteins were found to have six conserved domains which are believed to have different functions (Poch et al., 1990; Sidhu et al., 1993).

1.4 Virus structure

Paramyxoviruses are generally spherical (Fig 1.3) but may also have a pleomorphic or filamentous shape (Fig 1.4) as seen by electron microscopy.

Diameter of the virus can range from 150 to 300 nm. This is due mainly to the non-rigid lipid viral envelope derived from the host cell membrane. Within the lipid envelope, transmembrane viral proteins like the fusion (F) protein, attachment (G) protein and small hydrophobic (SH) protein can be found. These proteins are usually glycosylated but the type and extent of glycosylation depends on the host cell mechanism. The matrix (M) protein can be found just inside the envelope and provides a degree of structure to the virus particle.

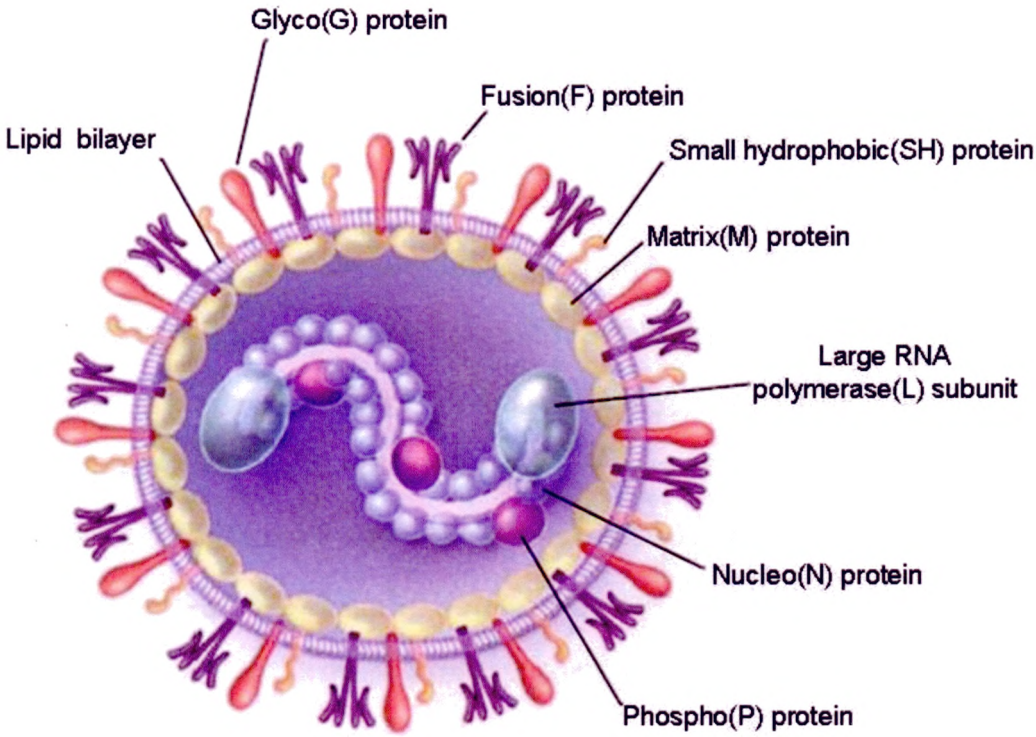

Figure 1.3. Schematic diagram of human metapneumovirus particle, adapted from Boivin. All the virus proteins are shown except the M2-1 and M2-2 proteins which are thought to be associated with the RNP replication complex.

The nucleo(N)protein, phospho(P)protein and RNA polymerase(L) form the transcription and replication mechanism of the virus. The M2-1 and M2-2 proteins are thought to be involved in regulatory functions and may be associated with the RNP complex. Most of the current knowledge of HMPV structure was elucidated from studies on related viruses like hRSV, measles virus and parainfluenza viruses.

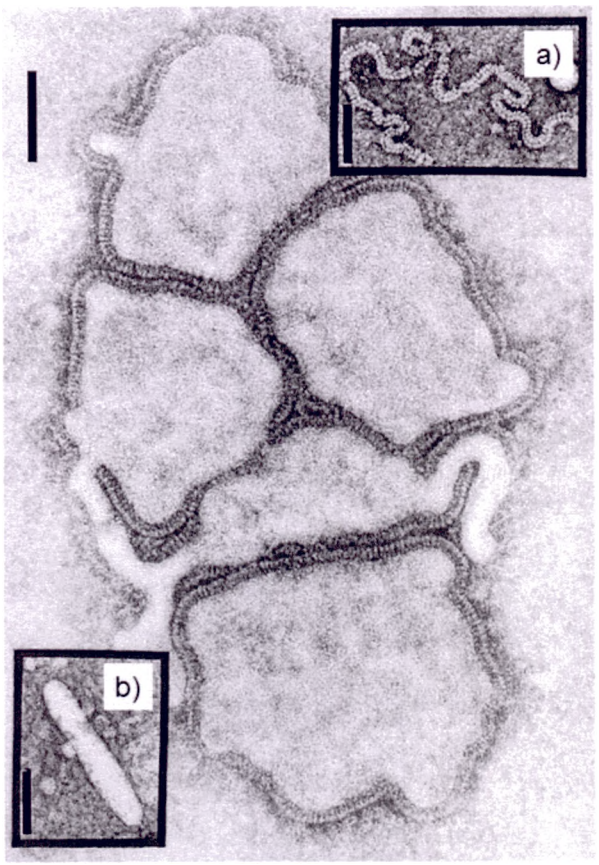

Figure 1.4. Electron micrograph of HMPV particles using negative staining taken from (Peret et al., 2002). Main image shows the pleomorphic form of HMPV. a) image of the nucleocapsid, b) image of the rod-shaped form of HMPV. The thick vertical bars represent a length of 100nm.

1.5 Replication of HMPV

HMPV infects the human host via the respiratory tract. Transmission of the virus is by airborne droplets or aerosol. An infected person coughs, sneezes or comes into contact with a susceptible person and the virus is passed on at close proximity. This mode of transmission is very similar to most respiratory viruses: by aerosol or close contact (Ansari et al., 1991). A recent publication (Tollefson et al., 2010) studied the stability of HMPV particles in the environment. They found that HMPV was very resistant to freeze-thawing with a loss of viability of less than 1 $\log_{10}$ value after 10 freeze-thaw cycles. This is different from hRSV which loses 2 $\log_{10}$ viability after 5 freeze-thaw cycles (Gupta et al., 1996) . HMPV was also shown to be viable for up to 2-6 hours on non-porous (metal or plastic) surfaces similar to hRSV (Hall et al., 1980) . This has implications for nosocomial and community transmission of HMPV because the virus no longer requires an infected host to be in close proximity to a susceptible host. Fomite transmission requires stricter preventive measures especially in areas of

high human traffic. Upon entering the upper respiratory tract, the virus attaches to the epithelial cells using the attachment (G) protein which binds to specific host cell receptors. The fusion (F) protein, which is thought to be in close proximity to the G protein, then undergoes a conformational change and triggers cell fusion (refer to section 1.11). This mechanism is known as receptor-mediated fusion. However, another theory has recently been put forward (Schowalter et al., 2006b) which suggests that the trigger for F protein fusion in HMPV could be due to low pH. The mechanism will also be discussed later in section 1.12. When the viral RNA is released into the host cell cytoplasm (Fig 1.5), the RNP starts to transcribe coding (positive) strands of mRNA for the various genes starting from N towards L. The mRNAs are 5' capped and 3' polyadenylated. As the polymerase moves from the 3' end to the 5' end, it pauses and restarts at each gene. This linear transcription results in a gradually decreasing concentration of mRNA from N to L. This translates into decreasing concentrations of N protein to L protein in the cell cytoplasm. Slowly, the various viral proteins (N, P, M, L) start to assemble. The transmembrane proteins (F, G, SH) are transported via the secretory pathway (endoplasmic reticulum and Golgi) to the cell membrane. At a critical concentration of M2-1 protein witihin the cell, the M2-1 protein starts to modify the RNP to transcribe full-length coding strands of RNA to serve as templates for synthesis of more negative-strand genomic RNA which will be packaged into new viral capsids. The new viral particles bud out from the cell membrane to infect neighbouring cells. The Dutch scientists (van den Hoogen et al., 2001) attempted to infect young turkeys, chickens and macaques with HMPV to determine if HMPV was an avian transmitted disease or a human originated one. None of the birds showed any symptoms and no virus replication was detected in them. However, viral nucleic acid was detected in the macaques, and some of them showed clinical symptoms. They came to the conclusion that HMPV was a primate-associated virus. Five years later, another group (Velayudhan et al., 2006) tried to infect groups of young turkeys separately with the 4 genotypes of HMPV compared with APVc as a control. They found that all 4 genotypes of HMPV produced short-lived and mild symptoms in the

turkeys. Viral RNA was also detected by RT-PCR in tissue samples. These results seem to suggest that the predecessor of HMPV may have crossed from birds to humans.

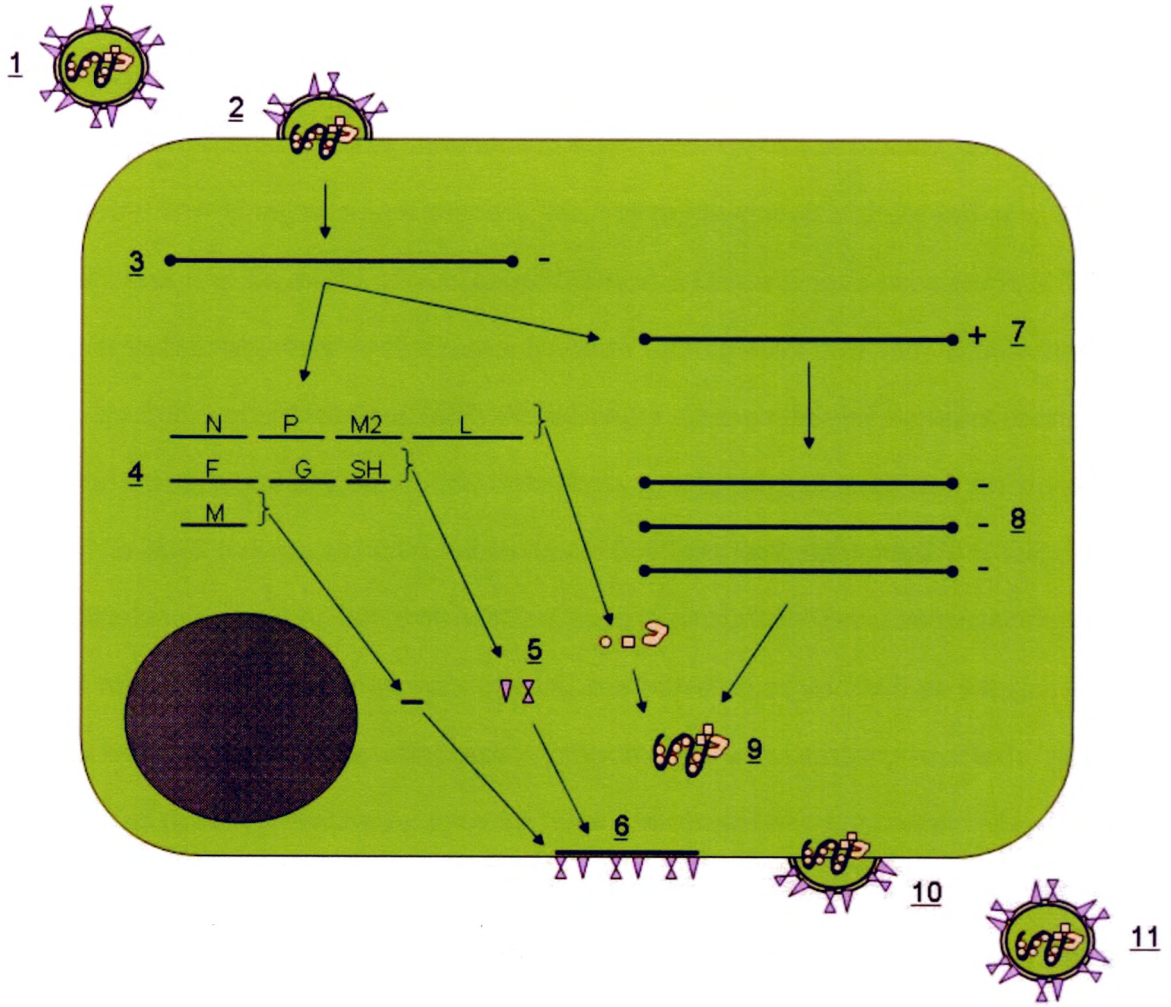

Figure 1.5. Life cycle of HMPV- a typical paramyxovirus. (1) A mature virus particle comes into close proximity with a susceptible host cell. The G protein attaches to specific host cell receptors and the F protein induces cell fusion by a change in structural conformation. (2) After fusion of the viral membrane with the host cell membrane, the contents of the viral capsid enter the cytoplasm. (3) The RNP complex initiates transcription of the negative strand viral RNA producing (4) positive strand mRNA which code for the various viral proteins. (5) the proteins are either RNP related, membrane bound, or structural. (6) The membrane bound proteins are processed via the ER and Golgi and transported to the cell surface where they aggregate with the M protein and form a new virus capsid. (7) Full length positive-strand RNA is transcribed to serve as a template for synthesis of (8) new negative-strand genomic RNA. (9) The new genome assembles with the newly synthesized RNP proteins and moves towards the cell surface. (10) As a new virus particle forms by budding as the components of the mature virus gradually assemble. (11) The virus is released from the cell surface and is now able to infect a new host cell.

Other research using animal models (MacPhail et al., 2004) (Hamelin et al., 2005) (Kuiken et al., 2004) have shown that hamsters, ferrets, cotton rats, BALB/c mice, and

African green monkeys are potentially useful animals to replicate HMPV infection in humans.

1.6 Worldwide incidence of metapneumovirus

Within a few years after the first discovery of HMPV, the number of reports of HMPV isolated from clinical samples increased. In continental Europe; HMPV was detected in France in 2001-2002 (Freymouth et al., 2003) where the prevalence was 6.6%, in Italy HMPV prevalence over 3 seasons from 2000-2002 varied from 37 to 7 to 43% (Maggi et al., 2003) with one-third of the HMPV-positive cases also infected with another respiratory virus. This study also found HMPV RNA in the blood of 30% of positive patients. In Austria, a long-term study collected 3576 samples and detected HMPV in 202 (5.6%) of them (Aberle et al., 2010). A study in Ireland found that 2.4% of 171 adult bronchioalveolar lavage specimens were positive for HMPV (Carr et al., 2005), but surprisingly, no HMPV was detected in 122 nasal specimens from children. In Spain in 2004, 16.2% of children with respiratory infection below 1 year of age were found to have HMPV which made it the second most prevalent respiratory virus in children after hRSV (Ordas et al., 2006). A study across 3 consecutive winter seasons from 2005-2008 in Greece found about 6% of 380 samples positive for HMPV, with 7 of these cases being co-infected with influenza A virus (Gioula et al., 2010). The incidence of HMPV was higher in the younger age groups (under 18 years) compared to influenza virus. Scandinavian countries also isolated HMPV: 21% of 236 children were found with HMPV during one winter season in Norway (Dollner et al., 2004), and half were found to have underlying chronic disease. This was in contrast to a study in Denmark where only 2.9% of 374 children were HMPV-positive and had mild symptoms compared to hRSV-infected children (von Linstow et al., 2004). In Finland, 8% of 132 children were HMPV-positive but the study was restricted to those suffering from acute wheezing (Jartti et al., 2002). In North America, a study in the United States in 2001-2002 found the prevalence of HMPV at 6.4% with one rare suspected case of

nosocomial transmission of HMPV (Esper et al., 2003). Another retrospective American study from 2001-2004 tested 1294 samples and found 34 (2.6%) positive for HMPV (Gray et al., 2006a) mainly in children below 9 years old. In Canada, a study found HMPV in 14.8% of 445 specimens in all age groups but a higher rate of hospitalization incidents for those younger than 5 years and older than 50 years old (Bastien et al., 2003b). Studies were also done in Latin America. The first study in Mexico (Noyola et al., 2005) on 558 nasal wash specimens from children under 3 years found 6.1% infected with HMPV, again making HMPV the second most isolated respiratory virus. A group in Brazil (da Silva et al., 2008) found 5.6% of 142 specimens positive for HMPV. A recently published study on 545 samples from Chile had a HMPV detection rate of 10.2% and some of the isolates were classified by phylogenetic analysis into a novel A3 subgroup (Escobar et al., 2009). In Uruguay, 8% of 217 samples were found positive for HMPV and sequence data based on the nucleoprotein and attachment genes detected genotypes A2, B1 and B2 (Pizzorno et al., 2010). A study involving 420 patients from both Peru and Argentina detected HMPV in only 2.3% of the samples (Gray et al., 2006b). On the other side of the Pacific, a research group in Australia (Nissen et al., 2002) found evidence of HMPV in 3 patients with respiratory infection as early as 2002. In New Zealand (Werno et al., 2004), 2-5% of children with bronchiolitis and pneumonia were infected with HMPV. A serological study in Japan found 72.5% of a sample population had antibodies against HMPV demonstrating that HMPV had been circulating in the Japanese population for quite some time (Ebihara et al., 2003). From 2003-2005, a study in Korea found 7.3% of 381 nasopharyngeal samples from children positive for HMPV by RT-PCR (Chung et al., 2006). Researchers in Taiwan (Wang et al., 2006) also found HMPV in children hospitalised for respiratory tract infections but disease symptoms were mainly mild. The prevalence of HMPV over a one year period in Hong Kong was 5.5% out of 587 respiratory samples (Peiris et al., 2003). In Hunan province, China, 6.8% of 661 children with acute respiratory tract infection were positive for HMPV and over half were co-infected with another respiratory virus like hRSV (Xiao et al., 2010). Researchers in Thailand worked with the Dutch scientists to

detect HMPV in 4.2% of 120 children with respiratory disease (Thanasugarn et al., 2003). In 2010, the presence of HMPV in the Philippines was first reported (Furuse et al., 2010). However, only two out of 465 samples (0.5%) were positive for HMPV. More recent studies from countries in the Middle East like Jordan (Kaplan et al., 2006) and Israel (Regev et al., 2006) have also isolated HMPV from specimens taken from children. The Israeli study was done on 388 respiratory samples and HMPV was detected in 10.8% of them with co-infections rarely detected. In Egypt, adults with lower respiratory tract infection were tested for HMPV (El Sayed Zaki et al., 2009) and 13.6% were found positive. In addition, 4.5% were found to be co-infected with *Streptococcus pneumoniae* bacteria. In the last three to four years, there have been reports of HMPV isolated in the African continent. A case controlled study in Kenya found HMPV in 3% of 759 clinical samples (Berkley et al., 2010) taken from children seen at a district hospital.

A few long-term studies on HMPV infection have been done. A four year study in Australia from 2001 to 2004 looking at just over 10,000 samples (Sloots et al., 2006b) detected HMPV in 7.1% of them. The peak of the HMPV season was from winter to spring and there was annual change in subgroups in most of the years. A retrospective study in the United States (Williams et al., 2006b) tested 2,384 samples collected from 1982 to 2001 and detected HMPV RNA in 5% of the samples. The season was from December to May and all four subgroups were detected with some years showing multiple subgroups circulating in the population. A German study from 1996 to 2006 based on a surveillance network for respiratory diseases tested 18,899 samples (Weigl et al., 2007). An Austrian study on respiratory samples collected between 1987 to 2008 detected HMPV in 5.6% of 3576 samples (Aberle et al., 2010). The researchers found that one subgroup of HMPV predominates in any one season and the change in predominant subgroups occurs every one to three years. In addition, they observed that the peak of HMPV infection shifts from the typical winter-spring months to the summer months every other year. Another recent study in Sweden on 4,989 samples collected from 2002 to 2006 detected HMPV in 2.9% of the total (Rafiefard et al.,

2008). The numbers for HMPV were the highest in March and much more of subgroup A was detected than subgroup B. In temperate climates, there is a distinctive peak of HMPV infections during the winter and early spring months. However, in tropical climates, there is a less pronounced seasonal fluctuation with HMPV infections generally occurring all year round (Loo et al., 2007). HMPV is clearly a ubiquitous virus responsible for approximately 5% of respiratory tract infections in the human population.

1.7 Metapneumovirus in Singapore

So far no study has been performed in Singapore to determine the prevalence of HMPV in the local population. A study was done between 1999 and 2002 by respiratory disease physicians at Kandang Kerbau Women's and Children's Hospital (KKH) in Singapore (Goh, 2002) who found that the prevalence of HMPV infection in 287 children seen at the emergency department for asthmatic conditions was 5.2% (15 cases). Despite the restricted cohort, this study gave useful information that HMPV infection could have a role in the exacerbation of asthma attacks. This has been observed with other respiratory viruses. Another study done between 2004 and 2005 at the National University Hospital (Ong et al., 2007) on an even more restricted cohort of 60 children with asthma and wheezing found 13.3% (8 cases) infected with HMPV. The most recent study was completed by our group in NTU from 2005 to 2007 based on nasopharyngeal swabs taken from 500 children admitted to KKH for respiratory disease. We found the prevalence of HMPV to be 5.8% (29 cases) (Loo et al., 2007). The presence and distribution of HMPV in Singapore is no different from that found in other parts of the world. Our group in NTU recently published a review on HMPV in 2008 (Sugrue et al., 2008).

1.8 Characteristics of HMPV infection

HMPV has been found to cause both lower and upper respiratory tract infection (Sugrue et al., 2008). Lower respiratory tract infection (LRTI) usually includes symptoms like wheezing, bronchitis, bronchiolitis and pneumonia and is generally defined as an infection from the trachea downward into the lungs. Upper respiratory tract infection (URTI), on the other hand, is an infection of the nose, throat, larynx (e.g. laryngitis) and upper trachea. URTI can occasionally involve the ear (e.g. otitis media) and this has been shown to be one of the most commonly associated symptoms of HMPV infection (Heikkinen et al., 1999; Williams et al., 2006a). Other general symptoms like fever and cough can surface. These symptoms are indistinguishable from hRSV infection. The incubation period from the initial contact with the virus to developing full-blown symptoms has been estimated at four to six days (Ebihara et al., 2004c) which is quite typical of other respiratory viruses. Research on mouse models have determined that HMPV can persist in the lungs for several weeks despite the presence of neutralizing antibodies (Alvarez et al., 2004b). This indicates that HMPV is somehow able to evade the host immune system for a significant length of time. (Liu et al., 2009) showed that HMPV could actually remain persistent and undetected within the nerve cells in the lungs of BALB/c mice. After treatment with a glucocorticoid (dexamethasone), the virus was found to be able to reactivate and re-infect respiratory epithelial cells in close proximity. This new knowledge will have a great impact on clinical management of HMPV disease. More will be discussed in the following section on immune response to HMPV (section 1.10). At one end of the spectrum, infected individuals can be asymptomatic or show very mild symptoms. One study in Italy found HMPV in 4% of asymptomatic volunteers (Bruno et al., 2009) which suggest that community spread of HMPV may be due to asymptomatic carriers. Another study by (Falsey et al., 2006) did not detect any HMPV in a non-infected control group of 158 adults. HMPV infections with potentially more severe outcomes have been reported, e.g. HMPV-associated encephalitis (Schildgen et al., 2005) and other forms of central

nervous system infection manifested as febrile seizures (Arnold et al., 2009), both of which are life-threatening. Patients who are immunocompromised are also susceptible to serious HMPV infections. In 2003, there was a case report of a fatal infection of HMPV in a patient after haematopoietic stem cell transplantation (Cane et al., 2003). Another death was reported of a post-transplant patient in 2006 who had HMPV infection and rapidly progressing lung cancer (Huck et al., 2006b). However, in the latter case, the cause of death could not be accorded to HMPV alone even though it was the only pathogen isolated from bronchoalveolar lavage. One study found influenza virus and HMPV to be the most common respiratory viruses isolated from HIV-positive adults receiving anti-retroviral drug therapy (Klein et al., 2010). HMPV and other respiratory viruses have been detected in a percentage of post-transplant lung patients (Kumar et al., 2010) and this has been suggested as the cause of organ rejection. Another study has implicated HMPV in the role of asthma exacerbation (Williams et al., 2005). The possibility of genogroup A causing more severe disease than genogroup B was raised by (Vicente et al., 2006) and more recently by (Arnott et al., 2011), but other groups did not confirm this finding (Debur et al., 2010; Pitoiset et al., 2010). A recent serological study of a community in Taiwan using an ELISA platform found 53.2% of preschoolers seronegative, 88.3% of school children seropositive and 93.7% of adults seropositive (Huang et al., 2010). Sera from 137 people without respiratory symptoms were tested for HMPV antibodies in Croatia (Ljubin Sternak et al., 2006) and the highest titers were in children aged 1 to 2 years. This means that most of the population would have been exposed to HMPV during their early school-going age and would benefit the most from any sort of vaccination program. Re-infection has been shown to occur in HMPV by scientists in Canada (Pelletier et al., 2002) and Japan (Ebihara et al., 2004a). This may be a result of incomplete immune protection which has also been shown in hRSV (Handforth et al., 2000). However, both cases of re-infection of HMPV were reported in young children who may be more susceptible due to their less mature immune system. Compared to hRSV, which usually affects children under two months old, HMPV infection tends to

occur in slightly older children from three to twelve months in age (Boivin et al., 2003; Ebihara et al., 2004b; Morrow et al., 2006; Peiris et al., 2003; Williams et al., 2004). Compared to studies focused on HMPV infection in children, fewer groups looked at the effect of HMPV infection in the elderly. A retrospective study on some elderly patients infected with HMPV found that those with underlying conditions are at greater risk of severe disease and even death (Boivin et al., 2002). Other studies in Japan (Honda et al., 2006), Canada (Boivin et al., 2007), the United States (Liao et al., 2012; Louie et al., 2007), Australia (Osbourn et al., 2009) discovered that HMPV outbreaks are a major cause of morbidity in long-term care facilities which cater to the needs of elderly persons. Reported fatality rates were as high as 33%. Bosis and colleagues studied the impact of HMPV disease on children and their families. Their publications (Bosis et al., 2005; Bosis et al., 2008) concluded that families with HMPV or influenza-infected children were more prone to fall ill, require more trips to the doctor, require more anti-pyretic medicines and miss out on school or work. The impact of HMPV on the economic burden of families is considerable and may be a significant public health problem.

1.9 Co-infection with other respiratory pathogens

There have been a few reports describing the incidence of co-infections of HMPV and other common respiratory viruses in patients. One group in the United Kingdom found that co-infection with HMPV and hRSV led to more severe respiratory disease (Greensill et al., 2003). The same group of researchers further calculated that co-infection with HMPV and hRSV would increase the risk of a patient requiring mechanical ventilation by ten times (Semple et al., 2005). Another group in China calculated that co-infection of HMPV with another respiratory virus increased the hospitalization rate (Xiao et al., 2010). In contrast, a few studies did not find any conclusive link between co-infection and disease severity (Al-Sonboli et al., 2006; Chan et al., 2003; Mackay et al., 2006). A group in Hong Kong tested patient samples

collected during the severe acute respiratory syndrome (SARS) outbreak in 2003 and found that about 12% of 48 the samples were positive for both SARS coronavirus and HMPV (Chan et al., 2003). An Egyptian study found one-third of HMPV infected adults also had *Streptococcus pneumoniae* (El Sayed Zaki et al., 2009) but there was no strong evidence of increased severity of disease. Other factors like genetic disposition or environmental effects may also contribute to disease severity.

1.10 Immunological response to HMPV infection

The effect of HMPV infection on the immune response was studied by a few groups. (Laham et al., 2004) analysed the cytokines in nasal washes taken from infants with respiratory symptoms. They compared the level of six cytokines in specimens positive for influenza virus, hRSV and HMPV (Fig 1.6).

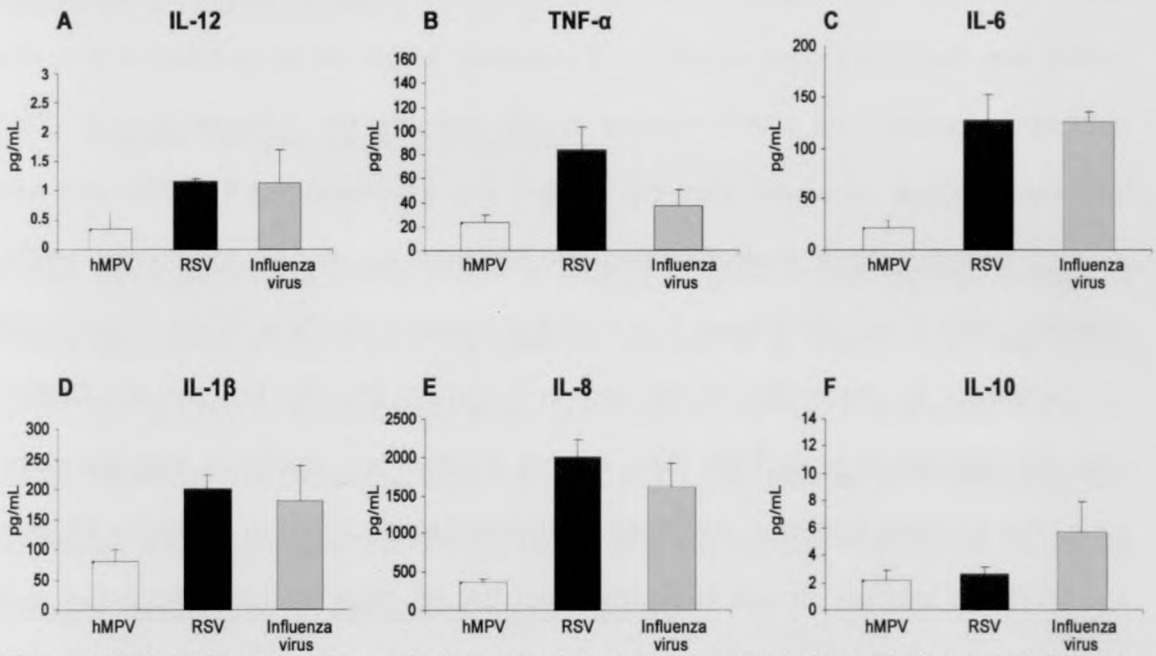

Figure 1.6. Cytokine levels in respiratory samples of infants adapted from Laham *et.al.* (Laham et al., 2004). The infants were infected with either human metapneumovirus (hMPV), human respiratory syncytial virus (RSV) or influenza virus. TNF-α-tumour necrosis factor alpha, IL-interleukin. A-IL12, B-TNF-α, C-IL-6, D-IL-1β, E-IL-8, F-IL-10. The vertical bars are the mean values ± standard error of the mean (SEM).

(Melendi et al., 2007) performed a follow-up experiment and studied the effect of the same three viruses on another set of three cytokines (Fig 1.7).

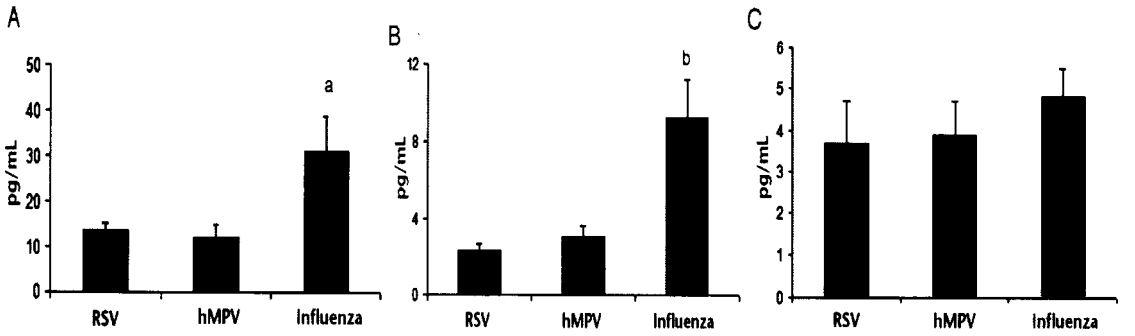

Figure 1.7. Cytokine levels in respiratory samples of infants modified from Melendi *et.al.* (Melendi et al., 2007). The infants were infected with either human metapneumovirus (hMPV), human respiratory syncytial virus (RSV) or influenza virus. A-IFN-γ (interferon gamma), B-IL-4, C-IL-13. The vertical bars are the mean values ± SEM.

The earlier study showed that, compared to hRSV and influenza virus, HMPV has a rather poor ability to trigger an inflammatory cytokine response. Only similar IL-10 cytokine levels were observed between hRSV and HMPV. This is despite the fact that both viruses are more related to each other than with influenza virus and that both viruses cause similar symptoms in infected individuals. The authors suggested that both hRSV and HMPV cause disease by different mechanisms. In the later study, HMPV was found to trigger a high IL-13 response compared to IL-4 and IFN-γ. The authors suggested that HMPV causes a shift towards the T-helper type 2 (Th2) immune response. However, they did not find any association of this Th2 shift with disease severity. Other research used BALB/c mice as models for human HMPV infection. (Kolli et al., 2008) found that in HMPV infection, the CD4(+) and CD8(+) cells are necessary for eradication of the virus in a primary infection but only the CD8(+) cells are required to protect the mice against a secondary challenge with the same virus. The mouse model was also used by (Darniot et al., 2009) to study the effect of age on HMPV infection. It was found that older BALB/c mice produced more IL-4, IL-6 and slightly more CD4(+) cells and this may be the cause of higher mortality of aged mice than young mice. Another study by (Dinwiddie and Harrod, 2008) found that HMPV is able to impair the IFN-α signaling pathway in cells by interfering with the activation of signal transducers and activators of transcription type 1 (STAT1) phosphorylation. This is very different from the closely related hRSV which uses its NS1 protein to perform a similar function (Moore et al., 2008). The ability of HMPV to

activate the expression of retinoic acid inducible gene 1 (RIG-1) and another associated protein melanoma differentiation associated gene 5 (MDA-5) was shown in A549 cells (Liao et al., 2008). These two proteins are part of a cytosolic viral sensor system which recognizes foreign 5' triphosphate RNA (Hornung et al., 2006; Pichlmair et al., 2006). HMPV G (Bao et al., 2008b) and P (Goutagny et al., 2010) proteins have been shown to inhibit the action of RIG-1 activity and thereby have the ability to downregulate the host immune response against itself. According to Bao et. al., the HMPV G protein binds to RIG-1 and this association interferes with RIG-1-dependant transcription. Because of this, the downstream activation of antiviral cytokine transcription factors e.g. NF-kB is hampered. Goutagny et. al. found that only the B1 subgroup phosphoprotein inhibited type 1 IFN response by preventing RIG-1-mediated sensing of viral 5'-triphosphate RNA. The possible mechanisms for the blocking action of B1 subgroup P protein include its higher affinity for viral RNA or higher expression level of B1 subgroup P protein.

1.11 Human metapneumovirus diagnostics

Unlike other paramyxoviruses, HMPV is difficult to grow in cell culture. Isolates of HMPV have been grown in tMK cells (van den Hoogen et al., 2001), HEp2 cells (Chan et al., 2003), Vero cells (Biacchesi et al., 2003) and LLC-MK2 cells (Deffrasnes et al., 2005). However, the cytopathic effects (CPE), if any, can take up to 14 days to show. Published observations on the CPE by HMPV (Fig 1.8) include formation of hRSV-like syncytia, rounding up of cells and cellular destruction.

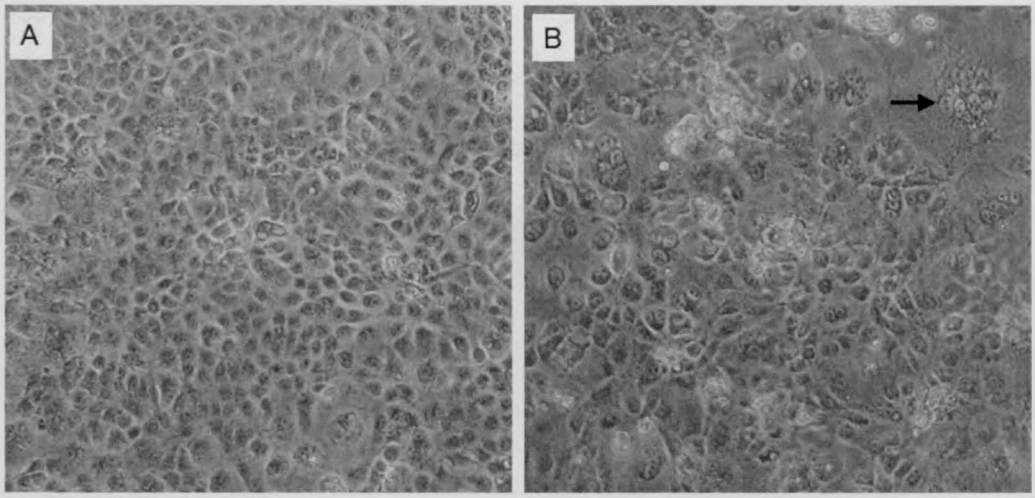

Figure 1.8. LLC-MK2 cells viewed under an inverted microscope using a 10x objective. (A) Uninfected cells after 1 week. (B) Cells infected with HMPV after 1 week showing extensive damage, rounding-up and syncytia formation (arrow).

Even after observing CPE, the follow-up identification test by immunofluorescence microscopy for the virus would require at least another day's work. This is certainly a huge drawback when this method is used in the diagnostic (and research) laboratory setting. There is no common cell line that offers the best condition for virus growth. In addition, a typical diagnostic laboratory cannot afford to stock four different cell lines just to culture one species of virus. On top of these considerations, the lengthy turn-around-time required to observe CPE in cells means that most patients would most likely have recovered from a HMPV infection by the time a diagnosis is made. No surprise then that few diagnostic laboratories are willing to take on culture tests for HMPV which can cost about S$150-200 per test. A research group in the UK tried using a less common cell line 16HBE140 to culture HMPV from clinical samples (Ingram et al., 2006). They found these cells superior to the LLC-MK2 cells used by many laboratories. HMPV cultured in 16HBE140 cells did not require the addition of trypsin into the growth media which is a huge advantage. Alternative methods to detect HMPV rapidly in clinical settings have been in developed as early as 2003. These protocols range from conventional end-point reverse-transcription polymerase chain reaction (RT-PCR) tests (Chan et al., 2003; McAdam et al., 2004) to more sophisticated real-time RT-PCR methods (Cote et al., 2003; Mackay et al., 2003; Maertzdorf et al., 2004). Antibodies developed for ELISA and immunofluorescence

assay (IFA) (Ebihara et al., 2005; Ishiguro et al., 2005) have also come into use. Tests based on IFA can be performed in one day, making the results more relevant to patient management. The cost of each test usually does not amount to more than S$80 (about the price of a standard bacterial culture with Gram stain). The only initial investment needed is the purchase of a fluorescence microscope and some plasticware. Many manufacturers of IFA kits for the detection of HMPV include good control slides which are very helpful for the less confident medical technologist. The sensitivity of IFA tests is in the range of 40-80%. This large variation is due to human factors like quality of specimen collection and technologist experience. Despite some disadvantages, IFA tests are popular amongst diagnostic laboratories that do not have a sophisticated setup for RT-PCR-based tests. KKH is currently using an IFA antigen detection kit from Diagnostic Hybrids Inc, USA which was recently evaluated (Aslanzadeh et al., 2008). There are few commercial ELISA-based tests for HMPV currently either detecting viral antigens or host antibodies. ELISA tests for antibodies are especially useful for screening large numbers of samples, e.g. when trying to determine the level of seroconversion of a local population (Leung et al., 2005). Some diagnostic laboratories may prefer to use ELISA if they already have the setup for performing such tests. RT-PCR-based tests for the detection of HMPV has been increasing because of its superior sensitivity (>80%) and specificity compared to IFA and culture. RT-PCR tests can cost between S$80-120 which would be cheaper than culture but more expensive than IFA. Conventional RT-PCR using a normal thermal cycler and agarose gel electrophoresis is slowly giving way to real-time RT-PCR using fluorescent dyes and real-time thermal cyclers. These new instruments can produce results in a few hours making same-day results a reality. Not surprisingly, as more and more cases of HMPV infection are diagnosed, the demand from physicians for the testing of HMPV has also increased (Aramburo et al., 2011). Diagnostic laboratories now have to consider including HMPV detection as part of their repertoire.

1.12 HMPV fusion and attachment proteins – process of cell fusion

The F protein of HMPV is a type I transmembrane viral fusion protein (Fig 1.9). It is immunogenic and is synthesized as an inactive precursor molecule F_0 with a size of 539 amino acids.

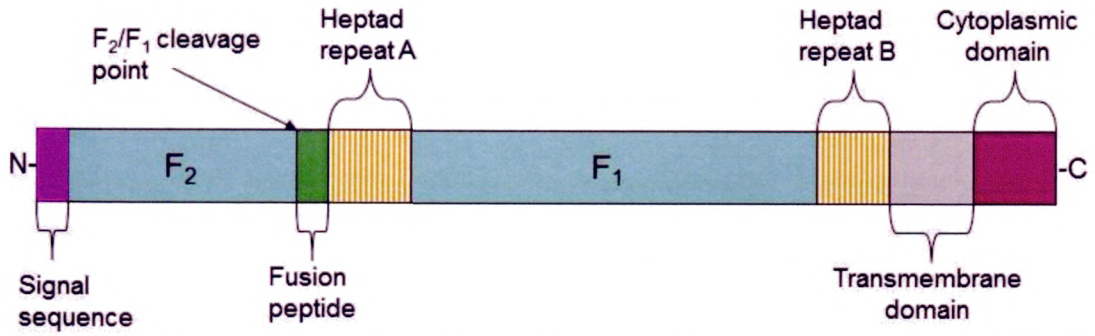

Figure 1.9. Simplified representation of the major domains in the fusion protein of HMPV. The N- and C- terminals are shown on the left and right of the diagram respectively. Refer to Chapter 3 for the detailed nucleic acid and amino acid sequences.

The N-terminal contains the signal sequence of the protein which is required for secretion. It also contains the cleavage site for a trypsin-like protease. The trypsin cleavage site within the F protein of HMPV is preceded by the proline-arginine-glutamine-serine-arginine (PRQSR) motif at positions 98-102. This motif is different from those found in other paramyxoviruses (Fig 1.10).

		102
hRSV	...NNRARR↓	ELP.....LSKKRKRR↓ FLG...
bRSV	...FSRAKR↓	GIP.....MGKKRKRR↓ FLG...
PVM		.....KSK-RKKR↓ FLG...
HMPV		.....IENPRQSR↓ FVL...
APVC		.....IMSPRKAR↓ FVL...
APVB		.....ILSHRKKR↓ FVL...
APVA		.....LSSPRRRR↓ FVL...

Figure 1.10. Cleavage sites for fusion protein of members of the Pneumovirinae subfamily. Arrows indicate the cleavage sites. The number indicates the amino acid position with respect to HMPV. hRSV-human respiratory syncytial virus, bRSV-bovine respiratory syncytial virus, PVM-pneumonia virus of mice, HMPV-human metapneumovirus, APV A/B/C-avian pneumovirus type A/B/C.

Most of the viruses in the Pneumovirinae family have several basic amino acids (arginine, lysine) which can be cleaved by the enzyme furin which is quite ubiquitous.

HMPV and APVC cleavage sites are only susceptible to trypsin-like enzymes which probably restricts their infectivity to certain cell types.

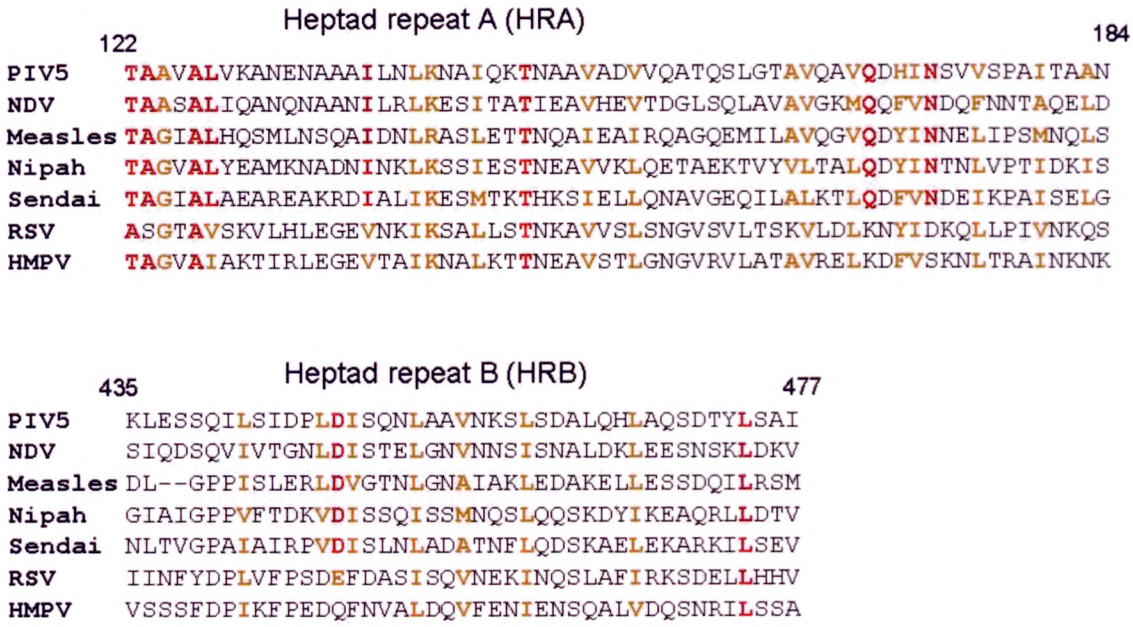

Figure 1.11. Alignment of the heptad repeat A (top) and B (bottom) regions of a few paramyxoviruses from (Lamb et al., 2006). Identical amino acid residues are highlighted in red. Similar residues are highlighted in yellow. Numbers indicate the amino acid positions with reference to PIV5. PIV5-parainfluenza virus 5, NDV-Newcastle disease virus, RSV-human respiratory syncytial virus, HMPV-human metapneumovirus.

Within the fusion protein, there are 2 heptad repeat domains (HRA and HRB) which are fairly conserved within the paramyxovirus family (Fig 1.11) and a fusion peptide which have a role in host invasion (Russell and Luque, 2006). The transmembrane region is located near the C-terminal. The F protein of HMPV was found to be fairly conserved among the various genogroups (Biacchesi et al., 2003; Boivin et al., 2004; Galiano et al., 2006; Yang et al., 2009). The F gene nucleotide sequences between HMPV genogroups A and B have an identity of approximately 84-94% and those within the same genogroup can have as high as 96-98% identity. The amino acid sequences between genogroups A and B share about 94-96% identity and can be >99% identical within the same genogroup. The hydropathy plot for the F protein is shown below (Fig 1.12).

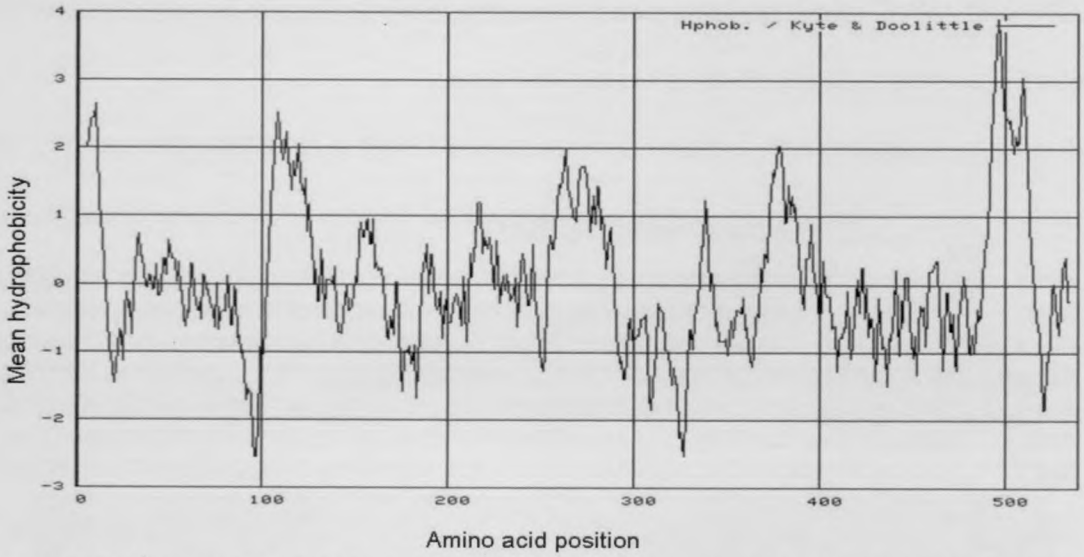

Figure 1.12. Kyte and Doolittle hydropathy plot for the F protein of HMPV. Hydrophobic regions are plotted above the zero horizontal axis. Hydrophilic regions are plotted below the zero horizontal axis. The horizontal scale indicates the amino acid positions of the proteins. The proposed transmembrane domain (approximately positions 490 to 520) corresponds to the area of high hydrophobicity. The cytoplasmic tail is from position 520 to the end. The external domain is from position 0 to 490. The hydrophobic fusion peptide corresponds to positions 100 to 120.

(Schowalter et al., 2006b; Schowalter et al., 2009) suggested that both low pH and trypsin cleavage are essential for the cell fusion activity of F protein. However this was disputed by (Herfst et al., 2008) who found that low pH induced fusion in HMPV was not universal but due to a substitution of the glutamate residue by glycine at position 294 of the F protein. (Schowalter et al., 2009) later clarified that some strains of HMPV may have their fusion activity enhanced by low pH and that the effect of endocytosis inhibitors (Bafilomycin A1, concanamycin A, monensin, dynasore) on the efficiency of HMPV infection point to endocytosis as a possible mechanism for HMPV entry. hRSV was also shown to use clathrin-mediated endocytosis as a method of cell entry (Gutierrez-Ortega et al., 2008; Kolokoltsov et al., 2007).

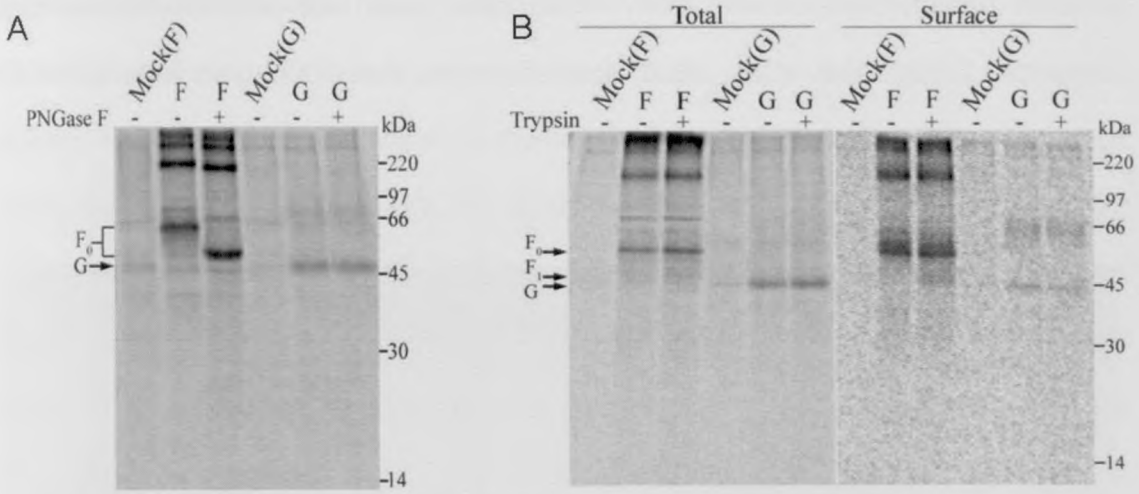

Figure 1.13. Western blot of HMPV F and G proteins adapted from (Schowalter et al., 2006b). (A) Treatment of F and G proteins with enzyme peptide N-glycosidase F (PNGaseF) which removed N-linked glycan chains from the protein. No visible change is noticed in the G protein. The F protein size is reduced by approximately 10 kDa which is consistent with the removal of three N-linked glycan chains from the protein. (B) The action of trypsin on the total and surface expressed F and G proteins of HMPV. Trypsin does not cleave the G protein at all. There is a small proportion of F total and surface protein cleaved by trypsin as shown by the smaller product F_1. F_0 indicates the uncleaved F protein.

(Schowalter et al., 2006b) used PNGaseF to remove all the N-linked glycan chains from the F protein of HMPV (strain CAN97-83) (see Fig 1.13 A). They confirmed that all three N-linked glycan sites are utilized. They also studied the effect of removing the three N-linked glycosylation sites on the cell fusion function of the F protein. When each of the three asparagine residues (at positions 57, 172 and 353) were individually point mutated to alanine, it was observed that the mutation at position 353 reduced cell fusion activity the most whereas the mutation at position 57 reduced cell fusion activity the least. They observed that like other paramyxovirus fusion proteins (Russell and Luque, 2006), the inactive F_0 protein of HMPV needs to be cleaved into its active components F_1 and F_2. They demonstrated the action of trypsin on the total and surface expressed uncleaved F protein (Fig 1.13 B). (Shirogane et al., 2008) managed to propagate HMPV efficiently in Vero cells which constitutively express the serine protease TMPRSS2. Another study attempted to eliminate the dependence of F protein-mediated fusion on trypsin by creating trypsin-independent F mutants (Biacchesi et al., 2006) but found this did not increase virus replication in animal models. It is possible that the HMPV F protein utilizes similar mechanisms for cell entry

as other paramyxoviruses like hRSV which have been well studied (Colman and Lawrence, 2003; Lamb et al., 2006; Russell and Luque, 2006) and referred to as receptor-mediated fusion.

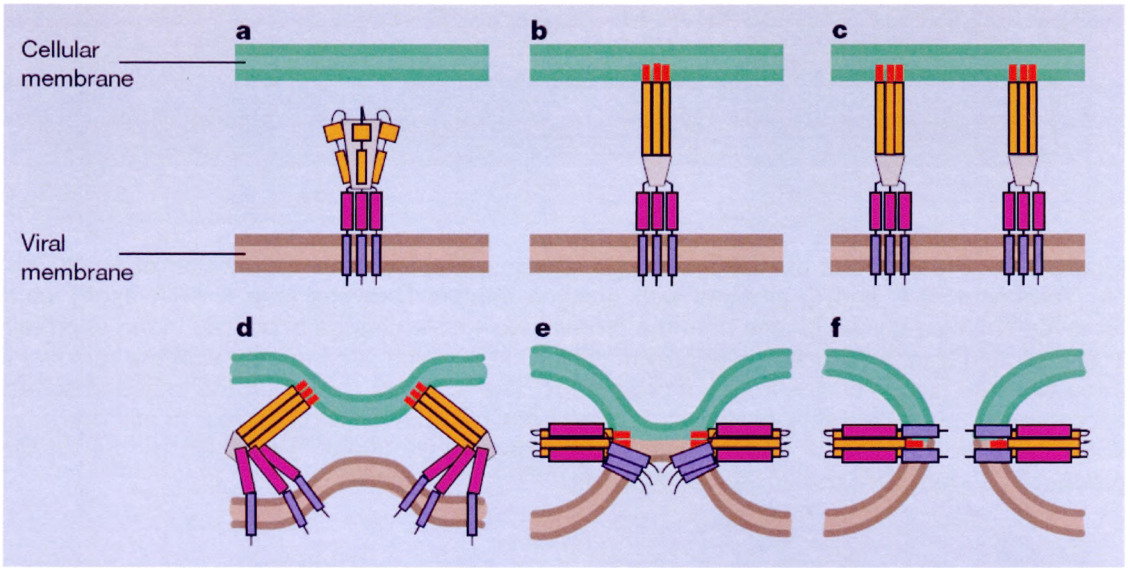

Figure 1.14. Suggested mechanism of paramyxovirus fusion protein action (Jardetzky and Lamb, 2004). (a) The pre-fusion protein generally exists as a trimer in metastable conformation with the transmembrane domain (purple) inserted into the virus envelope. The heptad repeats A (orange) and B (pink) are also shown. The F protein would have been cleaved by a protease to enable proper folding and exposure of the fusion peptide (red). (b) Binding to a host cell receptor by the attachment protein triggers a conformational change in the fusion protein trimer which results in the fusion peptide inserting into the host membrane. (c) Multiple trimers are required to activate the membrane fusion process. (d) The trimers start to fold to a lower energy state and pulls the two lipid membranes towards each other. (e) The two sets of heptad repeats come together forming a restricted hemifusion stalk that allows the lipids in the outer leaflets of the membranes to mix. (f) The folding process is completed forming the most stable form of the fusion protein,with the fusion peptide and transmembrane domain anti-parallel to each other. Only stages (a) and (f) have been observed by crystallography, but the other stages are supported by biochemical data.

Receptor-mediated fusion takes place when the virus is in close proximity to a susceptible host cell. The attachment protein (G) first binds to a cell surface receptor. The mechanism of the action of the G protein is not well understood but probably involves a conformational change in the protein after receptor binding which in turn activates the fusion (F) protein. Thermal energy is also required for fusion. The virus-host cell fusion process (Fig 1.14) is a complex one which consists of several steps. These include: dimpling, lipid stalk formation, hemifusion, transient pore formation and pore enlargement. Since the fusion of two distinct lipid bilayer membranes does not spontaneously occur in nature, the F protein is required to bring about this via

conformational changes. The F protein exists as a trimer under natural conditions. Cleavage of F_0 into F_1 and F_2 are necessary for the subsequent steps. Other well-studied type I viral fusion proteins are the haemaglutinnin (HA) protein from influenza A virus, the gp41 protein from HIV, the S protein from SARS coronavirus and the GP protein of Ebola virus. The pre-fusion form of the F protein (Fig 1.14 a) has been demonstrated in parainfluenza virus 5 (PIV5) by (Yin et al., 2006). The shape of the pre-fusion protein is similar to a mushroom where the stalk is formed by HRB and the transmembrane domain anchors the protein in the lipid membrane. The globular structure is formed by the folded domains of HRA, fusion peptide and the F_2 fragment. At this point the fusion peptide is folded inwards within the globular structure. Slight refolding is triggered by the attachment of the G protein to the surface receptor. The next stage is the formation of the pre-hairpin intermediate (Fig 1.14 b) where the coils of HRA form a triple coiled structure to project the now exposed fusion peptide into the host cell membrane.

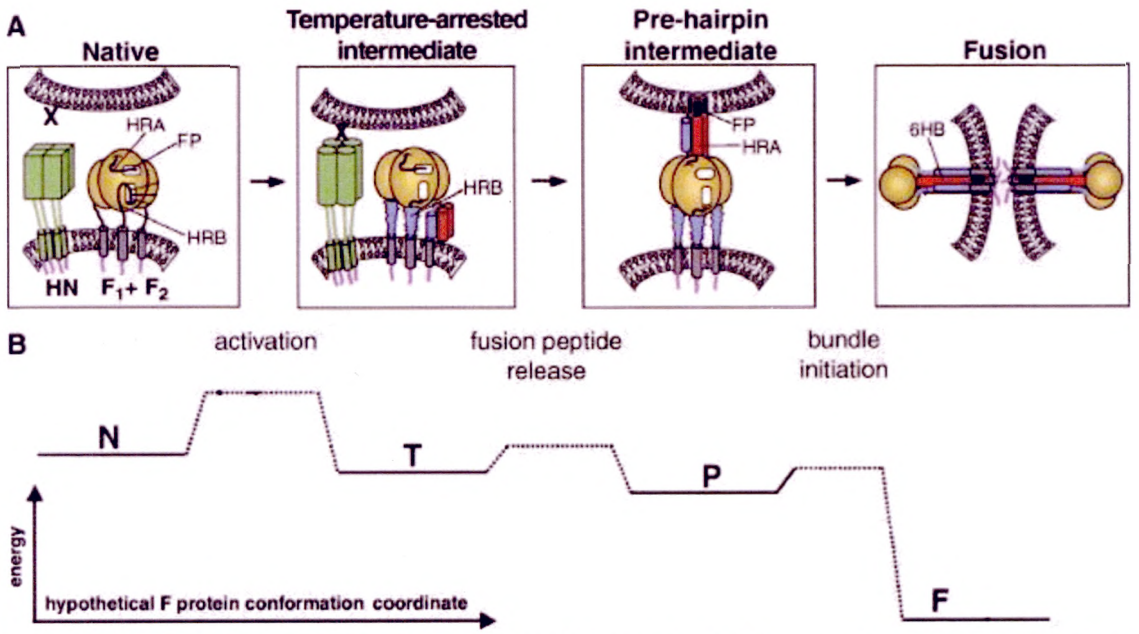

Figure 1.15. A proposed model of the various energy states of the paramyxovirus fusion protein adapted from (Russell et al., 2003). A) The four steps of membrane fusion. FP-fusion peptide, HRA-heptad repeat A, HRB-heptad repeat B, HN-haemagglutinnin neuraminidase, F1 and F2-fusion protein, 6HB-six helical bundle. B) The graph of the energy states of the various fusion intermediates.

The final conformation of the fusion protein is the post-fusion (fusogenic) form (Fig 1.14 f) where the triple coils of HRA and HRB fold towards each other. This action moves the fusion protein into the lowest energy state. A diagram of the various energy states of the trimeric fusion protein is shown in Fig 1.15. The HRB triple coils slot into the grooves formed by the triple coils of HRA to form the six helical bundle (6HB). This 6HB structure was resolved in parainfluenza virus 3 (PIV3) (Yin et al., 2005) and Newcastle disease virus (NDV) (Chen et al., 2001). Both groups of researchers managed to purify soluble forms of the cleaved F protein and found that they spontaneously folded into the post-fusion form. It is possible that the metastable pre-fusion form could be held in place by the presence of the transmembrane region and serve as a source of potential energy which can be released during the folding process (Bissonnette et al., 2009; Waning et al., 2004).

The G protein of HMPV is a type II transmembrane protein. It has a transmembrane region near the N-terminal (Fig 1.16). The G protein is similar in structure to the mucin-like proteins which are a highly glycosylated group of proteins produced by epithelial cells.

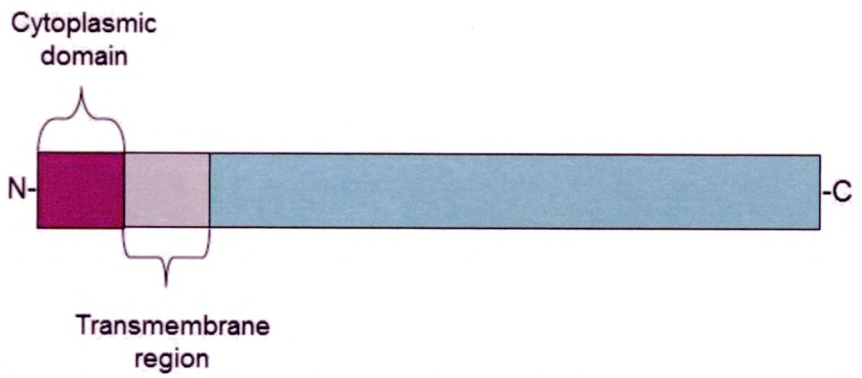

Figure 1.16. Simplified representation of the major domains in the attachment protein of HMPV. N- and C-terminals are shown on the left and right of the diagram respectively. Refer to Chapter 3 for detailed nucleic acid and amino acid sequence.

The nucleotide sequences of G genes are highly variable (Bastien et al., 2004; Biacchesi et al., 2003; Galiano et al., 2006; Peret et al., 2004) with identity between A and B genogroups of only 45-79% compared to 74-100% within the same genogroup. The amino acid sequences between genogroups A and B have only 31-67% identity

compared to 91-100% within the same genogroup. The earliest work to study the characteristics of the G protein was by (Peret et al., 2004). They analysed the G proteins of 25 HMPV isolates and compared them according to their genogroup. The isolates belonging to genogroup A had G proteins that were about 219 amino acid residues in length. G proteins belonging to genogroup B were about 236 residues in length. Althought the nucleic acid and amino acid sequences between genogroups were clearly different, the Kyte and Doolittle (Kyte and Doolittle, 1982) hydrophobicity profiles (Fig 1.17) turned out very similar, especially the position of the transmembrane domain. This suggests that despite the differences in sequence identity and length, the G proteins of both HMPV subgroups probably have the same functional role. It was also determined that the variation of the G protein is not significantly due to repeated passage of the virus through cell culture. (Bastien et al., 2004) compared both subgroups of HMPV G protein by Western blot (Fig 1.18).

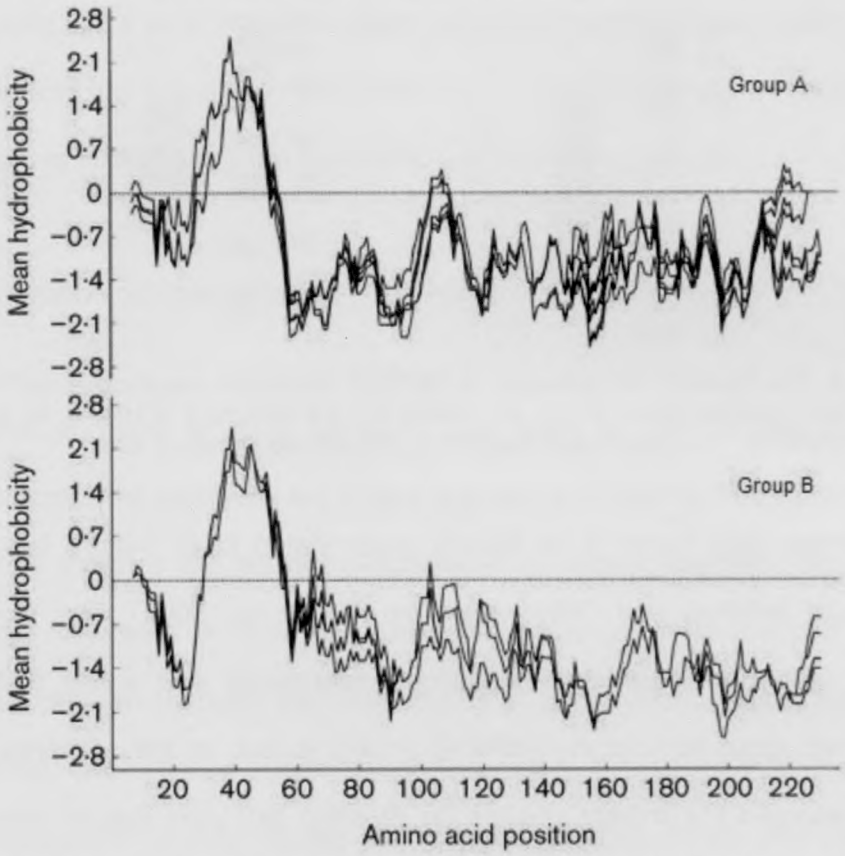

Figure 1.17. Kyte and Doolittle hydropathy plots for the G proteins of HMPV subgroups A and B adapted from (Peret et al., 2004). Hydrophobic regions are plotted above the horizontal axes. Hydrophilic regions are plotted below the horizontal axes. The horizontal scale indicates the amino acid positions of the proteins. The proposed transmembrane domain (approximately positions 30 to 55) corresponds to the area of high hydrophobicity. The cytoplasmic tail is from position 0 to 30. The external domain is from position 55 onwards.

The G protein from the A genogroup produced a different pattern on Western blot from the G from the B genogroup (Bastien et al., 2004) which seems to indicate that the glycosylation characteristics between genogroup A and B are very different (Fig 1.18). Both G proteins were noted to run at a much larger size than the expected 25-27 kDa. The subgroup A protein exhibits a protein smear between 60-80 kDa and another product at 50 kDa. The subgroup B protein shows a protein smear between 45-60 kDa. (Schowalter et al., 2006b) also analysed the G protein of Canadian HMPV strain CAN 97-83 which belongs to the A subgroup. They found that the G protein expressed on the cell surface showed a smear of size 60-70 kDa and a minor band at 45 kDa (Fig 1.13 B). This profile is similar to that observed in Fig 1.18.

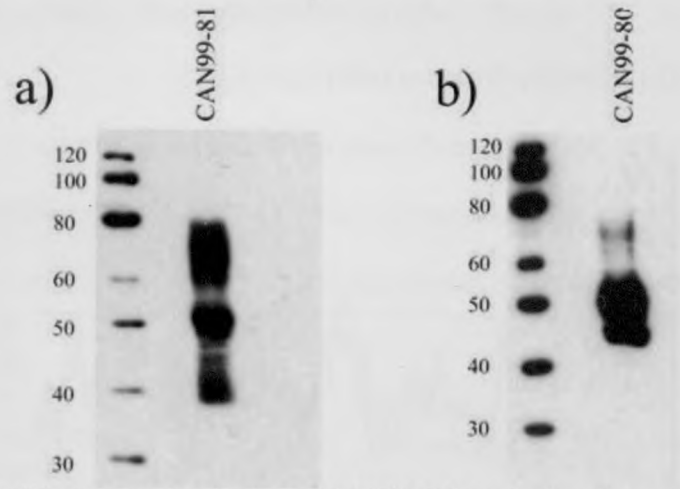

Figure 1.18. The Western blot detection of HMPV G from both subgroup A and B. Photograph modified from (Bastien et al., 2004). a) CAN99-81 is a subgroup A HMPV. b) CAN99-80 is a subgroup B HMPV. The protein size markers on the left are shown in kDa.

The G protein was found to be heavily glycosylated in its mature form due to the presence of N-linked and O-linked sugars (Liu et al., 2007). The same group of scientists also performed deglycosylation experiments and found that the smear observed at about 90 kDa in HMPV G protein is due to the presence of O-linked glycans, whereas the smaller species on Western blot were due to various N-linked glycosylated forms of G protein. A study using deletion mutants of G protein resulted in reduced virus replication in hamsters (Biacchesi et al., 2004) but also suggested that the F protein and not the G protein was an essential component of virus replication.

Another work suggested that the G protein interacts with glycosaminoglycans as part of their attachment strategy (Thammawat et al., 2008). The authors found that the HMPV G protein interacts with heparin and treatment of HEp-2 cells with soluble heparin reduces the infectivity of HMPV. This heparin-binding phenomenon has been observed in experiments involving the closely-related hRSV (Feldman et al., 1999; Shields et al., 2003). (Wyde et al., 2004) experimented with heparin as a potential anti-viral against HMPV and noted that it had similar activity against hRSV but not against parainfluenza virus type 3 nor measles virus. Few detailed structural studies on paramyxovirus attachment proteins have been performed. One of them involved the haemagglutinnin-neuraminidase (HN) protein of PIV5 by (Yuan et al., 2005). They found that the HN protein exists in the form of a tetramer and that the N-terminal stalk was essential for maintaining this tetrameric structure. Changes in the C-terminal domain of the HN protein after receptor binding may be the trigger or signal for the F protein to initiate fusion. This may serve as a model for HMPV G protein binding action. HMPV F and G protein interaction has not been studied but this could prove useful in understanding the mechanism of HMPV entry into host cells.

1.13 Glycosylation of virus proteins in mammalian and insect cells

Some proteins encoded by virus genomes are found on the surface of the viral envelope. Examples of these are the F and G proteins of HMPV. The mature form of these envelope proteins are usually glycosylated to varying degrees. Glycosylation refers to sugar molecules or chains covalently bound to certain amino acid residues. Viral envelope proteins undergo two major types of glycosylation: N-linked (reviewed by (Elbein, 1991) and O-linked glycosylation (reviewed by (Van den Steen et al., 1998). N-linked glycosylation occurs at the asparagine residues which are part of an asparagine-X-serine/threonine (N-X-S/T) motif (refer to Fig 1.19). HMPV F has three of these N-X-S/T motifs: N57 in the F2 fragment, N172 and N353 in the F1 fragment. There are generally three varieties of N-linked glycosylation side chains in mammalian

cell systems: the immature (high mannose), mature (complex) or hybrid type, and these are usually indicative of the different levels of processing.

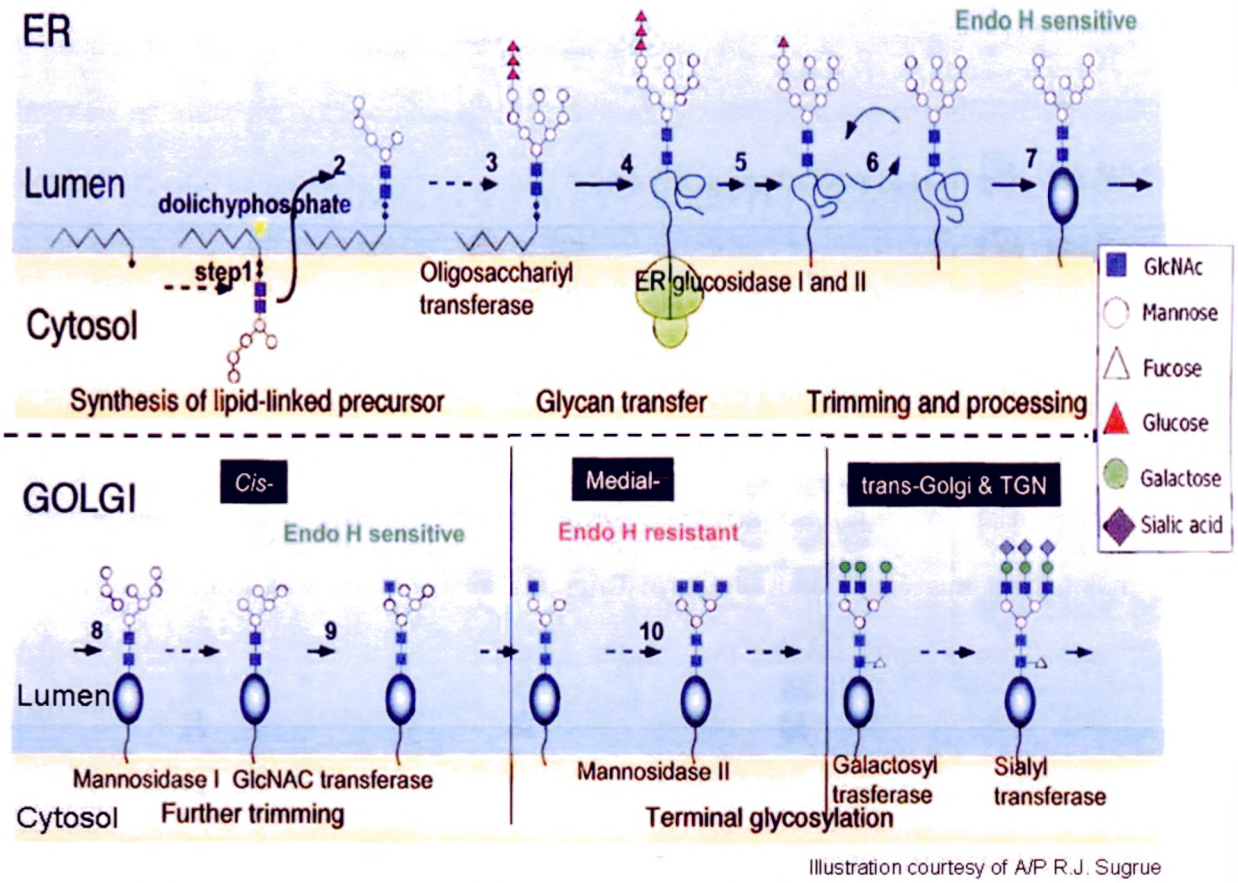

Illustration courtesy of A/P R.J. Sugrue

Figure 1.19. Illustration of the process of N-linked glycosylation of proteins in mammalian cells. The ER is the location of the start of synthesis. This begins when the first N-glycan chain is linked to a lipid-based molecule (dolichol phosphate) found within the membrane of the ER. The addition of the first N-glycan chain of 5 mannose and 2 N-acetylglucosamine molecules ($Man_5GlcNAc_2$) occurs on the cytosolic side of the ER. The N-glycan chain then flips into the lumen of the ER where the size of the N-glycan chain is gradually increased to the $Glc_3Man_9GlcNAc_2$ precursor form. The precursor form is then transferred to an appropriate asparagine residue in the growing polypeptide chain by an oligosaccharyl transferase enzyme. The glucose molecules are gradually removed by glucosidases in the ER as the synthesis of the protein is completed and transits from the ER to the Golgi. Once the glucose molecules are removed, the N-glycan chain is considered to be the high mannose form. Within the cis-Golgi, mannosidase enzymes further trim the N-glycan chain to leave a shorter intermediate ($Man_5GlcNAc_2$) form. A transfer of a single N-acetylglucosamine molecule to the α1-3 branch mannose chain results in a hybrid ($GlcNAcMan_5GlcNAc_2$) form. The hybrid and high mannose N-glycans are susceptible to cleavage by endoglycosidase H (EndoH). In the medial Golgi, additional trimming and processing of the N-glycan chain results in the core $Man_3GlcNAc_2$ that can possess 2-4 chains of N-acetylglucosamine. The N-glycan chain is now in the complex form. Finally in the trans-Golgi, additional molecules of galactose (Gal) or N-acetylgalactosamine (GalNAc) and sialic acid are added to the chains. Occasionally, fucose sugars are added to the N-glycan chain at the first N-acetylglucosamine residue.

Initiation of N-linked glycosylation takes place in the endoplasmic reticulum (ER) when a precursor complex of 3 glucose, 9 mannose and 2 N-acetylglucosamine molecules ($Glc_3Man_9GlcNAc_2$) are linked to an asparagine residue.

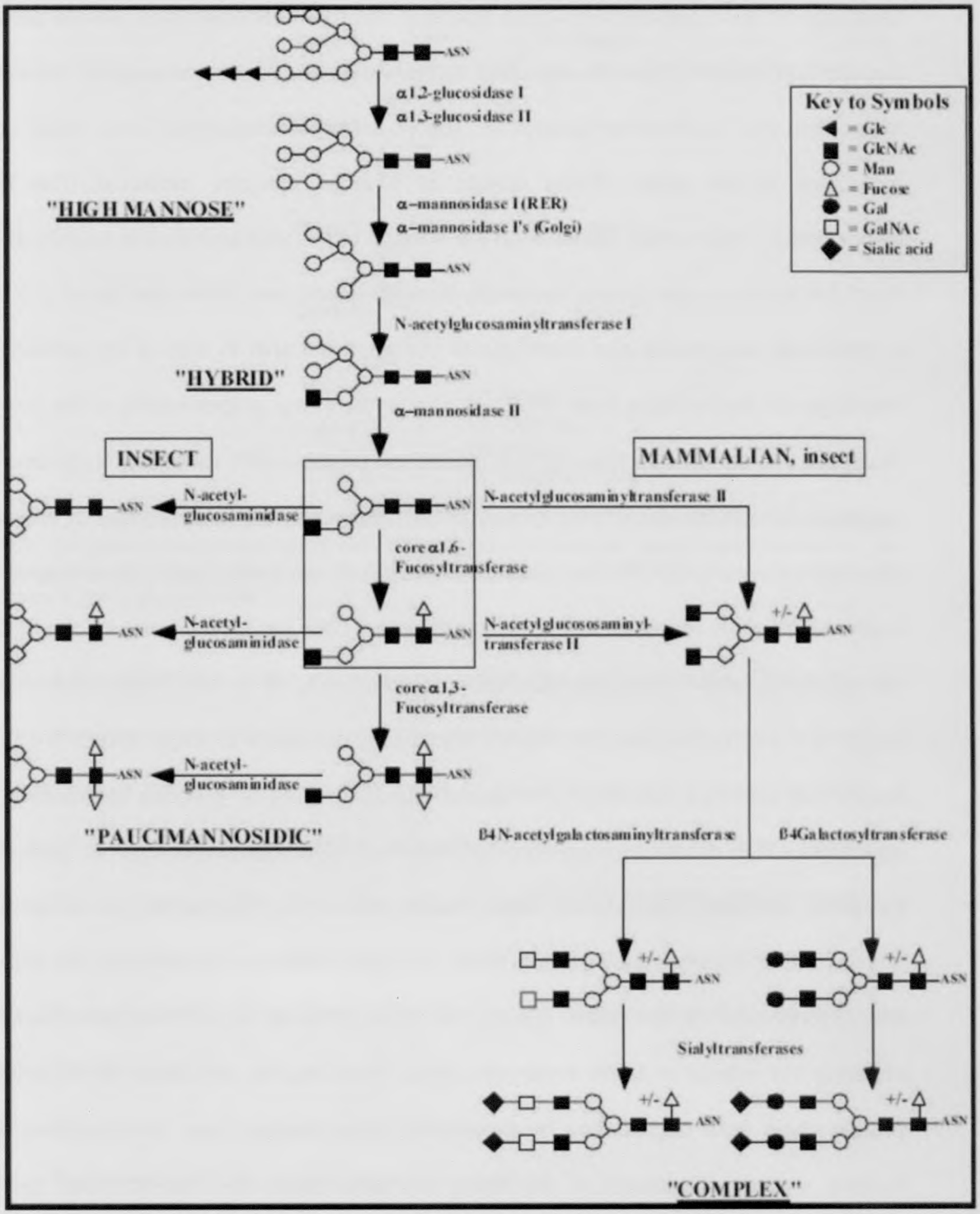

Figure 1.20. Illustration of the differences in the N-linked glycosylation pathways of insect and mammalian cells (Shi and Jarvis, 2007). The formation of high mannose and hybrid chains have been shown together with the associated enzymes. The square box indicates the $GlcNAcMan_3GlcNAc_2$(±α1-6Fucose) intermediate. Insect cells produce N-acetyl glucosaminidase which trims the terminal GlcNac leaving the $Man_3GlcNAc_2$(Fucose) structure known as paucimannose. A second fucose molecule may be added to the α1-3 site of the first GlcNAc molecule. Mammalian cells, on the other hand, add another GlcNAc via N-acetylglucoaminyl transferase II to produce the first complex N-glycan chain. Subsequent enzymatic additions of galactose (Gal) or N-acetyl galactosamine (GalNAc) followed by terminal sialic acid molecules complete the N-glycosylation pathway.

Cleavage of the 3 glucose molecules results in the high mannose form. As the protein transits from the endoplasmic reticulum to the Golgi, sequential cleavage of mannose molecules and addition of galactose (or N-acetylgalactosamine) and sialic acid molecules to the sugar chains results in a large complex molecule. The final glycosylated protein which appears on the surface of the viral envelope is usually made up of 2-4 mature sugar chains. Generally these N-linked side chains are about 2-3 kDa in molecular weight and can contribute to the apparent shift in size of the protein. N-linked glycan chains have been shown to play a role in the proper folding of the protein molecule (Parodi, 2000). Experiments based on proteins with defective N-glycans do not pass through the secretory pathway.Within the insect cells, the process of N-linked glycosylation is slightly different (refer to Fig 1.20). The initiation and processing of the N-glycan chain is identical to that in mammalian cells up to the point of the hybrid $Man_5GlcNAc_2$ and $GlcNAcMan_3GlcNAc_2$ intermediates. It is after this intermediate stage that the mammalian and insect processing pathways diverge. Insect N-glycan chains will undergo trimming by N-acetyl glucosamidase to produce paucimannose structures. The most common form of O-linked glycosylation occurs at serine or threonine residues. Sometimes these modifications are referred to as mucin-type glycosylations because they are thought to be responsible for the formation of mucus-like glycoprotein layers (also known as mucoproteins or mucopolysaccharides) covering the outside of some eukaryotic cells. These mucins are known to protect the protein chain from degradation by proteases. Other studies have demonstrated that mucins are also important in protecting the virus from the host immune system (Rawling and Melero, 2007; Sugrue, 2007).

These are generally formed by an N-acetylgalatosamine linked to a serine or threonine residue in the Golgi which in turn is bonded to a combination of galactose, N-acetylglucosamine or sialic acid molecules in a sequential reaction (see Fig 1.21).

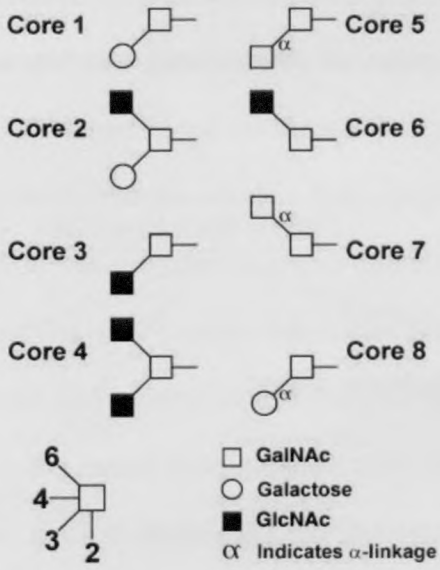

Figure 1.21. Illustration of the 8 possible core structures for O-glycan chains (Jensen et al., 2010). Linkages not indicated by "α" are "β" linkages. The linkage position and numbering can be referred to the icon in the lower left corner. Gal-galactose, GalNAc-N acetylgalactosamine, GlcNAc-N acetylglucosamine.

O-linked glycosylations, unlike the N-linked variety, are highly variable. They generally do not give rise to predictable sugar chain composition and this can result in a myriad of glycoprotein forms. Even though a single O-glycan chain has a molecular mass of less than 1 kDa, the sheer number of possible sites for O-linked side chains in a transmembrane protein can result in a shift in size from 10-100 kDa. The G protein in HMPV has between 4-6 possible sites for N-linked glycans but approximately 10-12 times the number of O-linked sites (estimated by the number of serine and threonine residues in the protein).

1.14 Baculovirus and its derived expression system

Baculovirus belong to the baculoviridae family of insect viruses which naturally infect larvae of the lepidopteran (butterfly and moth) order of insects. Baculoviruses are divided into 3 main genera (Fig 1.22). Genus A viruses are also known as nuclear polyhedrosis viruses (NPV). Genus B viruses are also known as granulosis viruses (GV). Genus C viruses are also known as the non-occluded viruses. The NPV are further divided into 2 main groups known as the singly-enveloped nuclear polyhedrosis

viruses (SNPV) and multiply-enveloped nuclear polyhedrosis viruses (MNPV). SNPVs only have one viral capsid per virion unlike MNPVs which can have multiple viral capsids per virion.

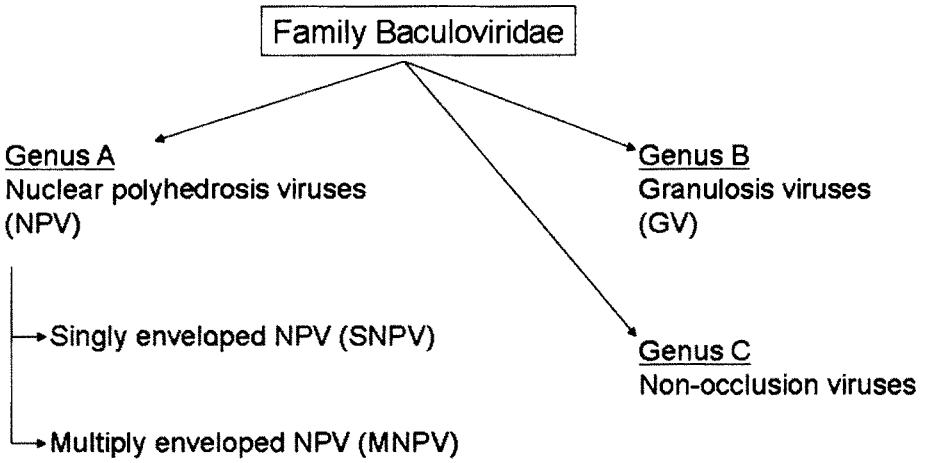

Figure 1.22. Classification of the Baculoviridae family of viruses and its three genera.

The virus used in this study is derived from the *Autographa californica* (alfalfa looper) multiply-enveloped nuclear polyhedrosis virus (AcMNPV). The size of the virus capsid ranges from 30-50 nm. The virus genome is composed of circular double-stranded DNA which is approximately 130 kb long. The virus life cycle is divided into 2 main phases (Fig 1.23): the occluded virus (OV) and the budded virus (BV) phases. These 2 phases are also known as primary and secondary infection. The BV form of the virus consists of the viral DNA encased in a capsid which is surrounded by a lipid envelope derived from the host cell. The lipid envelope contains the GP64 protein which is known to be involved in fusion with uninfected cells (Monsma et al., 1996) via attachment to cell surface receptors (Westenberg et al., 2007). Once the BV fuses with the new cell membrane, it is endocytosed. Cellular endosomes fuse with the BV endosome under acidic conditions to release the viral capsid into the cytoplasm. The viral capsid moves into the nucleus where the viral DNA is released and transcription initiates. Within the nucleus, replication of the virus occurs and this produces more viral capsids which exit the nucleus and bud out from the cell membrane to form progeny BV particles. The OV form of the virus contains the same basic BV form enclosed in a

polyhedron (PH) matrix. This matrix is resistant to environmental stress like heat and light allows the OV particle to remain on plant leaves for extended periods of time until other insect larvae ingest the OV forms found on the leaves. In the insect gut, the OV form loses the polyhedron matrix due to the alkaline lysis, thus releasing the occlusion derived virions (ODV). The ODV fuse with the columnar epithelial cells and release the viral capsid into the cytoplasm. The viral capsids can either proceed to the nucleus for viral replication or be transported to the basal side of the cell membrane to bud out into BV forms. The infected cells in the insect midgut do not develop OV forms. In the early stage of infection (0-12 hours), there is increasing cell activity as the virus prepares for replication as the growth and division of the cell rapidly ceases. The BV forms can be detected from 6-36 hours post-infection. This is known as the late stage of infection. During this stage, the cell nuclei can be seen to be enlarged. The OV forms start to appear from 24 hours onwards only during the very late stage of secondary infection. It is during this stage that the cells start to die and lyse. Upon cell lysis, the accumulated OV forms are released into the environment.

Cell lines from *Spodoptera frugiperda* (fall armyworm) can be used to grow and amplify the virus particles. Two common variants of these cell lines are Sf9 and Sf21. These cells can be grown as adherent cells in standard tissue culture flasks or as a suspension in shaking flasks. They have a round shape with a distinctive clear halo surrounding the cell when viewed under a microscope. Another cell line is from *Trichoplusia nii* (alfalfa looper), usually known as High Five cells. These cells are usually used for high level of protein expression and can only be grown adhered to tissue culture flasks. These cells have polygonal shape like some mammalian cell lines.

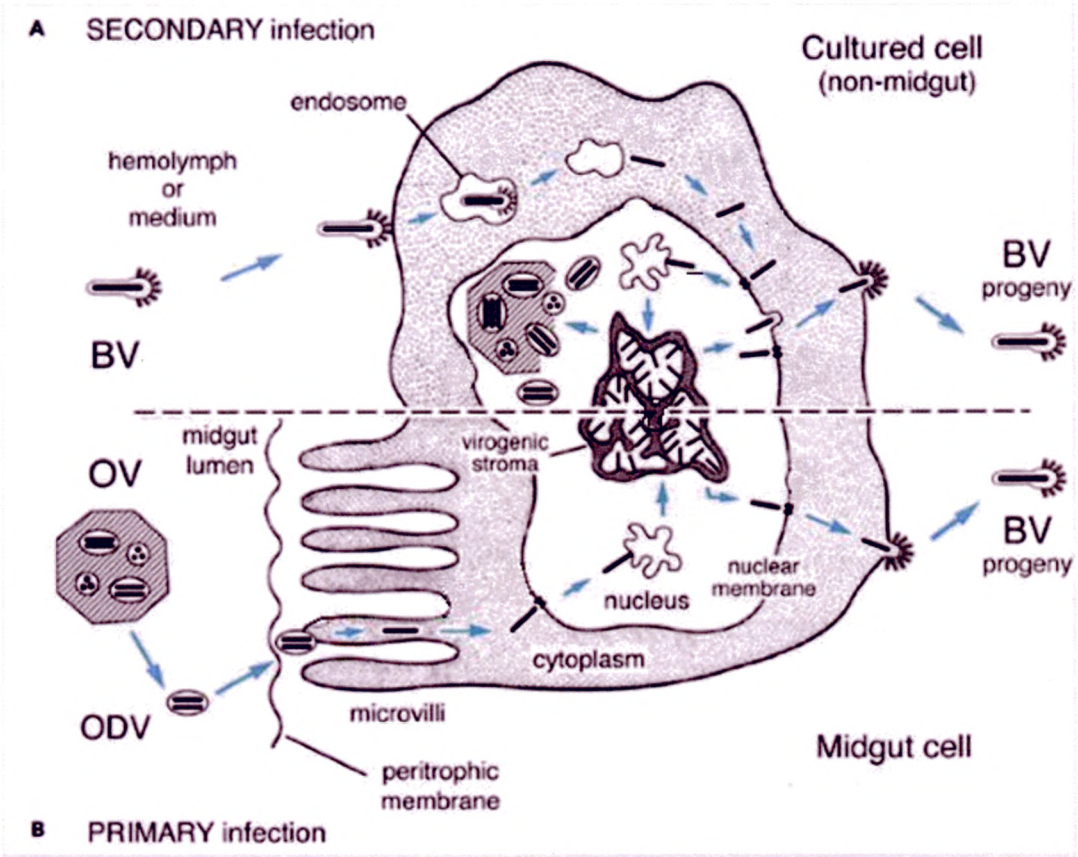

Figure 1.23. Illustration of baculovirus life-cycle from Fields Virology (Fields et al., 2007). Both primary infection (B) and secondary infection (A) processes are shown. The primary infection begins with the OV form of the virus in the midgut and this occurs when the insect larvae ingest the OV particle. The secondary infection begins with the BV form and is a result of cell-to-cell spread of the virus in culture or non-gut cells of insects.

Some of the genes in AcMNPV are non-essential for infection and replication in host cells. Two of these genes: the polyhedron (PH) gene and p10 protein gene can be replaced with foreign gene sequences of various proteins of interest to allow the recombinant expression of proteins driven by the strong PH and p10 gene promoters (Condreay and Kost, 2007). A major advantage of using baculovirus expression systems is that they are extremely safe since there is no possibility that humans can be infected by baculovirus. In addition, protein expressed in baculovirus can undergo post-translational modification unlike in prokaryotic systems which do not modify recombinant expressed proteins. However, some of the post-translational modifications, like N-linked glycosylation, which occur in baculovirus are somewhat different from that in mammalian cells. This has already been discussed in the previous section.

1.15 Development of anti-virals, vaccines and virus-like particles

There is a need to develope vaccines against HMPV because of the impact of HMPV infection on vulnerable groups like the young, the elderly and the immunocompromised. Early attempts at producing a vaccine used the strategy of immunizing cotton rats (Yim et al., 2007) and macaques (de Swart et al., 2007) with formalin-inactivated virus. Unfortunately, in both instances, the animals pre-exposed to formalin-inactivated virus developed serious secondary hypersensitivity reactions when challenged subsequently with the same live virus which resulted in significant respiratory tissue damage. These cotton rats developed pneumonitis and alveolitis. These macaques developed tracheo-bronchitis and alveolitis. The results of these experiments ruled out the use of formalin-inactivated virus for human use. In the 1960s, similarly prepared vaccines for hRSV and measles virus resulted in severe pulmonary disease (Fulginiti et al., 1967) and the death of two children (Kim et al., 1969) due to a similar hypersensitivity reaction. Experiments on cotton rats with formalin-inactivated parainfluenza 3 virus also triggered hypersensitivity (Ottolini et al., 2000). Other alternative strategies for vaccine production were studied. Live, attenuated vaccines (reviewed by (Buchholz et al., 2006) involving the deletion of G, M2-2 protein or substitution of the P protein have been tested with promising results. Another option is the production of a chimeric protein from parainfluenza 3 virus and HMPV F protein which has been shown to work well in animals (Tang et al., 2005). Ryder and colleagues studied the possibility of using the secreted ectodomain of HMPV G protein as vaccine in cotton rats (Ryder et al., 2010) but concluded that even though there were high levels of antibodies produced against HMPV G, they were not protective against repeat virus challenge. (Deffrasnes et al., 2008b) screened over 200 synthetic molecules and shortlisted two siRNA molecules which showed good activity in inhibiting HMPV replication. One siRNA molecule targets the N protein mRNA while the other targets the P protein mRNA. These two siRNA molecules seemed to work even if there were one or two mismatches in the sequences. (Miller et al., 2007) attempted to

construct peptide inhibitors against the heptad repeat regions of the HMPV F protein. They made analogues to the heptad repeat regions A and B which had high thermal stability and could bind to the virus heptad repeats to prevent the natural formation of the six helical bundle of the virus fusion protein thereby preventing virus-host cell fusion (Fig 1.24). (Deffrasnes et al., 2008a) also constructed peptide inhibitors to the heptad repeat regions and found one of their molecules to be highly effective at reducing viral loads in the lungs of test animals.

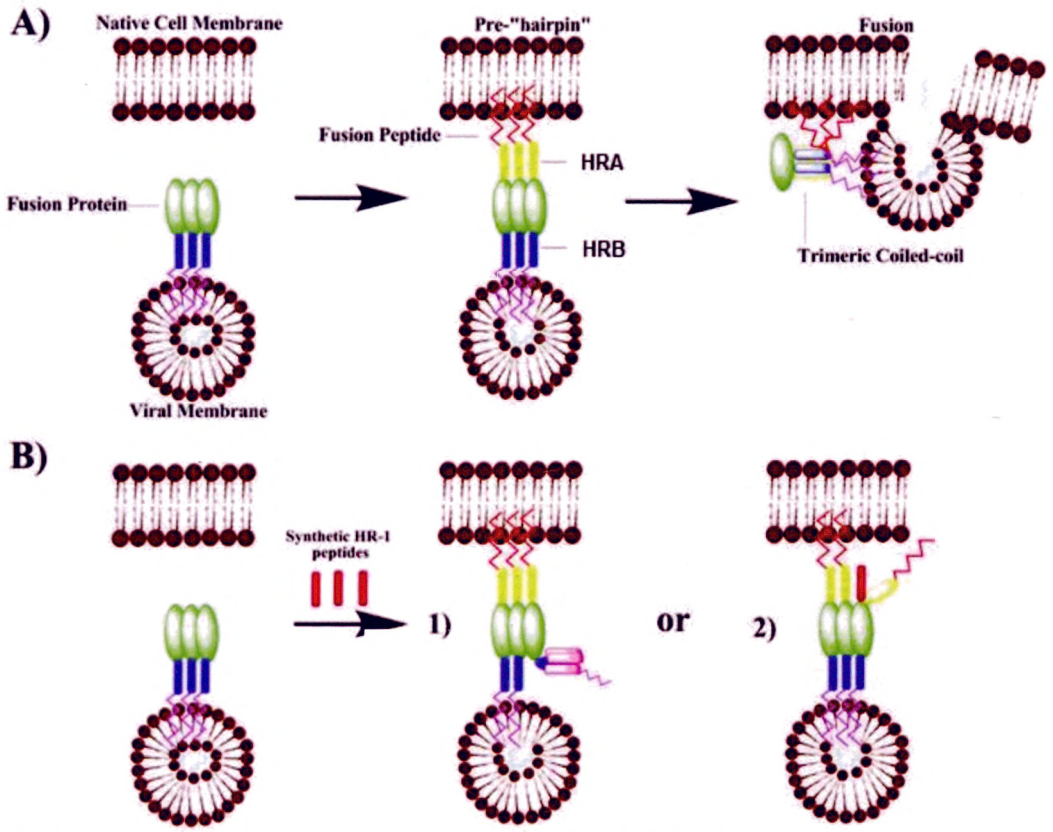

Figure 1.24. Illustration of the action of the fusion protein of HMPV in the absence and presence of fusion inhibitors from (Miller et al., 2007). (A) The normal process of virus-host cell fusion triggered by the fusion protein. The fusion peptide extends into the host cell membrane followed by the conformational change in the fusion protein which results in the overlapping of the two heptad repeat regions (HRA,HRB) to form the coiled coil structure to bring about the fusion of the virus and host cell membranes. (B) The presence of synthetic HRA peptides can interfere with this process by (1) forming a trimer and competitively binding the HRB region or (2) displacing the normal HRA and preventing the fusion peptide insertion.

(Wyde et al., 2003) experimented with ribavirin (a licensed anti-viral compound used to treat serious hRSV infections), immune globulin designed for intravenous use (i.v.IG) and palivizumab (humanized monoclonal antibody against hRSV) against hRSV and HMPV in tissue culture cells. Both ribavarin and i.v.IG were able to reduce hRSV and

HMPV titres equally. However, ribavarin is known to have many side-effects which may outweigh its beneficial uses (NLM, 2010). (Hamelin et al., 2006) also tested the effect of ribavirin and glucocorticoid on HMPV-infected BALB/c mice. They found that ribavirin was effective in reducing the viral load and inflammation in the mice whereas glucocorticoid was only effective in reducing inflammation. Another compound known as NMSO3 was tested on tissue culture cells infected with HMPV (Wyde et al., 2004). This compound was previously found to be effective at inhibiting hRSV-infected cotton rats and tissue culture cells (Kimura et al., 2000). NMSO3 was able to inhibit replication in HMPV-infected cells specifically during the virus attachment and penetration phases. This observation is interesting considering that a later work by (Kimura et al., 2004) found that NMSO3-resistant hRSV strains carried mutations in the G protein implying that the mechanism of action of NMSO3 may be the interference of host-virus interaction.

Virus-like particles (VLPs) are artificially synthesised virus shells lacking the genes within the viral capsid. The complexity of the live virus will have an impact on the complexity of synthesis (Noad and Roy, 2003). Non-enveloped viruses are the least complex because they usually only require one or two major capsid proteins to form a viral capsid structure. VLPs of enveloped viruses are more challenging to produce because they contain additional transmembrane proteins in the envelope. In paramyxoviruses, VLPs can be produced by the transfection of 3-4 plasmids into a permissive cell line. The plasmids are expression vectors compatible to the cells used and fused with a viral protein gene which is known to be essential for viral capsid synthesis. The viral protein genes transfected normally include those for the nucleoprotein, matrix protein and fusion and/or attachment protein. VLPs have been made from parainfluenza 1 virus (Coronel et al., 1999) using nucleoprotein and matrix protein; from simian virus 5 (SV5) (Schmitt et al., 2002) and Newcastle disease virus (NDV) (Pantua et al., 2006) using nucleoprotein, matrix protein, haemagglutinnin/neuraminidase protein and fusion protein; from Nipah virus (NiV)

(Patch et al., 2007) using nucleoprotein, matrix protein, fusion protein and attachment protein. Other than the work on NDV, all the other three virus proteins were expressed in HEK 293T cells using the pCAGGS vector. Since VLPs do not contain any viral genomic information, they are non-infectious, yet have been shown to elicit very good immune responses via the cellular and humoral pathways (Tacket et al., 2003) and have been demonstrated to be more immunogenic than monomeric proteins (Tamminen et al., 2012). In addition, VLPs can be applied to vaccine production (Madhan et al., 2010), virus structural studies, replication mechanisms and drug delivery mechanisms. So far, the only baculovirus-derived VLP vaccine approved for human use is the the Cervarix vaccine (Harro et al., 2001) against human papillomaviruses. It is a relatively simple VLP vaccine consisting of one structural viral protein and it remains to be seen if more complex VLPs can be applied just as successfully.

1.16 Aims of this research project

The aims of this research project are:

1) To determine the prevalence of HMPV in Singapore children admitted to hospital for respiratory symptoms and to screen patient specimens for the presence of other newly discovered or less commonly detected respiratory viruses.
2) To study the interaction between the fusion and attachment proteins of selected clinical HMPV isolates by expressing the proteins in tissue culture cells and to assess the role of certain domains of the fusion and attachment proteins by mutation studies.
3) Compare the characteristics of expressed HMPV fusion and attachment proteins in insect cells to those of mammalian cells.

4) To investigate the possibility of producing virus-like particles in both mammalian and insect tissue culture cells with the intention to applying them to the production of vaccines for humans or antibodies for routine diagnostic use.

Chapter 2. Materials and Methods

2.1 Collection and screening of clinical specimens

2.1.1 Ethics approval for the use of patient specimens

Prior to the commencement of the research project, written approval of the Institutional Review Board (IRB) of KKH was sought for the collection of 200 patient specimens for screening for HMPV. This figure was later revised upwards to 500 patient specimens. The IRB is responsible for overseeing the ethical aspects of research done in KKH. In order to receive IRB approval, the main condition which needed to be met was that specimens had to be anonymised and given a unique identifier, and therefore cannot be used to trace any information about the original patient. The IRB approval number is EC/043/2004.

2.1.2 Collection of specimens

Clinical specimens used for the study were derived from nasopharyngeal swabs (Copan, Italy). These swabs (Fig 2.1) consist of a thin aluminium shaft with a Dacron tip which can be transported in a sponge soaked in virus maintenance media containing the antibiotic gentamicin and the antifungal amphotericin B. The swab must be gently inserted into the nostril and slowly pushed inward until the tip contacts the inner wall of the nasopharynx. The swab must be left for a few seconds, or rotated gently, then slowly withdrawn and placed into the transport tube. Specimens for this study were collected by the ward staff and dispatched to the microbiology laboratory for routine screening of respiratory viruses.

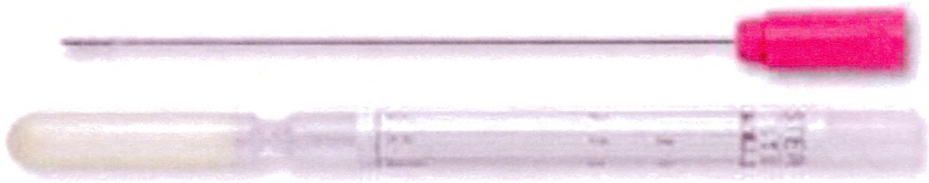

Figure 2.1. Nasopharyngeal swab used for obtaining samples from patients.

2.1.3 Screening for common respiratory viruses

Upon arrival in the laboratory, the nasopharyngeal swabs were vortexed in a capped 15 ml tube containing 0.5 ml of phosphate-buffered saline (PBS) to dislodge the nasopharyngeal cells. The resulting cell suspension was then applied to a Teflon-coated 12-well slide for air-drying in a biosafety cabinet followed by fixing in cold acetone. The fixed cells were then air dried and overlaid with a commercial screening reagent (D3 Ultra Respiratory Virus Screening Kit, Chemicon-Millipore, USA) for the detection of antigens of 7 common respiratory viruses: hRSV, influenza A and B virus, parainfluenza 1, 2 and 3 virus and adenoviruses. The slides with reagents were incubated at 37°C for 15 minutes in a humid container. After incubation, the slides were washed in a shaking tray of PBS for 5 minutes. After washing, the slides were air-dried again before mounting with buffered glycerol and a coverslip. The slides were examined under a fluorescence microscope (Leica DMLB, Leica, Germany) with a FITC filter. Specimens which showed a positive result for the presence of any of the 7 respiratory viruses would contain "apple-green" fluorescent cells (Fig 2.2) under light of wavelength 480 nm. The positive sample can next be tested against individual antibody reagents to confirm the identity of the viral pathogen.

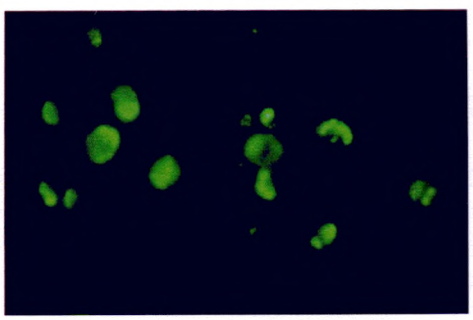

Figure 2.2. Photograph of clinical sample positive for influenza B. The nasopharyngeal cells were stained with specific antibodies for influenza B.

2.2 Nucleic acid detection of other respiratory viruses

2.2.1 Extraction of viral nucleic acids from specimens

The starting material for nucleic acid extraction was 140 µl of the nasopharyngeal cell suspension in PBS. The Viral RNA Mini Kit (Qiagen, Germany) was used according to the manufacturer's instructions. Briefly, the volume of cell suspension was mixed with 560 µl of AVL buffer in a microcentrifuge tube and incubated at room temperature for 10 minutes. Next, 560 µl of absolute ethanol was added to the tube and the entire solution was spun through a column to bind the nucleic acids. The column was then washed by spinning through consecutively with 500 µl of two wash buffers (AW1 and AW2). After a final spin-dry at maximum speed, the nucleic acids were eluted with 60 µl of RNase-free water. The nucleic acid extracts were stored at -80°C until ready for use.

2.2.2 Detection of human metapneumovirus

Detection of human metapneumvirus RNA was carried out by real-time RT-PCR based on the protocol by (Maertzdorf et al., 2004). The amplification target was the nucleoprotein (N) gene of HMPV and this was determined to be a consensus region within the 2 main serogroups and 4 subserogroups. The reagents were from the OneStep RT-PCR kit (Qiagen, Germany) and prepared according to the manufacturer's instructions. The amplification reactions were run on a RotorGene 3000 instrument (Corbett Research, Australia). The amplification conditions and primer/probe sequences are shown below:

Forward primer, NLN-F:	5'-cat ata agc atg cta tat taa aag agt ctc-3'
Reverse primer NLN-R:	5'-cct att tct gca gca tat ttg taa tca g-3'
Probe, NLN-P:	FAM 5'-tgy aat gat gag ggt gtc act gcg gtt g-3' TAMRA

Reverse transcription	50°C for 30 min	
Initial denaturation	95°C for 15 min	
Denaturation	95°C for 20 s	}
Annealing/extension	60°C for 60 s	}45 cycles, detection at FAM channel

Samples that showed the characteristic amplification curve were regarded as positive for HMPV and the cycle threshold (Ct) values were recorded.

2.2.3 Detection of human bocavirus

The RNA extracts were also screened for the presence of human bocavirus (HBoV) according to the protocol by (Sloots et al., 2006a) which used conventional PCR followed by agarose gel electrophoresis to target part of the NS1 gene of HBoV (see primers and conditions below). Platinum Taq DNA polymerase Kit (Invitrogen, USA) was used. Amplified DNA fragments (290 bases) from HBoV-positive samples were purified and extracted (refer to section 2.3.2) and confirmed by sequencing using the same primers for PCR (Tan et al., 2009b).

Forward primer, HBoV01.2: 5'-tat ggc caa ggc aat cgt cca ag-3'
Reverse primer, HBoV02.2: 5'-gcc gcg tga aca tga gaa aca ga-3'

Reverse transcription	50°C for 20 min	
Initial denaturation	95°C for 15 min	
Denaturation	94°C for 20 s	}
Annealing	56°C for 20 s	}45 cycles
Extension	72°C for 30 s	]

2.2.4 Detection of human coronavirus

Detection of human coronavirus (HCoV) was performed by SYBR-green real-time RT-PCR according to (Escutenaire et al., 2007) which targets the orf 1b region of HCoV. The SYBR-Green RT-PCR kit (BioRad, USA) was used in conjunction with the i-Cycler (BioRad, USA). Only samples which showed the characteristic amplification curve and a melting temperature (Tm) of between 75.5°C and 80.8°C were classified as positive for HCoV. Amplified DNA fragments (179 bases) from HCoV-positive samples were purified by agarose gel extraction (refer section 2.3.2) and confirmed by sequencing using the same primers for PCR (Tan et al., 2009b).

Forward primer, 11-FW:	5'-tga tga tgs ngt tgt ntg yta yaa-3'	
Reverse primer, 13-RV:	5'-gca twg trt gyt gng arc ara att c-3'	
Reverse transcription	50°C for 40 min	
Initial denaturation	95°C for 5 min	
Denaturation	94°C for 40 s	}
Annealing	50°C for 40 s	}50 cycles
Extension	72°C for 40 s	]
Melt curve analysis	95°C for 1 min 55°C for 45 s 0.5°C increments to 95°C	

2.2.5 Detection of human rhinovirus

Detection of human rhinovirus (HRV) was carried out by RT-PCR according to the method by (Hayden et al., 2003). The target is the 5' untranscribed region of the virus genome. A combination of Superscript reverse transcriptase/Platinum Taq (Invitrogen, USA) reagent was used and the reaction was performed on a LightCycler instrument (Roche Diagnostics, Germany). Serotyping of the various HRV isolates was based on a previous publication (Tan et al., 2009a).

2.3 Analysis of amplified viral genes

2.3.1 Amplification of HMPV genes

The nucleoprotein (N), phosphoprotein (P), matrix (M) protein, fusion (F) protein and attachment (G) protein of all HMPV isolates were subjected to RT-PCR using the OneStep RT-PCR kit (Qiagen, Germany) protocol with touch-down modification and primers designed to target the coding regions of the N, M, P and F genes of HMPV strain JPS03-240 (GenBank AY530095), and with G gene primers published by (Ludewick et al., 2005). The primer sequences are shown in Table 2.1:

N gene	hmtpNS5F 5'-gcg cgg atc cat gtc tct tca agg gat t-3'	hmtpN1237R 5'-gcg cgg atc ctt act cat aat cat ttt gac t-3'
P gene	hmtp1209JAPPF 5'-atg tcg ttc cct gaa gga aaa gat att c-3'	hmtp2093JAPPR 5'-tta aac tac ata att aag tgg taa at-3'
M gene	hmtp2126JAPMF 5'-atg gag tcc tat ctg gta gac a-3'	hmtp2890JAPMR 5'-tta tct gga ctt cag cac ata tc-3'
F gene	hmtp3103JAPFF 5'-atg tct tgg aaa gtg gtg atc at-3'	hmtp4632JAPFR 5'-cta act gtg cgg tat gaa gcc-3'
G gene	hmtpGunivF 5'-gag aac att cgr rcr ata gay atg-3'	hmtpGunivR 5'-aga tag aca ttr aca gtg gat tca-3'

Table 2.1. The forward and reverse primers used for the amplification of HMPV N, P, M, F and G genes.

Reverse transcription	50°C for 30 min	
Initial denaturation	95°C for 15 min	
Denaturation	95°C for 20 s	}
Annealing	65°C (-0.5°C per cycle)for 20 s	}30 cycles
Extension	72°C for 90 s	]
Final Extension	72°C for 10 min	

The total volume (50 µl) of the reaction mixes were run on a 1% agarose gel at 120V for 30-45 min. The amplified gene fragments were then excised and gel-purified as described below (section 2.3.2). The purified PCR products were then quantitated using a NanoDrop spectrophotometer (Thermo Fisher Scientific Inc, USA).

2.3.2 Agarose gel electrophoresis and DNA extraction

DNA was separated on a 1% (w/v) agarose gel (BioRad, USA) in 1x TBE buffer (1st Base Pte Ltd). About 2-3µl of 0.1% ethidium bromide (BioRad, USA) was added into the agarose solution before casting. The gels were run at 120 V for 30 min. The DNA bands were viewed on a UV Transilluminator (Syngene, UK). If a DNA band needed to be purified from the gel, it was excised and extracted with a QIAquick Gel Extraction Kit (Qiagen, Germany) according to the manufacturer's instructions.

2.3.3 Gene sequencing

The reagent BigDye Terminator v3.1 ready reaction mix (Applied Biosystems, USA) was used to sequence the amplified viral genes. According to the manufacturer's

recommendation, between 5-20 ng (for products of length 500-1000 bases) or 10-40 ng (for products of length 1000-2000 bases) of purified PCR product were used as sequencing templates. The reaction mix was prepared as follows : 4 µl BigDye Terminator v3.1 ready reaction mix, 2 µl of a 10 µM primer (forward or reverse) solution, 1-4 µl of quantitated, purified PCR product and nuclease-free water to final volume of 10 µl. The reaction mix was loaded into the PCR machine and run with the condition as follows:

Initial denaturation	96°C for 1 min	
Denaturation	96°C for 10 s	}
Annealing	50°C for 5 s	}25 cycles
Extension	60°C for 4 min	]

The samples were then sent to for sequencing analysis.

2.3.4 Sequence alignment

Once the gene sequences were returned from the sequencing companies, they were visually checked using BioEdit Sequence Alignment Editor (Hall, 1999). The forward and reverse sequences were then compared (reverse sequences were first reverse-complemented using the website http://www.bioinformatics.org/sms/rev_comp.html). Once the forward and reverse sequences were matched, they were aligned with known reference sequences from GenBank. Sequences from avian pneumovirus type c (APVc) were used as outgroups. The alignments were performed by ClustalX v2.0.12 software (Larkin et al., 2007). After alignment, the same software was used to plot a neighbour-joining tree (using 1000 bootstrap replicates). This same method was also used to compare amino acid sequences translated from the gene sequences using a web-based DNA/RNA translator program (http://www.fr33.net/translator.php).

2.3.5 Plotting phylogenetic trees

The neighbour-joining tree was visualised using MEGA 4 software (Tamura et al., 2007). The phylogenetic trees were formatted to the standard rectangular tree with the APVc gene outgroup at the extreme end of the tree. The final image was then saved in TIFF format.

2.3.6 Submission of the gene sequences

The sequences from the HMPV, HBoV, HCoV and HRV isolates were collated and submitted to GenBank. Either the program Sequin or Bankit was used for submission and can be obtained from the GenBank website (www.ncbi.nlm.nih.gov/genbank).

2.4 Construction of mammalian expression vectors

2.4.1 Initial cloning of virus gene PCR products

The N gene of SIN05-NTU70, M and P genes of SIN05-NTU84, F gene of SIN06-NTU271 and G genes of both SIN06-NTU271 (GA) and SIN06-NTU272 (GB) were chosen for cloning into a PCR cloning vector for further studies. Approximately 100 ng of PCR product was ligated to 50 ng of the pDrive cloning vector (Qiagen, USA) at 4-16°C for 30 min according to the manufacturer's instructions. A total of 2 µl of the ligation mix was added to 50 µl of ice-thawed EZ competent cells (Qiagen, USA) and held on ice for 5 min before heat-shock in a 42°C water bath for 30 s, after which the cells were returned into ice for 2 min. Subsequently, 250 µl of SOC media was added to the cells and 50-100 µl of the mixture was spread on pre-warmed Luria-Bertani (LB) agar (Difco Laboratories, USA) containing ampicillin (MP Biomedicals Inc, USA), IPTG (100µl of 0.1M, Fermentas, EU) and X-Gal (250µl of 40mg/ml, Fermentas, EU). The

plates were incubated at 37°C overnight and the white colonies were selected for screening by PCR. The remaining ligation mix was stored at -20°C for future use.

2.4.2 Cloning of virus genes

2.4.2.1 Vaccinia T7 vector (pcDNA3.1(-))

The F and GA genes from SIN06-NTU271 and the GB gene from SIN06-NTU272 were amplified from the pDrive vector construct (refer to 2.4.1) using specifically designed primers (Table 2.2). The forward primer included a recognition sequence for the XhoI [CTCGAG] restriction enzyme (Promega Corp, USA) and the reverse primer included a recognition sequence for EcoRI [GAATTC] restriction enzyme (Promega Corp, USA). The amplification was performed with the Expand High Fidelity PCR system (Roche Applied Sciences, USA) with touch-down modification as shown below:

F	NTU271Fforwardmod 5'-gc ctc gag gtt atg gct tgg aaa-3'	NTU271Freversemyc 5'-gc gaa ttc cta cag atc ctc ttc tga gat gag ttt ttg ttc act gtg cgg tat gaa gcc-3'
GA	G271pcDNA31F 5'-gc ctc gag acc atg gct ctt caa ggg att tc-3'	G271pcDNA31flagR 5'-gc gaa ttc cta ttt atc gtc atc gtc ttt gta atc tat tgt tgg tgt gct ggt-3'
GB	NTU272GpcDNAF 5'-gc ctc gag acc atg gaa gta aga gtg gag-3'	NTU272GpcDNAflagR 5'-gc gaa ttc cta ttt atc gtc atc gtc ttt gta atc act act tgg aga aga tgt-3'
Screening/ sequencing	T7pro/for 5'-taa tac gac tca cta tag gg-3'	pcDNA3.1rev 5'-tag aag gca cag tcg agg-3'

Table 2.2. Primers for cloning of F, GA and GB genes into pcDNA3.1(-) together with the primers used for PCR screening and sequencing of clones.

Reverse transcription	50°C for 30 min	
Initial denaturation	95°C for 15 min	
Denaturation	95°C for 20 s	}
Annealing	65°C (-0.5°C per cycle)for 20 s	}30 cycles
Extension	68°C for 90 s	]
Final Extension	68°C for 10 min	

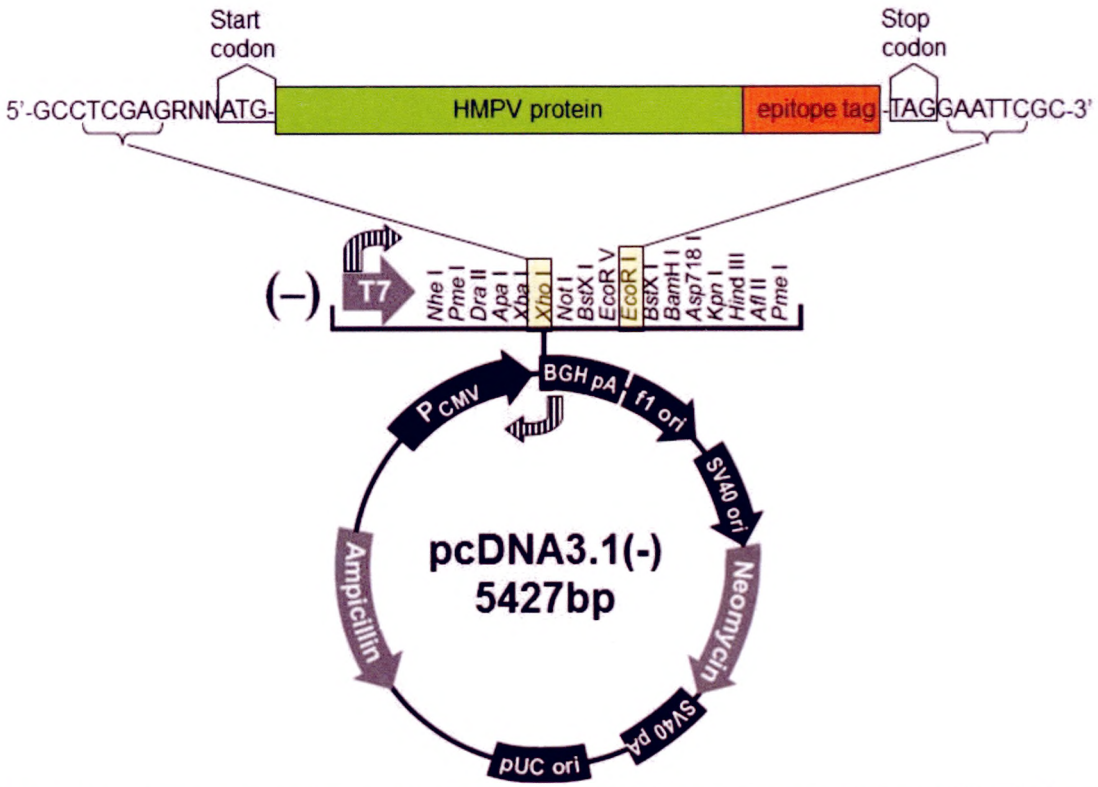

Figure 2.3. Construction of recombinant expression plasmid containing SIN06-NTU271 F and G protein genes and SIN06-NTU272 G protein gene in pcDNA3.1(-) using *Xho*I and *Eco*RI restriction sites. Epitope tag is either cmyc for F or FLAG for GA and GB. Curved arrows indicate the location of the forward and reverse primers for PCR screening and sequencing.

The cloned F gene was designed with a cmyc [EQKLISEEDL] tag at the C-terminal whereas the cloned GA and GB genes were designed with a FLAG [DYKDDDDK] tag at the C-terminal (Fig 2.3). The amplified gene products were digested overnight at 37°C with EcoRI and XhoI simultaneously in 1X Buffer H and 1X BSA (Promega Corp, USA) as was the pcDNA3.1(-) plasmid (Invitrogen, USA). After restriction digestion, the plasmid, F and GA/B genes were purified using QIAquick Gel Extraction kit (Qiagen, Germany) and eluted into 30µl water. The plasmid and digested F and GA/B inserts were ligated overnight at 16°C using T4 DNA ligase (Roche Applied Sciences, USA). The ligation mix was added into a tube of either DH5α or TOP10 chemical competent cells (Invitrogen, USA) and left on ice for 30 min followed by heat shock at 42°C for 30 s, then put back on ice for 2 min. The cells were then shaken at 37°C for 1 hour in 250 µl SOC medium (Invitrogen, USA) before plating on pre-warmed LB agar (Difco Laboratories, USA) plates containing 100 µg/ml ampicillin (MP Inc, USA). After overnight incubation at 37°C, colonies on plates were screened by PCR using primers

targeting the insert and flanking regions of the pcDNA3.1(-) plasmid (refer to 2.4.4). Expected amplified product was the size of insert plus 200 bp of forward and reverse flanking regions.

2.4.2.2 Chicken beta-actin promoter vector (pCAGGS)

The F and GA protein genes from SIN06-NTU271 and the GB protein gene from SIN06-NTU272 were amplified from their respective recombinant pcDNA3.1(-) plasmids using specifically designed primers (Table 2.3). The forward primer included a recognition sequence for the KpnI [CCTAGG] restriction enzyme and the reverse primer included a recognition sequence for XhoI [CTCGAG] restriction enzyme. As in the earlier section 2.4.2.1, the F gene was designed with a cmyc tag and the GA and GB genes were designed with a FLAG tag at the C-terminal (Fig 2.4).

F	F271pCAGGf 5'-gc ggt acc gtt atg gct tgg aaa gtg gtg-3'	F271pCAGGmycR 5'-gc ctc gag cta cag atc ctc ttc tga gat gag ttt ttg ttc act gtg cgg tat gaa gcc-3'
GA	G271pCAGGf 5'-gc ggt acc atg gag gtg aaa gta-3'	NTU271GpCAGGsFLAGr 5'-gc ctc gag cta ttt atc gtc atc gtc ttt gta atc tat tgt tgg tgt gct ggt-3'
GB	NTU272GpCAGGSf 5'-gc ggt acc atg gaa gta aga gtg gag-3'	NTU272GpCAGGSFLAGr 5'-gc ctc gag cta ttt atc gtc atc gtc ttt gta atc act act tgg aga aga tgt-3'
M	M84pCAGGf 5'-gc ggt acc att atg gag tcc tat ctg-3'	M84pCAGGr 5'-gc ctc gag tta tct gga ctt cag cac-3'
N	N70pCAGGf 5'-gc ggt acc atg gct ctt caa ggg att-3'	NTU70pCAGGsNmycR 5'-cgc ctc gag cta cag atc ctc ttc tga gat gag ttt ttg ttc ctc ata atc att ttg act gtc-3'
Screening/ sequencing	pCAGGSfor2 5'-tag cta gag cct ctg cta ac-3'	pCAGGSrev 5'-cag aag tca gat gct caa g-3'

Table 2.3. Primers for cloning of F, GA and GB genes into pCAGGS together with the primers used for PCR screening and sequencing of clones.

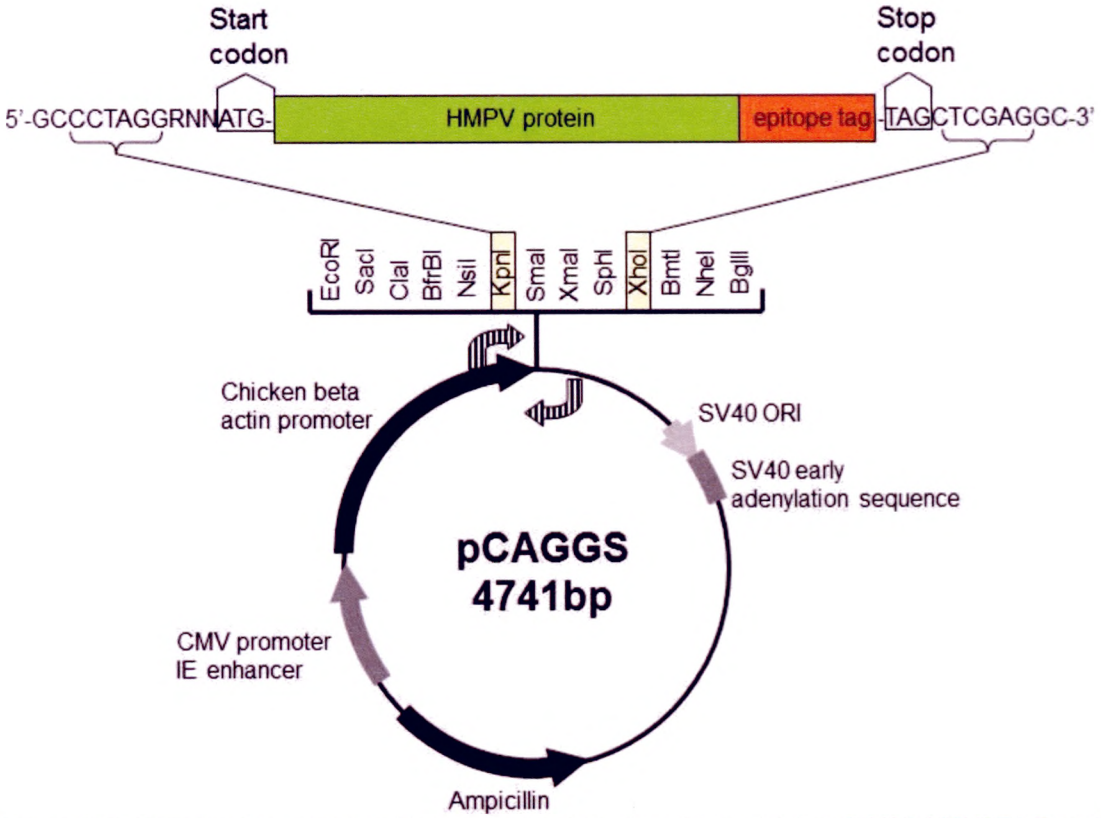

Figure 2.4. Construction of recombinant expression plasmid containing SIN06-NTU271 F and G protein genes and SIN06-NTU272 G protein gene in pCAGGS using *Kpn*I and *Xho*I restriction sites. Epitope tag is either cmyc for F or FLAG for GA and GB. Curved arrows indicate the location of the forward and reverse primers for PCR screening and sequencing.

The PCR, post-PCR purification and ligation protocols are the same as that used for pcDNA3.1(-) recombinants (refer to 2.4.2.1). Restriction digestion of PCR products with KpnI and XhoI had to be performed sequentially overnight at 37°C in Buffer J and Buffer D, respectively (both containing 1X BSA, Promega Corp, USA) as with the pCAGGS plasmid. After restriction digestion, the plasmid, F and GA/B genes were purified using QIAquick Gel Extraction kit (Qiagen, Germany) and eluted into 30 µl water. After ligation, the transformation, colony screening, plasmid purification and checking of sequences were identical to the protocols in the previous section 2.4.2.1, with the exception of using the insert flanking primers for pCAGGS recombinant plasmids (Table 2.3).

2.4.3 Construction of truncated virus genes

Truncated forms of HMPV F and GA proteins were constructed by using primers that eliminate the cytoplasmic tail of the protein ($F_{\Delta CT}$ and $GA_{\Delta CT}$) or both the transmembrane

$GA_{\Delta TM}$	NTU271pCAGGsGfwd-TM 5'-cgc ggt acc atg gac tac aca ata caa aaa ac caca-3'	NTU271GpCAGGsFLAGr (see Table 2.3)
$GA_{\Delta CT}$	NTU271pCAGGsGfwd-CY 5'-cgc ggt acc atg gta atc ctc ata gga ata act aca-3'	NTU271GpCAGGsFLAGr (see Table 2.3)
$F_{\Delta TM}$	F271pCAGGf (See Table 2.3)	NTU271pCAGGsFmyc-TM 5'-cgc ctc gag cta cag atc ctc ttc tga gat gag ttt ttg ttc gcc agt gtt ccc ttt ctc tgc-3'
$F_{\Delta CT}$	F271pCAGGf (See Table 2.3)	NTU271pCAGGsFmyc-CY 5'-cgc ctc gag cta cag atc ctc ttc tga gat gag ttt ttg ttc gat tat aat gaa gat gct-3'
F515	F271pCAGGf (See Table 2.3)	NTU271pCAGGSF515 5'-ccg ctc gag cta cag atc ctc ttc tga gat gag ttt ttg ttc ctt gat tat aat gaa gat-3'
F516	F271pCAGGf (See Table 2.3)	NTU271pCAGGSF516 5'-ccg ctc gag cta cag atc ctc ttc tga gat gag ttt ttg ttc ttt ctt gat tat aat gaa-3'
F517	F271pCAGGf (See Table 2.3)	NTU271pCAGGSF517 5'-ccg ctc gag cta cag atc ctc ttc tga gat gag ttt ttg ttc tgt ttt ctt gat tat aat-3'
F518	F271pCAGGf (See Table 2.3)	NTU271pCAGGSF518 5'-ccg ctc gag cta cag atc ctc ttc tga gat gag ttt ttg ttc ctt tgt ttt ctt gat tat-3'
F519	F271pCAGGf (See Table 2.3)	NTU271pCAGGSF519 5'-cgc ctc gag cta cag atc ctc ttc tga gat gag ttt ttg ttc ttt ctt tgt ttt ctt-3'
F524	F271pCAGGf (See Table 2.3)	NTU271pCAGGSF524 5'-cgc ctc gag cta cag atc ctc ttc tga gat gag ttt ttg ttc agg tgc ccc cgt tgg-3'
F529	F271pCAGGf (See Table 2.3)	NTU271pCAGGSF529 5'-cgc ctc gag cta cag atc ctc ttc tga gat gag ttt ttg ttc acc act cag ctc tgg-3'
F534	F271pCAGGf (See Table 2.3)	NTU271pCAGGSF534 5'-cgc ctc gag cta cag atc ctc ttc tga gat gag ttt ttg ttc gcc att att tgt gac-3'

Table 2.4. Primers for cloning of F and GA mutant or truncated genes into pCAGGS. The primers used for PCR screening and sequencing are the same as those in Table 2.3.

region and cytoplasmic tail ($F_{\Delta TM}$ and $GA_{\Delta TM}$). In addition, eight F protein constructs were made which had various lengths of the cytoplasmic tail region truncated (F515, F516, F517, F518, F519, F524, F529, F534). All F protein mutants were created with a cmyc tag while all GA protein mutants were created with a FLAG tag at their C-terminal

just like the wild-type proteins. The method of plasmid construction was the same as that in the previous section (2.4.2.2).

2.4.4 Screening of clones by PCR

Colonies derived from pDrive vector showed blue and white differentiation. The white colonies were picked with a sterile 10µl pipette tip and inoculated into 20µl of sterile water. One blue colony was always selected as a negative control. Colonies derived from pcDNA3.1(-) or pCAGGS vectors all appeared white and between 4-10 were picked for screening each time. The colony screening PCR was done using the specific primers mentioned in Tables 2.3 and 2.4. The PCR reaction mix (Invitrogen, USA) was prepared as follows: 1 µl of 10X PCR buffer, 1 µl of 2 mM dNTP, 0.3 µl of 50 mM $MgCl_2$, 0.2 µl of 10 mM forward primer, 0.2 µl of 10 mM reverse primer, 0.1 µl Platinum Taq polymerase, 2.2 µl of nuclease free water and 5 µl of cell suspension. The cycling conditions are shown below:

Initial denaturation	95°C for 3 min	
Denaturation	95°C for 20 s	}
Annealing	50°C for 20 s	} 25 cycles
Extension	72°C for 90 s	]
Final extension	72°C for 5 min	

Primers for PCR screening of pDrive plasmids:

Forward (M13, -20)	5'-gta aaa cga cgg cca gt-3'
Reverse (M13, -24)	5'-gga aac agc tat gac cat g-3'

If the colony screen was positive, the remainder of the cell suspension was added to 5 ml of LB ampicillin broth and shaken overnight at 37°C.

2.4.5 Extracting the plasmids

The 5 ml of overnight bacterial suspension was divided into two portions. About 4.6 ml of the suspension was used to extract the recombinant plasmid using the QIAprep Spin

Miniprep kit (Qiagen, Germany) according to the manufacturer's instructions. The final plasmid solution was quantitated by a NanoDrop spectrophotometer.

2.4.6 Confirming the plasmid sequence

The plasmid stock was checked by restriction digest with the same enzymes used for cloning and by sequencing with the screening primers. The 2 expected restriction fragments should consist of one of the same length as the cloned gene and the other of the same length as the vector. The sequencing result should show no mutations compared to the original gene. Once the sequence was determined to be correct, the recombinant plasmid was used for transfection.

2.4.7 Storage of clones

The remaining 0.4 ml of the turbid bacterial suspension was mixed with 0.1 ml sterile glycerol (Sigma-Aldrich, USA) to make a stock for freezing at -80°C. This stock could be used to generate more plasmids, if necessary.

2.5 Analysis of protein expression in mammalian cells

2.5.1 Growing and maintaining mammalian cells

HEK 293T, HEp-2 and Vero cells were maintained and propagated with DMEM+GlutaMAX (Life Technologies, USA) supplemented with 10% v/v fetal bovine serum (Life Technologies, USA), penicillin 100 UI/ml and streptomycin 100 µg/ml (Life Technologies, USA). The cells were kept in tissue culture flasks (Corning or Nunc, USA) and subcultured when the cells reached approximately 90% confluency. When subculturing, the cells were first rinsed with sterile PBS pH 7.2, then incubated with a small volume of Trypsin-EDTA 0.25% (w/v) until the cells could be dislodged by

tapping. Fresh DMEM+GlutaMAX media with supplements was added to neutralise the trypsin. A small proportion of the cells was transferred to a new flask with fresh media. The cells were incubated at 37°C with 5% CO_2. To calculate the cell density, a haemocytometer (Heinz Herenz GmbH, Germany) was used. Trypan Blue stain (Sigma-Aldrich, USA) was used to distinguish the viable cells while counting.

2.5.2 Transfection of cells

When seeding plates or dishes with mammalian or insect cells, a general guide was used to calculate the optimal seeding density (Table 2.5). There were slight variations in the exact number between the various cell lines depending on the size of the cell and the growth rate.

Well type/size	**Seeding density (cells/well)**	**Confluent density (cells/well)**
96-well plate	2.5×10^4	1×10^5
24-well plate	5×10^4	2×10^5
12-well plate	1×10^5	4×10^5
6-well plate/35mm dish	3×10^5	1.2×10^6
60mm dish	8×10^5	3.2×10^6

Table 2.5. A summary of the various plates and dishes used for growing cell lines and their respective recommended seeding densities and confluent densities.

2.5.2.1 Using pcDNA3.1(-) plasmids

Cells at almost confluent density (Table 2.5) were infected with modified vaccinia virus Ankara strain (MVA-T7) (Wyatt et al., 1995) containing the T7 bacteriophage RNA polymerase gene at a multiplicity of infection (MOI) value of 1. The MVA-T7 was allowed to infect for 1 hour at 37°C. The media was then changed to antibiotic-free media. TransIT-LT1 reagent (Mirus Bio LLC, USA) was used to transfect the recombinant plasmids into the cells. Cells were incubated at 37°C for 24 hours before harvesting and dissolving in Laemmli or Denaturing buffer (see 2.5.3).

2.5.2.2 Using pCAGGS plasmids

Cells at almost confluent density (refer Table 2.5) were transfected in antibiotic-free media using Lipofectamine 2000 (Invitrogen, USA) for the recombinant pCAGGS plasmids according to the manufacturer's instructions. Transfected cells were incubated at 37°C for 48 hours before harvesting and dissolving in Laemmli buffer or Denaturing buffer (see 2.5.3).

2.5.3 Harvesting cells for Western blot

Media was removed completely and the cells were washed with 1x PBS. Between 50-100µl of 1x Laemmli or Denaturing buffer was applied on the cells sufficient enough to cover the dishes or plates surface. The cells were then scraped and collected in a microcentrifuge tube. The lysates were heated at 100°C for 10 min before being sonicated (2x 5 s pulses on a Vibra-cell sonicator, Sonics & Materials Inc, USA) to shear genomic DNA. After that, the lysates were boiled again for 3 min. The lysates were then loaded on SDS-PAGE gel. An alternative method to sonication was used when the lysate contained radioisotopes. The genomic DNA was sheared by repeated pumping using a syringe and a fine gauge needle.

2.5.4 SDS-PAGE and Western blotting

SDS-PAGE gels were cast in a cassette (BioRad, USA) with an appropriate percentage (usually 10%) of acrylamide. After the gels had set, they were loaded into the SDS-PAGE Tank (BioRad, USA) and filled with 1x SDS-PAGE running buffer. Samples in 1x Laemmli buffer were then loaded into the wells together with a protein size marker (BioRad, USA). Samples were run at 200 V for 45-60 min. The Immobilon-P membrane (Millipore, USA) was activated by soaking in methanol for a few minutes before being used for Western blot. Care was taken that the orientation of the gel and the membrane was correct. The gel should face the cathode (black terminal) and the membrane

should face the anode (red/white terminal). 1x transfer buffer was used to fill the gel tank and the transfer process was run at 100 V for 60 min. After the transfer, the membrane was blocked with 5% skim milk overnight before probing with antibodies the next day (refer to Table 5 below for antibodies). Membranes were washed twice with PBS-Tween (0.05% Tween 20) before probing with each primary and secondary antibody at room temperature and before signal detection. Detection of secondary antibodies was done using ECL chemiluminescence reagent (GE Healthcare, USA). The treated membrane was then exposed to X-ray film (Fuji Photo Film Co Ltd, Japan) from 30 s up to 1 hour. Films were developed in a Kodak Developer.

2.5.5 Glycosylation analysis of proteins

To study the action of enzymatic digestion of PNGase F (Peptide:N-glycosidase F, New England Biolabs, USA) and Endo H (Endoglycosidase H, New England Biolabs, USA) on the expressed F and G proteins, a portion of the harvested cells were lysed in Denaturing buffer (0.5% SDS and 40 mM DTT; New England Biolabs, USA) and heated at 100°C for 10 min. The lysates were incubated overnight in the presence of PNGase F with 1% NP-40 and 1x G7 buffer (50 mM sodium phosphate pH 7.5, New England Biolabs, USA) and Endo H with 1x G5 buffer (50mM sodium citrate pH 5.5, New England Biolabs, USA) according to the manufacturer's instructions at 37°C overnight. PNGase F cleaves almost all N-linked sugar side chains from proteins. Endo H cleaves immature sugar side chains (primarily high mannose or hybrid chains) from proteins.

2.5.6 Biotin labelling of cell surface proteins

Using the same protocol as 2.5.2, once the cells were transfected for 24 or 48 hours (depending on cell type and expression plasmid used), they were rinsed in PBS pH 8 before incubating in a 0.5 mg/ml solution of EZ-Link Sulfo-NHS-LC-LC-Biotin (Pierce

Biotechnology, USA). This compound labels amine groups (e.g. lysine residues on the extracellular surface) because of its hydrophilic nature. After surface labeling, the cells were rinsed with PBS pH 8 and lysed with RIPA buffer (1% NP-40, 1 mM EDTA, 0.1% SDS, 2 mM PMSF). The lysate was then spun at maximum speed in a microcentrifuge for 10 min. Some of the lysate was incubated overnight at 4°C with the appropriate antibody in binding buffer (0.5% NP-40, 1 mM EDTA, 0.25% BSA, 2 mM lysine). After binding, Protein A-Sepharose (Sigma-Aldrich, USA) was added to bind the antibodies by gentle agitation at 4°C for 90 min. After 90 min, the Protein A-Sepharose was spun down and washed twice with a low salt buffer (1X PBS, 1 mM EDTA, 1% Triton-X-100) before being treated with Laemmli buffer or Denaturing buffer (see 2.5.3) and heated at 100°C for 10 min before loading onto an SDS-PAGE gel.

2.5.7 Chemical crosslinking of proteins

The cells were transfected and incubated as described in the previous section 2.5.2. The cells were then treated with Dithiobis[succinimidylpropionate] (DSP, Pierce Biotechnology, USA) in DMSO at a varying concentrations (e.g. 0 mM, 0.1 mM, 0.5 mM and 1 mM) for 1 hour. This compound also labels amine groups (e.g. lysine residues) but is membrane permeable due to its hydrophobic nature. DSP treatment can be done with or without surface protein labelling with biotin. After labelling, the cells were rinsed with PBS, lysed with RIPA buffer and processed as in 2.5.3.

2.5.8 Radiolabeling of proteins

2.5.8.1 Labeling with ^{3}H-glucosamine

The pCAGGS recombinant F and GA/B plasmids were transfected into Vero and Hep2 cells in 60-mm dishes (Hep2 cells adhere better to dishes) in the same way as 293T cells as described above in section 2.5.2.2. At 4-6 hours post-transfection, the media

was changed and the cells left overnight at 37°C. The next day, the media was changed to glucose-free DMEM (Invitrogen, USA) containing 200 µCi/dish tritium-labeled glucosamine hydrochloride D-[6-^{3}H(N)]- (Perkin Elmer, USA). The cells were further incubated for 8 hours and harvested as in surface labeling experiments (section 2.5.3). Once the lysates were harvested and run on SDS-PAGE, the gel was fixed in 10% acetic acid for 10 min, soaked in NAMP100 Amplify (GE Healthcare, USA) for 20 min and vacuum-dried onto a blotting paper for 1 hour. The dried gels were then attached to cassettes and exposed to pre-flashed X-ray film for durations ranging from 1 day to a few months.

2.5.8.2 Labeling with ^{35}S-methionine and cysteine

HEp-2 cells were transfected with pCAGGS plasmids as described in section 2.5.2.2. Approximately 8-12 hours post-transfection, the media was changed to DMEM without methionine and cysteine (Invitrogen, USA) and 100 µCi/ml of EasyTag Expres^{35}s protein labeling mix (Perkin-Elmer, USA). The cell proteins were labelled for 24 hours before harvesting. The subsequent procedures were the same as the previous section 2.5.8.1.

2.5.9 Light microscopy

Cell cultures were monitored and analysed using a standard inverted light microscope (Leica, Germany). Cells could be viewed and photographed through a 10X or 20X objective using an attached digital camera (Olympus, Japan).

2.5.10 Immunofluorescence microscopy

Various HMPV proteins (including F, GA/B, M, N) were singly expressed or co-expressed in Hep2 cells or Vero cells seeded at 60-80% confluency onto 10-12 mm

glass coverslips in 24-well plates. LLC-MK2 cells were infected with the clinical HMPV strain for 7 days before fixing. The transfections were performed in the same manner as in 2.5.2.2, incubated at 37°C for 16-24 hours before the cells were washed twice with PBS and fixed with a cold methanol:acetone (1:1) mixture for 15 minutes. After fixing, the cells were probed with the respective anti-myc, anti-FLAG or anti-6His antibody at 1:100 dilution in PBS (anti-M and anti-F58 antibodies were used neat), then washed twice again with PBS and probed with anti-mouse fluorescein isothiocynate (FITC) conjugate (an alternative to FITC known as Alexa Fluor 488 was also used) at 1:100 dilution or anti-rabbit Alexa Fluor 555 conjugate at 1:1000 dilution in PBS. Both primary and secondary antibodies were incubated at room temperature for 1 hour. After incubating with the secondary antibodies, the coverslips were finally washed twice with PBS before mounting. The coverslips were then mounted on a clean glass slide by inverting the cell-attached surface over a drop of glycerol-based mounting media (Dakocytomation Fluorescence Mounting Medium, Dako, USA) and sealing with nail varnish. The slides were observed under an immunofluorescence microscope using a 20X and 100X objective (Nikon Eclipse 80i, Japan). Images were captured by QCapture Pro software (QImaging, USA). Colours were artificially added to the images according to the actual fluorophore colours.

2.5.11 Confocal microscopy

The same coverslips which were prepared for immunofluorescence microscopy could also be viewed under a Zeiss 510 laser scanning confocal microscope (Carl Zeiss GmbH, Germany). Image sections of 8 to 12 slices of the fluorescent cells at 100X magnification were captured and these were compiled to produce an image of distribution of the various proteins stained by the fluorophores in the HEp-2 and Vero cell types. Coefficient of co-localisation, overlap (Manders) coefficient and Pearson's correlation coefficient were calculated by the Zen 2007 software (Carl Zeiss GmbH, Germany).

2.5.12 Ultracentrifugation of proteins in sucrose gradient

Separation of expressed HMPV F and G proteins was also achieved by ultracentrifugation (150,000g, 4°C for 18 hours) on a continuous 5-30% sucrose gradient using a Himac CP90WX preparative ultracentrifuge (Hitachi Koki, Japan) with a P40ST rotor. The various sucrose solutions were prepared in PBS+1% Triton-X-100. After centrifugation, the gradient was harvested into about 12 fractions of 1 ml each in a microcentrifuge tube. A sample of each fraction was mixed with 5x Laemmli buffer and analysed by SDS-PAGE. Some of the fractions were immunoprecipitated with the various antibodies depending on which proteins were to be isolated. Proteins crosslinked by DSP and/or surface-labeled with biotin (e.g. co-expressed F and GA/B proteins) were also studied using this method.

2.5.13 Flow cytometry analysis of surface protein expression

Surface expression of GA protein alone and GA plus F protein was analysed by flow cytometry. The primary reason for this was that the FLAG tag on the GA protein is located at the C-terminal and is exposed on the extracellular surface and therefore could easily be detected by anti-FLAG antibodies. HEp-2, Vero E6 and 293T cells were transfected (as in 2.5.2.2) and incubated for 24 hours at 37°C. Cells were then dislodged and harvested by washing with PBS+1 mM EDTA. The harvested cells were centrifuged at 1000g for 5 min and washed with PBS+1% FBS. The cell density was adjusted to $1x10^7$ per ml. 50 µl of the cell suspension was mixed with 50 µl of rabbit anti-FLAG antibody (diluted 1:100 with PBS+3% BSA) and incubated for 30 min on ice. After that, the cells were centrifuged at 1000g for 5 min and washed twice with PBS+1% FBS. 100 µl anti-rabbit FITC conjugate (diluted to 1:100 with PBS+3% BSA) was added to the cell pellet and incubated for 30 min on ice in the dark. Finally, the cells were washed twice with PBS+1% FBS and resuspended in a total of 200 µl of

PBS+1% FBS. The cells were passed through a FACScalibur instrument (BioRad, USA) for analysis. Graphs were plotted using the instrument software.

2.6 Maintaining and handling insect cells

2.6.1 Growing and maintaining insect cells

Two types of insect cell lines were used in this study. One was the Sf9 cell line derived from *Spodoptera frugiperda* (fall armyworm) and the other was the HighFive cell line derived from *Trichoplusia nii* (cabbage looper). The Sf9 cells were generally used for growing the recombinant viruses and plaque titering. The HighFive cells were used for protein expression work. Both cell types were maintained in Sf-900 II Serum free medium (SFM) supplemented with 10% v/v Fetal Calf Serum (Life Technologies, USA), penicillin 100 UI/ml and streptomycin 100 µg/ml (Life Technologies, USA). The cells were grown in tissue culture flasks (Corning or Nunc, USA) and subcultured when the cells reached approximately 90% confluency. When subculturing, the cells were either dislodged by gentle spraying of the media or with a cell scraper. A small quantity of old cells was introduced into a new flask with fresh supplemented SFM. The cells were then incubated at 28°C. If the cells need to be counted before seeding, a haemocytometer was used (as described in section 2.5.1).

2.6.2 Cryopreserving insect cells

Insect cells can be stored in liquid nitrogen for long periods. Cryovials (Nunc, USA) were filled with 1 ml of approximately $1x10^6$ or $1x10^7$ cells in SFM. Between 7.5-10% of DMSO was added to the media to protect the cells from freeze-thaw damage. Recovery of these frozen cells can be achieved by thawing to room temperature followed by centrifuging the cells (1000g) for a few minutes and replacing the media

with fresh supplemented SFM. The cells can then be transferred to a flask for incubation.

2.6.3 Plaque purification and titering of virus

Sf9 cells were used for plaque purification to isolate the correct virus clone expressing the proteins of interest. The Sf9 cells were seeded in 6-well plates to achieve 50% confluency. The cells were left to attach to the plate surface for 1 hour. Starting from the neat P2 virus, serial ten-fold dilutions were made and 0.1ml of each dilution was used to infect a single well. The dilutions used were from 10^{-2} to 10^{-7}. The diluted viruses were left to infect for 1 hour. During the infection time, a 1% agarose overlay was made by mixing a 1:4 volume of 4% low melting point agarose and 1xSFM 900 with 10% FBS and antibiotics, respectively. After the infection time, the cells were rinsed with 1xPBS and gently layered with the 1% agarose overlay and left to solidify. The 6-well plate was left at 28°C for up to 2 weeks and checked for plaque formation. The plaques were counted and the virus titre was calculated based on the following formula:

$$\text{Virus titre (PFU/ml)} = \frac{\text{number of plaques}}{\text{Dilution factor x inoculum volume (ml)}}$$

When the virus clones needed to be selected, a pipette tip (100 µl) was attached to a pipette and used to punch a hole in the middle of a plaque colony. The agarose gel plug picked up by the pipette tip was then dispensed into a microcentrifuge tube containing SFM 900 and mixed well. Several agarose gel plugs were picked and used to infect Sf9 cells. Each of the purified viruses was tested by harvesting the cells 2 days post-infection and dissolving in 1xLaemmli buffer before running on SDS-PAGE. Western blot was performed to confirm the correct protein expression.

2.6.4 Infecting insect cells

When the insect cells reached the desired density in a flask, plate or dish; they were infected with virus by adding the appropriate volume of prepared virus stock solution. The multiplicity of infection (MOI) is defined as the ratio of viruses to cells under experimental conditions and this was calculated from the values of virus titre and cell density. There was no need to remove the existing media. The container was rocked gently every 15-20 min for 1 hour to evenly distribute the virus inoculum. The cells were left in 28°C for up to 3 days.

2.7 Construction of insect expression vectors

2.7.1 Amplification of target virus genes

The HMPV proteins (F, FDTM, GA, M and N) were cloned into baculovirus vectors for expression in insect cells. The primers are shown in Table 2.6 below.

F	Derived from pcDNA3.1(-) vector	Derived from pcDNA3.1(-) vector
$F_{\Delta TM}$	NTU271Fforwardmod 5'-gc ctc gag gtt atg gct tgg aaa-3'	NTU271pFBDFmyc-TM 5'-cgc ggt acc cta cag atc ctc ttc tga gat gag ttt ttg ttc gcc agt gtt ccc ttt ctc tgc-3'
GA	G271pENTRf 5'-cacc atg gag gtg aaa gta gag-3'	G271pENTRflagr 5'-cta ttt atc gtc atc gtc ttt gta atc tat tgt tgg tgt gct ggt-3'
M	hmpv-M-for(1-1) 5'-gc ctc gag acc atg gag tcc tat ctg gta gac-3'	NTU84pFBDMrev 5'-cgc ggt acc cta tct gga ctt cag cac ata tc-3'
N	hmpv-N-forward(1-7) 5'-cacc atg gct ctt caa ggg att c-3'	hmpv-N-reverse(1-8) 5'-gaa tcc ctt gaa gag cca ggg tga agg gct cc-3'

Table 2.6. Primers for cloning of F, $F_{\Delta TM}$, GA, M and N genes into baculovirus vectors. The "cacc" bases required for the pENTR vectors (GA and N) are underlined.

The F protein was derived from the pcDNA3.1(-)/F-myc recombinant plasmid (refer to section 2.4.2.1) and thus there was no need to perform any PCR amplification. The GA and N protein genes were amplified from their respective pDrive vectors (refer to section 2.4.1) using primers targeting the GA and N genes respectively, but with 4

nucleotides (CACC) added to the 5' end of the forward primer to allow the PCR product to integrate into a Gateway pENTR directional TOPO vector (Invitrogen, USA). According to the manufacturer's instructions, the PCR products must be blunt-ended and can be produced by a proofreading DNA polymerase. A recombination reaction occurs via a topoisomerase enzyme resulting in a pENTR vector with the gene of interest. The difference between the pENTR vectors of GA and N genes was that the GA vector has a FLAG tag and stop codon integrated into the gene. The FdTM and M protein genes were amplified from their respective pDrive vectors (refer to sections 2.4.1) using the primers shown. A slight modification was the alteration of the restriction site at the 3' end from *Eco*RI to *Kpn*I.

2.7.2 Cloning of target genes

2.7.2.1 Constructing the F-myc baculovirus vector

The HMPV F gene was amplified from the pcDNA3.1(-)/F-myc vector by culturing up the *E.coli* stock in LB ampicillin broth overnight and extracting the plasmid by QIAprep Spin Miniprep Kit (Qiagen, Germany). The purified plasmid was digested with *Xho*I and *Kpn*I. The vector, pFastBacDual (Fig. 2.5, Invitrogen, USA) was also digested with the same enzymes.

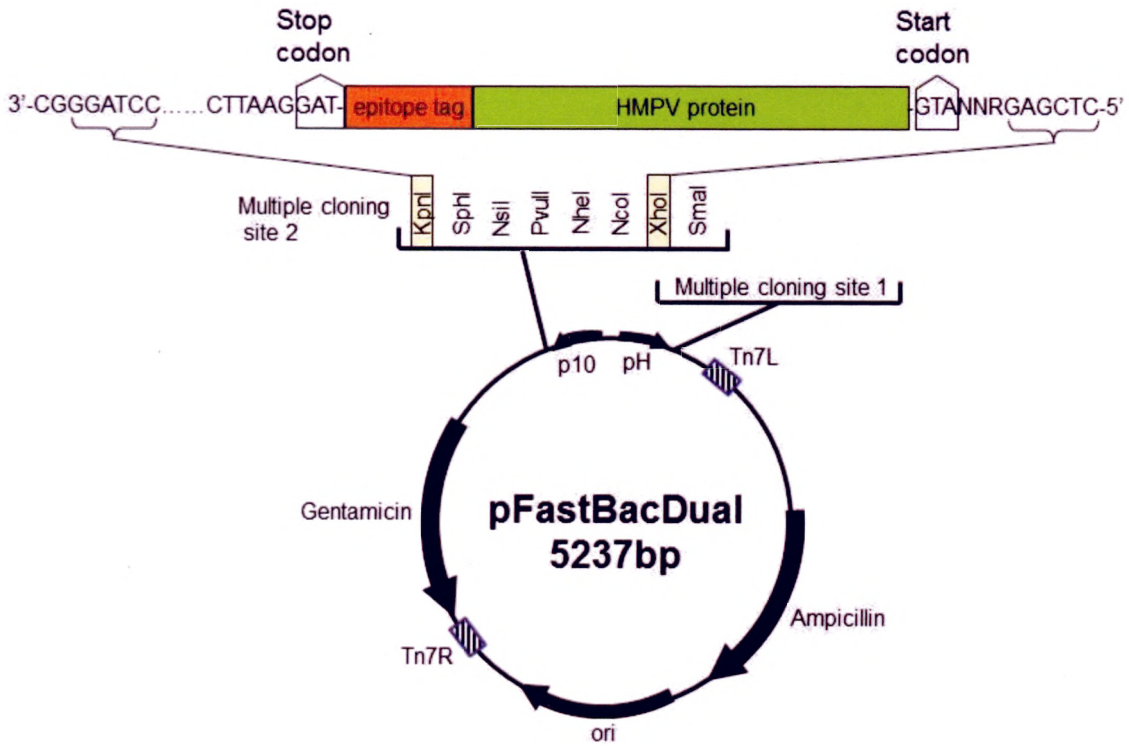

Figure 2.5. Construction of recombinant expression plasmid containing SIN06-NTU271 F protein gene using *Xho*I and *Kpn*I restriction sites. Epitope tag is myc. The Tn7L/R regions mark the location of the recombination zone with the baculovirus genome. There are 2 multiple cloning sites in this vector and each is controlled by a strong promoter i.e. p10 (10kDa protein) gene and polyhedrin gene (pH).

Once the insert and vector were ligated (refer to section 2.4.2.1), the recombinant pFastBacDual/F-myc plasmid was transformed into *E. coli* DH10Bac (Invitrogen, USA) containing a baculovirus shuttle vector (bacmid). Recombination took place via the transposon elements Tn7R/L on the pFastBacDual plasmid and the attTn7 site on the bacmid. The resulting recombinant bacmid containing F-myc gene (bac-F) was purified according to the manufacturer's instructions. A small quantity of purified bac-F was checked by PCR using the F gene-specific primers. The cloning scheme is shown in Fig. 2.6.

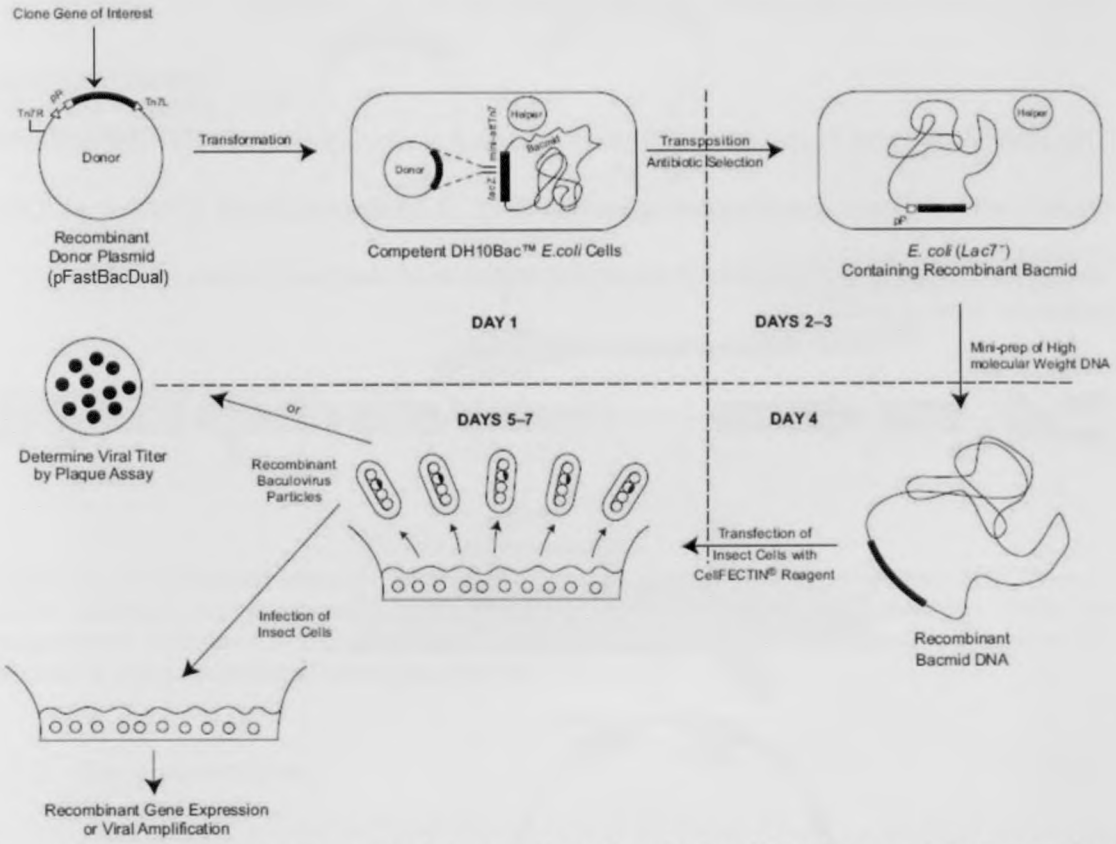

Figure 2.6. A schematic diagram of the workflow for cloning HMPV genes into baculovirus shuttle vector by transposon-activated recombination. This image was modified from the Bac-to-Bac Baculovirus Expression System instruction manual (Invitrogen, USA). The helper plasmid in the DH10Bac cell provides the Tn7 transposition function. Bac-F, bac-$F_{\Delta TM}$ and bac-M were constructed using this method.

2.7.2.2 Constructing the M and $F_{\Delta TM}$-myc baculovirus vectors

The HMPV M and $F_{\Delta TM}$ genes were amplified by PCR from the pDrive plasmids. Using the primers in Table 2.6, the two protein genes were amplified and digested with *Xho*I and *Kpn*I. The subsequent steps were similar to the previous method for F-myc (refer to 2.7.2.1). The recombinant baculovirus genes are referred to as bac-M and bac-$F_{\Delta TM}$. The bac-M and bac-$F_{\Delta TM}$ was checked by PCR in the same way as the bac-F in the previous section 2.6.2.1.

2.7.2.3 Constructing the GA-FLAG and N-6His baculovirus vectors

The HMPV GA and N genes which were previously cloned into pENTR vectors were mixed with a linear baculovirus genome (Fig. 2.7, BaculoDirect C-terminal DNA, Invitrogen, USA) and recombined according to the manufacturer's instructions.

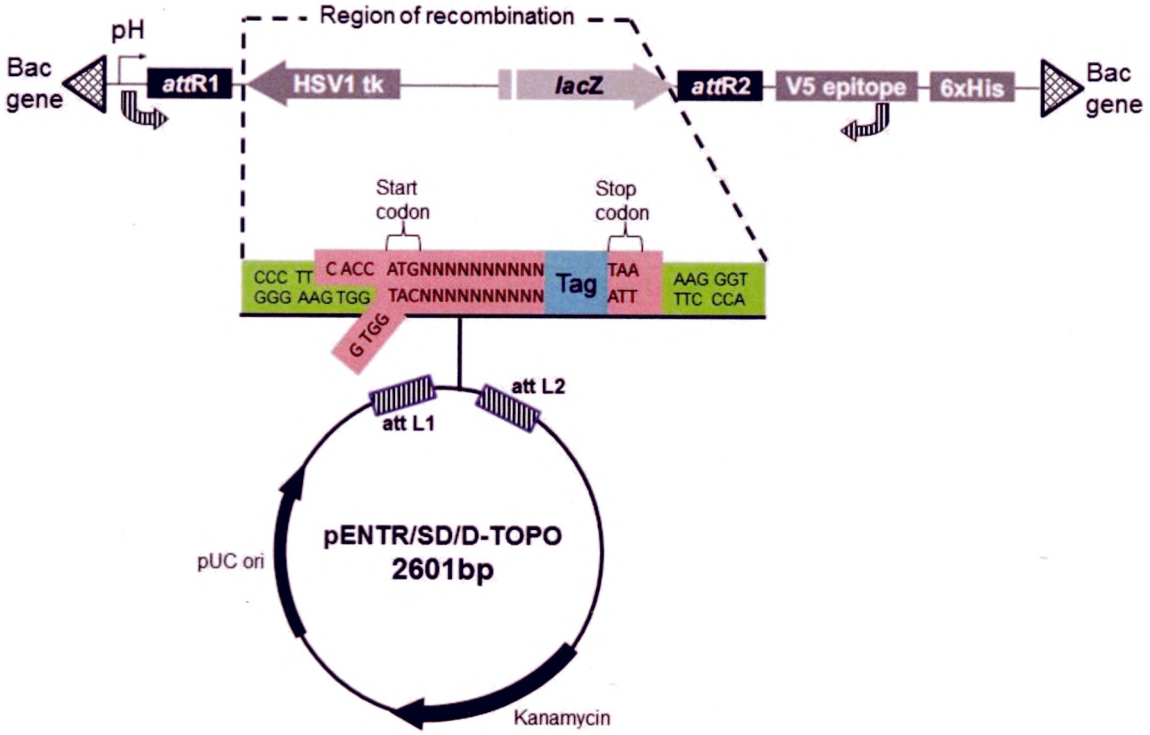

Figure 2.7. An illustration of the pENTR TOPO directional cloning vector (modified from Invitrogen, USA) and its area of recombination with a Baculodirect vector. The pENTR vector is shown containing an insert with the 5' "CACC" sequence, a tag (optional) and a stop codon (optional). The attL1/2 and attR1/2 sites are the recombination sites. The pH arrow indicates the location and direction of the strong polyhedrin gene promoter. The baculovirus linear DNA is the fragment containing the attR1 to 6xHis (5' to 3') coding regions. The arrows at the pH and V5 region are primer locations for PCR screening.

The GA gene which had a FLAG tag and a stop codon in the reverse primer coded for a GA protein with a FLAG tag. The N gene which has neither tag nor stop codon in the reverse primer coded for a N-6His fusion protein. Once the recombination took place, the recombinant baculovirus genomes (bac-GA and bac-N) were ready for transfection. A small quantity of purified bac-GA and bac-N was checked by PCR using the gene-specific primers or the polyhedron (5'-aaa tga taa cca tct cgc-3') and V5 (5'-acc gag gag agg gtt agg gat-3') primer pair. The cloning scheme is shown in Fig. 2.8.

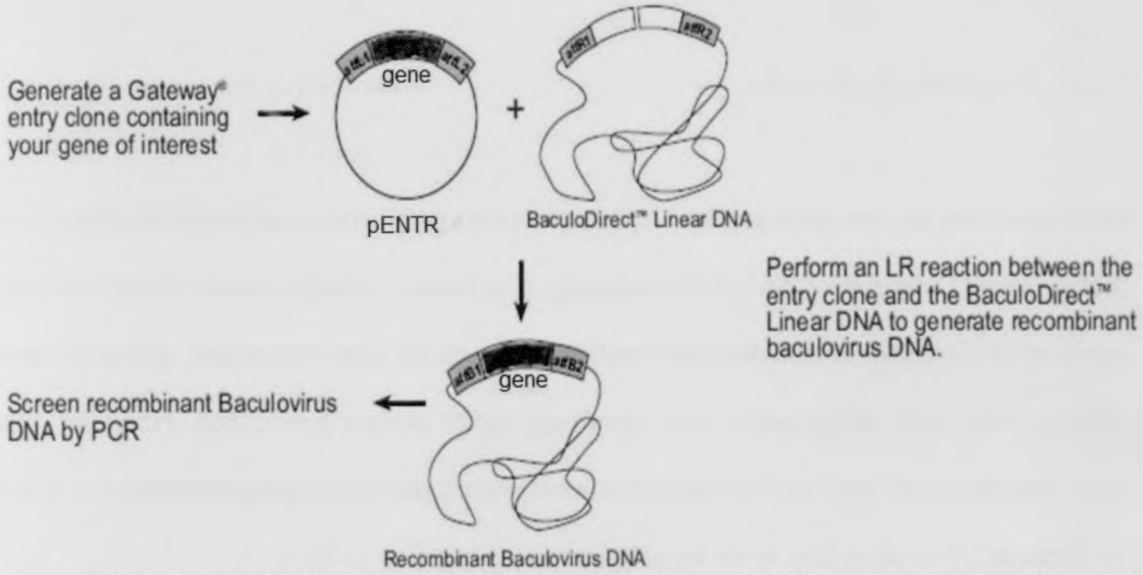

Figure 2.8. A schematic diagram of the workflow for cloning HMPV genes into pENTR entry vector followed by topoisomerase recombination. This image was modified from the BaculoDirect Baculovirus Expression System instruction manual (Invitrogen, USA). Bac-GA, and bac-N were constructed using this method.

2.7.3 Storage of clones

Once the clones for the bacmids were confirmed by PCR and Western blot, the *E. coli* cells containing the constructs (pFasBacDual or pENTR) and the purified bacmid solutions can be stored at -80°C for future use.

2.7.4 Transfection of bacmids or recombinant baculovirus DNA

The recombinant baculovirus genes (bac-F, bac-GA, bac-M, bac-N and bac-$F_{\Delta TM}$) were transfected into Sf9 cells using CellFECTIN reagent (Invitrogen, USA) according to the manufacturer's instructions in 6-well plates. Once the transfection is completed, viral replication takes place like an actual virus infection. For the first 2-3 days post-infection, the budded virus was extruded into the culture medium. The medium was harvested 3 days post-infection and used to infect fresh Sf9 cells in 6-well plates to produce the first generation progeny virus (P1). A second generation progeny virus (P2) was prepared in the same way. Subsequently, the P2 virus could be be used for plaque purification to obtain the correct clones.

2.7.5 Preparing virus stocks

Once the virus clones were purified by plaque purification (see section 2.6.3), the virus stocks could be prepared by propagating the virus in flasks until the P2 or P3 generation. The media was then harvested into a 15 ml tube. A second round of virus plaque assay was performed in the same way as for plaque purification. However, this time, the virus titre was calculated based on the number of plaques formed (see 2.6.3 for formula). The virus titre is necessary for the calculation of MOI.

The virus titres for the various virus stocks were determined to be:

Bac-F: 4.0×10^7 PFU/ml Bac-GA: 1.65×10^7 PFU/ml

Bac-M: 1.5×10^7 PFU/ml Bac-N: 6.6×10^7 PFU/ml Bac-$F_{\Delta TM}$: 1×10^7 PFU/ml.

2.8 Analysis of protein expression in insect cells

Most of the methods used for the analysis of protein expression in insect cells were identical to those used for mammalian expressed proteins. Two main exceptions were the time-course experiment, which determines the optimal time of incubation for best expression, and the MOI experiment which determines the optimal MOI to be used.

2.8.1 Harvesting insect cells for Western blot

After the cells were incubated for 2 days, they were harvested by either gentle spraying of the media or with a cell scraper. The cells were centrifuged at 3000g to remove the supernatant and 1x Laemmli buffer was added. The cells were then heated at 100°C for 10 min and sonicated. The Western blot protocols were identical to theose described in section 2.5.3.

2.8.2 Time-course experiment

The time-course experiment was carried out by infecting Sf9 and HighFive cells at M.O.I=1 and incubating the cells for 1, 2 and 3 days. Western blot was used to determine the incubation time which produced the best expression levels.

2.8.3 Determining optimal multiplicity of infection (MOI)

The MOI experiment was also carried out by infecting Sf9 and HighFive cells. This time, the number of days before harvesting was set according to the results from the time-course experiment. Cells were infected at MOI values of 1, 5 and 10. Western blot was performed to determine the optimal MOI to be used.

2.8.4 Immunofluorescence and confocal microscopy

Cells were seeded on coverslips (refer to 2.5.10) for 1 hour and infected with the various bacmids for 1 hour. The cells were then left overnight at 28°C. The next day, the cells were fixed with methanol/acetone (1:1) and stained according to the methods in section 2.5.10. Confocal microscopy was also performed in the same way as in section 2.5.11.

2.8.5 Western blot analysis

Western blot was performed on harvested insect cells in a similar way to section 2.5.4. The glycosylation analysis of insect cell-expressed proteins was also carried out in the same way as in section 2.5.5.

2.8.6 Radiolabeling of proteins

The HMPV proteins expressed by insect cells were analysed by radiolabeling with ^{35}S. After 24 hours post-infection in a 60 mm dish, the media was replaced with methionine and cysteine-free SF-900 II SFM (Invitrogen, USA). Radiolabelling with ^{35}S was performed by adding the isotope at the concentration of 100 µCi/dish. The cells were harvested and subsequently subjected to SDS-PAGE.

2.9 Virus-like particle analysis

2.9.1 Labeling cells with gold particles

Cells expressing HMPV proteins were prepared in the same way as for immunofluorescence microscopy. After overnight infection, the cells were fixed with 0.1% glutaraldehyde in PBS overnight at room temperature. The next day, the cells were washed 3 times with PBS, the primary anti-FLAG antibodies were added (1:100) and incubated for 4 hours at room temperature. The coverslips were washed 3 times with PBS and incubated with a secondary anti-rabbit antibody conjugated to colloidal gold (10 nm) particles (Sigma-Aldrich, USA) for 4 hours at room temperature. After washing 3 times with PBS, the cells were placed in a final fixative of 2.5% glutaraldehyde overnight at room temperature. The coverslips were then subjected to critical point drying and carbon-coated.

2.9.2 Field emission scanning electron microscopy

Viewing of the samples was performed on a JSM 7000 series field emission scanning electron microscope (FE-SEM) (JEOL, Japan) at 5 kV. Images were taken at various magnifications ranging from 20,000x to 100,000x. Both

secondary electron image (to show topology) and backscatter image (to show the gold particles) were collected and these could be superimposed into a combined image.

2.9.3 Removing VLP filaments from the cell surface

The mechanical shearing method was performed by douncing the cell suspension in a 1 ml dounce homogenizer for 40 times. The freeze-thaw method was performed by dipping the cell suspension into an ethanol-dry ice mixture until the liquid was frozen, then quickly immersing the frozen cells into a 37°C water bath until the suspension thawed. Three cycles of freeze-thaw were used.

2.9.4 Ultracentrifugation of virus-like particles

The protocol for ultracentrifugation of VLPs was the same as that for the F and G protein studies except for a few conditions. All ultracentrifuging was performed at 200,000g at 4°C. The discontinuous sucrose gradient was prepared by layering three solutions of 20%, 50% and 60% sucrose. Discontinuous gradients were centrifuged for 1 hour. Continuous sucrose gradients were prepared by layering solutions of 10% to 60% in 5 % intervals and left to equilibrate overnight before use. Continuous gradients were centrifuged for 18 hours. All sucrose solutions were prepared in TEN (10 mM Tris-Cl pH 8, 0.1 mM EDTA, 100 mM NaCl) buffer.

2.10 Reagent List

2.10.1 General Reagents

All general reagents used in this experiment were of analytical grade obtained from Sigma Adrich, Becton-Dickinson, Bio-Rad, Invitrogen, USB Corp., QIAGEN, unless

otherwise stated. For work where sterility was required, all of the reagents were either autoclaved at 121 °C for 20 min or filter-sterlilised through a 0.22 µm membrane. (Nalgene). Primers and probes for amplification were synthesised by either 1st Base, Singapore, AIT Biotech, Singapore or Proligo Singapore. Sequencing reactions were sent to either 1st Base or AIT Biotech, Singapore.

2.10.2 Cells and virus

HMPV clinical strain	A174, DSO, Singapore
HEK (human embryonic kidney) 293T	ATCC CRL11268, USA
Vero (African green monkey kidney) E6	ATCC CRL1586, USA
HEp-2 (human laryngeal carcinoma)	ATCC CCL23, USA
LLC-MK2 (Rhesus monkey kidney)	ATCC CCL7.1, USA
Sf 9 (*Spodoptera frugiperda*, fall armyworm)	Invitrogen, USA #11496
High Five (*Trichopulsia nii*, cabbage looper)	Invitrogen, USA #B855
Max Efficiency DH10Bac chemical competent cells	Invitrogen, USA #10361
Max Efficiency DH5α chemical competent cells	Invitrogen, USA #18258
One Shot TOP10 chemical competent cells	Invitrogen, USA #C4040
EZ competent cells (from PCR cloning plus kit)	Qiagen, USA #231224

2.10.3 Antibodies

Mouse anti-cmyc monoclonal antibody, 1:100 (immunofluorescense assay), 1:5000 (Western blot) Cell Signaling Technology, USA #2276

Rabbit anti-FLAG polyclonal antibody, 1:100 (immunofluorescence assay), 1:5000 (Western blot) Sigma-Aldrich, USA #F7245

Mouse anti-6His monoclonal antibody, 1:5000 (Western blot) GE Healthcare (Amersham), USA#27-4710-01

Mouse anti-M (HMPV) protein monoclonal antibody, neat (Western blot and immunofluorescence assay) Hybridoma clone #8A11,#3F8

Mouse anti-F (HMPV) protein monocloncal antibody, neat (Western blot and immunofluorescence assay) Gift from G. Toms, #F58

Mouse anti-F (hRSV) protein monoclonal antibody, neat (western blot and immunofluorescence assay) Commercial source

Goat anti-mouse IgG peroxidase conjugate, 1:10,000 (Western blot)
Sigma-Aldrich, USA #A4416

Goat anti-rabbit IgG peroxidase conjugate, 1:10,000 (Western blot)
Sigma Aldrich, USA #A0545

Goat anti-mouse IgG fluorescein conjugate 1:100 (immunofluorescence assay)
Sigma-Aldrich, USA #AP124F

Goat anti-rabbit IgG fluorescein conjugate 1:100 (immunofluorescence assay)
Sigma-Aldrich, USA #AP307F

Goat anti-rabbit IgG Alexa Fluor 555 conjugate 1:1000 (immunofluorescence assay)
Invitrogen, USA #A21428

Goat anti-mouse IgG Alexa Fluor 488 conjugate 1:100 (immunofluorescence assay)
Invitrogen, USA #A11001

2.10.4 Immunofluorescence reagents

Methanol:acetone, 1:1 (purchased separately)	Fisher Scientific, USA #1.00014.2500 and 1.106009.2500
Paraformaldehyde	ICN Biochemicals, Inc.
10X Phosphate-buffered saline pH 7.2	1st Base, Singapore #2041

2.10.5 Commercial kits

QIAamp Viral RNA Mini Kit	Qiagen, Germany #52906
QIAquick Gel Extraction Kit	Qiqgen, Germany #28706
QIAGEN PCR Cloning Plus Kit	Qiagen, Germany #231224
QIAGEN OneStep RT-PCR Kit	Qiagen, Germany #210212
QIAprep Spin Miniprep Kit	Qiagen, Germany #27106
HiSpeed Plasmid Midi Kit	Qiagen, Germany #12643
Platinum Taq DNA Polymerase	Invitrogen, USA #10966
Platinum Taq DNA Polymerase High Fidelity	Invitrogen, USA #11304

pENTR/SD/D-TOPO Cloning Kit	Invitrogen, USA #K242020

2.10.6 Cloning vector and *E. coli* growth media

pDrive (QIAGEN PCR Cloning Plus Kit)	Qiagen, Germany .#231224
pcDNA 3.1 (-)	Invitrogen, USA #V79520
pCAGGS	Gift from C.C. Broder
pFastBac Dual	Invitrogen, USA #10712
pENTR/SD/D-TOPO	Invitrogen, USA #K242020
LB (Luria-Bertani) Broth, Miller	LB powder containing 100 µg/ml ampicillin in 1 L water (Becton-Dickinson, Difco, USA #244620)
LB (Luria-Bertani) Agar, Miller	LB broth plus 1% agarose and 100 µg/ml ampicillin (Becton-Dickinson, Difco, USA #244520)
LB plate for blue/white colony screening	100 µl of 0.1 M IPTG (Fermentas, EU) and 250 µl of 40 mg/ml X-Gal (Fermentas, EU) were spread on the plate and incubated in 37°C for 1 hour. Plates were prepared fresh.
Ampicillin sodium salt	Fluka, Switzerland #10044
SOC Medium	Invitrogen, USA #15544034

2.10.7 Mammalian cell culture media

Cell Propagation Medium	DMEM+GlutaMAX(Gibco, USA) supplemented with 10% (v/v) fetal bovine serum (Gibco, USA) and Penicillin 100 UI/ml and Streptomycin 100 µg/ml (Gibco, USA)
Transfection medium	DMEM+GlutaMAX(Gibco, USA) supplemented with 10% (v/v) fetal bovine serum (Gibco, USA)
Dulbecco's modified Eagle medium+ GlutaMAX, 1X high glucose	Invitrogen, USA #10569
Heat-inactivated foetal bovine serum	Invitrogen, USA #10500
Phosphate buffered saline pH 7.2, 1X	Invitrogen, USA #20012
Penicillin-Streptomycin 100X (10,000 IU Penicillin and 10,000 µg Streptomycin)	PAA Laboratories #P11-010

Trypsin-EDTA 0.25% 1X	Invitrogen, USA #25200
Trypsin TCPK(L-1-tosylamido-2-phenylethyl chloromethyl ketone)-treated	Worthington, USA

2.10.8 Insect cell culture media

Cell propagation medium	SF-900 II SFM (serum-free medium) (Invitrogen, USA) supplemented with 10% (v/v) Fetal Calf Serum (Gibco, USA) and Penicillin 100 UI/ml and Streptomycin 100 µg/ml (Gibco, USA)
Cell overlay medium	9 ml of SF-900 II SFM (serum-free medium) (Invitrogen, USA) supplemented with 10% (v/v) Fetal Calf Serum (Gibco, USA) and Penicillin 100 UI/ml and Streptomycin 100 µg/ml (Gibco, USA) 3 ml of 4% (w/v) low melting point (LMP) agarose (BioRad, USA) in deionised water.
SF-900 II serum free medium (SFM) 1X	Invitrogen, USA #10902
Heat-inactivated fetal bovine serum	Invitrogen, USA #10500
Penicillin-Streptomycin 100X (10,000 IU Penicillin and 10,000 µg Streptomycin)	PAA Laboratories #P11-010
Phosphate-buffered saline pH 7.2, 1X	Invitrogen, USA #20012

2.10.9 DNA Analysis

1x TBE (Tris-Borate-EDTA)	100 ml of 10x TBE dissolved in 900 ml of deionised water to make 1 L of 1x TBE stock (1st Base, Singapore).
0.1% Ethidium Bromide	10 mg of Ethidium Bromide (BioRad, USA) dissolved in 10 ml of water.
1% Agarose gel	0.5 g of Agarose (Fermentas, EU) in 50 ml of 1x TBE.

2.10.10 Protein Analysis by SDS-PAGE

15% Resolving Gel	1980 µl of 30% Acrylamide/Bis solution

	(37.5:1, 2.6% C) (BioRad, USA #161-0158) 960 µl water 1000 µl Tris-Cl pH 8.8 (Promega, USA #H5135) 40 µl 10% SDS (sodium dodecyl sulphate) (BioRad, USA #161-0302) 40 µl 10% APS (ammonium persulfate) (Promega, USA #V3131) 4 µl TEMED (N,N,N,N-tetra methyl ethylenediamine) (BioRad, USA #161-0800)
12% Resolving Gel	1.6 ml of 30% Bis-Acrylamide (C : N = 1:29.9) 1.4 ml H2O 1 ml Tris-Cl pH 8.8 60 µl 10% SDS 60 µl 10% APS 6 µi TEMED
10% Resolving Gel	1.6 ml of 30% Bis-Acrylamide (C : N = 1:29.9) 1.4 ml H2O 1 ml Tris-Cl pH 8.8 60 µl 10% SDS 60 µi 10% APS 6 µl TEMED
4% Stacking Gel	266 µl of 30% Bis-Acrylamide (C : N = 1:29.9) 1333 µl H2O 375 µl Tris-Cl pH 6.8 15 µl 10% SDS 15 µl 10% APS 1.5 µl TEMED
Laemmli buffer 5x	31.25 ml 1M Tris-HCl pH 6.8 10 g SDS 25 ml Glycerol 750 µl Bromophenol Blue (2%) in ethanol 5 ml 2-mercaptoethanol Add ddH2O to 100 ml

Laemmli buffer 1x	Dissolve Laemmli buffer (5x) in deionised water in 1:5 ratio.
2-mercaptoethanol	(Merck, USA #8.05740.0250)
Isopropanol	(Merck, USA #1.09634.2500)

2.10.11 Western blotting

SDS-PAGE Running Buffer (1x)	57.6 g Glycine (BioRad, USA) 12 g Tris base (Sigma-Aldrich, USA) 4 g SDS (BioRad, USA) Add deionised water to 4 L
Transfer Buffer (1x)	3.03 g Tris base (BioRad, USA #161-0719) 14.41 g glycine (BioRad, USA #161-0718) 200 ml methanol (Fisher Scientific, USA) Deionised water to 1 L
1X PBS+0.05% Tween-20 (PBST)	100 ml of 10x PBS, 5 ml of 10% Tween-20, made up to 1 L with deionised water
5% (w/v) skimmed milk blocking solution	1 g skimmed milk powder in 20 ml PBST
Methanol	(Fisher Scientific, USA #1.106009.2500)
Ethanol	(Merck, Germany #1.00983.2500)
Glacial acetic acid	(Merck Germany #1.00063.2500)
10% Tween-20 (v/v) in water	(Amresco, USA #0777)

Chapter 3 Epidemiology of Respiratory Viruses in Singapore Children

Respiratory viruses are a major cause of morbidity in children worldwide. Even in developed countries like Singapore, preschool and school-going children frequently suffer from the effects of respiratory virus infection. Parents of ill children are more likely to bring them to a doctor compared to sick adults who may choose to self-medicate or allow the illness to run its course. Kandang Kerbau Women's and Children's Hospital (KKH) is the main paediatric hospital in Singapore which has more than 800 beds and boasts a wide range of medical specialities under one roof from neonatology to adolescent medicine, from oncology to infectious diseases, from endocrinology to reconstructive surgery. The children's emergency department sees more than 300-400 cases a day but not all patients require admission into hospital. The specimens collected for this study were from patients admitted to KKH for various respiratory-related symptoms. These include fever, cough, rhinitis, bronchiolitis, bronchitis, pneumonia, exacerbation of asthma, wheezing, pharyngitis, laryngitis and others. Samples were taken from the nasopharynx of patients which would give the best yield of cells infected by viruses. The laboratory in KKH uses a commercial kit to detect the presence of virus antigens in nasopharyngeal cells. This kit can only detect common viruses like influenza A/B virus, parainfluenza virus 1/2/3, hRSV and adenovirus. Although these viruses have been in the human population for many years, there are emerging viruses and "old" viruses which can also cause respiratory disease. One of the recently discovered viruses is human bocavirus (HBoV) which was discovered in human respiratory tissue in 2007 (Allander et al., 2005). In addition to HBoV, human coronavirus (HCoV) and human rhinovirus (HRV) which have been known for years to infect humans do not have readily available commercial reagents which can be used for detection in clinical samples. HRV is especially difficult because there are a large number of serotypes (about a hundred), making it very challenging to

design an assay which detects all serotypes. HMPV, HBoV, HCoV and HRV would require the use of PCR technology for detection. Even though the sensitivity of PCR is generally higher than that of antigen detection, it is expected that samples from symptomatic patients should still contain sufficient quantities of viral antigens to provide reliable results.

The aim of this chapter was to document the prevalence of respiratory viruses in Singapore children admitted to KKH for a variety of respiratory symptoms. Although the main focus of this study was HMPV, we took the opportunity to screen the patient specimens for some of the lesser known viruses. This would not only enable us to obtain clinical HMPV material with which to study the viral proteins, but also give us a more complete picture of the type of viruses which cause respiratory infections in children in Singapore.

3.1 The current situation in common respiratory virus infections

The results of the screening tests for the respiratory viruses are shown in Table 3.1. The nomenclature used for the clinical samples is SINyy-NTUxxx where "yy" denotes the last two digits of the year of isolation and "xxx" denotes a sequential sample number from 1 to 500 (refer to Appendix A for the complete sample list). It is important to note that the diagnosis indicated may not be the final one and the presence of a pathogen does not imply that it is the cause of the illness. Out of the 500 samples tested by the commercial immunofluorescence microscopy kit, the largest number of samples were positive for hRSV. This was detected in 59 samples (11.8%). Other viruses included parainfluenza 3 virus which was detected in 8 (1.6%) samples, influenza A virus and parainfluenza 1 virus both of which were detected in 4 (0.8%) samples, influenza B virus which was detected in 2 (0.4%) samples and adenovirus which was only found in 1 (0.2%) sample. Many studies have shown that hRSV is one of the most commonly isolated viruses in children. Freymuth (Freymuth et al., 2006)

detected hRSV in 43.6% of 263 children with respiratory disease. In addition, they found 8.8% infected with influenza viruses, 3.2% infected with parainfluenza viruses and 2.3% infected with adenoviruses. Templeton (Templeton et al., 2004) detected hRSV in 18.4% of 358 clinical specimens. They also tested the specimens for influenza A/B and parainfluenza viruses 1/2/3/4. These other viruses were only found in 1-2% of the specimens. Lee (Lee et al., 2007a) detected hRSV in about 12.6% of 103 samples and also detected between 1-5% of other respiratory viruses like influenza A/B, parainfluenza 1/3/4, and adenoviruses. Kuypers (Kuypers et al., 2006) tested 1138 clinical samples for common respiratory viruses. A combination of fluorescence microscopy and nucleic acid amplification tests detected hRSV in 20.8% of the samples, influenza A virus in 10.1%, parainfluenza viruses and adenoviruses in 1-4%. Based on the commercial kit used in our study, only 15.6% of the (78/500) samples tested positive for any of the seven common respiratory viruses listed in Table 3.1. Our positive detection rates are very similar to those from the four above-mentioned studies. There were no cases of multiple infections within the seven different viruses. This relatively poor detection rate is typical of immunofluorescence microscopy-based assays which have been shown to have sensitivities between 30-80% (Freymuth et al., 2006; Kuypers et al., 2006; Lee et al., 2007a; Templeton et al., 2004) compared to nucleic acid amplification-based assays like PCR. The reason for this large variation is mostly due to human factors like the technical skill and fluorescence interpretation of the medical technologist in the hospital laboratory. Improved skills and interpretation ability can only be achieved over years of experience. Not surprisingly, the use of recently developed but non-commercial PCR techniques detected another 27.2% (136/500) samples positive for other respiratory viruses not examined by the commercial kit.

	No. of Positives	% Positive
Respiratory syncytial virus	59	11.8
Influenza A virus	4	0.8
Influenza B virus	2	0.4
Parainfluenza 1 virus	4	0.8
Parainfluenza 2 virus	0	0
Parainfluenza 3 virus	8	1.6
Adenovirus	1	0.2
*Metapneumovirus	29	5.8
*Bocavirus	40	8.0
*Coronavirus	3	0.6
*Rhinovirus	64	12.8
Total (n=500)	**214**	**42.8**

Table 3.1. Results of the combined respiratory virus screening tests. The first seven viruses were detected by the commercial immunofluorescence microscopy kit using standard hospital protocols. The last four viruses (denoted by *) were detected by (reverse-transcription and) polymerase chain reaction depending on the type of nucleic acid in the virus.

Among these, there were 19 cases of dual infections. Nucleic acid amplification methods are less affected by the skill of the individual medical technologist (although a clear understanding of proper PCR workflow is necessary to prevent potentially disastrous amplicon contamination of the entire work area) and are gaining popularity as the method of choice in the modern diagnostic laboratory.

3.2 Human metapneumovirus isolates

A total of 29 samples were found to be positive for the presence of HMPV which translates to a prevalence of 5.8%. Of these 29 samples, none were found to have co-infection with other respiratory viruses. The presence of HMPV RNA in the clinical samples was determined by a published real-time RT-PCR protocol by (Maertzdorf et

al., 2004) and uses the technology of the dual-labeled fluorescent probe (see Fig 3.1). The probe is an oligonucleotide which is complementary to the PCR target region between the forward and reverse primers. The 5'-end of the probe is labeled with a 6-carboxyfluorecein (6-FAM) molecule and the 3'-end is labeled with a Black Hole Quencher 1 (BHQ-1) molecule. The 6-FAM molecule absorbs light at wavelength 492 nm and emits light at wavelength 517 nm. The BHQ-1 molecule absorbs light between 480-580 nm. If a light source about 492 nm is emitted, the 6-FAM molecule absorbs and re-emits 517 nm light waves. The nearby BHQ-1 molecule absorbs the light resulting in very low or no fluorescence. During the extension phase, the Taq DNA polymerase extends the nucleotides from the primers until it reaches the dual-labeled probe.

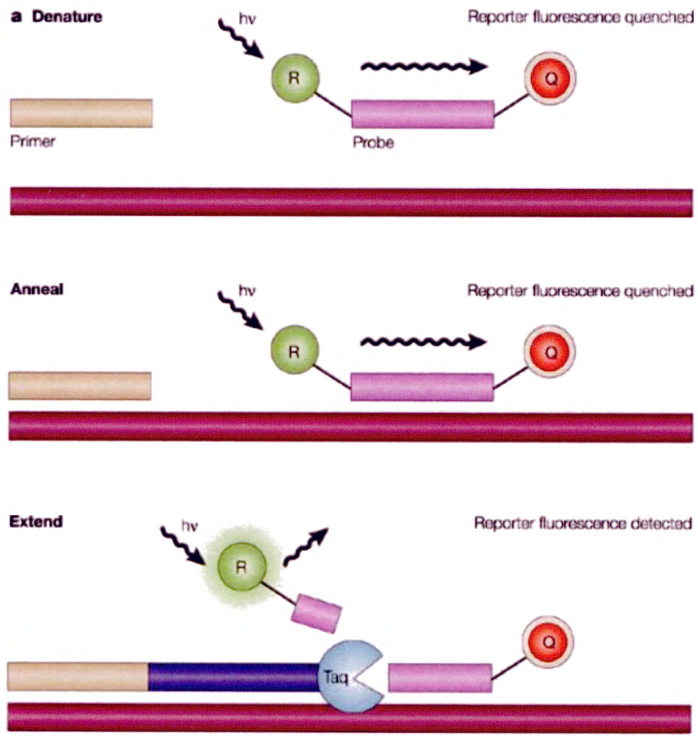

Figure 3.1. Illustration of the dual-labeled probe detection system for real-time polymerase chain reaction (adapted from (Koch, 2004)). The first step is denaturation where the primers and probe are not hybridized to the target DNA molecule. The second step is annealing where the primers and probe hybridise to the target DNA molecule. In the first two steps the proximity of the reporter (e.g. 6-FAM) and the quencher (e.g. BHQ-1) molecules results in little or no fluorescence. The third step is extension where the Taq DNA polymerase displaces the probe thereby releasing the reporter molecule to emit a second wavelength detectable by the instrument. R-reporter molecule, Q-quencher molecule, hv-incident light close to the absorption wavelength of the reporter molecule.

The 5'-3' exonuclease domain of the Taq DNA polymerase then cleaves the probe from the 5'-end to the 3'-end as it displaces and replaces the probe with a complementary DNA sequence. This releases the 6-FAM and BHQ-1 molecules into the solution. When the 6-FAM molecule is not in close proximity to the BHQ-1 molecule, any emitted fluorescence from the 6-FAM molecule will not be quenched and can be detected by the PCR instrument. The PCR instrument plots the graph of raw fluorescence versus cycle number. This graph is used to deduce the samples with positive amplification of HMPV RNA. The level of fluorescence in the reaction tube is proportional to the amount of free 6-FAM molecules which is proportional to the quantity of amplificons over the entire PCR run. The doubling of amplification products during PCR produces a sigmoidal curve (Fig 3.2). Negative samples do not show any increase in fluorescence. The instrument software then converts the graph of fluorescence versus cycle number to a graph of log fluorescence versus cycle number (Fig 3.3). This second graph is used to determine the cycle threshold (Ct) value that is usually within the exponential phase of the curve and can be used to estimate the starting amount of target (HMPV) RNA in the sample. Since a greater amount of starting RNA in the sample will result in a more rapid increase in PCR amplicons, the Ct value is therefore inversely proportional to the starting amount of target (HMPV) RNA.

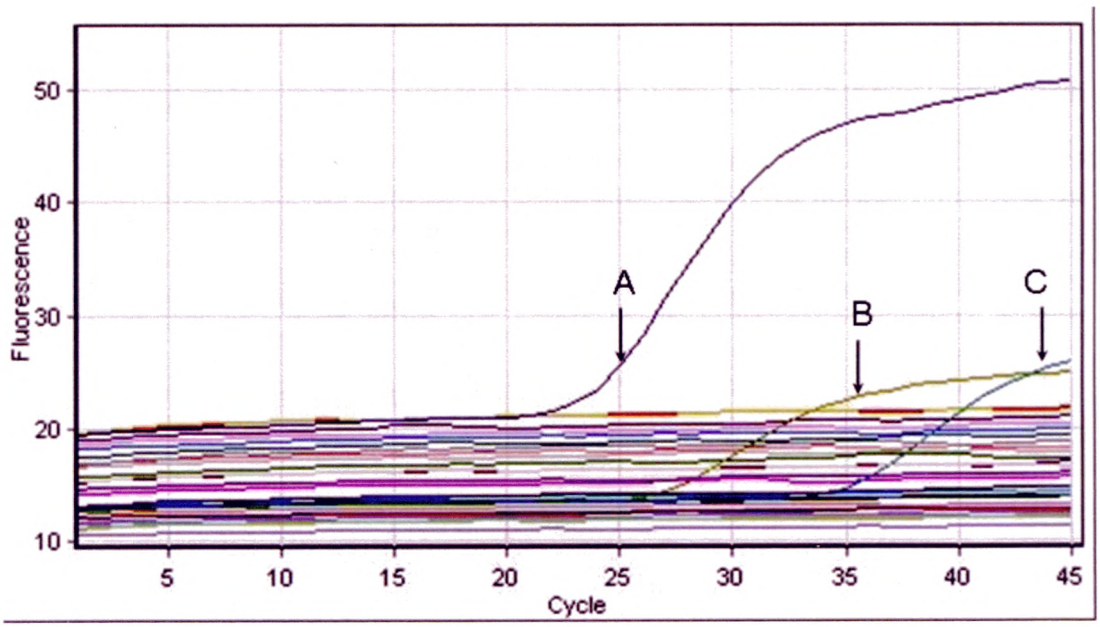

Figure 3.2. Real-time RT-PCR graph of fluorescence versus cycle number. Arrows A, B and C show 3 specimens positive for HMPV due to the increase in fluorescence levels. All the other specimens are negative as shown by the horizontal lines.

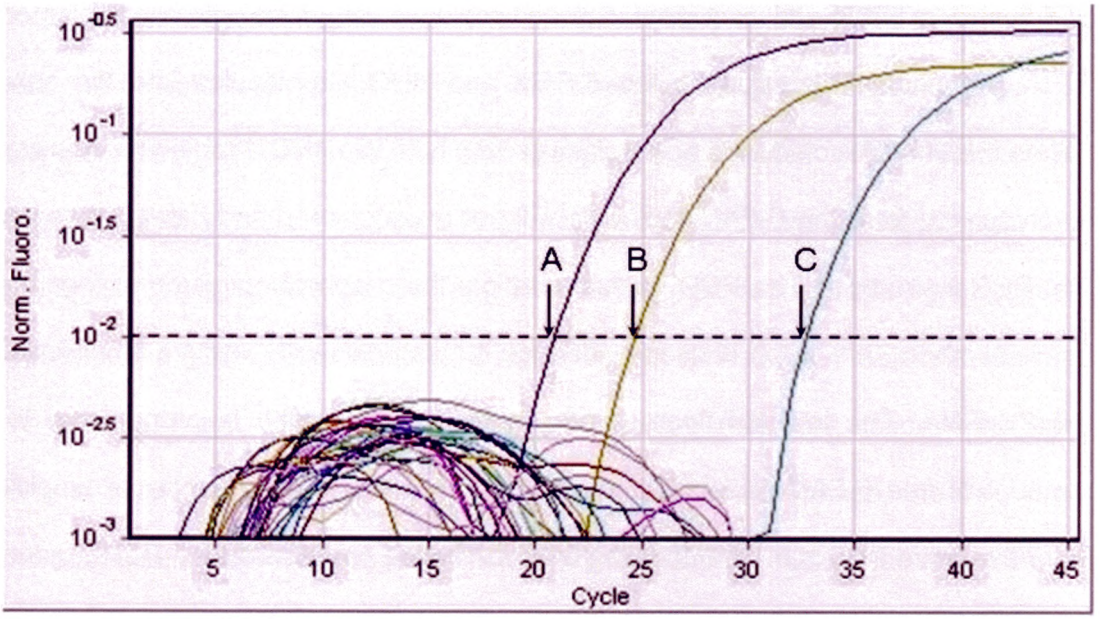

Figure 3.3. Real-time RT-PCR graph of log fluorescence versus cycle number (adapted from (Sugrue et al., 2008)). The dotted line shows the fluorescence level set as the threshold for positive amplification. Arrows A, B and C indicate 3 specimens positive for HMPV with Ct values of 20.9, 24.6 and 32.6 respectively.

The results for the screening of the 500 clinical samples, part of which have been published (Loo et al., 2007), are detailed in Appendix A. Of the total number of HMPV positive samples, 11 (37.9%) of the patients had infections of the upper respiratory tract [10 URTI, 1 pharyngitis], 9 (48.2%) had infections of the lower respirtory tract [2 chest infection, 3 bronchitis, 3 bronchiolitis, 1 pneumonia], 5 had asthmatic/wheezing conditions and the remaining 4 (13.8%) had either fits or fever. There was no predominant symptom among the patients with HMPV infection. Table 3.2 below shows the details of the HMPV isolates including their specimen number, diagnosis, HMPV genogroup and presence (if any) of other respiratory viruses in the same specimen.

Specimen number	Age group	Diagnosis indicated	PCR Ct value	HMPV geno group	Specimen number	Age group	Diagnosis indicated	PCR Ct value	HMPV geno group
SIN05-NTU14	1-3	Bronchiolitis	24.6	A2	SIN06-NTU272	3-10	URTI	21.9	B2
SIN05-NTU29	1-3	Febrile fit	34.8	A2	SIN06-NTU273	1-3	URTI	22.0	B2
SIN05-NTU50	<1	URTI	26.6	A2	SIN06-NTU277	3-10	URTI	23.8	B2
SIN05-NTU51	1-3	Bronchiolitis	34.9	A2	SIN06-NTU289	1-3	Bronchitis	26.4	A2
SIN05-NTU52	1-3	Pharyngitis	24.3	A2	SIN06-NTU384	1-3	Chest infection	20.4	A2
SIN05-NTU70	<1	Infantile pyrexia	18.4	A2	SIN06-NTU398	3-10	Asthma	19.6	B2
SIN05-NTU84	<1	URTI	28.7	A2	SIN07-NTU401	3-10	Acute bronchitis	31.5	A2
SIN05-NTU101	1-3	Bronchiolitis	31.9	A2	SIN07-NTU423	3-10	URTI	19.9	A2
SIN05-NTU102	1-3	Pneumonia	31.5	A2	SIN07-NTU442	3-10	Asthma	29.0	A2
SIN05-NTU135	1-3	URTI	21.3	B2	SIN07-NTU461	3-10	URTI	20.9	B1
SIN06-NTU187	<1	Wheezing	24.1	A2	SIN07-NTU480	3-10	Fever	24.6	A2
SIN06-NTU217	<1	Asthma	26.0	B1	SIN07-NTU481	3-10	URTI	32.6	A2
SIN06-NTU224	1-3	URTI	29.9	B2	SIN07-NTU489	3-10	Febrile fit	35.0	ND
SIN06-NTU232	1-3	Acute bronchitis	23.8	A2	SIN07-NTU495	3-10	Asthma	24.1	A2
SIN06-NTU271	>10	Chest infection	19.4	A2					

Table 3.2. All 29 HMPV clinical isolates. The specimen number is abbreviated from the original SINyy-NTUxxx format to show the running sample number only. The age group, clinical diagnosis, genogroup classification and co-infection viruses (if any) are also included in the table. Genogroup classification derived from P gene sequence analysis. ND-not determined.

Among the HMPV isolates, the first gene to be sequenced was the P gene. All the P genes from the clinical isolates were successfully amplified and sequenced except for isolate number SIN07-NTU489. The most probable reason for this was the low starting amount of target HMPV RNA in the clinical sample as indicated by the Ct value for the real-time RT-PCR which was 35.0. This was the highest value among the positive

HMPV isolates and suggests that the amount of starting HMPV RNA in that sample was close to the limit of detection for the test method. This observation is in agreement with similar test protocols employed by the Department of Pathology and Laboratory Medicine in KKH. Almost the entire P gene (884 bases) of the 28 remaining HMPV isolates were sequenced. The 21 sequences used in the 2007 publication (Loo et al., 2007) were submitted to GenBank under the accession numbers EF409351 to EF409371. Only the first 182 nucleotides of the P gene were used for the actual sequence analysis based on an earlier publication by (Mackay et al., 2004) The authors concluded that the sequence information obtained from the first 182 bases was sufficient to properly classify the four subgenogroups of HMPV. Our own phylogenetic analyses revealed that 20 isolates were assigned to the A2 subgenogroup, 6 to the B2 subgenogroup and 2 to the B1 subgenogroup. None of the HMPV isolates belong to the A1 subgenogroup. The phylogenetic trees of P (Fig 3.4), F (Fig 3.5), G (Fig 3.6), N (Fig 3.7) and M (Fig 3.8) genes are shown in the subsequent pages. Not all the N, M, F and G genes from the clinical strains of HMPV were amplified successfully. There were only 2 sequences of N genes (GenBank JQ309641 to JQ309642), 28 sequences of P genes (GenBank EF409351 to EF409371, JQ309666 to JQ309672), 23 sequences of M genes (GenBank JQ309643 to JQ309665), 16 sequences of F genes (GenBank EF397618 to EF397633) and 10 sequences of G genes (GenBank JQ309673 to JQ309682). This could have been due to factors such as minor variations in the PCR target region, sub-optimal reaction conditions or low numbers of target RNA in the clinical material. Despite having sequenced less than the expected number of HMPV genes, the results of the 4 phylogenetic trees clearly show that the genogrouping pattern is consistent among the different genes used for phylogenetic analysis. This observation is consistent with the fact that the HMPV genome is non-fragmented and not liable to re-assort like orthomyxoviruses (Kaverin, 2010). It is, therefore, unlikely that the genogrouping pattern of the HMPV isolates will be different based on different gene sequences. Based on the information from Table 3.2, there was no apparent difference in severity between the patients infected with HMPV genogroup A or B. Only

one sample (SIN05-NTU102) was obtained from a patient diagnosed with pneumonia which is the most severe condition in this group. HMPV genogroup A2 was isolated from this patient. However, this single severe case of HMPV A2 infection is not sufficient to be congruent with the observation by (Vicente et al., 2006). None of the patients infected with HMPV genogroup B had severe symptoms but again, there is unsufficient data to draw any conclusions. Since none of the HMPV positive samples were correspondingly infected with another respiratory virus, no conclusion about the increased severity of HMPV co-infection can be reached in this study. Infection of children with HMPV seems to be evenly spread throughout the different age groups but seldom occurs in those above 10 years old. The more severe conditions appear to manifest in children in the 1-3 year-old age group but this requires the analysis of a larger number of positive cases.

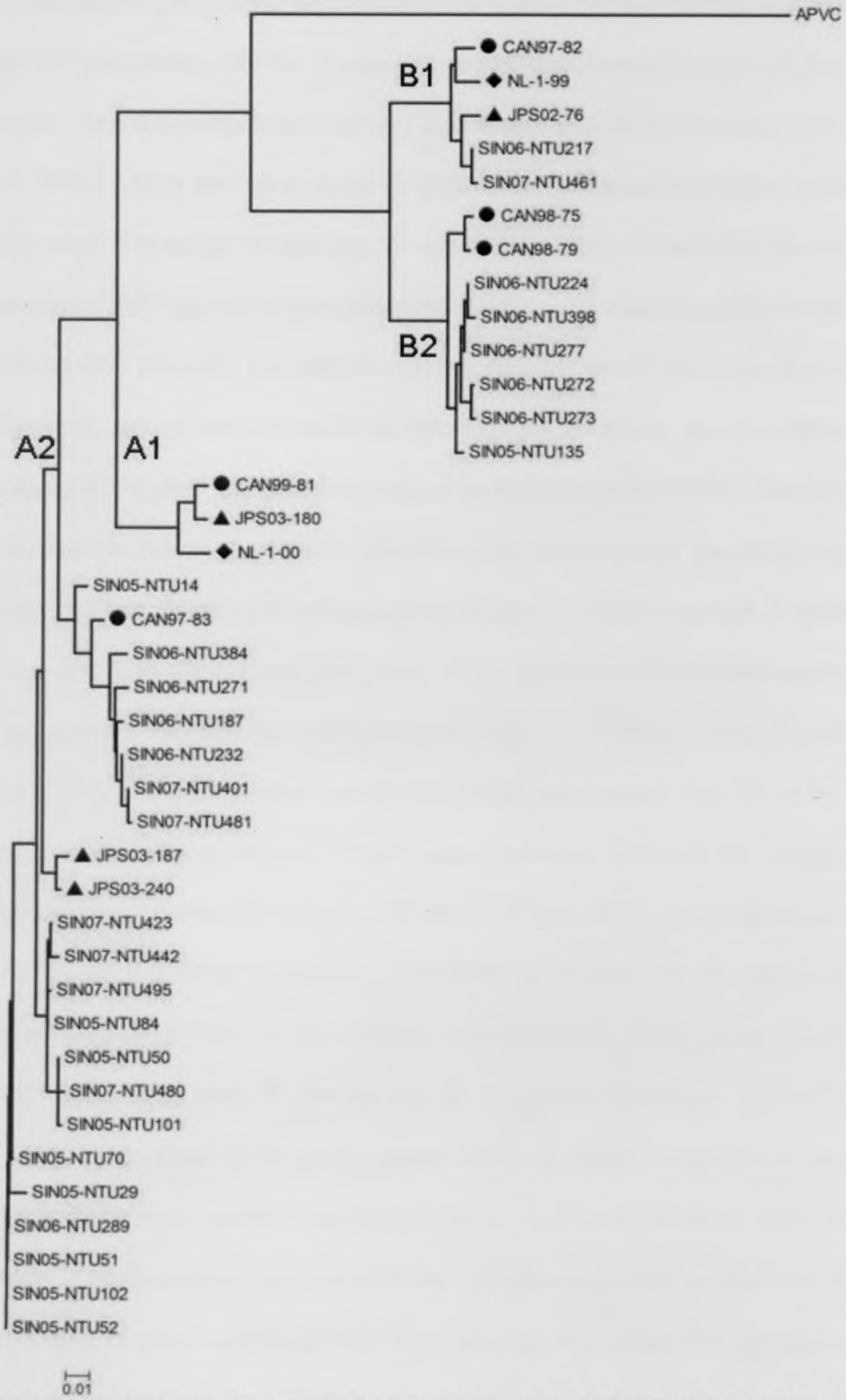

Figure 3.4. Phylogenetic relationship of P gene sequences of 28 HMPV isolates. Canadian strains [CAN97-82 GenBank AY145250, CAN97-83 GenBank AY297749, CAN98-75 GenBank AY297748, CAN98-79 GenBank AY145248, CAN-99-81 GenBank AY145249] are indicated by (●). Dutch strains [NL-1-99 GenBank AY525843, NL-1-00 GenBank AF371337] are indicated by (♦). Japanese strains [JPS02-76 GenBank AY530089, JPS03-180 GenBank AY530092, JPS03-187 GenBank AY530093, JPS03-240 GenBank AY530095] are indicated by (▲). HMPV isolates from this study are designated as SINyy-NTUxxx where "yy" is the year of isolation, "xxx" is the specimen number, SIN and NTU are abbreviations for Singapore and Nanyang Technological University respectively. Avian pneumovirus C (APVC) [GenBank AY590688] is used as an outgroup. A1, A2, B1 and B2 indicate the HMPV genogroups.

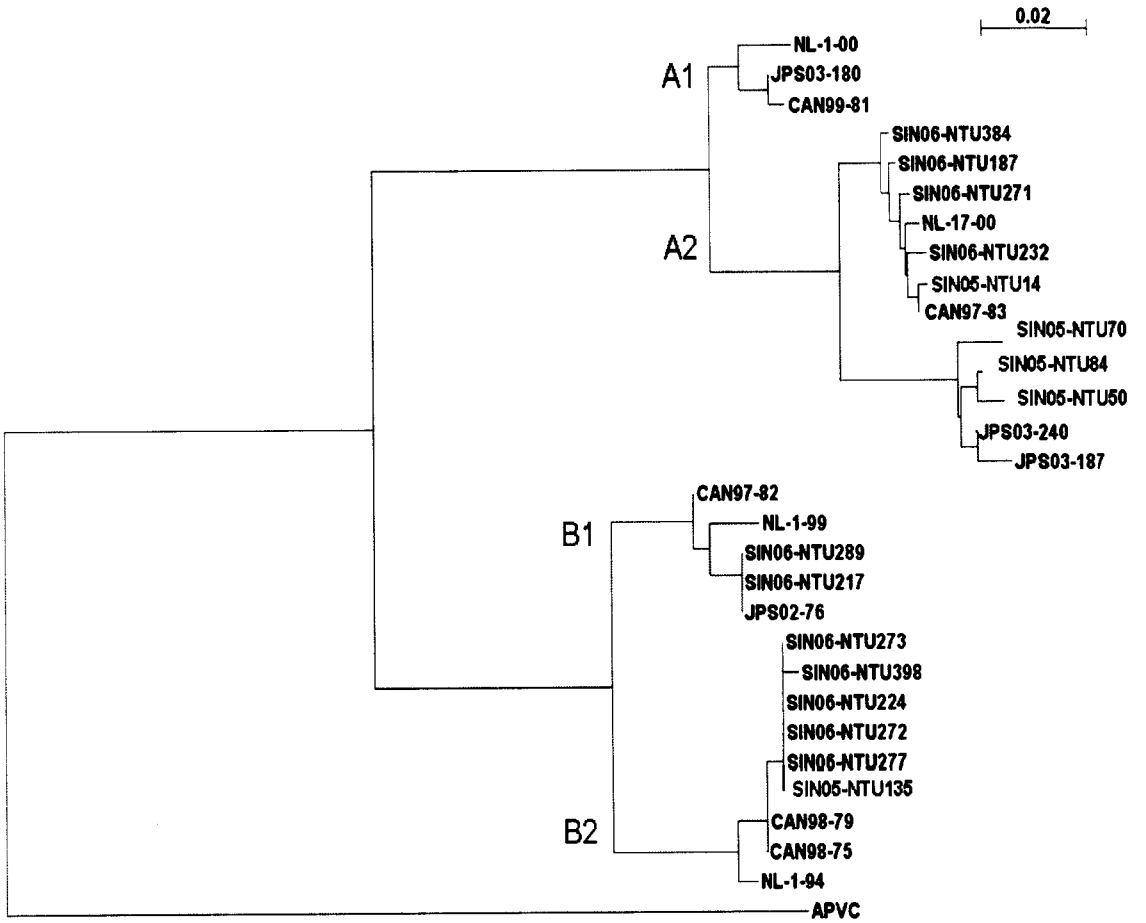

Figure 3.5. Phylogenetic tree of successfully sequenced HMPV F genes. Canadian strains are indicated by prefix CAN [CAN97-82 GenBank AY145295, CAN97-83 GenBank AY297749, CAN98-75 GenBank AY297748, CAN98-79 GenBank AY145293, CAN-99-81 GenBank AY145294]. Dutch strains are indicated by prefix NL [NL-1-94 GenBank AY304362, NL-1-99 GenBank AY525843, NL-1-00 GenBank AF371337, NL-17-00 GenBank AY304360]. Japanese strains are indicated by prefix JPS [JPS02-76 GenBank AY530089, JPS03-180 GenBank AY530092, JPS03-187 GenBank AY530093, JPS03-240 GenBank AY530095]. HMPV isolates from this study are written as SINyy-NTUxxx as explained under Fig 3.4. Avian pneumovirus type C (APVC) [GenBank AY590688] is used as an outgroup. A1, A2, B1 and B2 indicate the HMPV genogroups.

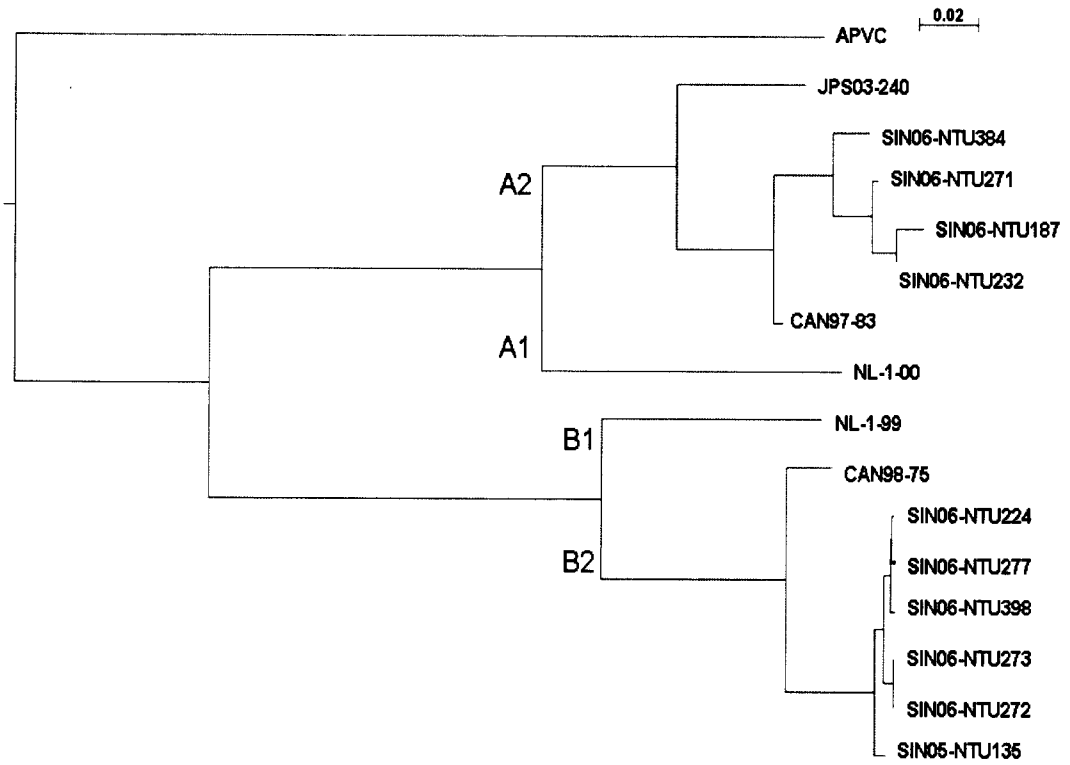

Figure 3.6. Phylogenetic tree of successfully sequenced HMPV G genes. Canadian strains are indicated by prefix CAN [CAN97-83 GenBank AY297749, CAN98-75 GenBank AY297748]. Dutch strains are indicated by prefix NL [NL-1-99 GenBank AY525843, NL-1-00 GenBank AF371337]. The Japanese strain is indicated by prefix JPS [JPS03-240 GenBank AY530095]. HMPV isolates from this study are written as SINyy-NTUxxx as explained under Fig 3.4. Avian pneumovirus type C (APVC) [GenBank AY590688] is used as an outgroup. A1, A2, B1 and B2 indicate the HMPV genogroups.

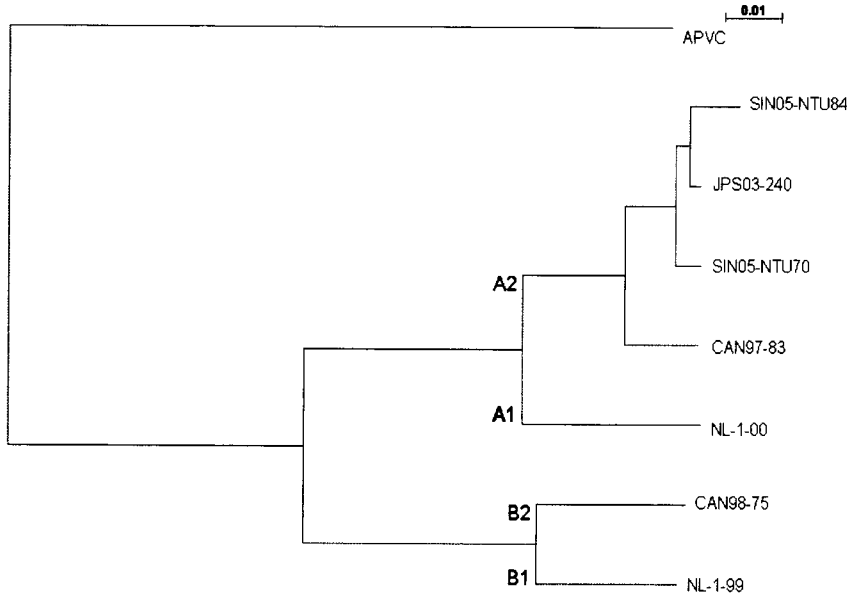

Figure 3.7. Phylogenetic tree of successfully sequenced HMPV N genes. Canadian strains are indicated by prefix CAN [CAN97-83 GenBank AY297749, CAN98-75 GenBank AY297748]. Dutch strains are indicated by prefix NL [NL-1-99 GenBank AY525843, NL-1-00 GenBank AF371337]. Japanese strains are indicated by prefix JPS [JPS03-240 GenBank AY530095]. HMPV isolates from this study are written as SINyy-NTUxxx as explained under Fig 3.4. Avian pneumovirus type C (APVC) [GenBank AY590688] is used as an outgroup. A1, A2, B1 and B2 indicate the HMPV genogroups.

Figure 3.8. Phylogenetic tree of successfully sequenced HMPV M genes. Canadian strains are indicated by prefix CAN [CAN97-83 GenBank AY297749, CAN98-75 GenBank AY297748]. Dutch strains are indicated by prefix NL [NL-1-99 GenBank AY525843, NL-1-00 GenBank AF371337]. Japanese strains are indicated by prefix JPS [JPS03-240 GenBank AY530095]. HMPV isolates from this study are written as SINyy-NTUxxx as explained under Fig 3.4. Avian pneumovirus type C (APVC) [GenBank AY590688] is used as an outgroup. A1, A2, B1 and B2 indicate the HMPV genogroups.

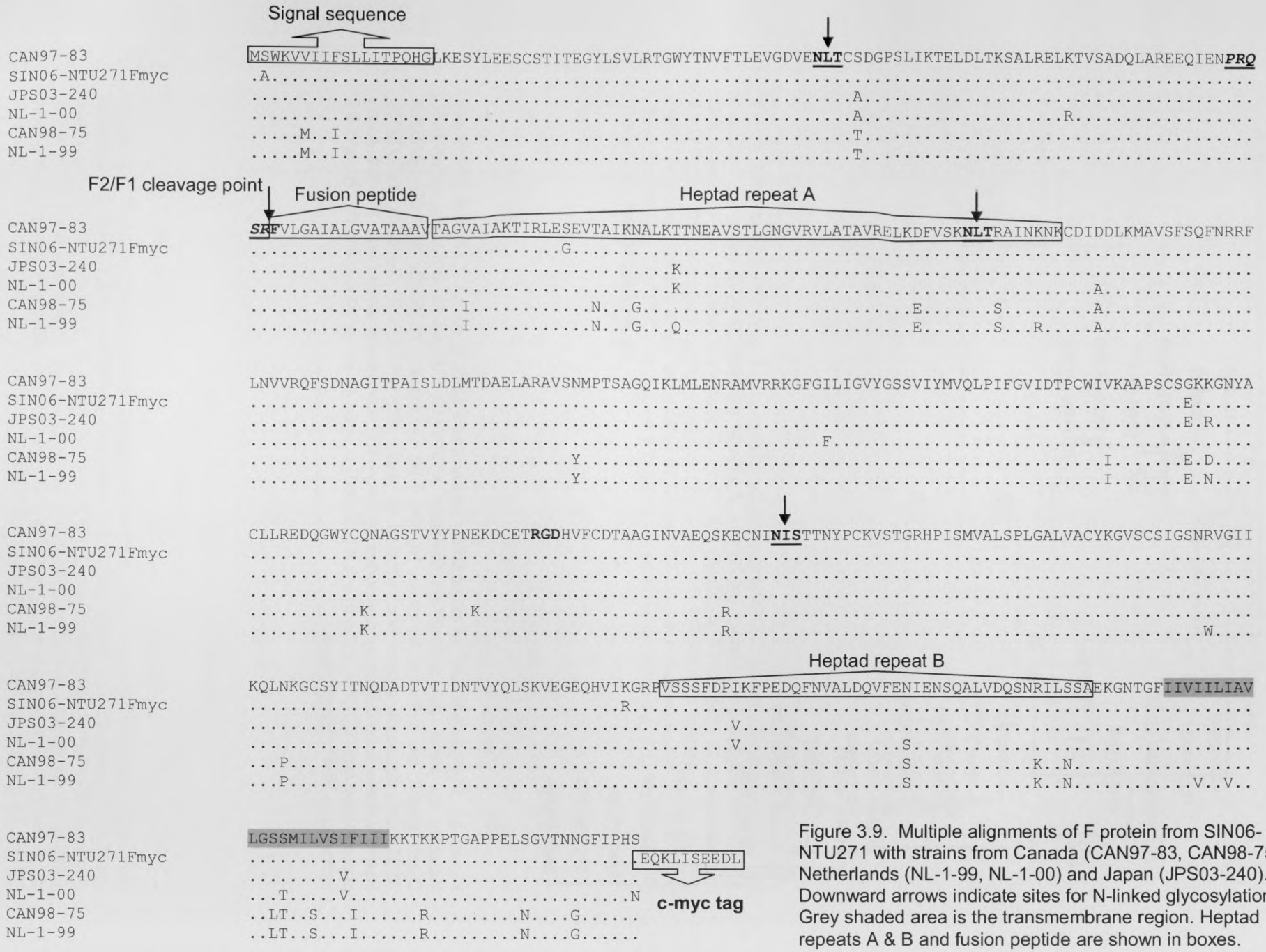

Figure 3.9. Multiple alignments of F protein from SIN06-NTU271 with strains from Canada (CAN97-83, CAN98-75), Netherlands (NL-1-99, NL-1-00) and Japan (JPS03-240). Downward arrows indicate sites for N-linked glycosylation. Grey shaded area is the transmembrane region. Heptad repeats A & B and fusion peptide are shown in boxes.

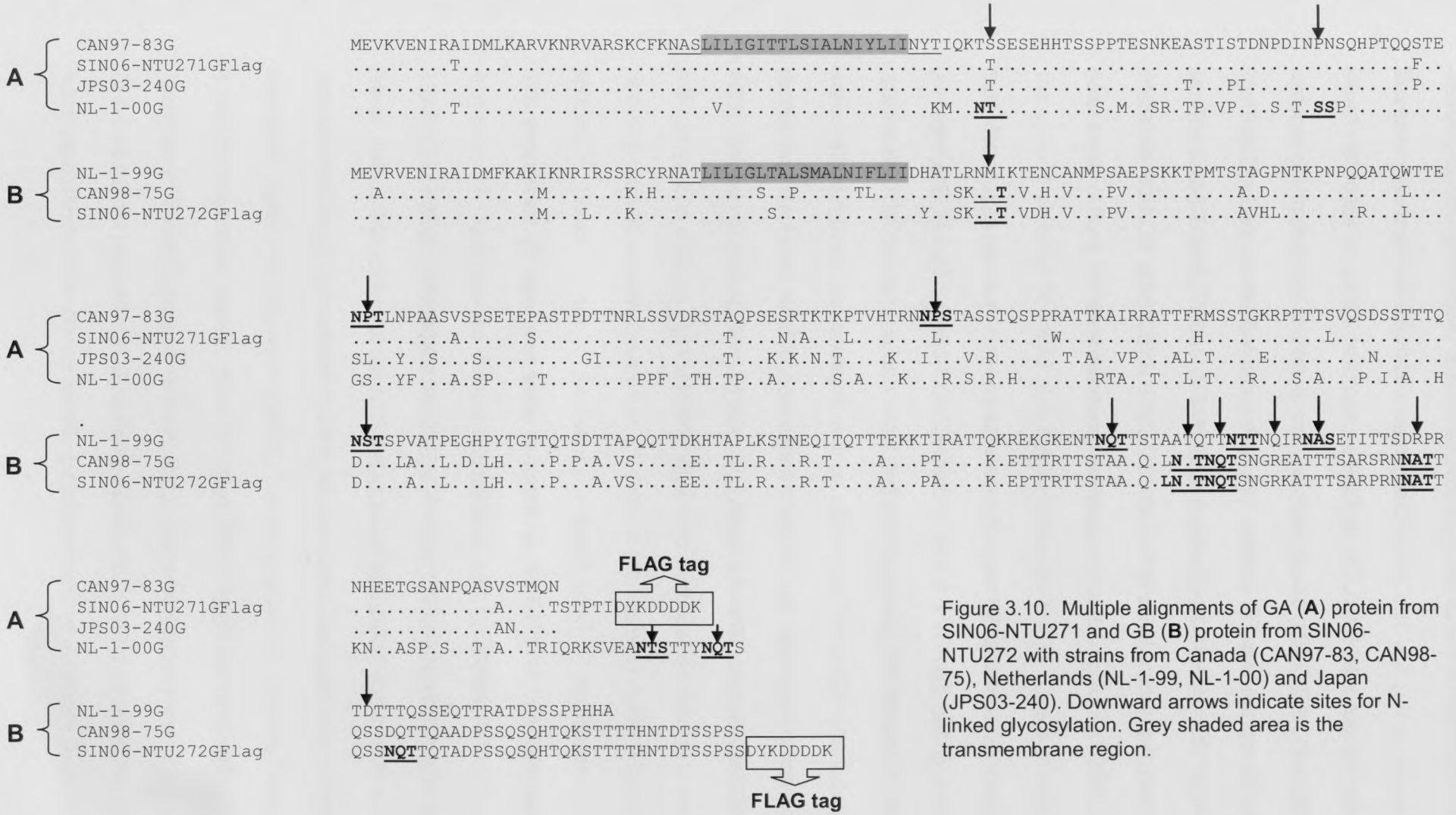

Figure 3.10. Multiple alignments of GA (**A**) protein from SIN06-NTU271 and GB (**B**) protein from SIN06-NTU272 with strains from Canada (CAN97-83, CAN98-75), Netherlands (NL-1-99, NL-1-00) and Japan (JPS03-240). Downward arrows indicate sites for N-linked glycosylation. Grey shaded area is the transmembrane region.

The detailed alignment of the amino acid sequence of F protein from isolate SIN06-NTU271 is shown in Fig 3.9. The detailed alignments of the amino acid sequences of GA protein from isolate SIN06-NTU271 and GB protein from isolate SIN06-NTU272 are shown in Fig 3.10. Both sets of alignments were obtained by comparison against published sequences of F and G proteins of isolates derived from Canada [CAN97-83 GenBank AY297749, CAN98-75 GenBank AY297748], Japan [JPS03-240 GenBank AY530095] and the Netherlands [NL-1-99 GenBank AY525843, NL-1-00 GenBank AF371337]. These two alignments provided the groundwork for the protein expression work in the next chapter.

The F protein of SIN06-NTU271 was aligned with known F protein sequences from representatives of the four genogroups including NL-1-99 (genogroup B1), NL-1-00 (genogroup A1), CAN98-75 (genogroup B2), CAN-97-83 (genogroup A2) and JPS03-240 (genogroup A2). Some of the motifs in the F protein of SIN0-NTU271 were identified by comparing with the known sequences. These included the signal sequence [MSWKVVIIFSLLITPQHG] which is known to facilitate the processing of the protein via the endoplasmic reticulum and Golgi; the cleavage location of a trypsin-like protease [PRQSR] which converts the inactive F_0 precursor molecule into the active F_1 and F_2 disulphide bond-linked molecule; the fusion peptide [FVLGAIALGVATAAAVTAGV] which is exposed after cleavage by the trypsin-like protease; the heptad repeats A [TAGVAIAKTIRLESEVTAIKNALKTTNEAVSTLGNGVRVLATAVRELKDFVSKNLTRAINKNK] and B [VSSSFDPIKFPEDQFNVALDQVFENIENSQALVDQSNRILSSA] which are important for the folding and fusion activity of the F protein and the transmembrane region of the protein [IIVIILIAVLGSSMILVSIFIII]. Finally, the three N-linked glycosylation sites were identified by the N-X-S/T motif. It was confirmed that the F proteins of all the genogroups were fairly conserved and greater than 90% identical. The F protein of SIN06-NTU271 had a c-myc peptide [EQKLISEEDL] added to the C-terminal to facilitate detection by immunoblotting and immunofluorescence. Since the F

proteins of HMPV are quite conserved, the F protein from SIN06-NTU271 was used in the subsequent protein expression experiments.

The G proteins of SIN06-NTU271 and SIN06-NTU272 were aligned with G protein sequences from representatives of the four main genogroups including NL-1-99 (genogroup B1), NL-1-00 (genogroup A1), CAN98-75 (genogroup B2), CAN-97-83 (genogroup A2) and JPS03-240 (genogroup A2). Some of the motifs in the G proteins of SIN06-NTU271 and SIN06-NTU272 were identified by comparing with the known sequences. These included the transmembrane domain [LILIGXXXXSXALNXXLII] and the various potential N-linked glycosylation sites [N-X-S/T]. The G proteins of both A and B genogroups were highly variable and shared less than 50% identity between genogroups. The G proteins of SIN06-NTU271 and SIN06-NTU272 had a FLAG peptide [DYKDDDDK] added to their C-terminal to facilitate detection by immunoblotting and immunofluorescence. The significant differences between the G proteins of the A and B genogroups prompted the use of both GA protein from SIN06-NTU271 and GB protein from SIN06-NTU272 for protein expression experiments.

3.3 Human bocavirus isolates

The prevalence of HBoV was found to be 8% (40/500) (Table 3.3). Of these 40 positive samples, 13 (32.5%) were detected in patients with upper respiratory tract infections [10 URTI, 3 laryngotracheobronchitis] while 14 (35%) were detected in patients with lower respiratory tract infections [3 bronchitis, 6 bronchiolitis, 4 pneumonia, 1 chronic lung disease], 6 (15%) had asthma and the remaining 7 (17.5%) were diagnosed with a variety of clinical conditions ranging from fever to gastritis to leukaemia. In addition, a total of 17 (42.5%) of the HBoV isolates were found in association with another respiratory virus in the same sample. Six isolates contained both HBoV and hRSV, 8 had both HBoV and HRV, 1 sample had both HBoV and parainfluenza 1 virus and 2 samples had both HBoV and parainfluenza 3 virus.

Specimen number	Age group	Diagnosis indicated	Other viruses present	Specimen number	Age group	Diagnosis indicated	Other viruses present
SIN05-NTU12	1-3	URTI	-	SIN06-NTU268	1-3	pneumonia	P3
SIN05-NTU22	<1	Febrile fit	-	SIN06-NTU275	3-10	asthma	-
SIN05-NTU46	<1	Bronchiolitis	-	SIN06-NTU290	1-3	bronchitis	P3
SIN05-NTU79	1-3	Herpangina	-	SIN06-NTU325	1-3	ALTB	P1
SIN05-NTU86	3-10	Asthma	-	SIN06-NTU328	<1	URTI	-
SIN05-NTU104	<1	Pneumonia	-	SIN06-NTU353	1-3	URTI	hRSV
SIN05-NTU150	1-3	?	-	SIN06-NTU371	3-10	bronchitis	-
SIN06-NTU159	1-3	bronchiolitis	hRSV	SIN06-NTU374	>10	URTI	-
SIN06-NTU165	1-3	CLD	hRSV	SIN06-NTU375	1-3	Asthma	-
SIN06-NTU167	1-3	URTI	-	SIN06-NTU399	1-3	Bronchiolitis	-
SIN06-NTU193	3-10	Asthma	-	SIN07-NTU421	<1	URTI	HRV
SIN06-NTU194	<1	URTI	hRSV	SIN07-NTU427	1-3	Croup	-
SIN06-NTU195	1-3	Acute bronchiolitis	-	SIN07-NTU430	3-10	?	hRSV
SIN06-NTU218	1-3	bronchiolitis	HRV	SIN07-NTU432	<1	Bronchiolitis	-
SIN06-NTU234	<1	URTI	HRV	SIN07-NTU441	3-10	ALL	HRV
SIN06-NTU243	<1	Croup	-	SIN07-NTU470	3-10	asthma	HRV
SIN06-NTU246	3-10	Pneumonia	-	SIN07-NTU494	1-3	URTI	-
SIN06-NTU250	<1	Infantile pyrexia	-	SIN07-NTU496	>10	Bronchitis	-
SIN06-NTU258	<1	URTI	hRSV	SIN07-NTU497	>10	pneumonia	HRV
SIN06-NTU263	>10	asthma	HRV	SIN07-NTU500	3-10	gastritis	HRV

Table 3.3. All 40 HBoV clinical isolates. The specimen number is abbreviated from the original SINyy-NTUxxx format to show the running sample number only. The age groups, clinical diagnosis and other viruses co-infected are also included in the table. (-)-no co-infection with other respiratory viruses determined.

Based on the age group information, most of the patients with HBoV are below 10 years old. In terms of severity, there does not appear to be a particular age group that is more vulnerable because patients with pneumonia or bronchiolitis come from all age groups. A recent publication by (Martin et al., 2010) found that HBoV could be detected for up to 75 days in children. This kind of prolonged shedding of virus is unusual among respiratory viruses, whereas it is more commonly observed in viruses causing gastroenteritis. It is also interesting to note that some recently discovered strains of HBoV (namely HBoV2, HBoV3 and HBoV4) have been known to cause gastroenteritis (Arthur et al., 2009; Chow et al., 2010; Kapoor et al., 2010) in adults and children. One report of HBoV isolated from urine was documented (Pozo et al., 2007) but hardly any conclusion can be drawn due to the very low incidence. Martin and co-workers also found that the presence of HBoV among children with (59%) and without (44%) symptoms were not significantly different. This implies a high level of asymptomatic carriage of HBoV. However, this finding is in contrast to the work by (Garcia-Garcia et al., 2008) who observed a significant difference in prevalence of HBoV between symptomatic (17%) and asymptomatic (5%) subjects. Sequence analysis of HBoV isolates using the partial NS1 gene showed that HBoV isolates from Singapore were highly similar to those found worldwide as shown below (Fig 3.11). Out of the 40 HBoV strains detected, 23 were found to have identical partial NS1 sequences. The sequences were submitted to GenBank under the accession numbers EU014167 to EU014206.

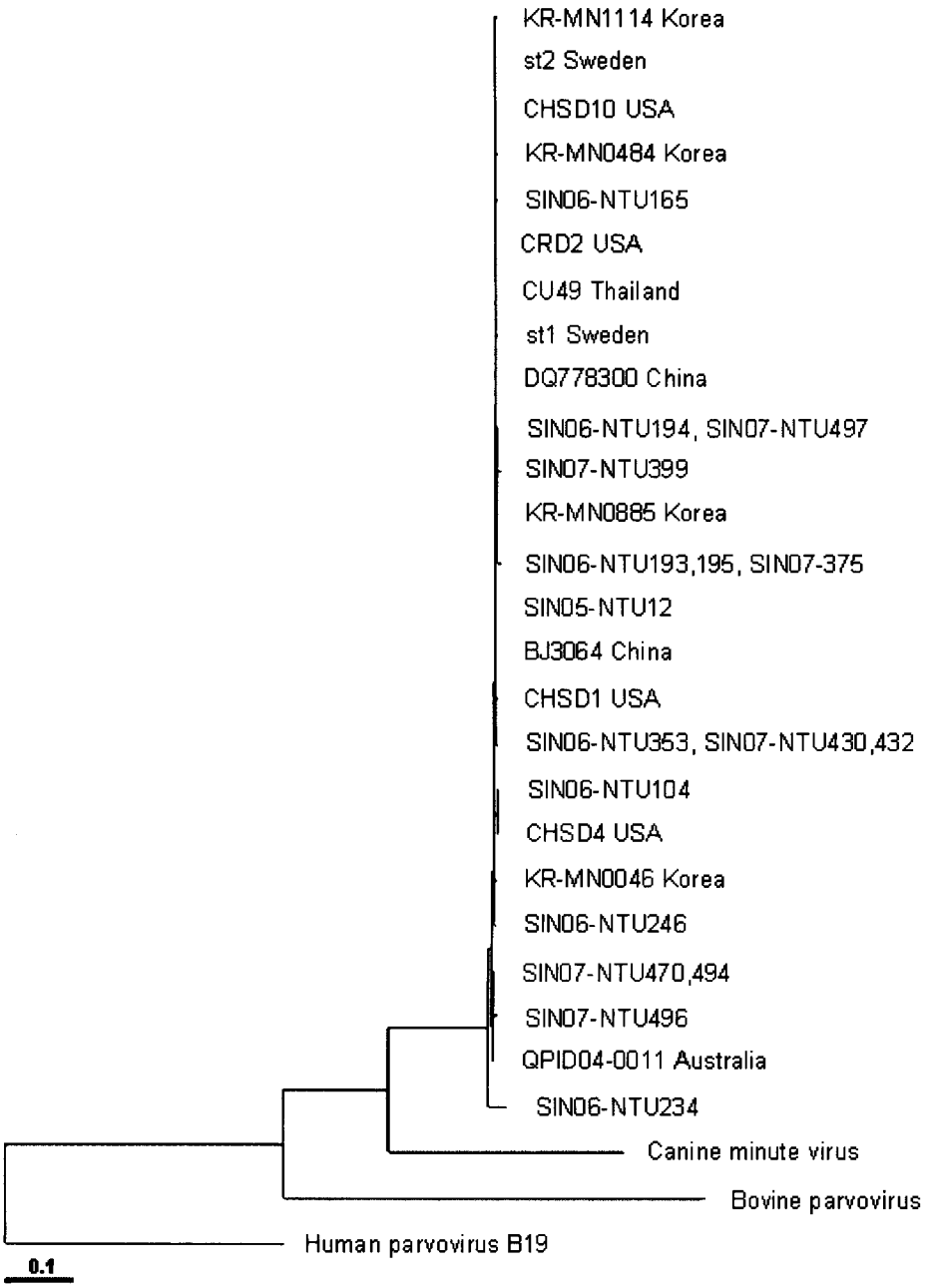

Figure 3.11. Phylogenetic relationship of the partial NS1 gene region for HBoV. #SIN05-NTU-12 is the representative strain for a cluster of 24 isolates, comprising of specimen numbers SIN05-NTU- 12, 22, 46, 79, 86, 150; SIN06-NTU-159, 167, 218, 243, 250, 258, 263, 268, 275, 290, 325, 328, 371, 374; and SIN07-NTU-421, 427 and 500, with 100% sequence similarity at the nucleotide level. Other HBoV strains are indicated by their countries of origin. Other bocaviruses are included in the tree as outgroups. HBoV isolates from this study are written as SINyy-NTUxxx as explained under Fig 3.4.

3.4 Human coronavirus isolates

HCoV was detected in only 3 samples (Table 3.4). After sequencing the partial orf 1b (replicase polyprotein gene) target fragment and aligning with known HCoV sequences,

1 isolate from a patient with bronchitis was identified as human coronavirus OC43. The other 2 isolates were identified as human coronavirus NL63. Both patients had laryngotracheobronchitis (also known as croup). This observation is in agreement with the findings of (van der Hoek et al., 2005), (Han et al., 2007) and (Wu et al., 2008). However HCoV NL63 was prevalent at higher rates in all three studies (5.2%, 1.7% and 1.3%, respectively). Our positive rate for HCoV NL63 was only 0.4% (2/500). Despite the small number of local HCoV NL63 isolates, the observed symptoms for both patients combined with results of other publications indicate that HCoV NL63 is one of the causative agents of croup in young children. None of the 3 patients had co-infection with other respiratory viruses. The results of this study have been published together with findings on bocavirus in Singapore (Tan et al., 2009b).

Specimen number	Age group	Diagnosis indicated	HCoV strain	Other viruses present
SIN06-NTU211	<1	ALTB	NL63	-
SIN06-NTU295	1-3	Bronchitis	OC43	-
SIN06-NTU395	<1	ALTB	NL63	-

Table 3.4. All 3 HCoV clinical isolates. The specimen number is abbreviated from the original SINyy-NTUxxx format to show the running sample number only. The age group, clinical diagnosis, subtype information and other viruses co-infected are also included in the table. (-)-no co-infection with other respiratory viruses determined.

Sequence analysis of HCoV isolates showed that the 2 HCoV NL63 isolates are similar to those from the Netherlands. The HCoV OC43 isolate is similar to the ATCC VR759 strain (Fig 3.12). The coronavirus sequences have been submitted to GenBank under accession numbers EU370700 to EU370702. Other strains of human coronaviruses previously published that were included in the sequence comparison were isolated from Australia, Germany, Hong Kong, Italy, Japan, Netherlands and USA (including the American Type Culture Collection or ATCC). Other coronaviruses used for the comparison were two strains of SARS coronavirus (CoV), one bovine coronavirus

(BCoV), one porcine epidemic diarrhea virus (PEDV), and transmissible gastroenteritis virus (TGEV) which infects pigs.

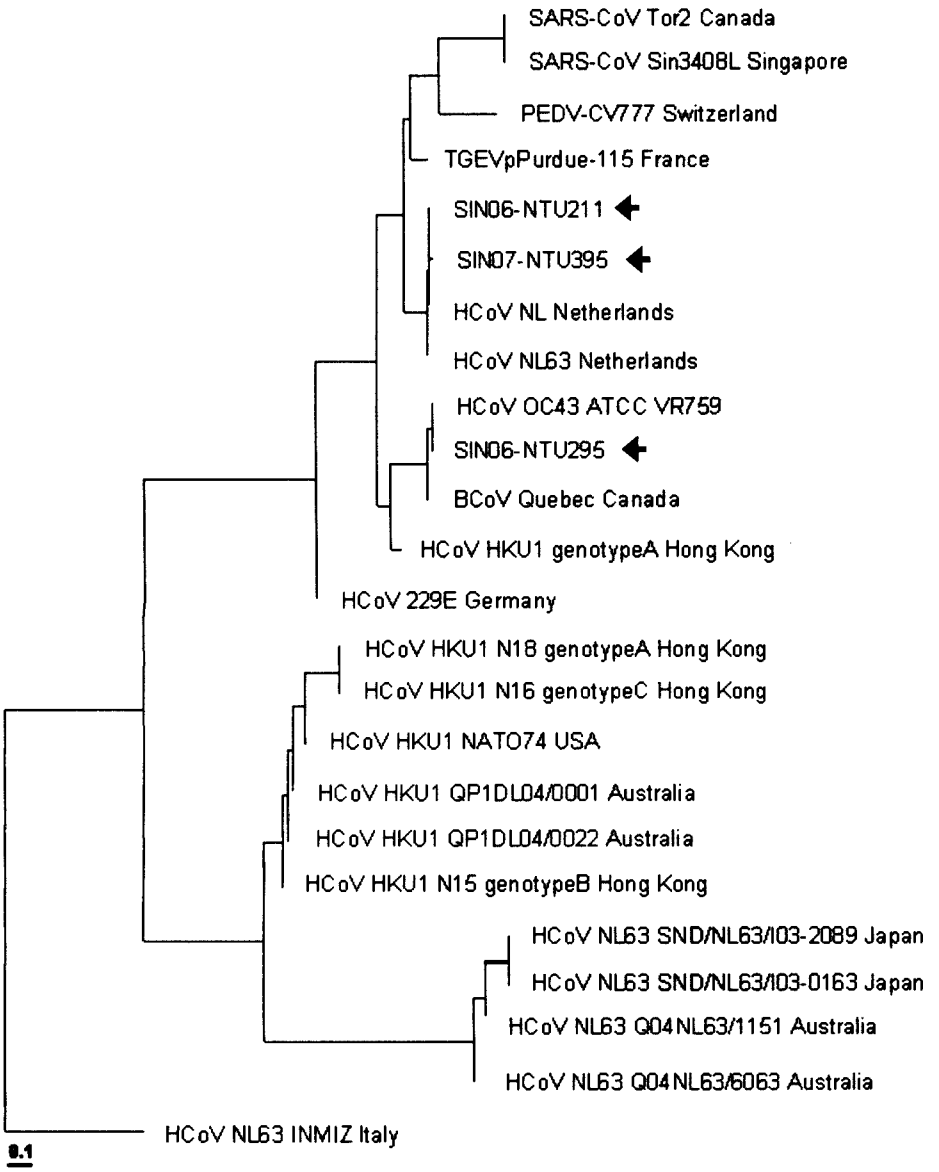

Figure 3.12. Phylogenetic analysis of the partial orf 1b region of HCoV isolates. The fragment length is approximately 100bp. The local isolates are highlighted with arrows and numbered SIN06-NTU211, 295 and SIN07-NTU395 according to the scheme explained in Fig 3.4. Other published human coronavirus strain sequences are indicated next to their country of origin: Australia [Q04NL63/1151 GenBank AY600446, Q04NL63/6063 GenBank AY600443, QP1DL04/0001 GenBank DQ190472, QP1DL04/0022 GenBank DQ206693], Germany [229E GenBank AF304460], Hong Kong [HKU1 N15 genotypeB GenBank DQ415911, HKU1 N16 genotypeC GenBank DQ415912, HKU1 N18 genotypeA DQ415914, HKU1 genotypeA GenBank AY597011], Italy [NL63 INMIZ GenBank EU030685], Japan [SND/NL63/I03-0163 GenBank AY662694, SND/NL63/I03-2089 GenBank AY662698], Netherlands [NL GenBank AY518894, NL63 GenBank AY567487], USA [HKU1 NATO74 GenBank EF077277], ATCC [OC43 VR759 GenBank AY391777]. Other coronavirus sequences are SARS coronavirus (CoV) [Canada Tor2 GenBank AY274119, Singapore Sin3408L GenBank AY559097], bovine coronavirus (BCoV) [Canada Quebec GenBank AF220295], porcine epidemic diarrhea virus (PEDV) [Switzerland CV777 GenBank AF353511], transmissible gastroenteritis virus (TGEV) [France Purdue-115 Z34093].

3.5 Human rhinovirus isolates

Human rhinovirus was detected in 64 samples giving a prevalence of 12.8% (Table 3.5). Of these, 19 isolates (29.6%) were from patients with lower respiratory tract infections [4 bronchitis, 11 bronchiolitis, 2 pneumonia and 2 chest infections], 17 (26.6%) isolates were from patients with upper respiratory tract infections, 11 (17.2%) isolates were from patients with asthma and 7 (10.9%) isolates were from patients with fits or fever. The remaining 10 isolates were from patients with gastritis, vomiting, leukaemia or other undefined symptoms. Among the 64 samples positive for HRV, 10 (15.6%) were detected together with other respiratory viruses [2 with hRSV, 8 with HBoV]. Two isolates SIN06-NTU263 and SIN06-NTU391 were found to belong to the newly discovered human rhinovirus group C (HRV-C) (Lamson et al., 2006). One patient with HRV-C had asthma while another had bronchiolitis. An earlier study in Hong Kong found 76% of patients with HRV-C had asthma (Lau et al., 2007). A Thai study also found HRV-C in a high proportion of children with asthma and wheezing (Linsuwanon et al., 2009). The significance of HRV-C in the local population cannot be determined until a wider study can be conducted using a larger population pool. Based on the age group information, most of the patients infected with HRV are under the age of 3 but the younger children may not necessarily have the more severe symptoms like pneumonia or bronchiolitis. Sequences for 58 of the 64 rhinovirus isolates were submitted to GenBank (GenBank accession nos. FJ645771–FJ645828). Out of the 64 HRV-positive samples detected, 47 (73.4%) belong to HRV-A, 9 (14.1%) belong to HRV-B and 2 (3.1%) belong to HRV-C (Fig 3.13). Six of the HRV isolates (SIN05-NTU121, SIN06-NTU316, SIN06-NTU372, SIN06-NTU382, SIN07-NTU439 and SIN07-NTU500) could not be subtyped due to low viral load in the samples. Hence, no sequence data were available for these 6 samples.

Specimen number	Age group	Diagnosis indicated	HRV group	Other viruses present	Specimen number	Age group	Diagnosis indicated	HRV group	Other viruses present
SIN05-NTU35	1-3	Bronchiolitis	A	-	SIN06-NTU316	1-3	URTI	Nd	-
SIN05-NTU58	3-10	URTI	A	-	SIN06-NTU324	3-10	?	B	-
SIN05-NTU62	3-10	?aspergillosis	A	-	SIN06-NTU334	<1	URTI	A	-
SIN05-NTU74	3-10	Asthma	A	-	SIN06-NTU336	<1	URTI	A	-
SIN05-NTU91	1-3	Infection	A	-	SIN06-NTU341	3-10	Asthma	A	-
SIN05-NTU107	1-3	Acute bronchiolitis	A	-	SIN06-NTU348	1-3	URTI	B	-
SIN05-NTU121	3-10	?	Nd	-	SIN06-NTU352	3-10	URTI	B	-
SIN05-NTU129	1-3	Bronchiolitis	A	-	SIN06-NTU354	3-10	URTI	A	-
SIN05-NTU144	<1	Bronchiolitis	A	-	SIN06-NTU372	<1	URTI	Nd	-
SIN06-NTU173	3-10	Bronchitis	A	-	SIN06-NTU380	<1	Overfeeding	A	-
SIN06-NTU177	<1	Bronchitis	A	hRSV	SIN06-NTU381	<1	Gastritis	A	-
SIN06-NTU179	1-3	URTI	A	-	SIN06-NTU382	<1	Infantile pyrexia	Nd	-
SIN06-NTU188	<1	URTI	A	-	SIN06-NTU391	<1	Bronchiolitis	C	-
SIN06-NTU196	<1	Vomiting	A	-	SIN06-NTU397	<1	Bronchiolitis	A	-
SIN06-NTU201	<1	URTI	A	-	SIN07-NTU404	<1	Bronchiolitis	A	-
SIN06-NTU205	1-3	Chest infection	A	-	SIN07-NTU405	1-3	Bronchitis	A	-
SIN06-NTU213	1-3	Afebrile fit	A	-	SIN07-NTU412	<1	NNP	A	-
SIN06-NTU218	1-3	bronchiolitis	A	HBoV	SIN07-NTU416	3-10	URTI	B	-
SIN06-NTU220	1-3	pneumonia	A	hRSV	SIN07-NTU421	<1	URTI	A	HBoV

Specimen number	Age group	Diagnosis indicated	HRV group	Other viruses present	Specimen number	Age group	Diagnosis indicated	HRV group	Other viruses present
SIN06-NTU234	<1	URTI	A	HBoV	SIN07-NTU425	3-10	Bronchiolitis	A	-
SIN06-NTU241	>10	Asthma	B	-	SIN07-NTU436	3-10	Asthma	A	-
SIN06-NTU245	<1	bronchiolitis	A	-	SIN07-NTU439	1-3	Asthma	Nd	-
SIN06-NTU252	3-10	URTI	A	-	SIN07-NTU441	3-10	ALL	A	HBoV
SIN06-NTU257	>10	Asthma	A	-	SIN07-NTU454	<1	NNP	A	-
SIN06-NTU260	<1	URTI	B	-	SIN07-NTU458	1-3	Bronchitis	A	-
SIN06-NTU263	>10	Asthma	C	HBoV	SIN07-NTU463	1-3	Kawasaki	B	-
SIN06-NTU278	<1	Fever	A	-	SIN07-NTU470	3-10	Asthma	A	HBoV
SIN06-NTU281	3-10	Gastritis	B	-	SIN07-NTU471	3-10	Asthma	A	-
SIN06-NTU301	<1	Whooping cough	A	-	SIN07-NTU478	1-3	Fever	A	-
SIN06-NTU302	1-3	Bronchiolitis	A	-	SIN07-NTU486	3-10	Asthma	A	-
SIN06-NTU304	1-3	Asthma	A	-	SIN07-NTU497	>10	Pneumonia	B	HBoV
SIN06-NTU308	1-3	Febrile fit	A	-	SIN07-NTU500	3-10	Gastritis	Nd	HBoV

Table 3.5. All 64 HRV clinical isolates. The specimen number is abbreviated from the original SINyy-NTUxxx format to show the running sample number only. The age groups, clinical diagnosis, subtype information and other viruses co-infected are also included in the table. Nd – subtype could not be determined, (-)-no co-infection with other respiratory viruses determined.

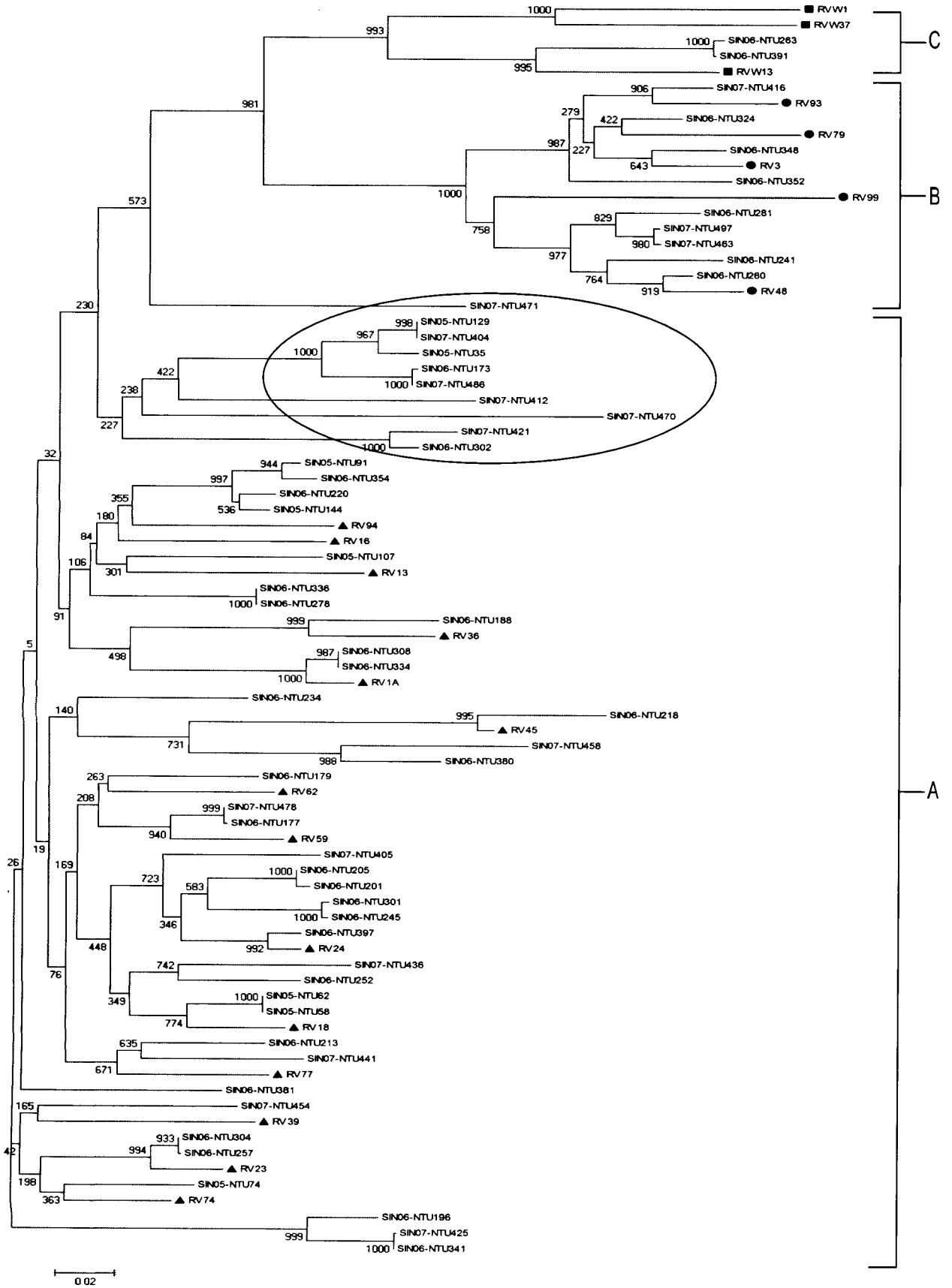

Fig 3.13. Phylogenetic relationship between rhinovirus isolates. The 5' non-coding region of the virus isolates were used for sequence comparison. Local isolates are denoted by SINyy-NTUxxx where "yy" is the year of isolation and "xxx" is the sample number. Isolates with the prefix RV and numbers are the various serotypes with sequences obtained from (Lee et al., 2007b). Strains within group A are highlighted by [▲]. Strains within group B are highlighted by [●]. Strains within group C are highlighted by [■]. Isolates within the large oval area have diverged from group A.

There was no apparent correlation between the severity of the respiratory disease and the HRV group infecting a patient. However, both patients who had pneumonia with HRV were also co-infected with another respiratory virus. Sample SIN06-NTU220 was found to contain both HRV-A and hRSV. Sample SIN07-NTU497 was found to contain both HRV-B and HBoV. The significance of these two cases of co-infection is uncertain.

3.6 Patterns of metapneumovirus, bocavirus, coronavirus and rhinovirus infections

From this study of 500 patient specimens, it is clear that HRV, HBoV and HMPV represent the most (12.8%), third (8%) and fourth (5.8%) frequent viruses detected in paediatric patients with respiratory infection, compared to hRSV which was the second most detected virus (11.8%). The most prevalent subgenogroup of HMPV was A2 followed by B2 and B1. This pattern is also observed in other parts of the world and the same genogrouping could be observed regardless of which gene (N, P, M, F or G) was used for phylogenetic analysis. The number of HCoV isolates was relatively low compared to HMPV and HBoV, and no distinct subtype was predominant. However, unlike HMPV and HCoV, HBoV appeared to show a high degree of genetic conservation, with most global isolates sharing greater than 90% similarity in the NS1 gene. This may be due to the fact that HBoV is a DNA virus. DNA replication usually has higher fidelity than RNA replication which is prone to high rates of mutation originating from the viral RNA polymerase. The role of HBoV in human disease is still unclear. With the discovery of new HBoV types, more evidence for the association of HBoV and human disease may be uncovered. For many years, HRV has been known to be a cause of the common cold. The large number of serotypes has been a huge obstacle in the development of a vaccine and suitable diagnostic tests. Greater interest in the study of HRV may lead to better treatment and detection options.

3.7 Chapter Summary

Almost every diagnostic laboratory in Singapore which can perform tests for respiratory virus antigens depends on the use of commercial kits. Such kits can usually detect common viruses such as influenza virus A and B, parainfluenza viruses 1, 2 and 3, hRSV and adenoviruses. Before 2008, reagents which could detect newly discovered viruses like HMPV and HBoV were not available for routine diagnostic use. Despite the fact that the existence of HRV and HCoV has been known for decades, their circulation in the local paediatric population was largely ignored by physicians. As awareness and interest in newly discovered respiratory viruses HMPV and HBoV grows, we can expect an increasing demand for such reagents for routine diagnostics. This will lead to better understanding of their prevalence and impact in the human population. A similar effect is likely to occur with regards to HRV and HCoV. Hopefully, this will occur as more studies based on community and hospital virus infections demonstrate that a higher proportion of respiratory virus infections are due to these previously overlooked viruses and that viable management options for these viral infections become available as a result of more intensive research. Information regarding the seasonality of virus isolates cannot be accurately determined because the samples were not collected continuously throughout the year.

Chapter 4 Study of Human Metapneumovirus Fusion and Attachment Proteins Cloned from Clinical Isolates

Being a member of the *Paramyxoviridae* family of viruses, HMPV depends on its viral envelope glycoproteins for cell-to-cell transmission. The fusion (F) and attachment (G) proteins are thought to have their own distinctive roles in the virus to cell fusion process. The association between the F and G proteins of the closely related hRSV on the surface cells have been shown by (Low et al., 2008). It has been suggested that hRSV cell-to-cell transmission begins with the G protein-mediated attachment to cell surface receptors (Levine et al., 1987). This is followed by the induced changes in the conformation of the F protein which then facilitates membrane fusion (Colman and Lawrence, 2003; Dutch et al., 2000). It is hypothesized that HMPV uses a similar mechanism for cell-to-cell transmission. In order to understand this mechanism, the F and G proteins of HMPV were chosen for further experimentation. Earlier work published on HMPV F and G proteins have primarily dealt with the individual proteins. Of the two proteins, the F protein is the more conserved (refer to Table 1.4 and Fig.3.9) with 94% similarity in the amino acid sequences between A and B genogroups. This could reflect a greater evolutionary pressure to maintain the structure of the F protein for proper functioning during virus infection. The G protein, on the other hand, is the most variable amongst all the HMPV proteins (refer to Table 1.4 and Fig. 3.10) with only 33% similarity between the amino acid sequences of A and B genogroups. This may be due to evasion of host recognition. Therefore, to ensure a more complete study of F-G protein interaction, one F protein from clinical isolate SIN06-NTU271 (genogroup A2) was chosen for the study, together with two different G proteins from clinical isolates SIN06-NTU271 (genogroup A2) and SIN06-NTU272 (genogroup B2). This was a strategy to determine if the significant differences between the two G proteins would result in contrasting levels of interaction with F. The two G proteins from

SIN06-NTU271 and SIN06-NTU272 were designated GA and GB, respectively. Since there were no readily available anti-F or anti-G antibodies, the genes for F, GA and GB were expressed with peptide tags. The F protein was tagged with c-myc peptide (EQKLISEEDL) and the GA/B proteins were tagged with a FLAG peptide (DYKDDDDK). Two mammalian expression systems were tested. The first was the modified vaccinia virus-driven expression system which can produce large quantities of protein but requires infection of the cells with a foreign virus. The second is a chicken beta-actin promoter driven expression system which is more representative of a mammalian protein expression system.

In this chapter, the aim was to characterize HMPV F and GA/B proteins expressed both singly and co-expressed in the same cells. Attempts were made to analyse the co-expressed proteins by various means, including chemical crosslinking reagents, confocal microscopy and sucrose gradient ultracentrifugation. The role of the cytoplasmic tails and transmembrane regions of the proteins were also studied with respect to the interaction between F and GA/B proteins.

4.1 Expression of F and G proteins using a vaccinia-driven expression system

4.1.1 Total protein expression

Using the MVA-T7 and pCDNA 3.1(-) system, expression of F proteins alone (Fig 4.1, lanes 1 to 3) and with GA protein (Fig 4.1, lanes 4 to 6) in Vero E6 cells are shown. The F protein shows a band at about 55 kDa (F_{55}) and another prominent band at about 145 kDa (F_{145}) which could possibly be a multimeric form of F. When treated with PNGaseF and EndoH most of the F protein is converted to the 51 kDa (F_{51}) form which suggests the presence of immature N-linked glycosylated forms of the F protein within the cell. When co-transfected with GA protein and treated with PNGaseF and EndoH, the F protein shows similar digest patterns.

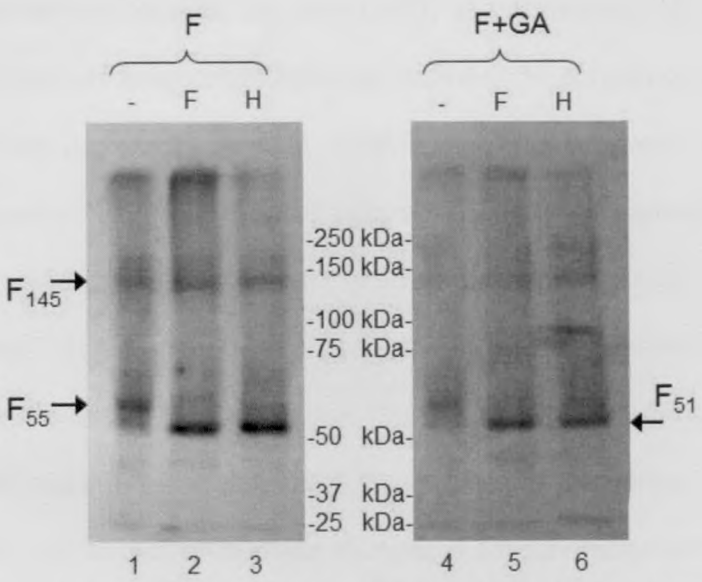

Figure 4.1. Expression of F (lanes 1 to 3) and F+GA (lanes 4 to 6) in Vero E6 cells probed with anti-myc antibody. (-)-Non enzyme treated, F-PNGaseF treated, H-EndoH treated. The various F protein forms are shown with their respective sizes in kDa.

When the GA protein was expressed alone in Vero E6 cells (Fig 4.2, lanes 1 to 3), there were two distinct bands at 40 kDa (GA_{40}) and 75 kDa (GA_{75}). There was also the appearance of a smear from 110 to 180 kDa. There was a slight reduction in the size of the GA_{40} and GA_{75} bands after treatment with PNGaseF and EndoH, suggesting the presence of N-linked glycosylated sugars.

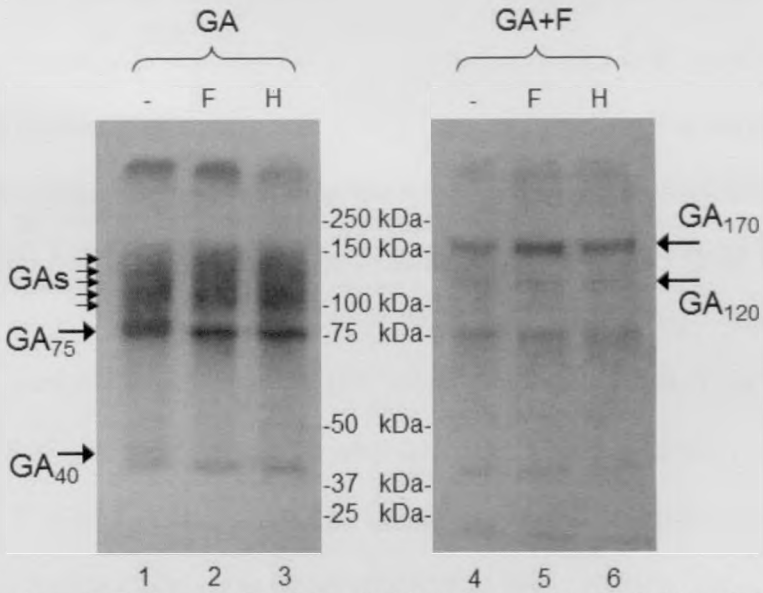

Figure 4.2. Expression of GA (lanes 1 to 3) and GA+F (lanes 4 to 6) in Vero E6 cells probed with anti-FLAG antibody. (-)-Non enzyme treated, F-PNGaseF treated, H-EndoH treated. The various GA protein forms are shown with their respective sizes in kDa. GAs-GA smear from 80-150 kDa.

However, the GA protein smear (GAs) was not affected by the enzyme treatments suggesting the presence of O-linked glycosylated sugars.The size of GA was much larger than the expected size of 24-25kDa. A factor which can alter the migration rate may be the presence of O-linked side chains. When GA was co-transfected with F (Fig 4.2, lanes 4 to 6), GA appeared as band sizes of GA_{40} and GA_{75}, and two additional bands at approximately 120 kDa (GA_{120}) and 170 kDa (GA_{170}). The four GA bands in lanes 4 to 6 of Fig 4.2 were apparently not affected by treatment with PNGaseF and EndoH which reinforces the suggestion that the GA protein is mainly O-linked glycosylated. The presence of F protein seemed to cause the GA protein to form distinct species of O-linked glycans instead of a heterogeneous smear. This could be due to the interaction of F with GA which may result in a conformational change in GA giving rise to differential or preferential glycosylation products.

4.1.2 Surface protein expression

Results for the surface expression of F alone (Fig 4.3) and in combination with GA (Fig 4.4, lanes 1 to 3) or GB (Fig 4.4, lanes 4 to 6) are shown below. The F protein present on the surface of Vero E6 cells is the mature N-linked 65 kDa form (F_{65}) characterized by its resistance to EndoH treatment (Fig 4.3, lane 3) but its digestion by PNGaseF (Fig 4.3, lane 2) into the smaller 58 kDa form (F_{58}). The co-transfection with either GA (Fig 4.4, lanes 1 to 3) or GB (Fig 4.4, lanes 4 to 6) did not alter the characteristics of F protein.

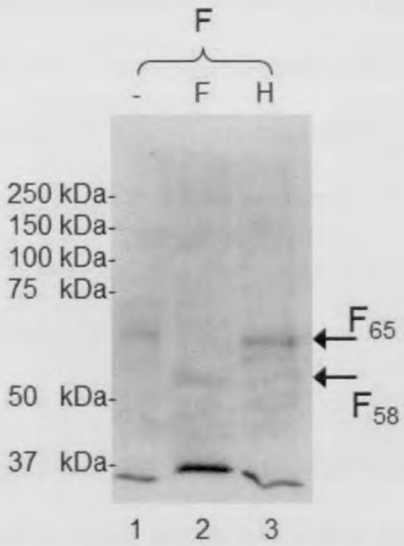

Figure 4.3. Surface expression of F protein in Vero E6 cells analysed by immunoprecipitation of biotin-labeled protein with anti-myc antibody. (-)-Non enzyme treated, F-PNGaseF treated, H-EndoH treated. The various F protein forms are shown with their respective sizes in kDa.

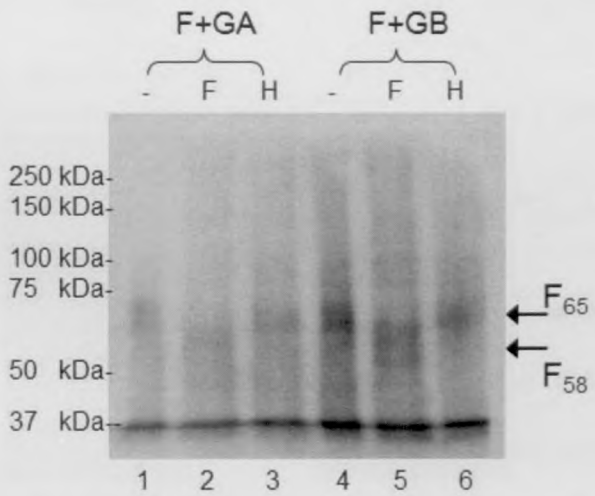

Figure 4.4. Surface expression of F+GA (lanes 1 to 3) and F+GB (lanes 4 to 6) proteins in Vero E6 cells analysed by immunoprecipitation of biotin-labeled protein with anti-myc antibody. (-)-Non enzyme treated, F-PNGaseF treated, H-EndoH treated. The various F protein forms are shown with their respective sizes in kDa.

Results for the surface expression of GA alone (Fig 4.5, lanes 1 to 3) and co-transfected with F (Fig 4.5, lanes 4 to 6); and GB alone (Fig 4.6, lanes 1 to 3) and co-transfected with F (Fig 4.6, lanes 4 to 6) are shown below. Surface-expressed GA showed two main species with sizes of 60 kDa (GA_{60}) and 120 kDa (GA_{120}) and a faint smear between the two bands. These two species were resistant to treatment with PNGaseF and EndoH (Fig 4.5, lanes 2 and 3). When co-transfected with F protein, the GA protein appeared as two different yet distinct 70 kDa (GA_{70}) and 170 kDa (GA_{170})

forms (Fig 4.5, lanes 4 to 6). The GA_{170} bands represent a possible oligomeric form of GA_{70}. This is analogous to the GA_{60} and GA_{120} forms seen in the singly transfected cells (Fig 4.5 lanes 1 and 3). Co-expression of F with GA appeared to cause a shift in the size of GA. The GA_{70} and GA_{170} species were also resistant to both PNGaseF and EndoH digestion.

Surface expressed GB (Fig 4.6, lanes 1 to 3) appeared as a smear from 50 kDa to 80 kDa (GB_{50-80}) and was resistant to EndoH treatment (Fig 4.6, lane 3), but showed a slight downward shift in size when treated with PNGaseF (Fig 4.6, lane 2). When co-transfected with F (Fig 4.6, lanes 4 to 6), a single band at about 80 kDa (GB_{80}) was observed, which was also resistant to both PNGaseF and EndoH digestion (Fig 4.6, lanes 2 and 3).

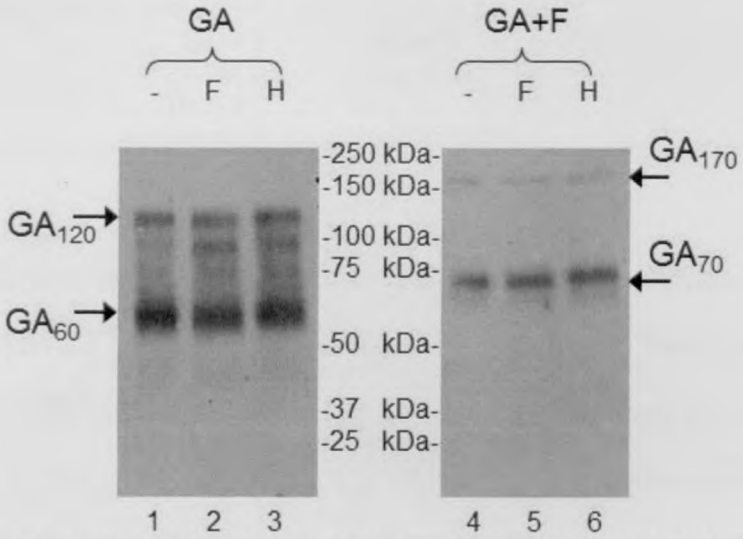

Figure 4.5. Surface expression of GA (lanes 1 to 3) and GA+F (lanes 4 to 6) in Vero E6 cells analysed by immunoprecipitation of biotin-labeled protein with anti-FLAG antibody. (-)-Non enzyme treated, F-PNGaseF treated, H-EndoH treated. The various GA protein forms are shown with their respective sizes in kDa.

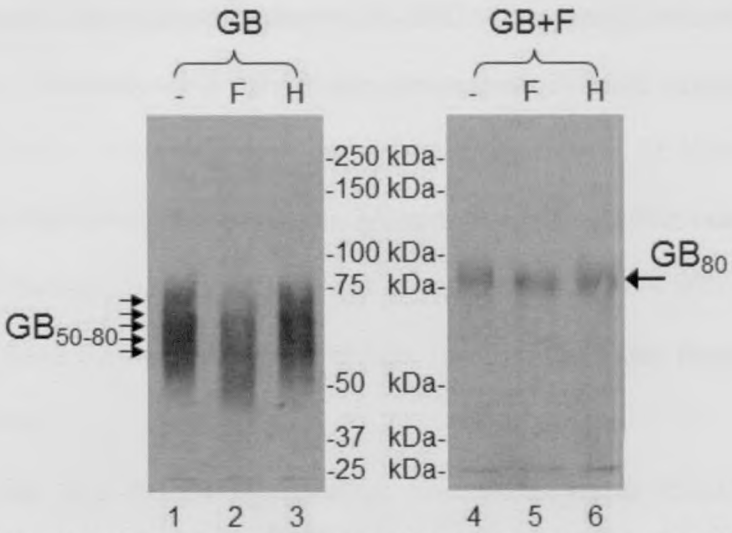

Figure 4.6. Surface expression of GB (lanes 1 to 3) and GB+F (lanes 4 to 6) in Vero E6 cells analysed by immunoprecipitation of biotin-labeled protein with anti-FLAG antibody. (-)-Non enzyme treated, F-PNGaseF treated, H-EndoH treated. The various GB protein forms are shown with their respective sizes in kDa.

4.1.3 Summary of F and G expression using MVA-T7/pcDNA 3.1(-) system

Using the MVA-T7 expression system with pCDNA3.1(-), the F protein was found to exist mainly as an immature form (F_{55}) within the Vero E6 cells and as a mature glycosylated form (F_{65}) expressed on the surface of the cells. Co-transfection with GA or GB protein did not alter the processing of the F protein which primarily contains N-linked sugar chains. There were differences between the GA and GB protein glycosylation patterns. The GA protein mainly contains O-linked sugar chains because treatment with PNGaseF and EndoH had little effect on it. The GB protein, on the other hand, may have a few significant N-linked sugar chains in addition to the O-linked sugars. This could be inferred by the slight reduction in size of the GB protein upon treatment with PNGaseF (Fig 4.6, lane 2). When both GA and GB proteins were co-expressed with F on the cell surface, there was a shift in the expression of GA and GB towards a single species (GA_{70} and GB_{80} in Fig. 4.5 and 4.6 respectively). This suggests that the presence of the F protein on the host cell surface can cause the GA or GB proteins to preferentially adopt one particular conformation. The vaccinia-driven expression system was used as a pilot study for F and G expression. It was

subsequently decided that the pCAGGS mammalian expression system (refer to next section 4.2) would be more representative of a human virus infection.

4.2 Expression of F and G proteins using a mammalian expression system

4.2.1 Total protein expression

Using the pCAGGS vector expression system, the F, GA and GB proteins were expressed singly and in combination in 293T cells. The expression of F protein alone (Fig 4.7, lanes 1 to 3) showed a major band at 60 kDa (F_{60}) and another prominent band at about 145 kDa (F_{145}) which probably represented the multimeric form of F protein. When treated with PNGaseF (lane 2) and EndoH (lane 3), most of the F_{60} protein was converted to a size of 51 kDa (F_{51}), indicating cleavage of immature N-linked sugar chains. This is comparable to the vaccinia-driven expression system in Fig.4.1. This suggests the presence of immature forms of the F protein in the cell. However, when F was co-expressed with GA protein (Fig 4.7, lanes 4 to 6) and treated with PNGaseF (lane 5) and EndoH (lane 6), the F_{60} protein shows little resistance to EndoH digestion suggesting that the F_{60} form of F protein is still an immature form.

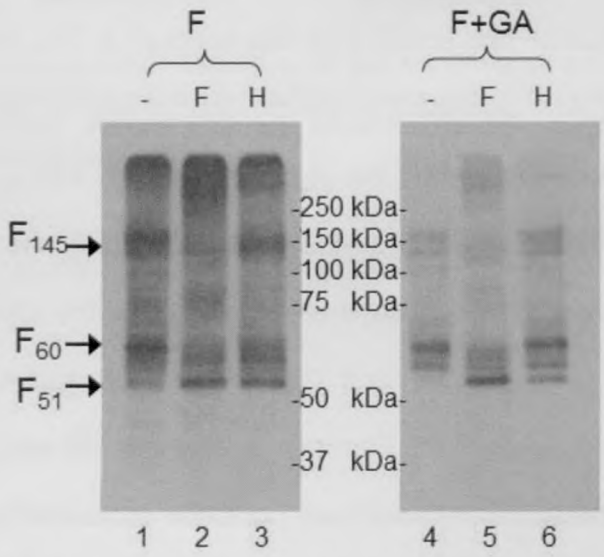

Figure 4.7. Expression of F (lanes 1 to 3) and F+GA (lanes 4 to 6) in 293T cells probed with anti-myc antibody. (-)-Non enzyme treated, F-PNGaseF treated, H-EndoH treated. The various F protein forms are shown with their respective sizes in kDa.

The immunoblot of the GA protein alone (Fig 4.8, lanes 1 to 3) showed a smear from 75 to 150 kDa. This smearing effect was a result of O-linked sugars and was not affected by digestion with PNGaseF (lane2) or EndoH (lane 3). When GA was co-transfected with F (Fig 4.8, lanes 4 to 6), GA appeared as a large molecular species of about 170 kDa (GA_{170}). GA_{170} was also not affected by treatment with PNGaseF (lane 5) and EndoH (lane 6), again suggesting that the GA170 protein is predominantly O-linked glycosylated.

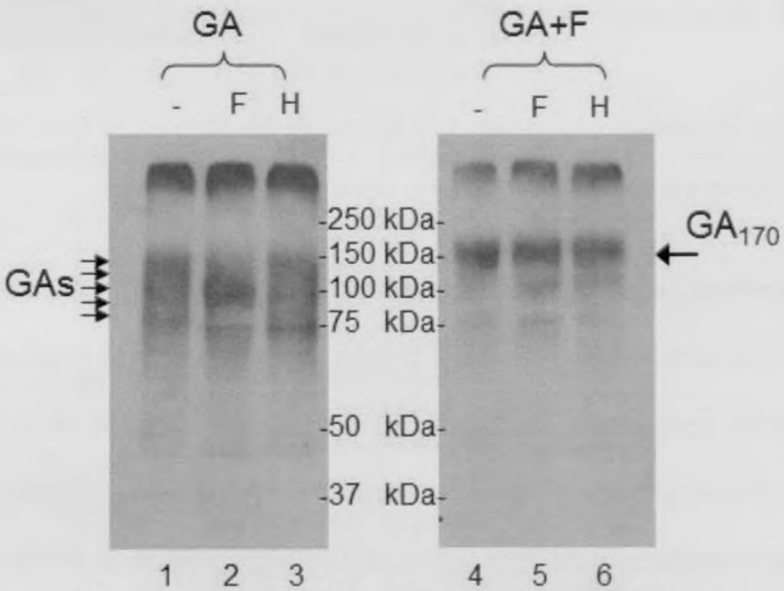

Figure 4.8. Expression of GA (lanes 1 to 3) and GA+F (lanes 4 to 6) in 293T cells probed with anti-FLAG antibody. (-)-Non enzyme treated, F-PNGaseF treated, H-EndoH treated. GAs-G protein smear from 75-150 kDa. The various GA protein forms are shown with the respective sizes in kDa.

As with the co-expression of F+GA, the co-expression of F+GB (Fig 4.9, lanes 4 to 6) showed a very similar pattern of the F_{60} and F_{51} proteins. There was also the presence of the multimeric form of F (F_{145}), indicating a relatively low impact of GB co-transfection on the expression of F protein.

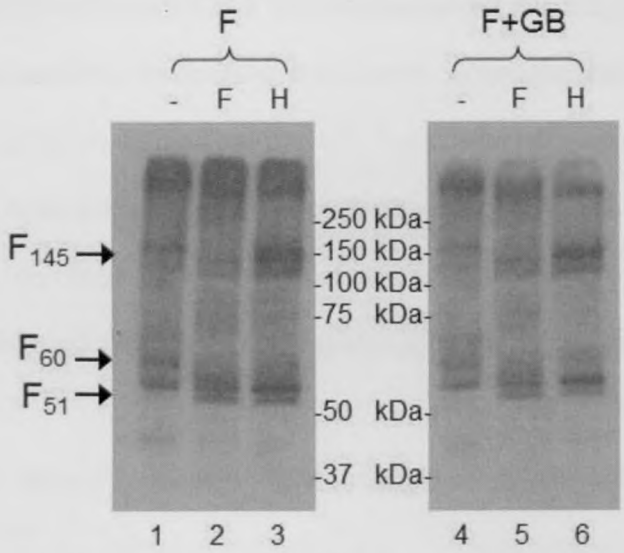

Figure 4.9. Expression of F (lanes 1 to 3) and F+GB (lanes 4 to 6) in 293T cells probed with anti-myc antibody. (-)-Non enzyme treated, F-PNGaseF treated, H-EndoH treated. The various F protein forms are shown with their respective sizes in kDa.

By comparison, when GB was co-expressed without F (Fig 4.10, lanes 1 to 3) and with F (Fig 4.10, lanes 4 to 6), GB was shown to be sensitive to PNGaseF (lanes 2 and 5) and EndoH treatment (lanes 3 and 6) with the appearance of a 40 kDa form of GB (GB_{40}) after enzyme treatment. This suggests that GB may possibly be modified by N-linked glycosylation. Another species of GB appeared as a smear from 50 to 80 kDa and this species was not significantly affected by PNGaseF and EndoH treatment either in the presence or absence of F protein was most likely due to O-linked glycosylation.

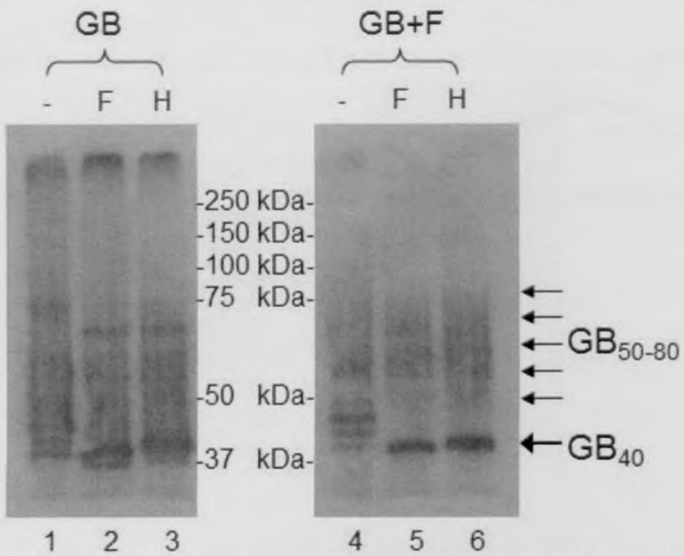

Figure 4.10. Expression of GB (lanes 1 to 3) and GB+F (lanes 4 to 6) in 293T cells probed with anti-FLAG antibody. (-)-Non enzyme treated, F-PNGaseF treated, H-EndoH treated. The various GB protein forms are shown with their respective sizes in kDa.

4.2.2 Surface protein expression

Results for the surface expression of F alone (Fig 4.11, lanes 1 to 3) and F+GA in combination (Fig 4.11, lanes 4 to 6) are shown below. The F protein present on the surface of 293T cells (Fig 4.11, lane 1) was primarily the mature triple N-link glycosylated, 65 kDa form (F_{65}). Treatment with PNGaseF reduced the F_{65} protein to a 58 kDa form (F_{58}). EndoH had no effect on F_{65} reflecting the mature state of the N-linked sugar chains.

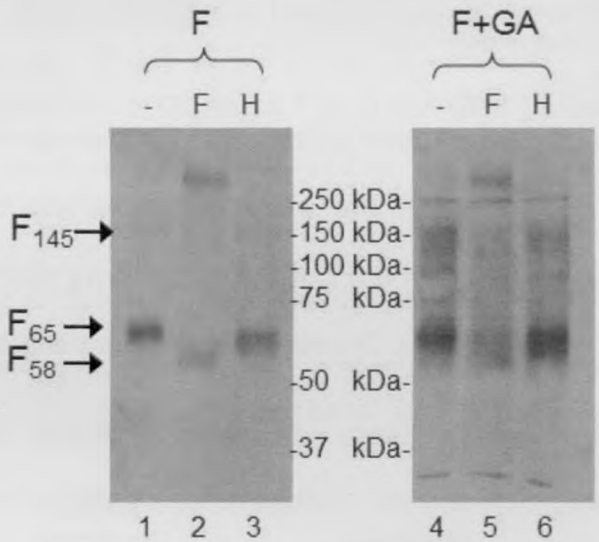

Figure 4.11. Surface expression of F (lanes 1 to 3) and F+GA (lanes 4 to 6) in 293T cells analysed by immunoprecipitation of biotin-labeled protein with anti-myc antibody. (-)-Non enzyme treated, F-PNGaseF treated, H-EndoH treated. The various F protein forms are shown with their respective sizes in kDa.

The presence of GA did not alter the processing of F protein significantly (Fig 4.11, lane 4) since the F protein still maintained the same size and digest pattern. When GA was expressed alone (Fig 4.12, lanes 1 to 3), it showed 2 forms of surface-expressed GA with sizes 60 kDa and 120 kDa (GA_{60}, GA_{120}). When co-expressed with F protein (lanes 4 to 6), the same two GA species shifted upwards in size (GA_{70}, G_{170}). This phenomenon was the same as that observed in the vaccinia-driven expression system (refer to Fig. 4.5). The smearing effect seen when GA was treated with PNGaseF (lanes 2 and 5) appeared to suggest that the N-linked sugars in GA have a role in forming distinct molecular sizes of the protein.

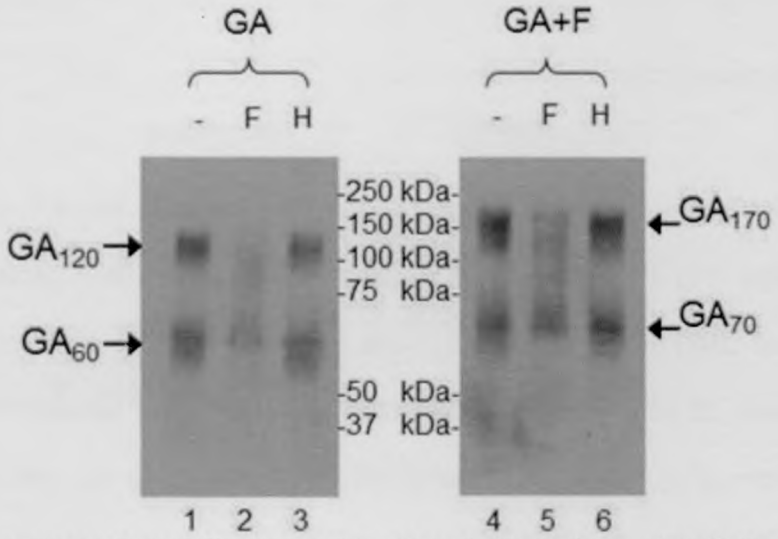

Figure 4.12. Surface expression of GA (lanes 1 to 3) and GA+F (lanes 4 to 6) in 293T cells analysed by immunoprecipitation of biotin-labeled protein with anti-FLAG antibody. (-)-Non enzyme treated, F-PNGaseF treated, H-EndoH treated. The various GA protein forms are shown with their respective sizes in kDa.

Results for the surface expression of F alone (Fig 4.13, lanes 1 to 3) and F+GB (Fig 4.13, lanes 4 to 6) in combination are shown below. As with F+GA (Fig 4.11), the presence of GB co-expressed with F (Fig 4.13) did not have much impact on F protein processing (Fig 4.13, lanes 4 to 6). Of interest is the faint trace of GB_{40} present in the co-transfected F+GB cells (Fig 4.13, lanes 5 and 6).

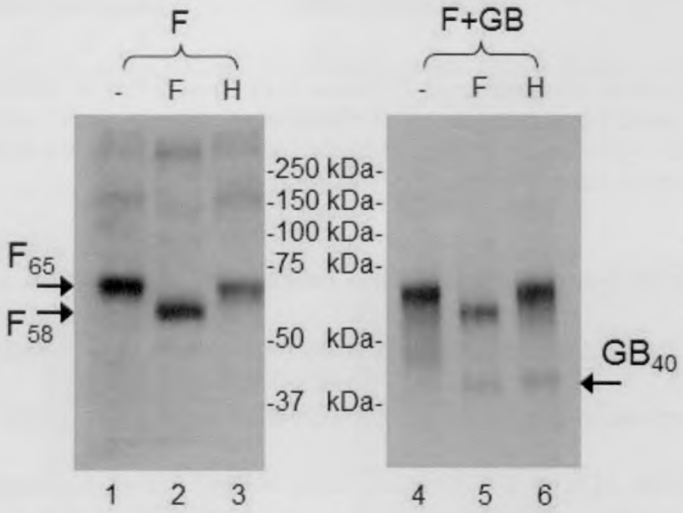

Figure 4.13. Surface expression of F (lanes 1 to 3) and F+GB (lanes 4 to 6) in 293T cells analysed by immunoprecipitation of biotin-labeled protein with anti-myc antibody. (-)-Non enzyme treated, F-PNGaseF treated, H-EndoH treated. The various forms of F and GB proteins shown with their respective sizes in kDa.

In Figure 4.14, we can observe that like GA (Fig 4.12), GB tends to shift to a larger molecular weight form when co-expressed with F. This is could be seen by the

reduction in the GB_{40} form (Fig 4.14, lanes 2 and 3) but increase in GB_{50-80} smear (Fig 4.14, lanes 5 and 6).

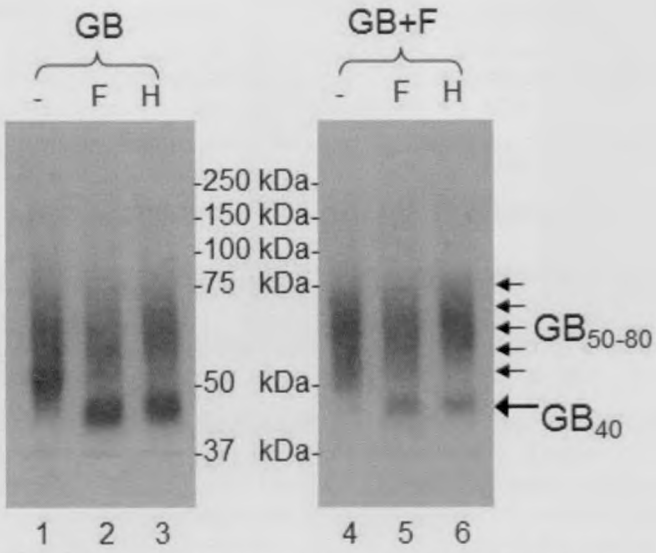

Figure 4.14. Surface expression of GB (lanes 1 to 3) and GB+F (lanes 4 to 6) in 293T cells analysed by immunoprecipitation of biotin-labeled protein with anti-FLAG antibody. (-)-Non enzyme treated, F-PNGaseF treated, H-EndoH treated. The various GB protein forms shown with their respective sizes in kDa.

As observed in Figure 4.13, when F is co-expressed with GB, a faint trace of GB_{40} was observed after immunoprecipitating with anti-myc antibody and treatment with PNGaseF or EndoH. This is indicative of a close association between F and GB proteins on the surface of 293T cells. In addition, there is also a possibility that there is a similar interaction between F and GA proteins, although there was no conclusive evidence of this by immunoprecipitation. This interaction will be discussed in the later section.

4.2.3 Radiolabeling of F and G proteins

The analysis of tritium-labeled F, GA, and F+GA proteins expressed in Vero E6 cells using the vaccinia-driven system (Fig 4.15) is shown below. Bearing in mind that the tritium label is attached to the sugar (glucosamine) molecules, only glycosylated F and GA proteins would be detected. The F_{65} protein band (Fig 4.15, lane 1) was comparable to that seen in non-radiolabeled surface expressed F_{65} protein (Fig 4.3

lane 1). Likewise, GA protein showed 2 species (Fig 4.15, lane 2) GA_{60} and GA_{120} similar to that seen in non-radiolabeled surface expressed GA proteins (Fig 4.5, lane 1). When F was co-expressed with GA, the F_{65} species was not altered (Fig 4.15, lane 3). This was comparable to the F_{65} in non-radiolabeled surface expression (Fig 4.4, lane 1). When GA was co-expressed with F, the larger molecular weight GA_{120} form (Fig 4.15, lane 4) predominated. This was different from the GA pattern seen in non-radiolabeled surface expression (Fig 4.5, lane 4). This implies that the higher molecular weight GA_{120} species is more N-linked glycosylated in the presence of F.

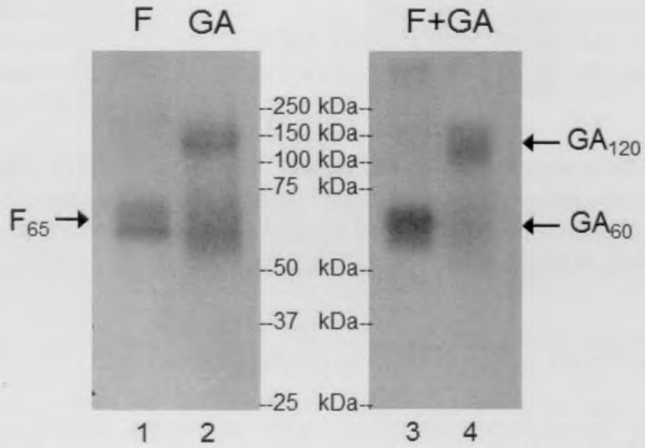

Figure 4.15. Radiolabeled single F, single GA and co-transfected F+GA in Vero E6 cells. Lanes 1 and 3 were immunoprecipitated with anti-myc antibody and lanes 2 and 4 were immunoprecipitated with anti-FLAG antibody.

F, GA and GB were expressed in HEp2 cells and labeled with tritiated glucosamine (Fig 4.16). The F protein was mainly in the form of the F_{65} monomer just as observed in the non-radiolabeled experiment (Fig. 4.11, lane 1). When co-expressed with either GA (Fig. 4.16, lane 5) or GB (Fig.4.16, lane 8), the F_{65} protein was unchanged compared to the singly expressed F_{65} protein (Fig 4.16, lane 1). The GA protein showed a similar size shift (Fig 4.16, lanes 3 and 4) in the presence of F protein as observed in non-radiolabeled surface expression using 293T cells (Fig 4.12, lanes 1 and 4). The GB protein showed a smear from 50-80 kDa but also displayed an increased predominance of a larger sized form closer to the 80 kDa size (Fig 4.16, lanes 6 and 7) when co-expressed with F protein.

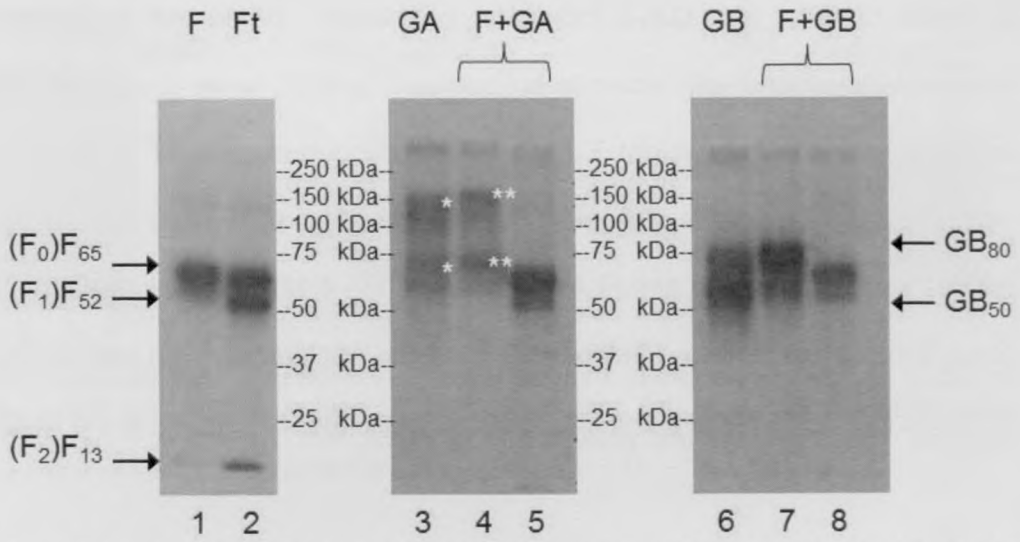

Figure 4.16. Radiolabeled single F, single GA/GB and co-expressed F+GA/GB in Hep2 cells. Ft - F protein treated with 0.5µg/ml trypsin for 2 hours at 37°C. Lanes 1, 2, 5 and 8 were immunoprecipitated with anti-myc antibody. Lanes 3, 4, 6 and 7 were immunoprecipitated with anti-FLAG antibody. "*" indicate the GA_{60} and GA_{120} proteins. "**" indicate the GA_{70} and GA_{170} proteins. Other protein bands are shown with their corresponding sizes in kDa.

There was no trace of the GB_{40} protein species. This is to be expected since GB_{40} only appeared when GB was treated with PNGaseF, and is therefore unglycosylated. The unglycosylated form of GB_{40} would not have been labeled with tritiated glucosamine. Another experiment performed was the action of trypsin on F protein. The 65 kDa F_{65} (F_0) protein (Fig 4.16, lane 1) was cleaved by trypsin (Fig 4.16, lane 2) into its 2 subunits F_{52} (F_1) and F_{13} (F_2) with sizes of approximately 52 kDa and 13 kDa, respectively. This demonstrates that the fully glycosylated and expressed F_{65} protein is functional and can be expected to behave predictably like the naturally produced viral fusion protein.

4.2.4 Crosslinking of F and G proteins

Immunoprecipitation of the surface-expressed and crosslinked F+GA proteins with anti-myc antibodies (Fig 4.17, lanes 1 to 4) demonstrated an increasing amount of GA (both GA_{70} and GA_{170}) species detected on the membrane in proportion to an increase in DSP concentration. Where no DSP was added (Fig 4.17, lane 1), the F_{65} protein band was observed. As the concentration of DSP was increased (Fig 4.17, lanes 2 to 4), the

2 bands of GA_{70} and GA_{170} increased in intensity. When the immunoprecipitated lysates were probed with anti-myc antibodies (Fig 4.17, lanes 5 to 8), the F_{65} protein and higher molecular weight F_{145} protein were detected in all lanes 5 to 8. This confirmed the presence of F protein in the lysates. When the immunoprecipitated lysates were probed with anti-FLAG antibodies (Fig 4.17, lanes 9 to 12), only the larger GA_{170} protein was detected in lanes 10 to 12 but not lane 9 which had no DSP added. This confirmed the presence of GA protein crosslinked to F protein in the lysates.

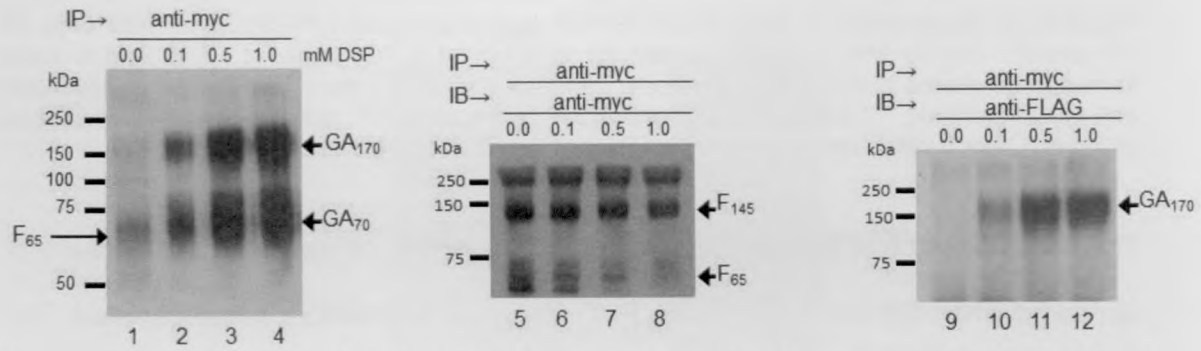

Figure 4.17. Crosslinking of F and GA in 293T cells. (Lanes 1-4) Immunoprecipitation of the cell lysate using anti-myc antibody to detect F protein. (Lanes 5-8) Immunoblot of lysate using anti-myc antibody. (Lanes 9-12) Immunoblot of lysate using anti-FLAG antibody. Numbers above the photos indicate DSP crosslinker concentrations in mM.

Immunoprecipitation of the surface-expressed and crosslinked F+GA proteins with anti-FLAG antibodies (Fig 4.18, lanes 1 to 4) only showed the presence of the 2 bands (GA_{70} and GA_{170}) of the GA protein. It is likely that the presence of F protein on the membrane was obscured by the high signal intensity of the GA proteins. When the immunoprecipitated lysates were probed with anti-myc antibodies (Fig 4.18, lanes 5 to 8), the higher molecular weight F_{145} protein was detected in lanes with DSP added (Fig 4.18, lanes 6 to 8). This confirmed the presence of F protein crosslinked to GA protein in the lysates. When the immunoprecipitated lysates were probed with anti-FLAG antibodies (Fig 4.18, lanes 9 to 12), only the higher GA_{170} protein was detected in all four lanes 9 to 12. The lower molecular weight GA_{70} protein is barely visible in lane 12. This confirms the presence of GA in the lysates.

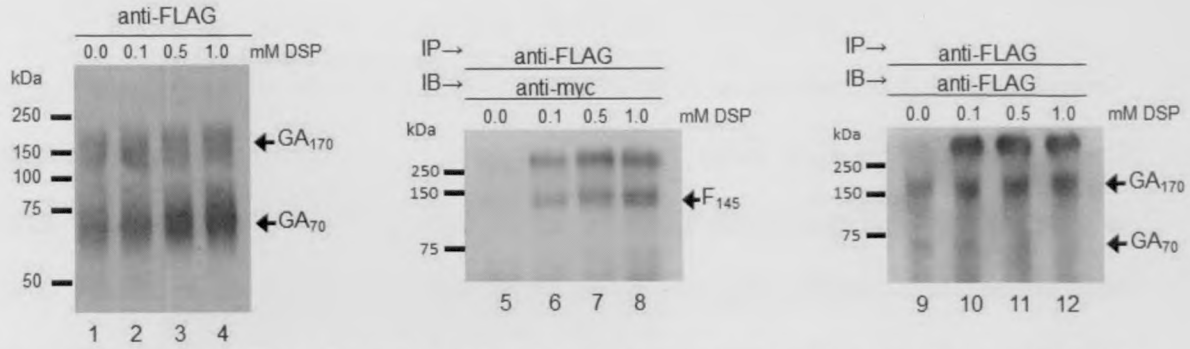

Figure 4.18. Crosslinking of F and GA in 293T cells. (Lanes 1-4) Immunoprecipitation of the cell lysate using anti-FLAG antibody to detect GA protein. (Lanes 5-8) Immunoblot of lysate using anti-myc antibody. (Lanes 9-12) Immunoblot of lysate using anti-FLAG antibody. Numbers above the photos indicate DSP crosslinker concentrations in mM.

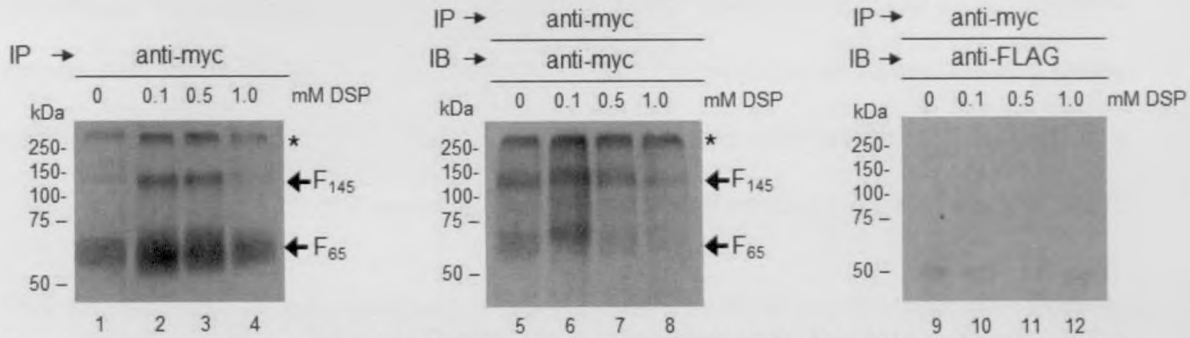

Figure 4.19. Crosslinking of F only in 293T cells. Immunoprecipitation of the cell lysate using anti-myc antibody to detect F protein (lanes 1 to 4). Immunoblot of lysate using anti-myc antibody. (lanes 5 to 8). Immunoblot of lysate using anti-FLAG antibody (lanes 9 to 12). Numbers above the photos indicate crosslinker concentrations in mM.

In order to exclude the possibility of the anti-myc antibody cross-reacting with the GA protein and the anti-FLAG antibody cross-reacting with the F protein, a control experiment was set up. 293T cells expressing only the F (Fig 4.19) or GA (Fig 4.20) proteins were crosslinked using the same concentration range of DSP (0, 0.1, 0.5, 1.0 mM).

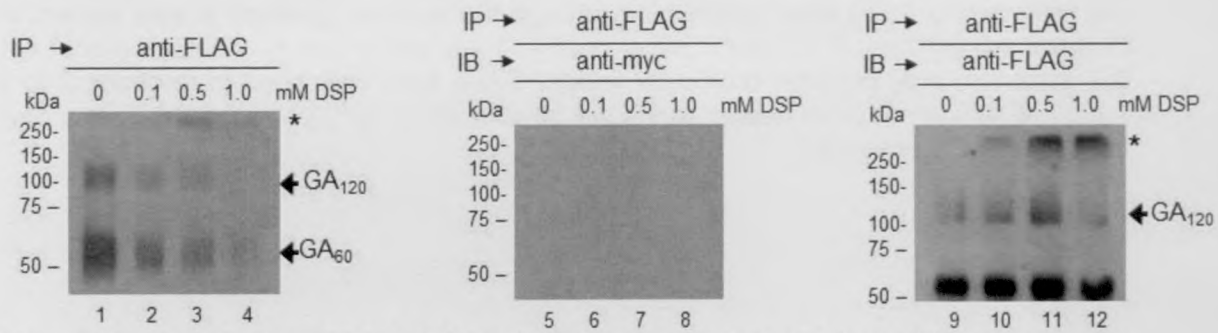

Figure 4.20. Crosslinking of GA in 293T cells. Immunoprecipitation of the cell lysate using anti-FLAG antibody to detect GA protein (lanes 1 to 4). Immunoblot of lysate using anti-FLAG antibody. (lanes 5 to 8). Immunoblot of lysate using anti-myc antibody (lanes 9 to 12). The bands of size 50 kDa in lanes 9 to 12 are due to the immunoglobulin heavy chain. Numbers above the photos indicate crosslinker concentrations in mM.

Crosslinking of F protein alone in 293T cells showed the two species F_{65} and F_{145} on the cell surface (Fig 4.19, lanes 1 to 4). This was confirmed by the immunoblot with anti-myc antibody (Fig 4.19, lanes 5 to 8). Crosslinking of GA protein alone in 293T cells showed two species GA_{60} and GA_{120} on the cell surface (Fig 4.20, lanes 1 to 4). This was confirmed by the immunoblot with anti-FLAG antibody (Fig 4.20, lanes 5 to 8). From the two control experiments using F and GA alone, we can see that there is an optimal concentration of DSP crosslinker within 0.1 to 0.5 mM DSP. Higher concentrations of DSP can result in the formation of large molecular weight aggregates which are not useful for studying protein interactions. These experiments also confirm that the two antibodies used are specific to the target proteins and show insignificant cross-reactivity (Fig 4.19 lanes 9 to 12 and Fig 4.20, lanes 5 to 8).

4.2.5 Sucrose gradient ultracentrifugation of F and G proteins

The fractions collected from ultracentrifugation in a continuous 5-30% sucrose gradient were analysed by Western blot (Fig 4.21 to 4.26). The first photo image (Fig 4.21) shows the immunoblot of the singly expressed F protein after centrifuging through the sucrose gradient. The F_{65} species was detected from fractions 2 to 9 and showed peaks at fractions 4 and 5. The F_{145} species was detected from fractions 4 to 12 and also showed peaks at fractions 4 and 5. A similar experiment using singly expressed GA protein (Fig 4.22) after centrifuging through the sucrose gradient is also shown. In this instance, only the high molecular weight GA_{170} form was seen in fractions 2 to 4 but peaking at fraction 3.

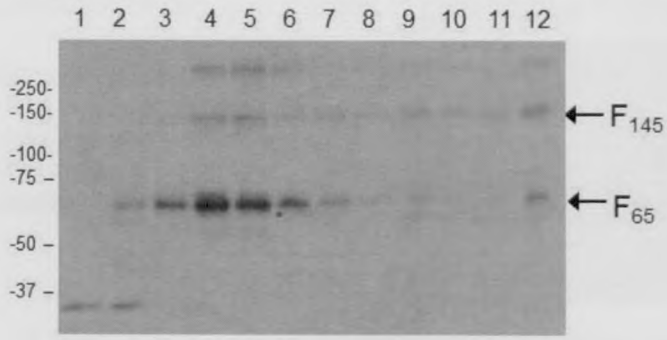

Figure 4.21. Western blot of all 12 fractions of F in a sucrose gradient probed with anti-myc.

Figure 4.22. Western blot of all 12 fractions of GA in a sucrose gradient probed with anti-FLAG.

The immunoblot of co-expressed F+GA protein centrifuged through the sucrose gradient is shown in Figures 4.23 and 4.24. The membrane probed with anti-myc antibody (Fig 4.23) detected the F_{65} and F_{145} proteins from fractions 2 to 5, which peaked at fractions 2 and 3. The membrane probed with anti-FLAG antibody (Fig 4.24) detected the GA_{170} protein from fractions 2 to 5, which also peaked at fractions 2 and 3. This suggests an association of F and GA which resulted in the two proteins migrating down the gradient at the same rate. After F and GA were co-transfected followed by addition of DSP crosslinker, the proteins were centrifuged through the same continuous sucrose gradient. Probing the fractions with anti-myc antibody (Fig 4.25) showed the F_{65} form in fractions 3 and 4, and the F_{145} form in fractions 3 to 8. Probing the fractions with anti-FLAG antibody (Fig. 4.26) showed the GA_{170} protein in fractions 2 to 8.

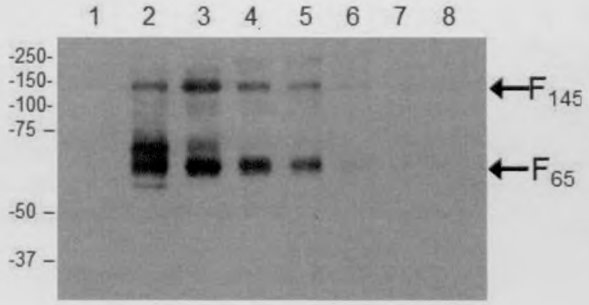

Figure 4.23. Western blot of the first 8 fractions of F+GA in a sucrose gradient probed with anti-myc. Fractions 9-12 did not show any detectable levels of protein.

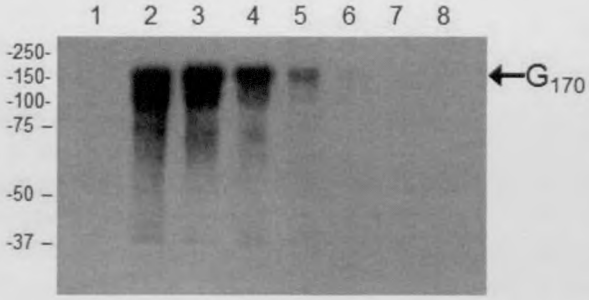

Figure 4.24. Western blot of the first 8 fractions of F+GA in a sucrose gradient probed with anti-FLAG. Fractions 9-12 did not show any detectable levels of protein.

There was co-migration of the F and GA proteins from fractions 3 to 8. This observation is similar to the previous experiment without DSP crosslinker (Fig 4.23 and 4.24), except that the F_{145} form of F protein was more predominant from fraction 4 onwards when crosslinker was applied.

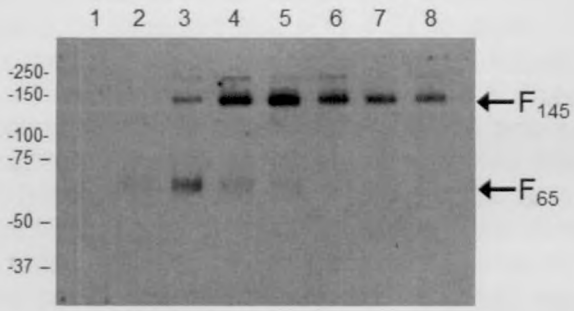

Figure 4.25. Western blot of the first 8 fractions of crosslinked F+GA in a sucrose gradient probed with anti-myc.

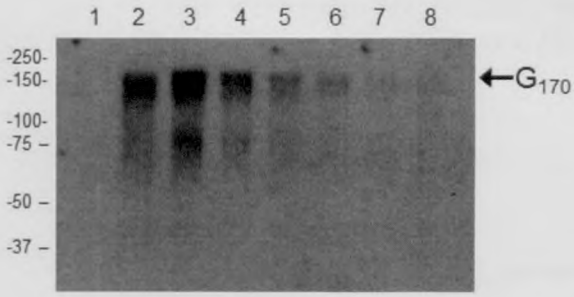

Figure 4.26. Western blot of the first 8 fractions of crosslinked F+GA in a sucrose gradient probed with anti-FLAG.

The appearance of GA_{170} in fraction 2 may be due to the presence of un-crosslinked GA protein.

4.2.6 Microscopy analysis of F and G expression

Images of HEp-2 cells under confocal immunofluorescence microscopy are shown below (Fig 4.27). The similar patterns of fluorescence between F and GA proteins may be due to co-localisation of the 2 proteins in parts of the cells. From the image (Fig 4.27, F_{WT}), the wild-type F protein can be seen to be well-distributed throughout the cell except the nucleus. The wild-type GA protein (Fig 4.27, GA_{WT}) shows concentrations around the edge (surface) of the cells.

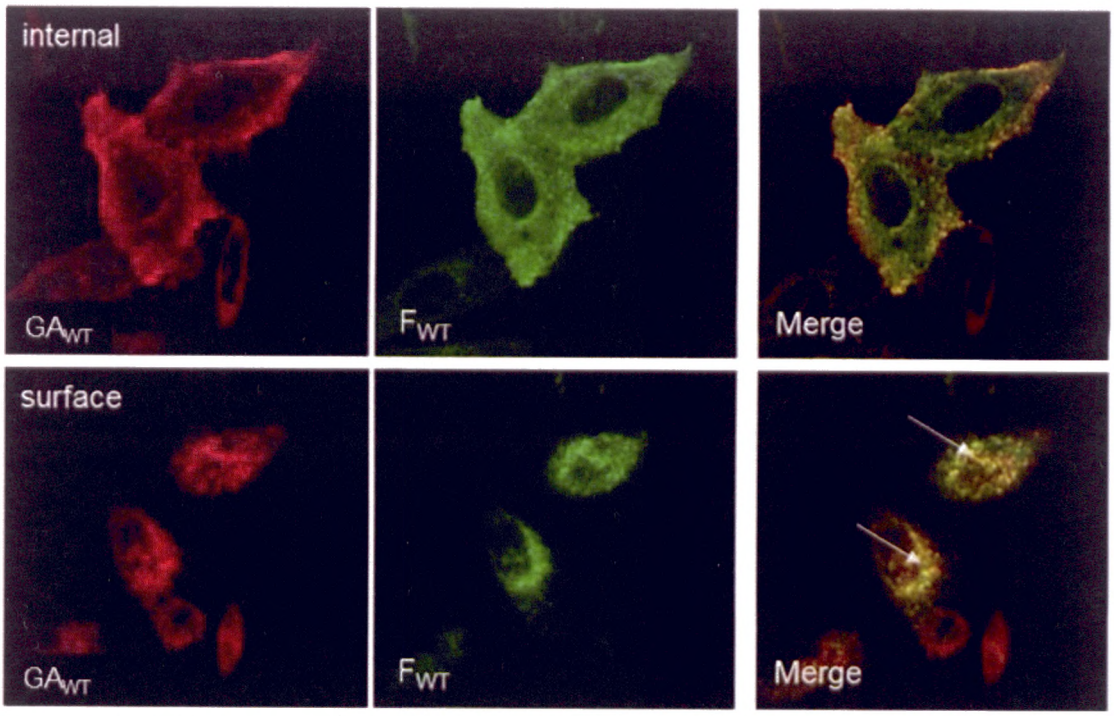

Figure 4.27. HEp-2 cells expressing wild type (WT) F and GA protein seen by a 100X confocal objective. F protein is labeled with green dye FITC. GA protein is labeled with red dye Alexa Fluor 555. When both colours are combined (Merge), the yellow coloured areas (white arrows) represent co-localisation of F and GA proteins in the cells. The internal (top row) and surface (bottom row) views of the cells are shown.

The extent of co-localisation of both F_{WT} (FITC) and GA_{WT} (Alexa Fluor 555) protein expression in the cells was obtained by combining the green channel (FITC) and red channel (Alexa Fluor 555) to produce a yellow colour which indicates the regions where both proteins are found together. The yellow colouration was more intense around the

edges of the cell (where the cell membrane is). When a cross-sectional image was obtained (Fig 4.28), the cell surface showed the greatest amount of yellow colour demonstrating co-localisation of F and GA on the cell surface. When the Carl Zeiss Zen 2007 (LSM) software was used to calculate the degree of co-localisation, 3 areas on the cell surface were selected. The average values for correlation R and R^2 were calculated to be 0.81±0.03 and 0.66±0.05, respectively.

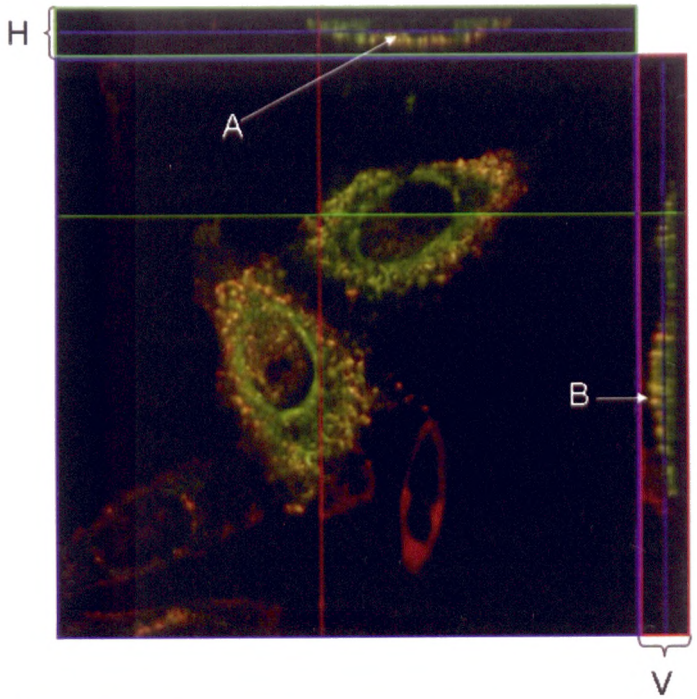

Figure 4.28. Same image of HEp-2 cells expressing F and GA protein seen in Fig 4.27. Horizontal (H) and vertical (V) cross-sectional images are shown at the top and right side of the main image respectively. Surface co-localisation of F and GA proteins (arrows A and B) are highlighted.

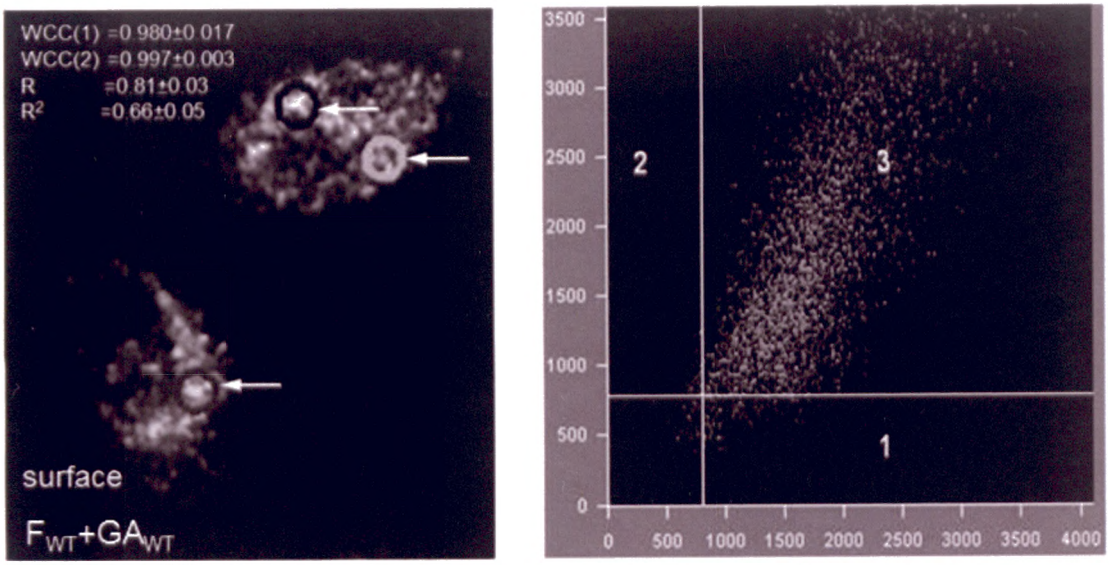

Figure 4.29. Analysis of the co-localisation of wild type F_{WT} and GA_{WT} proteins in HEp-2 cells. The three areas of co-localisation used for calculations are circled and indicated by arrows (left image). The surface view of the cells is shown. The scatterplot (right image) generated by the software shows region 1 (x-axis) representing the distribution of green pixels, region 2 (y-axis) representing the distribution of red pixels and region 3 representing the co-localisation of green and red pixels. Calculated values include the weighted co-localisation coefficient of the green channel (WCC1), red channel (WCC2) and Pearson's correlation coefficients (R and R^2).

These values strongly suggest co-localisation of F_{WT} and GA_{WT} proteins on the surface of the HEp-2 cells (Fig 4.29). Images obtained from both conventional and confocal microscopy of HEp-2 cells co-transfected with F_{WT} and GA_{WT} proteins suggest that both proteins associate on the surface and in certain locations within the cells. This is in line with the observation in the cell expression studies in previous sections which point to a close association between the F_{WT} and GA_{WT} proteins on the cell surface.

Images of Vero E6 cells under immunofluorescence microscopy are shown below (Fig 4.30). F_{WT} and GA_{WT} proteins show similar fluorescence patterns to those in HEp-2 cells (Fig 4.27). Using the same experimental conditions, Vero E6 cells co-transfected with F_{WT} and GA_{WT} proteins were also viewed under a confocal microscope. As seen in Figure 4.30, the F_{WT} protein is well-distributed throughout the cell except the nucleus (similar to Fig 4.27). The GA_{WT} protein is more concentrated near the edges of the cell and around the nucleus. When observing the merged green and red images, the yellow colouration was more intense around the nucleus of the cell and around the cell edges. A cross-sectional image (Fig 4.31) also demonstrated the presence of F_{WT} and GA_{WT} on the surface of Vero E6 cells.

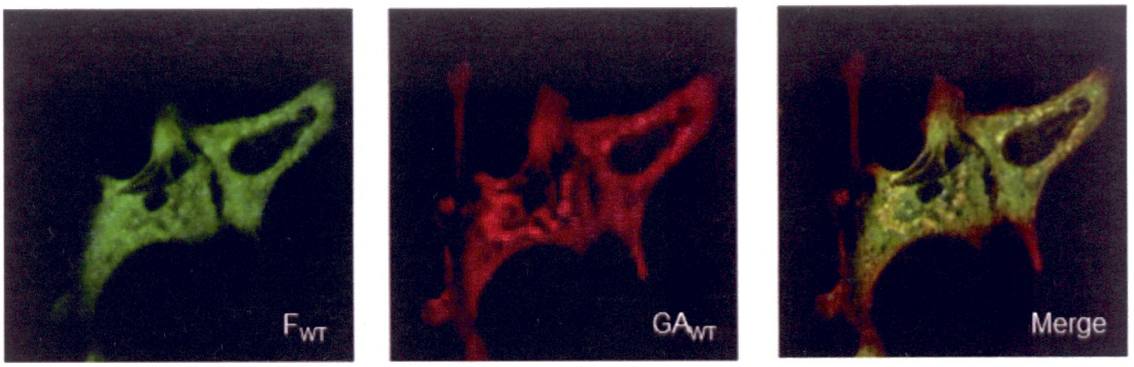

Figure 4.30. Vero E6 cells expressing wild type F_{WT} and GA_{WT} protein seen by a 63X confocal objective. F_{WT} protein is labeled with green dye FITC. GA_{WT} protein is labeled with red dye Alexa Fluor 555. When both colours are combined (Merge), the yellow coloured areas represent co-localisation of F_{WT} and GA_{WT} proteins in the cells. Only the internal view of the cells are shown.

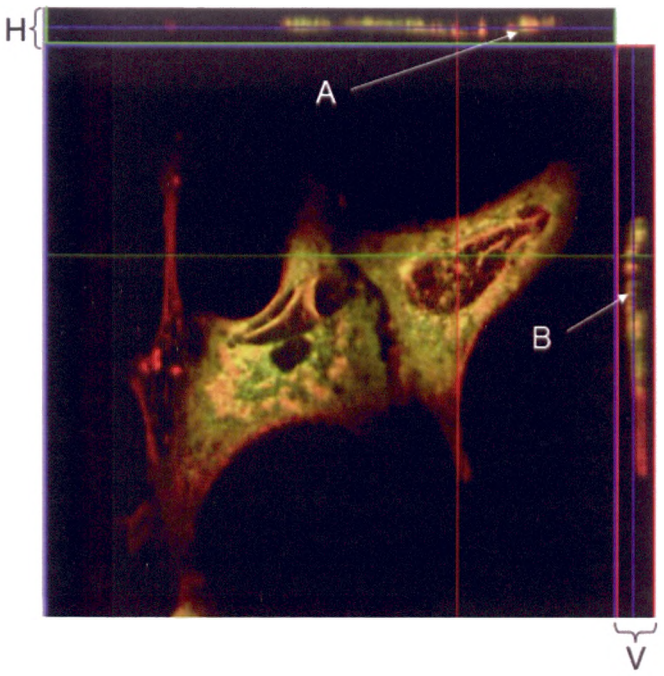

Figure 4.31. Same image of Vero E6 cells expressing F and GA protein seen in Fig 4.30. Horizontal (H) and vertical (V) cross-sectional images are shown at the top and right side of the main image respectively. Surface co-localisation of F and GA proteins (arrows A and B) are highlighted.

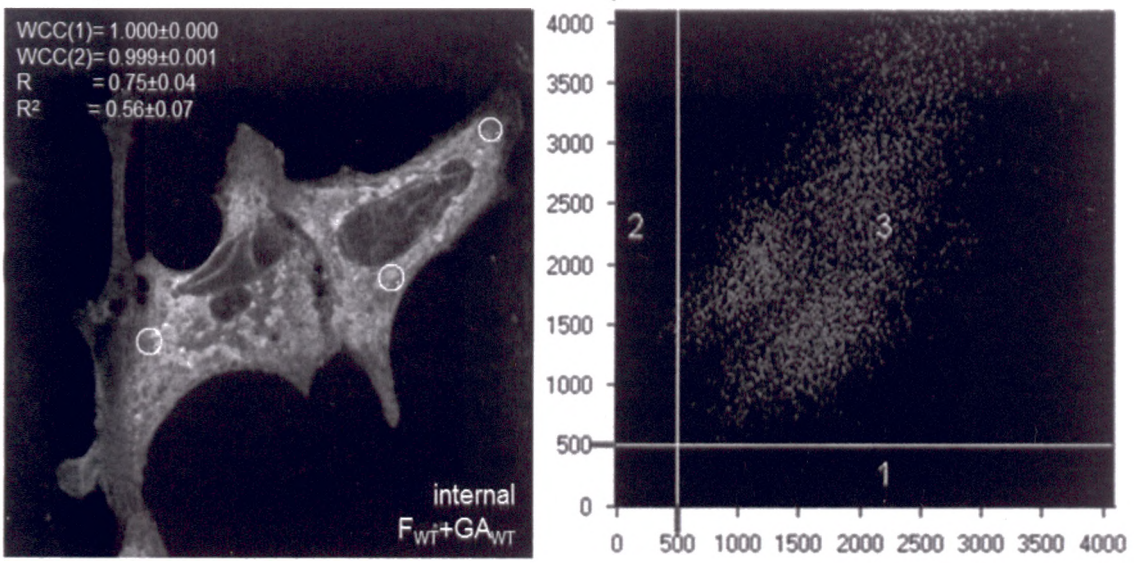

Figure 4.32. Analysis of the co-localisation of wild type F_{WT} and GA_{WT} proteins in Vero E6 cells. The three areas of co-localisation used for calculations are circled in the left image. The internal cross-section of the cells is shown. The scatterplot (right image) generated by the software shows region 1 (x-axis) representing the distribution of green pixels, region 2 (y-axis) representing the distribution of red pixels and region 3 representing the co-localisation of green and red pixels. Calculated values include the weighted co-localisation coefficient of the green channel (WCC1), red channel (WCC2) and Pearson's correlation coefficients (R and R^2).

The Carl Zeiss Zen 2007 (LSM) software was used to calculate the degree of co-localisation, 3 areas in the cell were selected (Fig 4.32). The average values for correlation R and R^2 were calculated to be 0.75±0.04 and 0.56±0.07, respectively. These values are similar to those obtained from the HEp-2 transfected cells suggesting that F and GA generally co-localise when expressed in mammalian cell-lines.

4.2.7 Flow cytometry analysis of F and G expression

The histograms plotted by the FACScalibur software are shown below (Fig 4.33). Using the wild type pCAGGS plasmid as a control, it was observed that the fluorescence intensity shown by the cells expressing only GA protein were almost identical to those cells expressing both GA and F proteins. The only exception was in 293T cells where cells expressing only GA protein had slightly higher intensity than those expressing both F and GA proteins. Generally this experiment showed that the presence of F did not affect the expression level of GA on the cell surface.

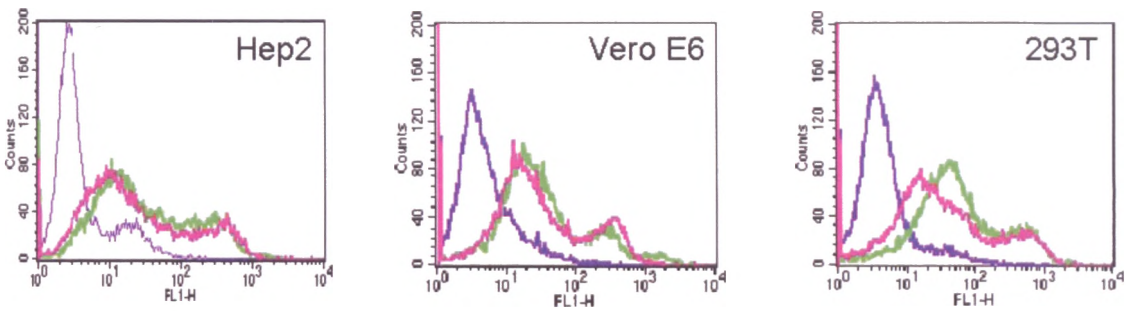

Figure 4.33. Data from FACS analysis of HEp-2, Vero E6 and 293T cells transfected with either wild type pCAGGS plasmid (purple line), pCAGGS/GA-FLAG plasmid (green line) or pCAGGS/GA-FLAG+pCAGGS/F-myc plasmids (pink line). The graphs are plotted using cell counts against fluorescence intensity (FITC channel).

4.2.8 Images of mammalian cell lines used

Digital images of the various cell lines used are shown to illustrate the effect of transfection on the cell morphology.

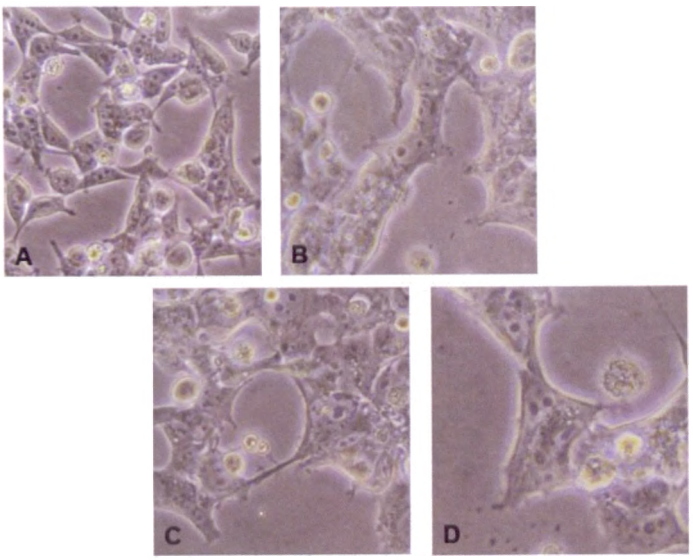

Figure 4.34. Images of 293T cells viewed under a 20X objective of an inverted microscope. Cells shown are (A) non-transfected, (B) transfected with F_{WT}, (C) transfected with GA_{WT} and (D) transfected with both F_{WT} and GA_{WT}. All images were taken 24 hpi.

The appearance of 293T cells (Fig 4.34) is usually round or star-shaped and are fairly well-spaced from each other. When the transfection reagent is added together with the plasmid, the cells started to clump together. Some cells showed signs of rounding-up. This phenomenon is more pronounced when both F and GA plasmids were transfected together.

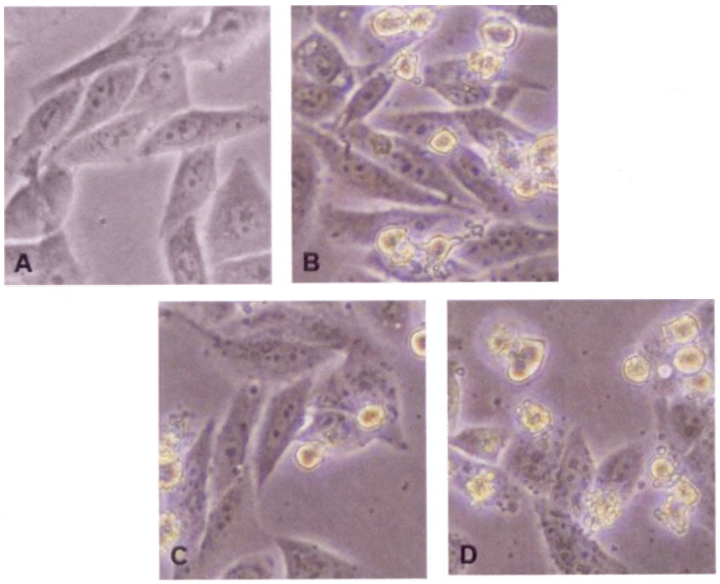

Figure 4.35. Images of HEp-2 cells viewed under a 20X objective of an inverted microscope. Cells shown are (A) non-transfected, (B) transfected with F_{WT}, (C) transfected with GA_{WT} and (D) transfected with both F_{WT} and GA_{WT}. All images were taken 24 hpi.

The shape of HEp-2 cells (Fig 4.35) is usually angular and the cells are regularly spaced apart. When the transfection reagent was added together with the plasmid, some of the cells started to deform and others showed signs of rounding-up. Just as in 293T cells, this occurrence was more evident when both F and GA plasmids were co-transfected.

4.2.9 Summary of F and G expression using pCAGGS/MCS system

When using the pCAGGS/MCS expression system, the expression of F protein was not significantly affected by the presence of GA or GB proteins. The main form of F protein present on the surface of 293T cells is the 65 kDa monomer, as was earlier observed in the vaccinia-driven expression system. Similarly with GA and GB expression on the cell surface, the presence of F had a tendency to shift the size of GA (Fig. 4.12) and GB (Fig. 4.14) proteins to the larger multimeric form. From the study of the surface expression of F and GA/B proteins, there were indications of co-precipitation of GA/B protein when lysates were pulled down with anti-myc antibody which binds only the F protein (Fig. 4.11 and 4.13). This association was further demonstrated by crosslinking of F and GA proteins before immunoprecipitation or Western blot and sucrose gradient analysis. When F and GA were crosslinked, the most predominant forms of the proteins were the higher molecular weight sizes (refer to Fig. 4.17 and 4.18). This may be due to F and GA multimers forming a complex on the cell surface as suggested by (Lamb et al., 2006). Analysis of the F (Fig. 4.21) and GA (Fig. 4.22) proteins singly on a continuous sucrose gradient showed that the two proteins migrated at different peak fractions (densities). However, when both proteins were co-expressed with (Fig. 4.25 and 4.26) and without (Fig. 4.23 and 4.24) crosslinking, the results showed that the F and GA proteins migrated within the same peak fractions. The confocal immunofluorescence images of F and GA co-transfected cells showed areas of co-localisation of F and GA proteins within the cell and on the cell surface in HEp-2 cells (Fig. 4.27 and 4.28), as well as in Vero E6 cells (Fig 4.30 and Fig 4.31). This cell surface association of F and GA/B proteins in HMPV supports the possibility that the action of F protein coupled with that of the GA/B protein is necessary for virus infection. This interaction of F and G proteins has already been demonstrated in a related virus hRSV (Feldman et al., 2001; Heminway et al., 1994; Low et al., 2008). In animals models, it has been shown that modifying the F protein to become trypsin-independent

(Biacchesi et al., 2006) does not improve infection rates, whereas G protein deletion mutants have reduced infectivity (Biacchesi et al., 2004). All these data suggests that F and G proteins are necessary for infection and are potential targets for antiviral therapy.

4.3 Expression of F and G protein mutants in mammalian cells

4.3.1 Western blot of cells expressing F and G mutants

F and GA mutants proteins were constructed as described in Methods (2.4.3). A schematic representation is shown in Fig 4.36. The various abbreviations used for the proteins are: F_{WT}, GA_{WT} and GB_{WT} denoting the wild-type F, GA and GB proteins; $F_{\Delta CT}$ and $GA_{\Delta CT}$ denoting the truncated F and GA proteins without the cytoplasmic tail; $F_{\Delta TM}$ and $GA_{\Delta TM}$ denoting the truncated F and GA proteins without the transmembrane region and cytoplasmic tail. All F proteins and mutants were constructed with a cmyc fusion tag, whereas all the GA proteins and mutants were constructed with a FLAG fusion tag. For better differentiation, the wild-type F and GA proteins were denoted by F_{WT} and GA_{WT}. These mutant proteins were transfected into 293T cells for 48 hours and analysed by Western blot (Fig 4.34, (B)). The two F protein mutants $F_{\Delta TM}$ (without transmembrane and cytoplasmic domain) and $F_{\Delta CT}$ (without cytoplasmic domain) have only one monomeric species unlike the wild-type protein (F_{WT}) which shows the monomeric and multimeric forms.

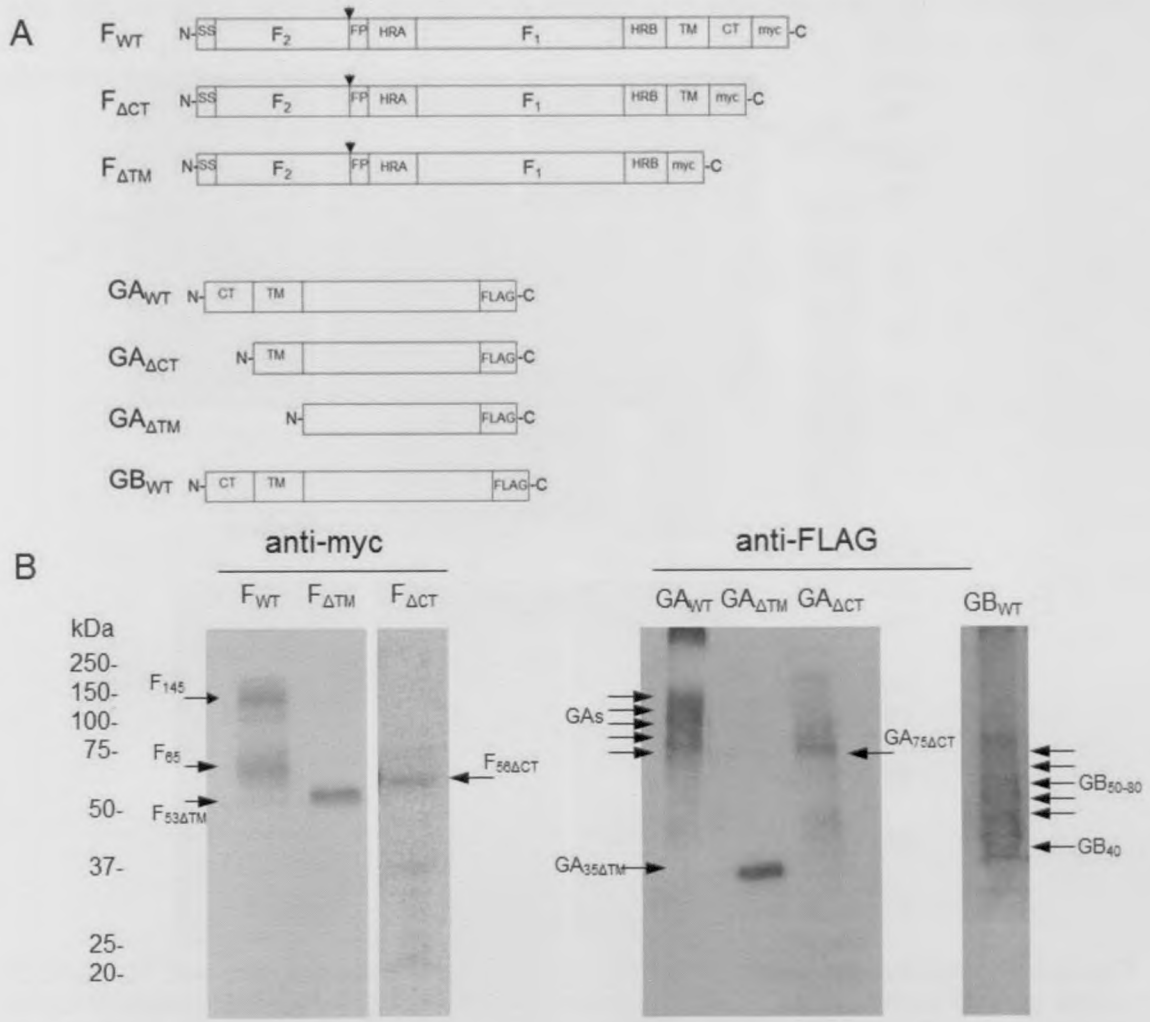

Figure 4.36. Illustration of the (A) mutant F and GA proteins constructed. "N" and "C" indicate the location of the N-terminal and C-terminal of the proteins. "SS" is the signal sequence, "FP" is the fusion peptide, "HRA" and "HRB" are the heptad repeats A and B, "TM" is the transmembrane region, "CT" is the cytoplasmic tail region, "F1" and "F2" are the two F protein subunits, the inverted arrows indicate the cleavage point of trypsin-like proteases. (B) Western blot of the various F and GA protein mutants. The GB protein is shown for comparison. The various species of the F and GA proteins are shown together with their sizes in kDa. The exposure for $F_{\Delta CT}$ was enhanced due to very low signal. GAs-GA smear from 75-150 kDa.

The mutant $GA_{\Delta TM}$ (without transmembrane and cytoplasmic domain) and the $GA_{\Delta CT}$ mutant (without cytoplasmic domain) both have one monomeric form, unlike the wild-type G protein (GA_{WT}) which has a highly glycosylated form observed as a smear.

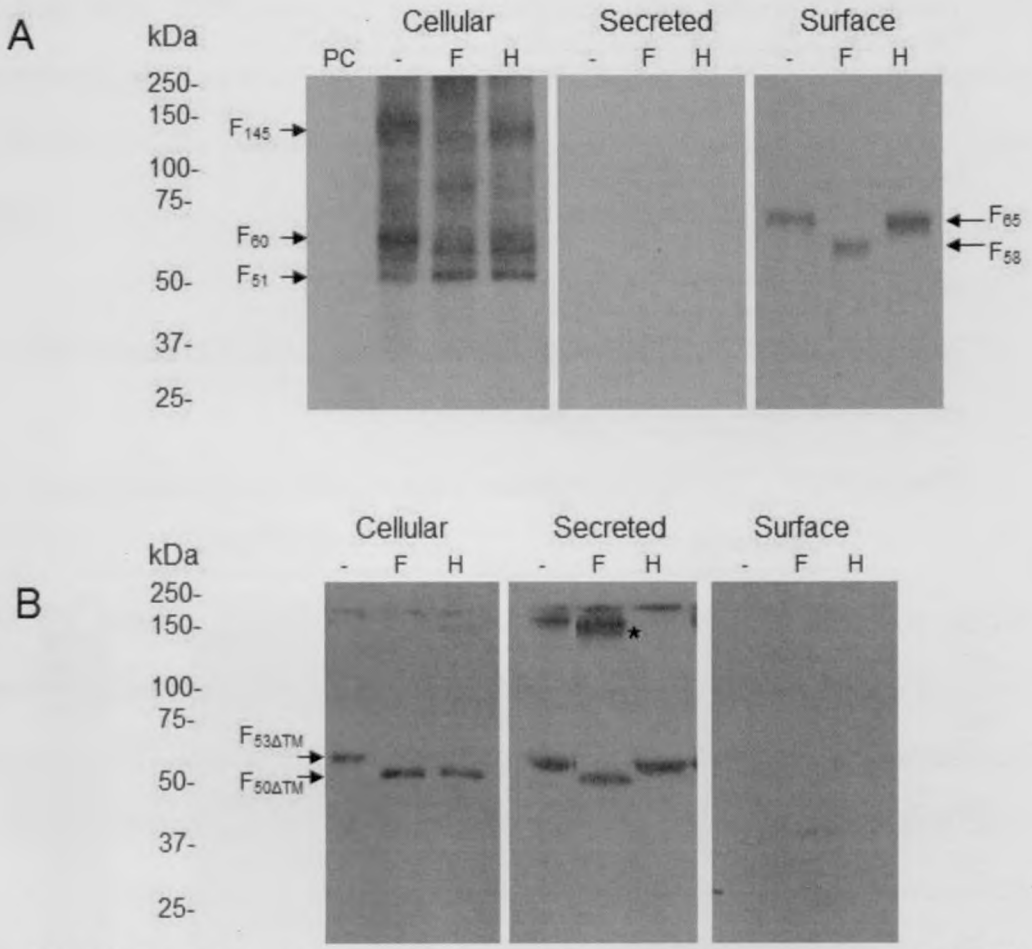

Figure 4.37. Glycosylation analysis of the F_{WT} (A) and $F_{\Delta TM}$ (B) by Western blot. PC-pCAGGS control plasmid transfected cells, (-)-non treated protein, F-PNGaseF treated protein, H-EndoH treated protein. The two F proteins were examined in the cellular form, secreted form and surface-expressed form. [*]-indicates high molecular weight aggregates of $F_{\Delta TM}$ protein. The various F protein forms are shown with their respective sizes in kDa.

Glycosylation studies were performed on F_{WT} and $F_{\Delta TM}$ (Fig 4.37) by treatment with PNGaseF and EndoH (described in Methods 2.5.5). The wild-type F protein was present in the cell and on the cell surface but was not secreted into the media. This was expected since the transmembrane region anchors the protein to the host cell membrane. On the other hand, the $F_{\Delta TM}$ protein was found in the cell and was secreted into the media but was not present on the cell surface. Thus, the lack of transmembrane domain means this protein cannot anchor itself in the host cell membrane but is able to be transported to the cell surface to be secreted. The $F_{\Delta CT}$ protein was not studied because of the very low levels of protein detected (Fig 4.36 B). The $F_{\Delta TM}$ protein was sensitive to PNGaseF suggesting that it is N-link glycosylated but

only the secreted form was resistant to EndoH probably because the secreted form contains mature N-linked sugars.

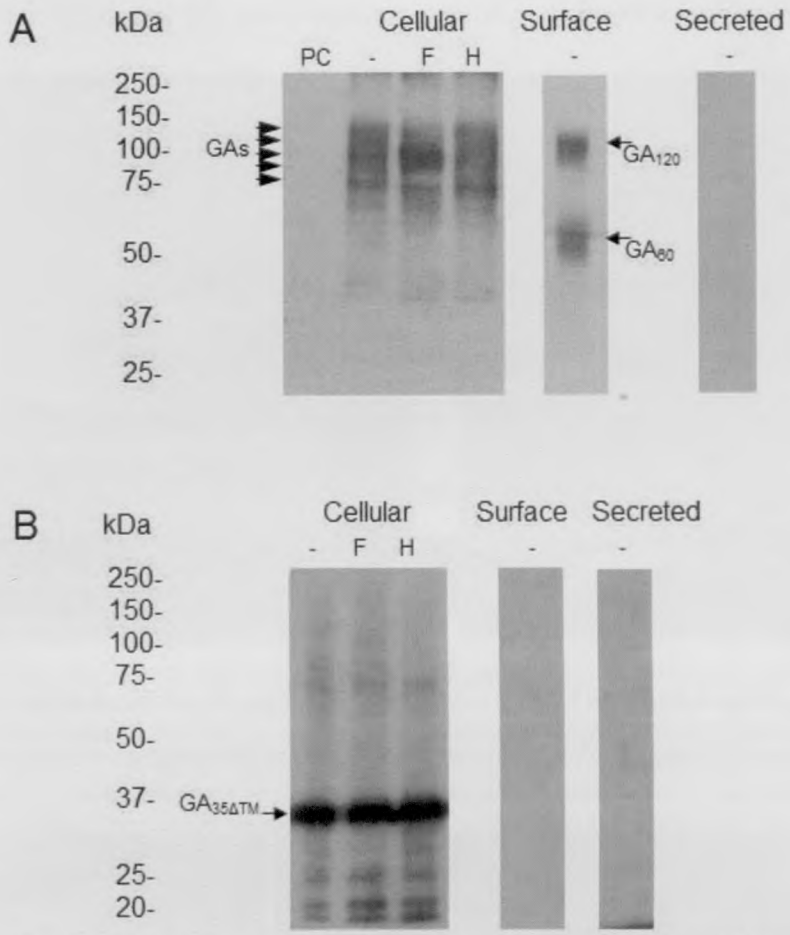

Figure 4.38. Glycosylation analysis of the GA_{WT} (A) and $GA_{\Delta TM}$ (B) by Western blot. PC-pCAGGS control plasmid transfected cells, (-)-non treated protein, F-PNGaseF treated protein, H-EndoH treated protein. The two GA proteins were examined in the cellular form, secreted form and surface-expressed form. GAs-GA smear from 75-150 kDa. The various GA protein forms are shown with their respective sizes in kDa. Surface expressed GA_{WT} treated with PNGasF and EndoH can be found in section 4.2.2 (Fig 4.12).

Glycosylation studies were also performed on GA_{WT} and $GA_{\Delta TM}$ (Fig 4.38) by treatment with PNGaseF and EndoH (described in Methods 2.5.5). The wild-type GA protein was present within the cell and on the cell surface but was not secreted into the media. This is expected since the transmembrane region anchors the protein to the host cell membrane. On the other hand, the $GA_{\Delta TM}$ protein was found in the cell but was not secreted into the media nor present on the cell surface. The transmembrane domain of the GA protein is not only the region which anchors the protein but seems to have a role in the export of the protein, unlike the F protein which has a signal sequence at the

N-terminal. The $GA_{\Delta CT}$ protein was not studied due to the low levels of expression (Fig 4.36 B).

4.3.2 Confocal immunofluorescence microscopy of cells expressing F and G combinations

Immunofluorescence images taken using a confocal microscope allowed the study of the pattern of mutant F and G proteins in HEp-2 cells. As described in Methods (2.4.3), truncated F and G protein constructs were made and these were co-transfected into HEp-2 cells according to the scheme shown below:

F wild type combinations	G wild type combinations
F_{WT} + $GA_{\Delta TM}$ (Fig 4.41, 4.42)	$F_{\Delta TM}$ + GA_{WT} (Fig 4.37,4.38)
F_{WT} + $GA_{\Delta CT}$ (Fig 4.43, 4.44)	$F_{\Delta CT}$ + GA_{WT} (Fig 4.39, 4.40)

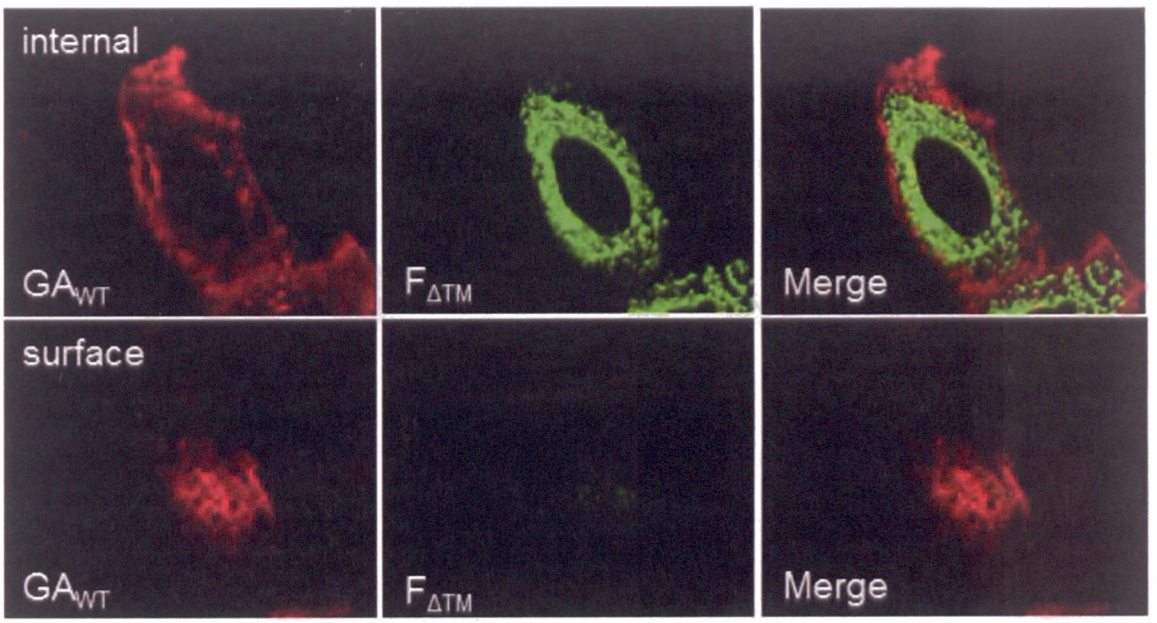

Figure 4.39. HEp-2 cells expressing wild-type GA_{WT} protein and transmembrane-region deleted $F_{\Delta TM}$ protein as seen by a 100X confocal objective. F protein is labeled with green dye FITC. GA protein is labeled with red dye Alexa Fluor 555. When both colours are combined (Merge), the yellow coloured areas represent co-localisation of F and GA proteins in the cells. The internal (top row) and surface (bottom row) views of the cells are shown.

When $F_{\Delta TM}$ was co-transfected with GA_{WT}, the GA_{WT} protein distribution in the cell was similar to that when co-transfected with F_{WT}. However, the distribution of $F_{\Delta TM}$ was

different from F_{WT}. $F_{\Delta TM}$ was found throughout the cytoplasm but not at the cell surface (Fig 4.39). In addition, the values obtained for Pearson's correlation (Fig 4.40) were 0.39 and 0.16 (R and R^2) which are not indicative of co-localisation of the two proteins.

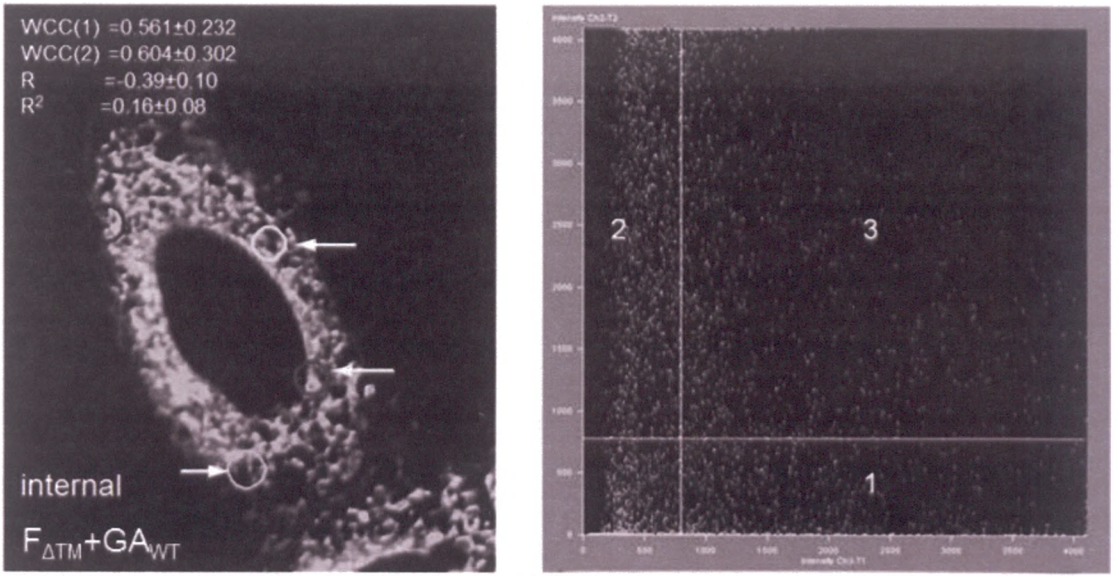

Figure 4.40. Analysis of the co-localisation of $F_{\Delta TM}$ and GA_{WT} proteins in HEp-2 cells. The three areas of co-localisation used for calculations are circled and indicated by arrows (left image). The internal view of the cell is shown. The scatteplot (right image) generated by the software shows region 1 (x-axis) representing the distribution of green pixels, region 2 (y-axis) representing the distribution of red pixels and region 3 representing the co-localisation of green and red pixels. Calculated values include the weighted co-localisation coefficient of the green channel (WCC1), red channel (WCC2) and Pearson's correlation coefficients (R and R^2).

When $F_{\Delta CT}$ was co-transfected with GA_{WT}, the GA_{WT} protein distribution in the cell was comparable to that when co-transfected with F_{WT}. The staining pattern observed for $F_{\Delta CT}$ was different from F_{WT}. $F_{\Delta CT}$ was only distributed around the perinuclear region (Fig 4.41) and not present on the cell surface. There appeared to be co-localisation of the GA_{WT} and $F_{\Delta CT}$ proteins within the perinuclear region. In addition, the values obtained for Pearson's correlation (Fig 4.42) were 0.76 and 0.58 (R and R^2) which was probably a result of the limited co-localisation of the two proteins around the nucleus.

When F_{WT} was co-transfected with $GA_{\Delta TM}$ (Fig 4.43), the distribution of F_{WT} in the cell was similar to that of F_{WT} co-transfected with GA_{WT} (Fig 4.27). However there was very little yellow area observed in the merged view and there was almost no trace of $GA_{\Delta TM}$ on the cell surface. Comparing this with the Pearson's correlation value in Figure 4.44 ($R=0.02$, $R^2=0.00$), there was clearly zero co-localisation between the two proteins.

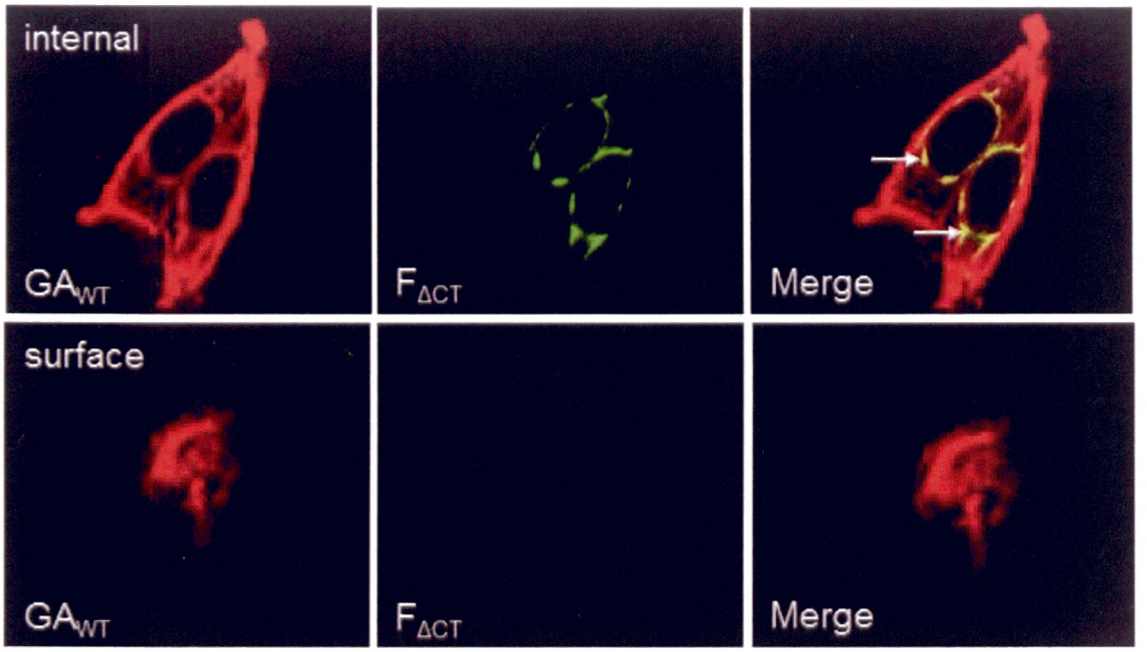

Figure 4.41. HEp-2 cells expressing wild-type GA_{WT} protein and cytoplasmic tail-region deleted $F_{\Delta CT}$ protein as seen by a 100X confocal objective. F protein is labeled with green dye FITC. GA protein is labeled with red dye Alexa Fluor 555. When both colours are combined (Merge), the yellow coloured areas represent co-localisation of F and GA proteins in the cells. The internal (top row) and surface (bottom row) views of the cells are shown. Arrows indicate the areas of co-localisation around the nucleus.

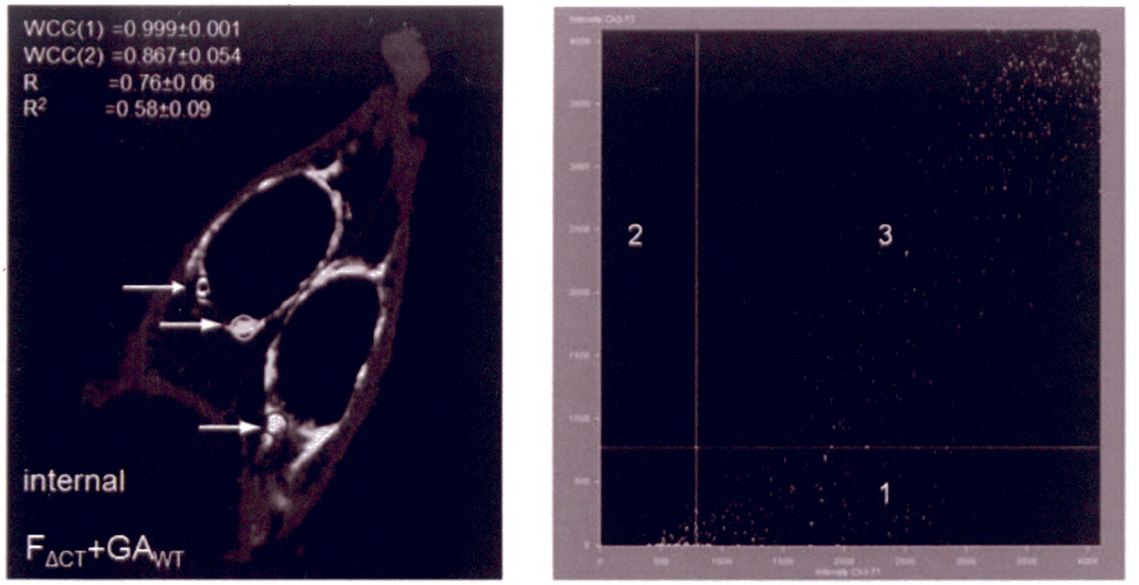

Figure 4.42. Analysis of the co-localisation of $F_{\Delta CT}$ and GA_{WT} proteins in HEp-2 cells. The three areas of co-localisation used for calculations are circled and indicated by arrows (left image). The internal view of the cell is shown. The scatteplot (right image) generated by the software shows region 1 (x-axis) representing the distribution of green pixels, region 2 (y-axis) representing the distribution of red pixels and region 3 representing the co-localisation of green and red pixels. Calculated values include the weighted co-localisation coefficient of the green channel (WCC1), red channel (WCC2) and Pearson's correlation coefficients (R and R^2).

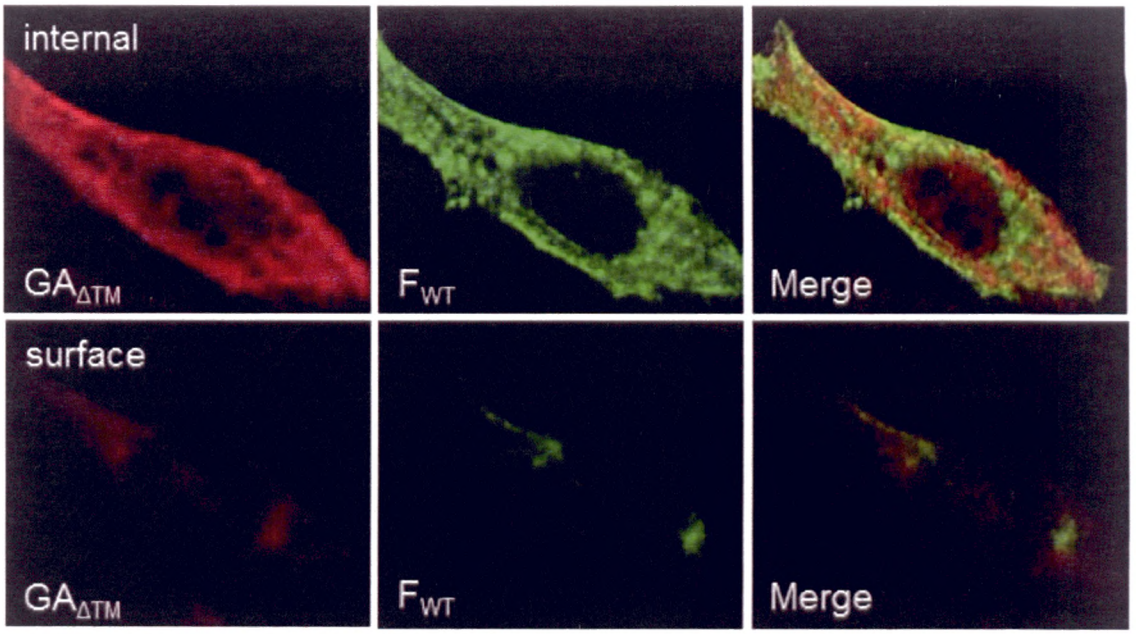

Figure 4.43. HEp-2 cells expressing wild-type F_{WT} protein and transmembrane-region deleted $GA_{\Delta TM}$ protein as seen by a 100X confocal objective. F protein is labeled with green dye FITC. GA protein is labeled with red dye Alexa Fluor 555. When both colours are combined (Merge), the yellow coloured areas represent co-localisation of F and GA proteins in the cells. The internal (top row) and surface (bottom row) views of the cells are shown.

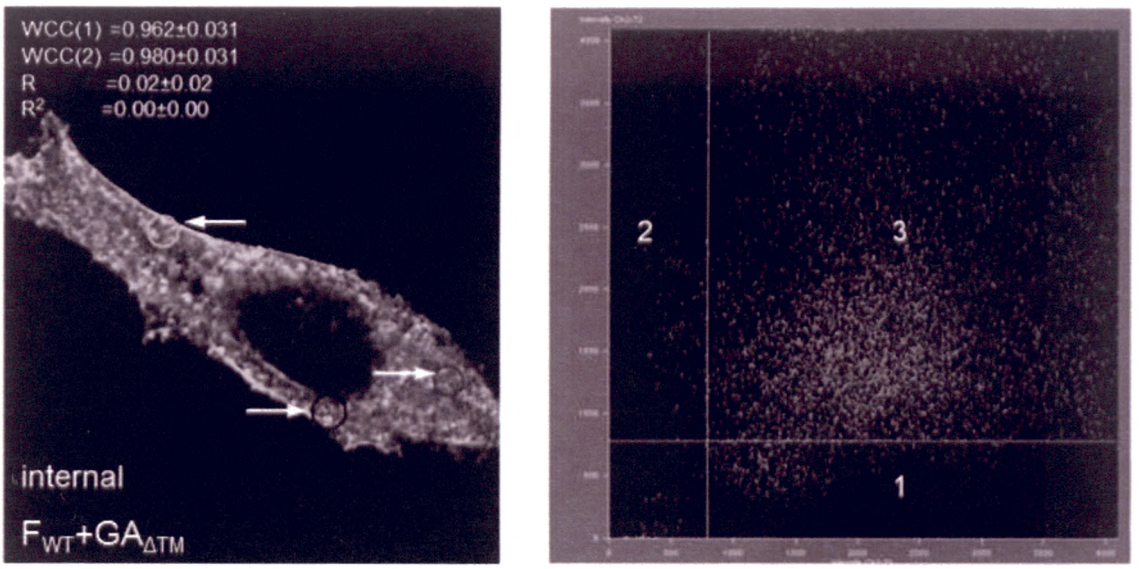

Figure 4.44. Analysis of the co-localisation of F_{WT} and $GA_{\Delta TM}$ proteins in HEp-2 cells. The three areas of co-localisation used for calculations are circled and indicated by arrows (left image). The internal view of the cell is shown. The scatteplot (right image) generated by the software shows region 1 (x-axis) representing the distribution of green pixels, region 2 (y-axis) representing the distribution of red pixels and region 3 representing the co-localisation of green and red pixels. Calculated values include the weighted co-localisation coefficient of the green channel (WCC1), red channel (WCC2) and Pearson's correlation coefficients (R and R^2).

When F_{WT} was co-transfected with $GA_{\Delta CT}$ (Fig 4.45), the distribution of F_{WT} in the cell was similar to that of F_{WT} co-transfected with GA_{WT} (Fig 4.27). The pattern of $GA_{\Delta CT}$ distribution was very similar to that of F_{WT} within the cell and on the surface.

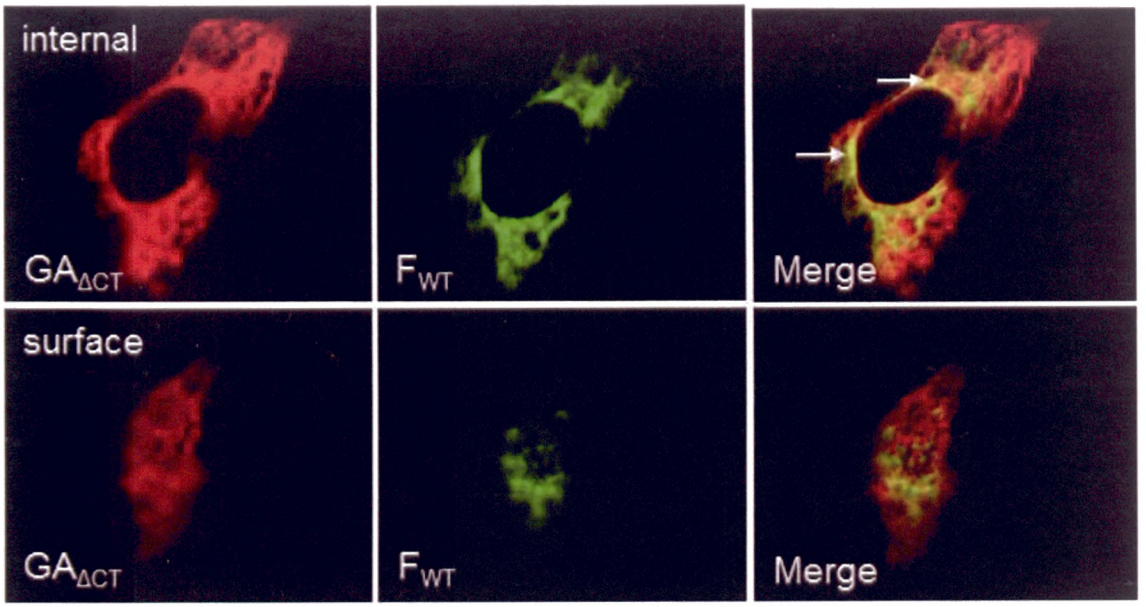

Figure 4.45. HEp-2 cells expressing wild-type F_{WT} protein and cytoplasmic tail-region deleted $GA_{\Delta CT}$ protein as seen by a 100X confocal objective. F protein is labeled with green dye FITC. GA protein is labeled with red dye Alexa Fluor 555. When both colours are combined (Merge), the yellow coloured areas represent co-localisation of F and GA proteins in the cells. The internal (top row) and surface (bottom row) views of the cells are shown. Arrows indicate areas of co-localisation around the nucleus.

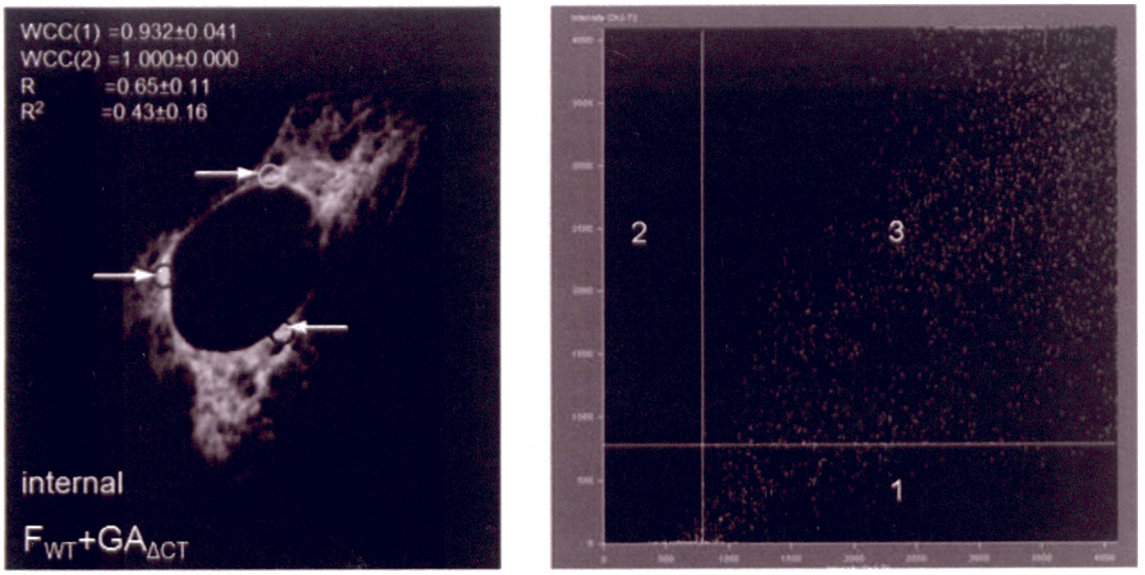

Figure 4.46. Analysis of the co-localisation of F_{WT} and $GA_{\Delta CT}$ proteins in HEp-2 cells. The three areas of co-localisation used for calculations are circled and indicated by arrows (left image). The internal view of the cell is shown. The scatteplot (right image) generated by the software shows region 1 (x-axis) representing the distribution of green pixels, region 2 (y-axis) representing the distribution of red pixels and region 3 representing the co-localisation of green and red pixels. Calculated values include the weighted co-localisation coefficient of the green channel (WCC1), red channel (WCC2) and Pearson's correlation coefficients (R and R^2).

Large areas of yellow in the merged image (white arrows) show co-localisation around the nucleus and on the surface. The Pearson's correlation values for this combination

of proteins (Fig 4.46) are R=0.65 and R^2=0.43. This suggests some degree of co-localisation although it may not be as high as the combination of F_{WT} and GA_{WT}.

4.3.3 Immunofluorescence microscopy of cells expressing F cytoplasmic-tail mutants

HEp-2 cells transfected with the various cytoplasmic-tail mutants of F protein (refer to Methods 2.4.3) were viewed under a fluorescence microscope. These images are shown in Figure 4.47 on the following page. There is a distinct pattern observed where the gradual reduction in the length of the cytoplasmic tail results in the increasing concentration of the mutant F protein around the perinuclear region of the cells corresponding to the location of the endoplasmic reticulum. The mutant F protein without a cytoplasmic tail is totally restricted to this region. This seems to imply a need for the cytoplasmic tail of the normal F protein in its processing to become a mature membrane-bound viral protein. In addition, the length of the cytoplasmic tail has an effect on the quantity of the mutant F protein within the cell. This is seen by the reduction in the fluorescence intensity as the cytoplasmic tail is reduced in length. The last two lysine residues closest to the transmembrane region (Fig. 4.47, images F514 and F515) seem to have the most significant effect on the processing of the mutant F protein.

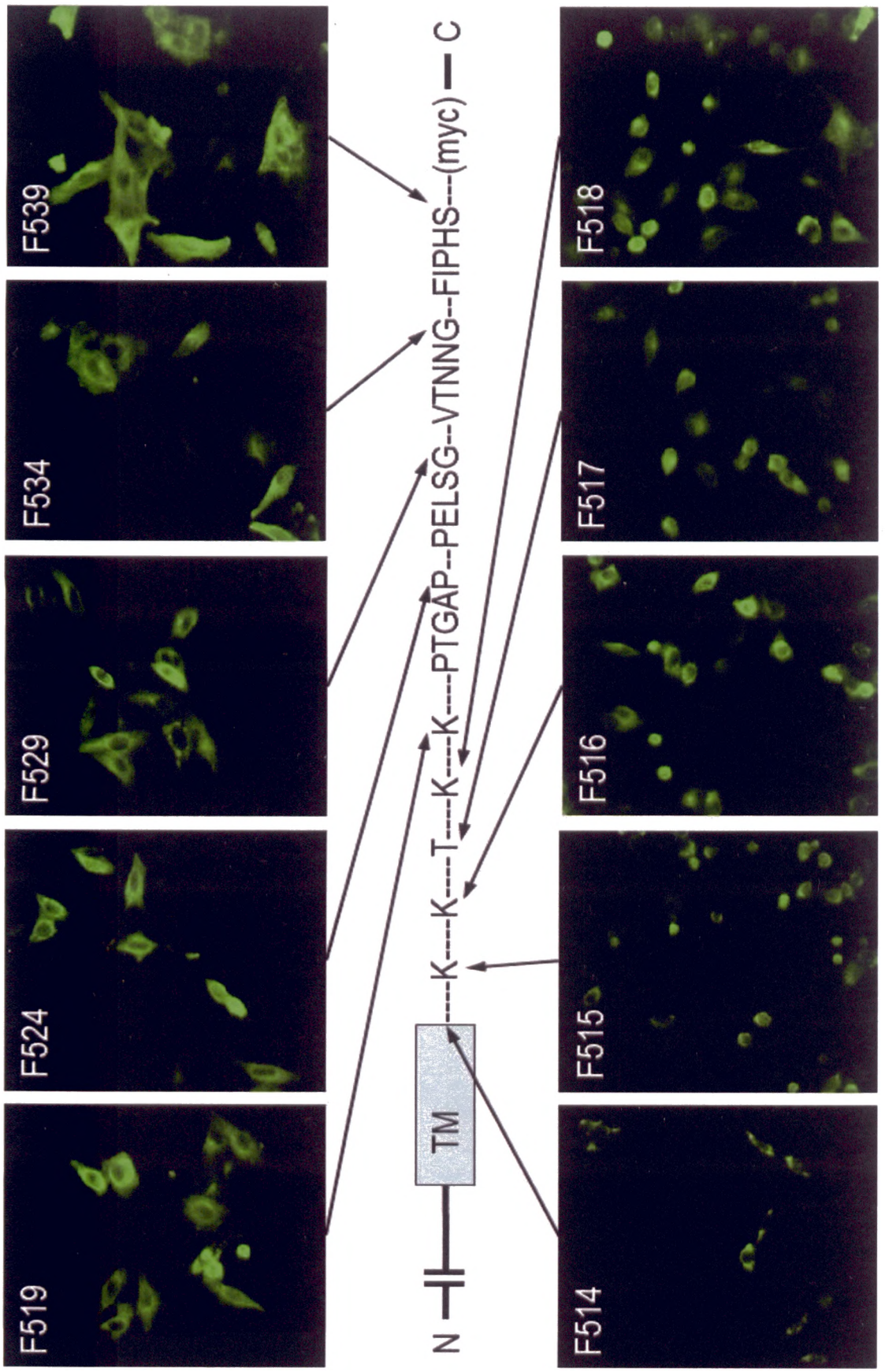

Figure 4.47. Immunofluorescence images of the various cytoplasmic tail deletion mutants of the F protein transfected in HEp-2 cells after 18 hours. The numbers indicate the last amino acid residue. 539 is the wild type and 514 has no cytoplasmic tail. All the F protein constructs have a myc tag at the C-terminal. TM-transmembrane region,

4.3.4 Western blot of cells expressing F cytoplasmic tail mutants

Western blot analysis was performed on the same F cytoplasmic tail mutant protein constructs transfected into 293T cells for 48 hours (Fig 4.48). The intensity of the signal on the membrane was highest in the wild-type protein and gradually decreased until there was very little signal from the F protein with no cytoplasmic tail ($F_{\Delta CT}$). This is in agreement with the observations of the immunofluorescence experiment described in the previous section. The monomeric form of the F protein was observed between the 54-58 kDa region.

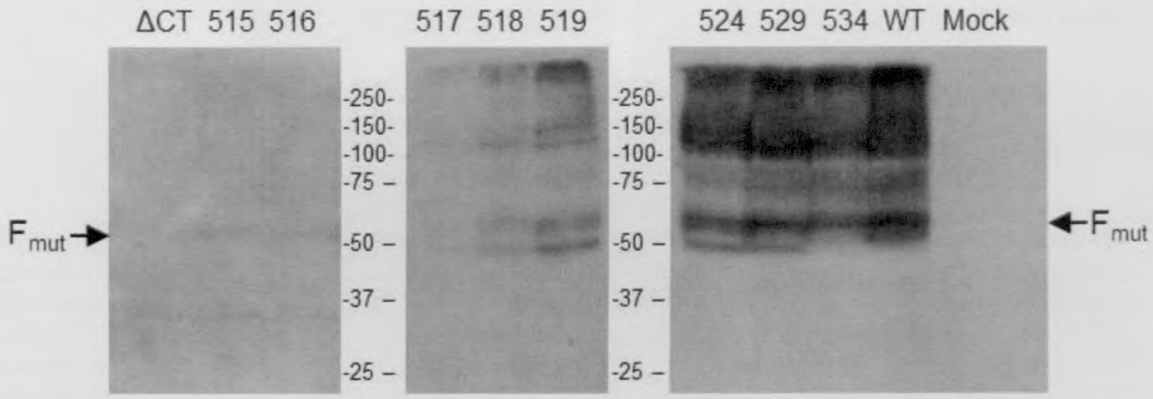

Figure 4.48. Western blot analysis of F cytoplasmic tail mutants which were probed with the anti-myc antibody. The numbers indicate the last amino acid residue of the mutant F proteins. Mock-mock transfected cells, WT-wild-type F_{WT} protein, ΔCT-$F_{\Delta CT}$ protein without cytoplasmic tail. The size range of the F mutants (F_{mut}) is approximately 54-58 kDa.

4.3.5 Summary of F and G mutant expression

In the F protein, the cytoplasmic domain plays an important role in the processing and maturation of the protein. A similar observation was made by a group which worked on hRSV (Oomens et al., 2006). The role of the cytoplasmic domain in the G protein is not as clear. Both proteins require their transmembrane region for anchoring to the host cell membrane but the G protein also requires it for proper processing and positioning at the host cell surface. This has been shown in hRSV G protein (Lichtenstein et al., 1996) as well.

4.4 Expression of M and N proteins in mammalian cells

4.4.1 Total protein expression

The pCAGGS vector expression system was utilized to express the HMPV M and N proteins singly in Vero E6 cells. The expression of N protein alone (Fig 4.49, lanes 1 and 2) showed a band at 43 kDa (N_{43}) which is the expected size for the monomeric form of N protein. The expression of M protein alone (Fig 4.49, lanes 3 and 4) showed a clear band at 28 kDa (M_{28}) corresponding to the expected size of the monomeric M protein. In the case of both proteins, there was a greater amount expressed after 2 days post-transfection compared to 1 day post-transfection.

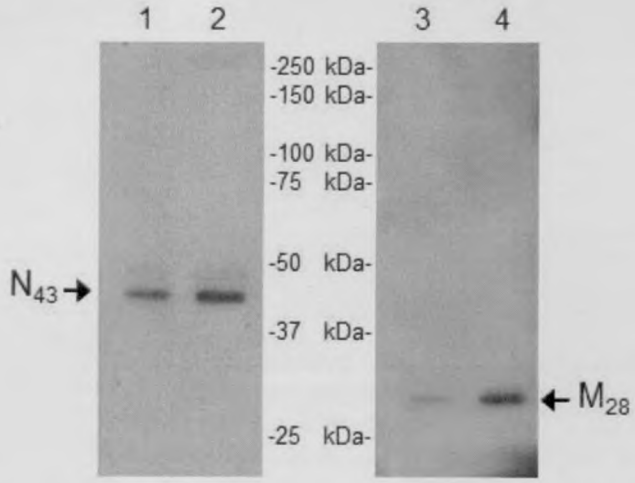

Figure 4.49. Western blot of N and M expressed in Vero E6 cells. Lanes 1 and 2, pCAGGS/N-myc expressed after 1 and 2 days, respectively. Lanes 3 and 4, pCAGGS/M expressed after 1 and 2 days, respectively. M and N proteins are shown with their respective sizes in kDa.

4.4.2 Microscopy analysis of M and N protein expression compared to F and GA

Images of Vero E6 cells under immunofluorescence microscopy are shown below (Fig 4.50). The N protein showed even staining throughout the cell except for the nucleus. The presence of a few inclusion bodies were also seen. The M protein staining pattern showed a web-like network probably involving cytoskeleton components. The F protein was also evenly distributed throughout the cell except the nucleus. There was an

accumulation of F protein around the perinuclear region which suggests endoplasmic reticulum and Golgi processing. The GA protein showed concentrations around the edge (surface) of the cells and the nucleus. In addition, there were fine filament-like projections from the cell surface.

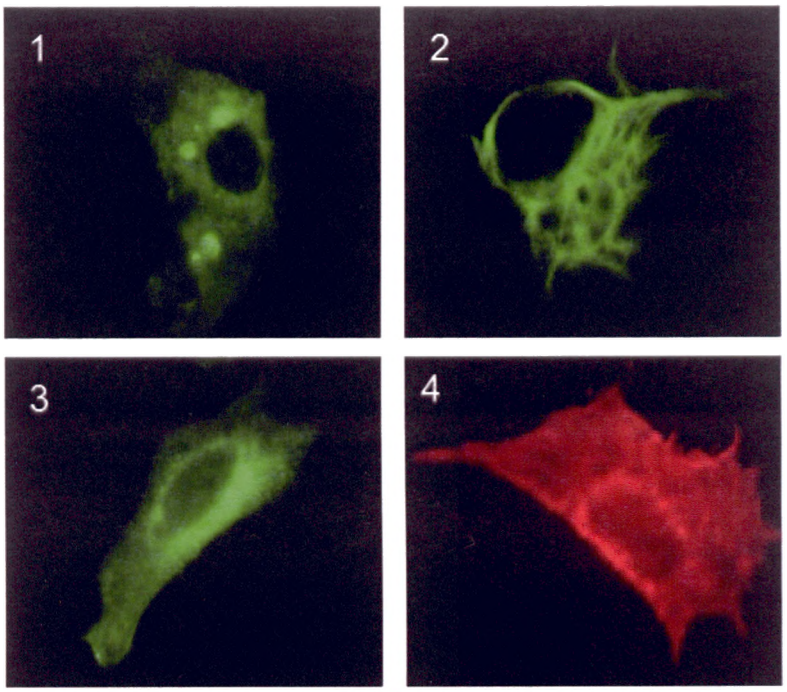

Figure 4.50. Immunofluorescence microscopy of Vero E6 cells expressing N, M, F and GA proteins. Image 1 shows Vero E6 cells transfected with pCAGGS/N-myc. Image 2 shows Vero E6 cells transfected with pCAGGS/M. Image 3 shows Vero E6 cells transfected with pCAGGS/F-myc. Image 4 shows Vero E6 cells transfected with pCAGGS/GA-FLAG. Cells transfected with N and F were stained with primary anti-myc antibody and secondary anti-mouse FITC conjugated antibody. Cells transfected with M were stained with primary anti-M antibody and secondary anti-mouse FITC conjugated antibody. Cells transfected with GA were stained with primary anti-FLAG antibody and secondary anti-rabbit AlexaFluor 555 conjugated antibody. The cells were observed under a fluorescence microscope and pictures were taken at 100X magnification.

4.4.3 Summary of M and N protein expression

The expressed HMPV M and N proteins in Vero E6 cells were observed in their native monomeric form without any indication of oligomerisation. This is not unexpected given that these two proteins are not found on the surface of the host cell or mature virus particle. The knowledge of the expected size for M and N proteins will be useful when producing VLPs in chapter 6.

4.5 Chapter summary

Using both the MVA-T7 expression system with pCDNA3.1(-) and the pCAGGS expression system, the F protein was found to exist as several immature forms within the transfected cells and as a mature form (F_{65}) expressed on the surface of the cells. Co-transfecting F with GA or GB protein did not alter the processing of the F protein significantly. The GA and GB proteins tend to form smears with one or two major bands reflecting a high level of O-linked glycosylation. When co-transfected with F, the GA/B proteins showed a shift in molecular weight suggesting that the presence of the F protein can cause the GA or GB proteins to preferentially adopt one particular conformation. There are differences between the GA and GB protein glycosylation patterns originating from the divergence of the GA and GB genes.

Protein construct	Total expression level	Surface expressed	Secreted
F_{WT}(F539)	Normal	Yes	No
$F_{\Delta TM}$	Normal	No	Yes
$F_{\Delta CT}$(F514)	Weak	No	ND
F534	Normal	ND	ND
F529	Normal	ND	ND
F524	Normal	ND	ND
F519	Normal	ND	ND
F518	Weak	ND	ND
F517	Weak	ND	ND
F516	Weak	ND	ND
F515	Weak	ND	ND
GA_{WT}	Normal	Yes	No
$GA_{\Delta TM}$	Normal	No	No
$GA_{\Delta CT}$	Weak	ND	ND
GB_{WT}	Normal	Yes	No
M	Normal	ND	ND
N	Normal	ND	ND

Table 4.1. Summary table of protein constructs used in this chapter. Total expression levels are classified into normal or weak. ND-not determined in mammalian cells.

When F and GA/B were crosslinked, the most predominant forms of the proteins on the cell surface were of higher molecular mass. This may be due to F and GA multimers forming a complex on the cell surface as suggested by Lamb (Lamb et al., 2006). Analysis of co-expressed F and GA proteins by sucrose gradient ultracentrifugation revealed that both proteins tended to co-migrate in the same few fractions thus

providing more evidence that there is some form of interaction. This is reinforced by the immunofluorescence images of F and GA co-transfected cells showing areas of co-localisation of F and GA protein. This cell surface association of F and G proteins in HMPV supports the possibility that the combined action of F and G protein is necessary for virus infection and are therefore potential targets for antiviral therapy. The association of F and G proteins with host cell proteins should be explored. Both the M and N proteins are thought to be intracellular. The M protein may be essential for virus formation given its structural role. Wild-type F_{WT}, GA_{WT} and GB_{WT} proteins are expressed strongly in mammalian cells and have been shown to be surface expressed but not secreted into the media. This is in agreement with their role as viral fusion and attachment proteins, respectively. Both proteins require their transmembrane region for anchoring to the host cell membrane and are therefore not found on the cell surface but $F_{\Delta TM}$ is secreted whereas $GA_{\Delta TM}$ is not. The G protein probably requires the transmembrane region for proper processing and positioning at the host cell surface xxx. Both $F_{\Delta CT}$ and $GA_{\Delta CT}$ were not well expressed in cells. The cytoplasmic domain of the HMPV F protein plays an important role in the processing and maturation of the protein but the role of the cytoplasmic region in the HMPV G protein has not yet been confirmed. A more in-depth study of the functions of the cytoplasmic tail domain of HMPV F and G proteins should be considered for the future.

Chapter 5 Expressing Human Metapneumovirus Proteins in Insect Cells

Recombinant baculoviruses are used in many studies to express genes. Since the first publication in 1983 (Smith et al., 1983), it has become a popular method for expressing proteins. The usual technique involves replacing the late virus polyhedrin gene with the gene of interest. Two different promoters (polyhedrin or p10) can be linked to the gene of interest. These strong promoters are able to produce large quantities of protein under the appropriate conditions. Other than high expression levels, the strengths of baculovirus technology are safety (only infects insect cells), post-translational modification (although not exactly the same as mammalian cells, refer to Fig 1.20) and ease of scaling up (insect cells can be grown in suspension cultures which can be applied to bioreactors). In this study, two methods were used to construct recombinant baculoviruses. The first method was via a shuttle vector and the second was by Gateway recombinant technology (Invitrogen, USA). The end products were recombinant baculoviruses for the HMPV F, GA, M, N and $F_{\Delta TM}$ proteins. As with all virus work, the virus titre for each recombinant baculovirus had to be determined so that the MOI values could be derived. Two specific insect cell lines (Sf9 and HighFive) were used. Each served a different purpose. The Sf9 cells were used mainly for cloning, propagating and purifying the recombinant baculoviruses. The HighFive cells were used for protein expression work. With each cell line, a series of preliminary experiments was performed including a time-course experiment and MOI experiment. The preliminary experiments served as a precursor to the VLP work in the following chapter. The expression and secretion of $F_{\Delta TM}$ protein was performed to assess the feasibility of using it to generate antibodies.

The aim of this chapter is to compare the characteristics of expression of HMPV fusion and attachment proteins in insect cells to that of mammalian cells. Another objective

was to compare and confirm the differences in expression levels between the two insect cell lines Sf9 and HighFive to decide which would be preferable for VLP production.

5.1 Baculovirus as an expression platform

5.1.1 Constructed baculovirus-expressed recombinant proteins

A total of 5 constructs were made using the baculovirus expression system. They are bac-F which expresses the HMPV F protein, bac-GA which expresses the HMPV GA protein, bac-M which expresses the HMPV M protein, bac-N which expresses the HMPV N protein and the bac-$F_{\Delta TM}$ which expresses the HMPV $F_{\Delta TM}$ protein. The use of wild-type AcMNPV was also employed as controls of viral infection and protein expression (Fig 5.1).

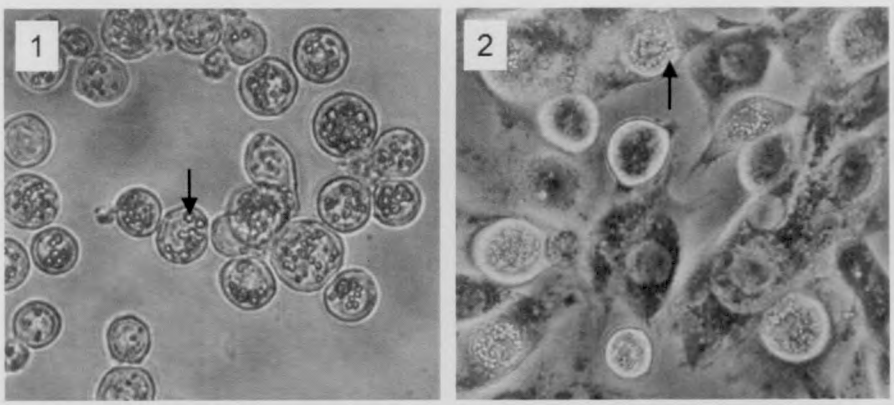

Figure 5.1. Cells infected with wild-type AcMNPV. Image 1, Sf9 cells infected with AcMNPV after 4 days. Image 2, HighFive cells infected with AcMNPV after 3 days. Both images were viewed using 20X objective on an inverted microscope. The arrows indicate the presence of refractile bodies called polyhedra in infected cells.

An example of the process of baculovirus vector construction can be demonstrated by the production of bac-M: The M gene was first amplified using the primers in section 2.7.1, the PCR product was then check on an agarose gel for the correct size (approximately 700 bases). The band was then purified by gel extraction and restriction-digested with both *Kpn*I and *Xho*I overnight (Fig 5.2, lane 3). The baculovirus

vector pFastBacDual (pFBD) was also restriction-digested with the same enzymes (Fig 5.2, lane 1).

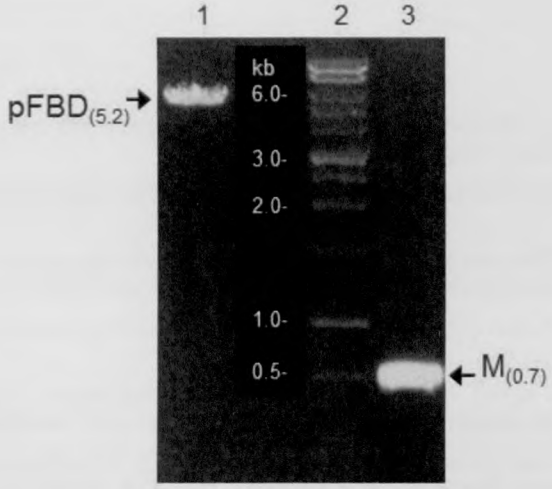

Figure 5.2. Restriction digest of pFastBacDual (pFBD) vector and amplified M gene insert. Both vector and insert were digested overnight with *Kpn*I and *Xho*I. The products were check by agarose gel electrophoresis (1% agarose) before ligation. Lane 1-digested pFBD vector, lane 2-molecular size marker, lane 3-digested M gene insert. Size markings are shown in brackets in kilobases (kb).

After purification of both digested M gene insert and pFastBacDual vector, they were ligated overnight before being used for transformation. The transformed DH10Bac *E.coli* cells were grown on selective media. Colonies were picked and grown in a selective broth to prepare the baculovirus genomic DNA. After DNA purification, the presence of the insert was confirmed by PCR (Fig 5.3) and agarose gel electrophoresis before transfection into Sf9 insect cells.

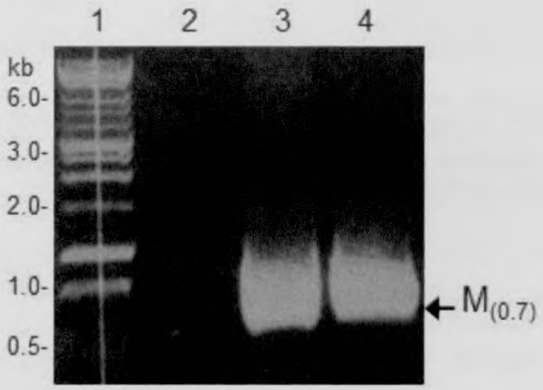

Figure 5.3. Confirming the presence of M gene insert in baculovirus vector. M gene was amplified using the same PCR primers in section 2.7.1 and the products run on 1% agarose gel. Lane 1-molecular size marker, lane 2-vector only control, lanes 3 and 4-recombinant baculovirus containing M gene insert (bac-M). Size markings are shown in brackets in kilobases (kb).

After transfection of Sf9 cells (refer to 2.7.4), the infected cells were incubated for 3 days before harvesting the recombinant bac-M virus from the culture supernatant.

5.1.2 Plaque titration of baculovirus constructs

Plaque assay was used to determine the viral titre for each of the recombinant baculoviruses expressing HMPV proteins. The virus titre values for each of the recombinant baculoviruses were: $4.0x10^7$ PFU/ml for bac-F, $1.65x10^7$ PFU/ml for bac-GA, $7.0x10^6$ PFU/ml for bac-M, $6.6x10^7$ PFU/ml for bac-N and $1.0x10^7$ PFU/ml for bac-$F_{\Delta TM}$. The wild type AcMNPV was also titred and a value of $4.4x10^7$ PFU/ml was obtained. The 6-well plates containing the various baculovirus constructs in dilutions were incubated for up to 2 weeks. Plaques were counted after visualizing with neutral red stain (Fig 5.4).

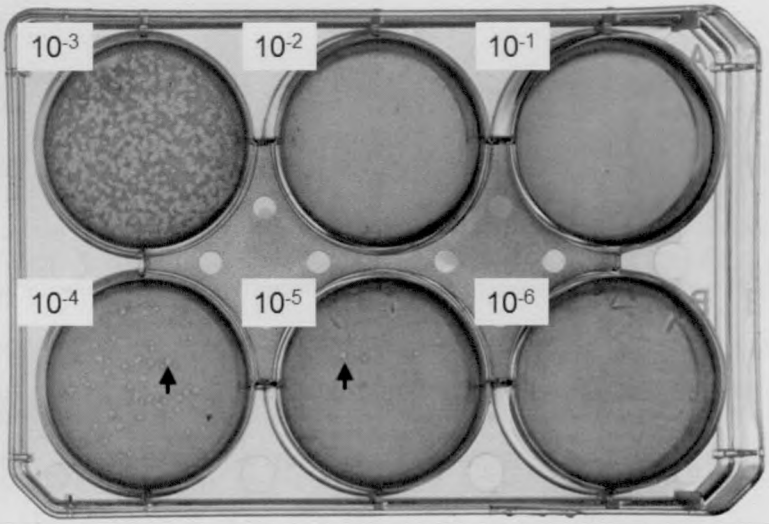

Figure 5.4 Plaque titration of recombinant baculovirus in Sf9 cells. An example of a 6-well plate used to determine the viral titre of a recombinant baculovirus expressing HMPV protein. The dilution values are shown next to each well. Black arrows indicate the positions of the virus plaques which appear as clear zones within the lawn of cells.

5.2 Expression of F and GA proteins in Sf9 cells

5.2.1 Time-course assay

The time-course assay was carried out to determine the optimal number of days of infection for protein expression. A one to three-day time course study was carried out with Sf9 cells infected with the baculovirus expressing F (bac-F) and baculovirus expressing GA (bac-GA).

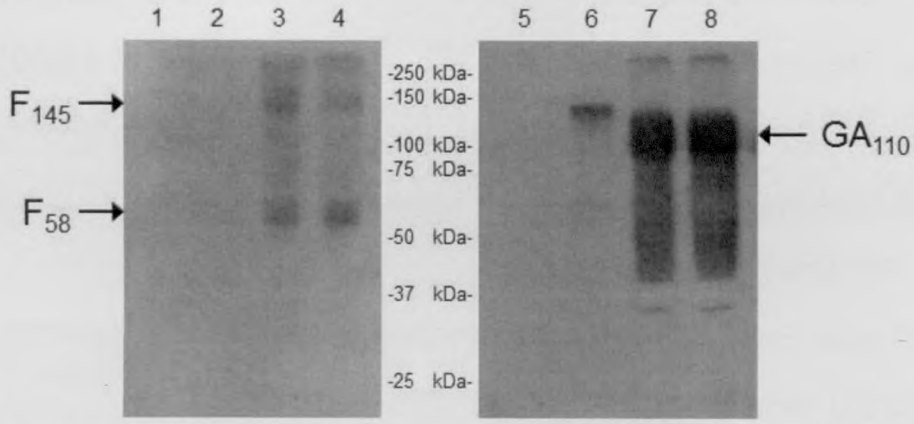

Figure 5.5. Time course assay using Sf9 cells infected with bac-F and bac-GA protein. Lane 1-mock infected Sf9 cells. Lanes 2 to 4-Sf9 cells infected with bac-F protein which were harvested after 1, 2 and 3 days post-infection, respectively. Lane 5-mock infected Sf9 cells. Lanes 6 to 8-Sf9 cells infected with bac-GA protein which was harvested after 1, 2 and 3 days post-infection respectively. Lanes 1 to 4 were probed with anti-myc antibodies and lanes 5 to 8 were probed with anti-FLAG antibodies. The major species of F and GA proteins are shown by the arrows.

Cells were infected at a multiplicity of infection (MOI) of 1 and were harvested after 1, 2 or 3 days. Western blot analysis was performed by probing with the appropriate antibodies and the results are shown in Fig 5.5. Both F and GA proteins were optimally expressed after 2 days post-infection since the 3-day expression levels did not show any significant increase over the 2-day expression levels. The expression of F protein showed the 2 main species F_{58} and F_{145} which are very similar to those observed with mammalian expression vectors (refer to chapter 4.1 and 4.2). The slightly smaller size of F_{58} compared to the F_{60} in mammalian cells could be due to differences in the size of the N-linked side chains. The GA protein showed a smear from 40-110 kDa, with a major species of size 110 kDa (GA_{110}).

5.2.2 Multiplicity of infection (MOI) assay

After determining the optimal incubation time post-infection, the optimal MOI had to be determined. Sf9 cells were infected with bac-F at MOI of 1, 3 or 5 and with bac-GA at MOI of 1 or 3. All cells were incubated 2 days post-infection before harvesting.

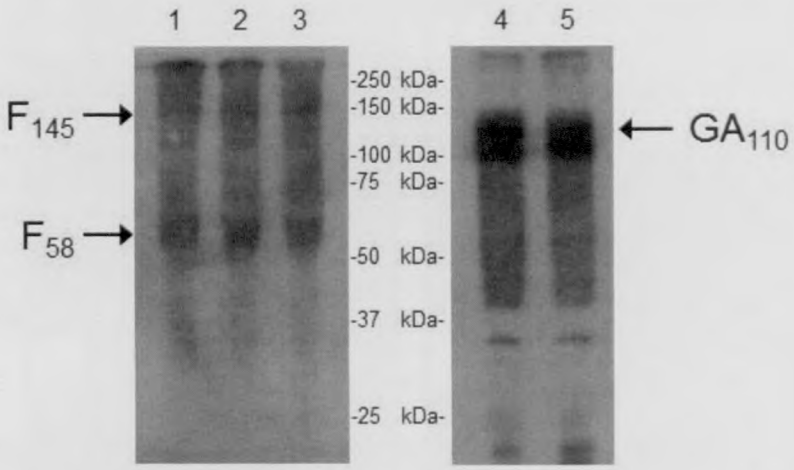

Figure 5.6. Multiplicity of infection (MOI) assay of Sf9 cells infected with bac-F and bac-GA proteins. Cells were harvested 2 days post-infection. Lanes 1 to 3-Sf9 cells infected with bac-F at MOI of 1, 3 and 5 respectively. Lanes 4 to 5-Sf9 cells infected with bac-GA at MOI of 1 and 3 respectively. Lanes 1 to 3 were probed with anti-myc antibodies and lanes 4 to 5 were probed with anti-FLAG antibodies. The major species of F and GA proteins are shown by the arrows.

Western blot analysis was performed by probing with the appropriate antibodies and the results are shown above (Fig 5.6). It was observed that for all MOI values used (3 for bac-F and 2 for bac-GA), there was no significant difference in the amount of protein expressed. Therefore, in the subsequent experiments, the Sf9 cells were infected with virus at an MOI of 1 and harvested 2 days post-infection.

5.2.3 Determining the specificity of the antibodies

To verify if the bands observed in immunoblotting were indeed specific for the F and GA protein, wild-type AcMNPV was used to infect Sf9 cells together with bac-F and bac-GA and probed with anti-myc and anti-FLAG antibodies.

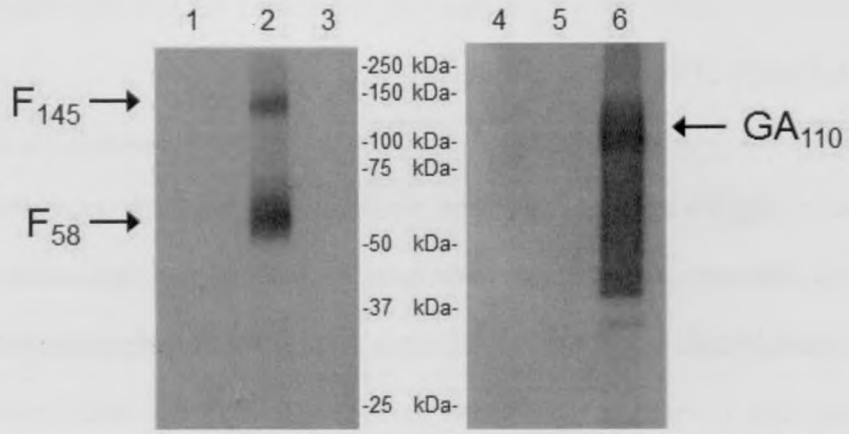

Figure 5.7. Infection of bac-F, bac-GA and wild-type AcMNPV in Sf9 cells. Lanes 1 to 3 were probed with primary mouse anti-myc antibody and secondary goat anti-mouse HRP conjugated antibody. Lanes 4 to 6 were probed with primary rabbit anti-FLAG antibody and secondary goat anti-rabbit HRP conjugated antibody. Lanes 1 and 4 were harvested from AcMNPV-infected cells. Lanes 2 and 5 were harvested from bac-F infected cells. Lanes 3 and 6 were harvested from bac-GA infected cells. The major species of F and GA proteins are shown by the arrows.

From the blots shown in Fig 5.7, it was observed that the anti-myc antibodies were specific for the F protein only and the anti-FLAG antibodies were specific for the G protein only. Neither of the antibodies cross-reacted with the wild-type virus or cell proteins. In this Sf9 cell-line, protein bands for bac-F were observed at 58 kDa (F_{58}) and 145 kDa (F_{145}) corresponding to the monomeric and multimeric forms of F protein, respectively. The F proteins are possibly triple N-glycosylated since it was shown to have 3 possible N-glycosylation sites (Schowalter et al., 2006a). The same molecular mass was observed in another study with baculovirus-expressed hMPV F protein (Ishiguro et al., 2005). The G protein appeared as a smear from 40-100 kDa, possibly due to the high degree of O-linked glycosylation but a distinct band was observed at about 110 kDa (GA_{110}). The native unglycosylated size of GA protein is predicted to be about only 24 kDa.

5.2.4 Morphology of Sf9 cells before and after infection

The morphology of the Sf9 cells was studied after infection with bac-F, bac-GA and wild-type AcMNPV at an MOI of 1. This was compared with non-infected cells. All the cells were observed 1 day post-infection (Fig 5.8).

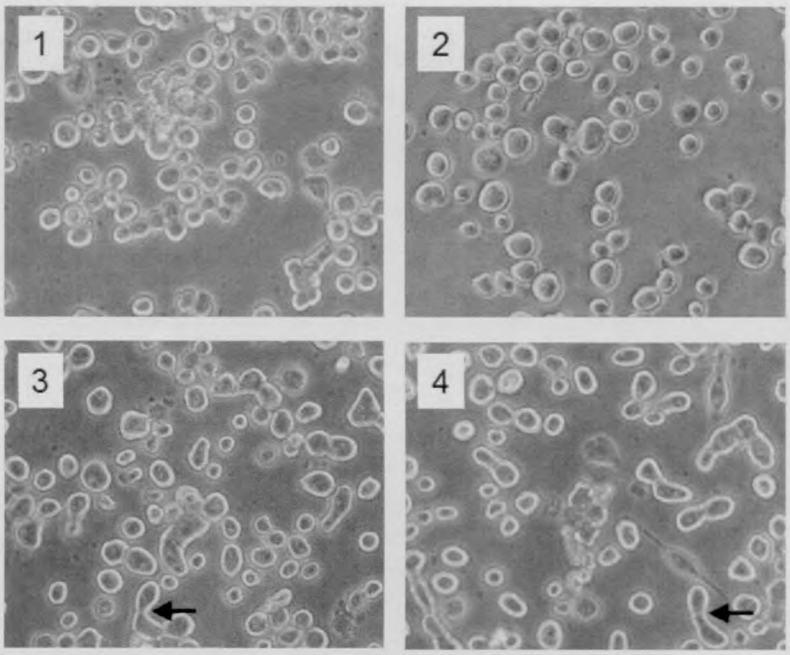

Figure 5.8. Morphology of Sf9 cells after 1 day post-infection. Image 1 shows mock-infected cells. Image 2 shows wild-type AcMNPV-infected cells. Image 3 shows bac-GA infected cells. Image 4 shows bac-F infected cells. Cells were observed under an inverted light microscope at 20X magnification. The arrows indicate the process of cell fusion occurring.

Compared to the mock infected cells, the cells that were infected with bac-F and bac-G appeared enlarged and showed signs of cell fusion (Fig 5.8, arrows). This fusion process is not likely to be due to the bac-F and bac-GA because cells infected with wild-type AcMNPV showed fusion characteristics as well although it was less pronounced. The most likely reason for this phenomenon is the action of baculovirus fusion protein GP64 which is responsible for cell-to-cell spread of the virus. Cells infected with bac-F and bac-GA showed more extensive cell damage on day 2 post-infection (image not shown).

5.2.5 Immunofluorescence microscopy of infected cells

Expression of F and GA proteins was studied using immunofluorescence microscopy (Fig 5.9). Cells mock-infected and infected with wild-type AcMNPV served as controls. After 1 days post-infection at an MOI of 1, the cells were fixed and permeabilised with methanol:acetone (1:1) prior to staining.

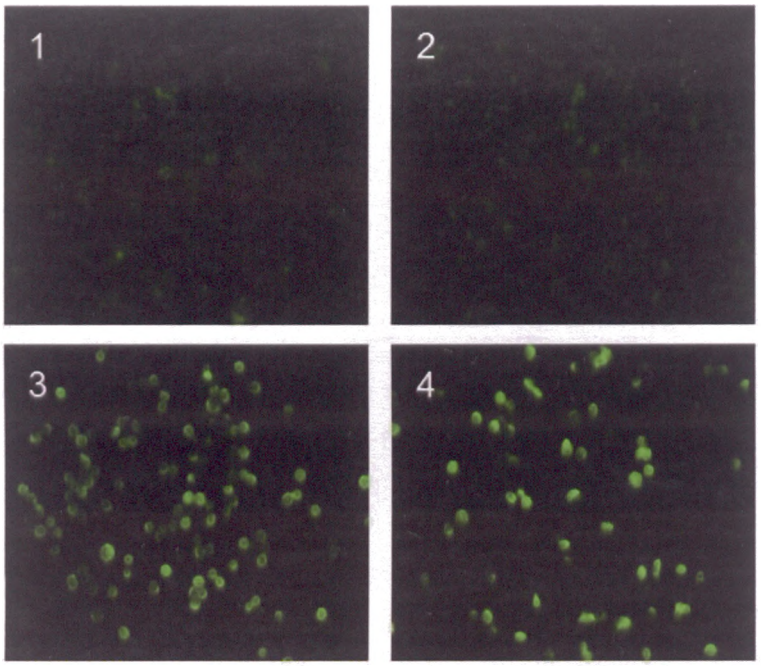

Figure 5.9. Immunofluorescence microscopy of Sf9 cells expressing F and GA proteins. Image 1 shows mock-infected Sf9 cells. Image 2 shows Sf9 cells infected with wild-type AcMNPV. Image 3 and 4 shows Sf9 cells infected with bac-F and bac-GA respectively. Cells infected with bac-F were stained with primary anti-myc antibody and secondary anti-mouse FITC conjugated antibody. Cells infected with bac-GA were stained with primary anti-FLAG antibody and secondary anti-rabbit FITC conjugated antibody. The mock-infected and AcMNPV infected cells were stained with both anti-myc and anti-FLAG antibodies followed by anti-mouse FITC and anti-rabbit FITC conjugated secondary antibodies. The cells were observed under a fluorescence microscope and pictures were taken at 200X magnification.

Intense fluorescence was observed in the cells infected with bac-F and bac-GA, thus confirming the expression of recombinant F and GA protein in these cells. This was in contrast to the mock-infected and AcMNPV-infected cells which only showed background staining. As a follow-up experiment, the expression of GA protein on the surface of Sf9 cells was investigated (Fig 5.10). Instead of fixing the cells with methanol:acetone (1:1), the cells were either fixed without permeabilisation using 4% PFA and probed with the antibodies or fixed with 4% PFA and permeabilised with 0.1%

saponin before probing with antibodies. This procedure is also able to verify the orientation of the myc (F) and FLAG (GA) tag of the proteins with respect to the host cell membrane.

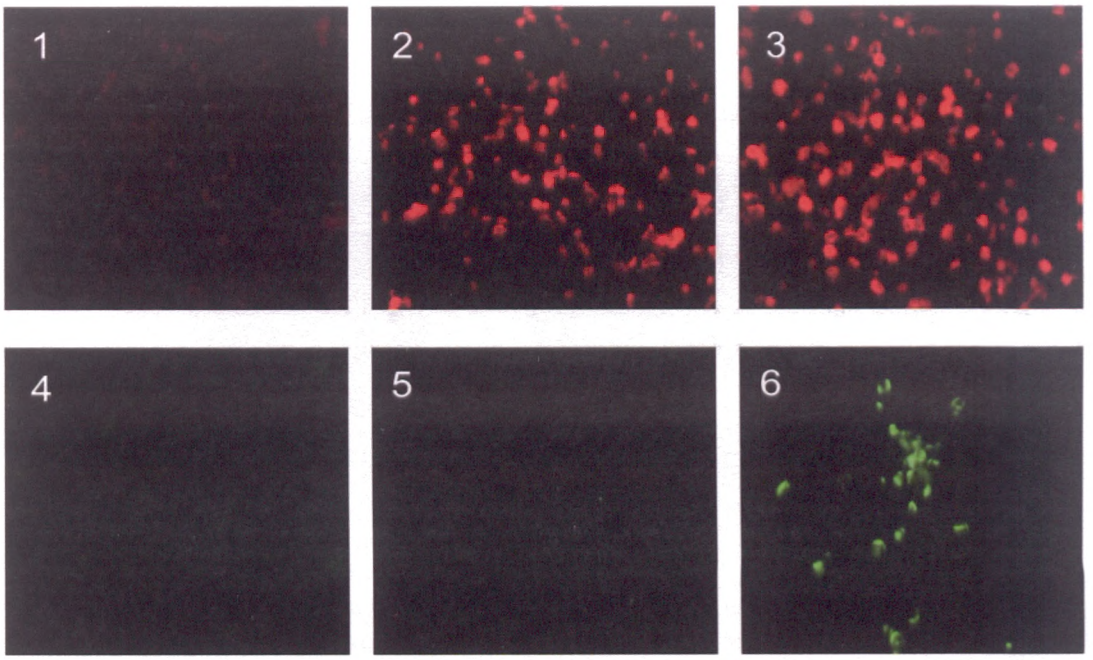

Figure 5.10. Surface expression of bac-F and bac-GA in Sf9 cells observed under immunofluorescence microscopy. Sf9 cells infected with bac-F were stained with primary anti-myc antibody and secondary anti-mouse FITC and cells infected with bac-GA were stained with primary anti-flag antibody and secondary anti-rabbit Alexa Fluor 555. AcMNPV-infected cells were stained with both anti-myc and anti-flag antibody followed by anti-mouse FITC and anti-rabbit Alexa Fluor 555 secondary antibodies. The cells were observed under a fluorescence microscope and pictures were taken at 200X magnification. (images 1 and 4): Cells infected with AcMNPV, (images 2 and 3): Cells infected with bac-GA, (images 5 and 6): Cells infected with bac-F. (images 2 and 5): Cells that were only fixed and not permeabilised. (images 1, 3, 4 and 6): Cells that were both fixed and permeabilised.

As expected, recombinant F protein was stained only when the cells were permeabilised as the myc tag was constructed on the intracellular C-terminus of the protein. On the other hand, the recombinant GA protein was stained regardless of the addition of 0.1% saponin because the FLAG tag was constructed on the extracellular C-terminus of the protein. This observation of the GA protein staining without 0.1% saponin also confirms the presence of the GA protein expressed on the cell surface.

5.2.6 Study of F and G glycosylation

Analysis of N-glycosylation in the expressed F and GA proteins were carried out using PNGase F and Endo H (Fig 5.11). The actions of these two enzymes have been described in the previous chapter.

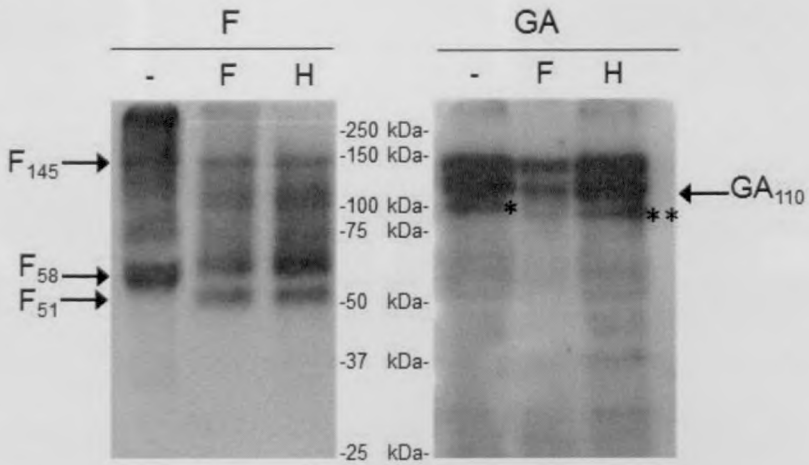

Figure 5.11. N-glycosylation analysis of total cell protein in Sf9 cells. Sf9 cells were infected with bac-F and bac-GA at an M.O.I of 1 and were harvested 2 days post infection. Cells were then treated with either Endo H or PNGase F enzyme. Cells that were not treated by enzymes served as controls. (-)- Non-treated cells, F:-PNGase F treated cells, H:-EndoH treated cells. The major F and G protein species are shown together with their expected sizes in kDa. (*) and (**) illustrate a slight reduction in size of a GA protein species.

It was observed that both the recombinant F and GA proteins were sensitive to PNGase F treatment as seen by the reduction in the molecular mass. The size of the F protein was reduced from 58 kDa to 51 kDa and the GA protein band (*) was slightly reduced in size (**). The intensity of the GA bands were also much less after PNGase F treatment. When both proteins were treated with Endo H, there was similar decrease in the sizes of F and GA, but this time, the intensity of the GA bands remained similar to the untreated GA protein. In order to determine if PNGase F had modified the GA protein such that it had aggregated and remained in the stacking gel, a repeat SDS-PAGE run was performed without the removing the stacking gel for immunoblotting (Fig 5.12).

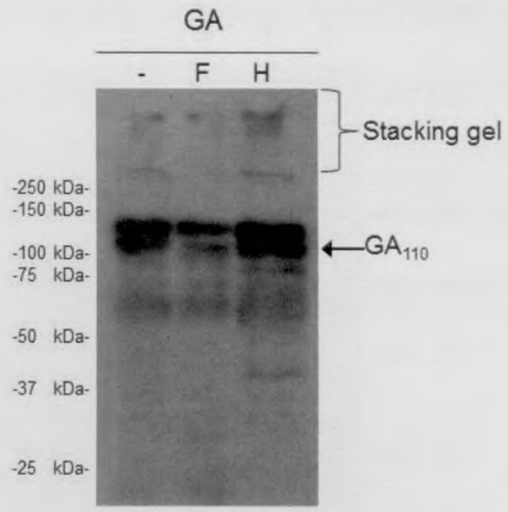

Figure 5.12. Observation of GA protein aggregates in stacking gel. (-)- Non-treated cells, F:-PNGase F treated cells, H:-EndoH treated cells. The position of the stacking gel is indicated.

However, no significant amount of protein was observed in the stacking gel. The reason for the loss of GA protein after PNGase F treatment remains unclear. After studying the total expressed protein, the expression of F and GA proteins on the surface of the cell was studied in the same baculovirus-insect cell system (Fig 5.13). The cells infected with bac-F and bac-GA were harvested 2 days post-infection. Wild-type AcMNPV-infected cells served as a control. Proteins on the cell surface were labeled with biotin and immunoprecipitated using the respective antibodies. As in the previous chapter, the proteins were bound to protein A-Sepharose and analysed by SDS-PAGE. The proteins were then probed with streptavidin-HRP conjugate. From the results in Fig 5.13, it can be concluded that there was a fair amount of non-specific reaction between the antibodies and other cellular proteins. The bac-F infected cells produced F proteins of size 65 kDa, 110 kDa and 145 kDa. The bands observed at 110 kDa and 145 kDa are possibly multimeric forms of the F protein which could either be a dimeric or trimeric form ,respectively, that is expressed on mammalian cell surfaces. The bac-GA infected cells revealed the GA proteins of sizes 60 kDa and 110 kDa. These could be the different types of glycosylated forms of the GA proteins. The 60 kDa band observed for the GA protein was similar to that observed in mammalian expressed pCAGGS/GA-FLAG in the previous chapter.

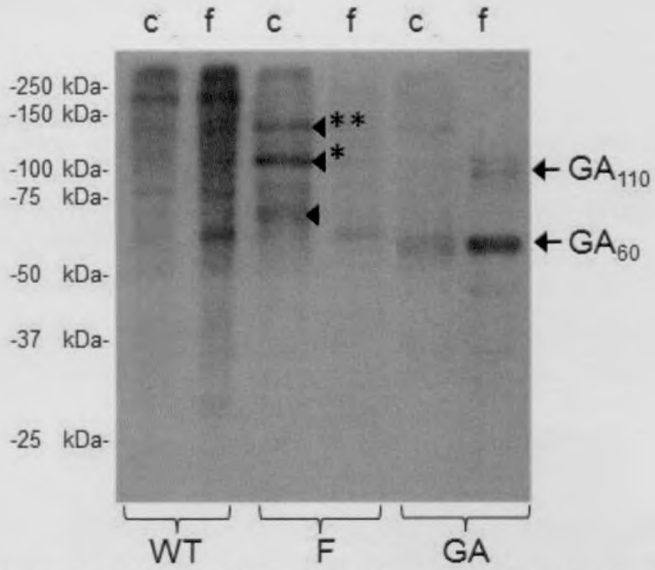

Figure 5.13. Surface expression of F and GA in Sf9 cells. Cells infected with wild type AcMNPV (WT), bac-F (F) and bac-GA (GA). Wild-type AcMNPV infected cells served as a control. Proteins were surface labeled with biotin and immunoprecipitated with with either anti-myc (c) antibody or anti-FLAG (f) antibody. The immunoprecipitated proteins were analysed by SDS-PAGE and probed with streptavidin-HRP. The GA species are shown with their corresponding sizes. (◀), (◀*) and (◀**) indicate the F protein monomer (65 kDa) and oligomers (110 kDa, 145 kDa) respectively.

The reason for the much higher mass compared to the predicted mass (24 kDa) could be attributed to the high proline content accounting for the anomalous migration of proteins on SDS gels (Wertz et al., 1989). There is less appearance of the smearing effect compared to that seen in total cell lysates (Fig 5.11) containing GA protein and this could be due to the lower heterogeneity of the glycosylations on the surface proteins. The study of surface expressed F and GA proteins in Sf9 cells appears to be more complex than in mammalian cells and requires more experimental work to obtain meaningful results.

5.2.7 Summary of F and G expression in Sf9 cells

The expression of HMPV F and GA proteins in Sf9 cells differ from those expressed in mammalian systems in terms of their size and glycosylation patterns. The expression of F protein in Sf9 cells was similar to that in mammalian cells where there are primarily two forms of the protein: a monomeric form and a oligomeric form. The slight difference in size between the mammalian (60 kDa, Fig 4.7) and insect (58 kDa, Fig 5.11)

expressed F proteins could be due to the difference in the N-linked sugar chains, since the F protein is almost exclusively modified by N-linked glycosylation. The GA protein is usually modified by O-glycosylation which can result in a more heterogeneous variety of protein sizes as observed in mammalian cells but the GA protein in Sf9 cells tends to form fewer distinct bands, suggesting that perhaps the process of O-glycosylation in insect cells is less complex.

5.3. Expression of F and GA proteins in HighFive cells

5.3.1 Time-course assay

Another time-course assay was carried out to determine the optimal number of days of infection for protein expression. A one to three-day time course study was carried out with HighFive cells infected with the bac-F and bac-GA. Cells were infected at a multiplicity of infection (MOI) of 1 and were harvested after 1, 2 or 3 days. Western blot analysis was performed probing with the appropriate antibodies and the results are shown in Fig 5.14 below.

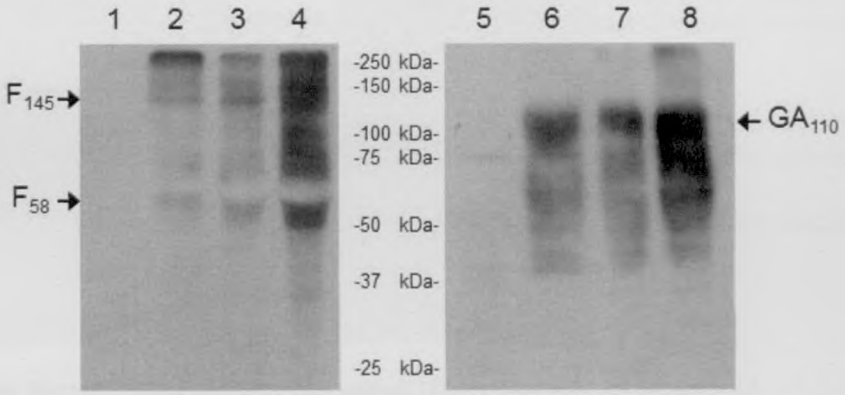

Figure 5.14. Time-course assay using HighFive cells infected with bac-F and bac-GA protein. Lane 1-mock infected HighFive cells. Lanes 2 to 4-HighFive cells infected with bac-F protein which was harvested after 1, 2 and 3 days post-infection, respectively. Lane 5-mock infected HighFive cells. Lanes 6 to 8-HighFive cells infected with bac-GA protein which was harvested after 1, 2 and 3 days post-infection respectively. Lanes 1 to 4 were probed with anti-myc antibodies and lanes 5 to 8 were probed with anti-FLAG antibodies. The major species of F and GA proteins are shown by the arrows.

Both F and GA proteins were maximally expressed after 3 days post-infection. The F protein displayed the 2 main species F_{58} and F_{145} which were identical in size to those seen in Sf9 cells and very similar to those observed in mammalian expression vectors (refer to chapter 4.1 and 4.2). The GA protein showed a smear from 40-110 kDa, with a major species of size 110 kDa (GA_{110}).

5.3.2 Multiplicity of infection (MOI) assay

After determining the optimal incubation time post-infection, the optimal MOI had to be determined. HighFive cells were infected singly with bac-F and bac-GA at a MOI of 1, 5 or10. All cells were incubated for 3 days post-infection before harvesting. Western blot analysis was performed by probing with the appropriate antibodies and the results are shown (Fig 5.15). It was observed that the optimal MOI for both bac-F and bac-GA expression is 1. Increasing the MOI did not significantly increase the level of protein expression. Subsequently, HighFive cells were infected at MOI of 1 and harvested at 3 days post-infection.

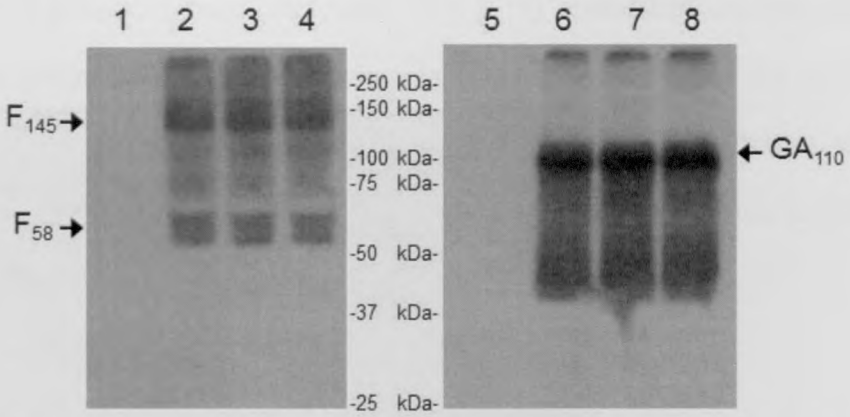

Figure 5.15. Multiplicity of infection (MOI) assay of HighFive cells infected with bac-F and bac-GA proteins. Cells were harvested 3 days post-infection. Lanes 1 and 5-HighFive cells infected with wild-type AcMNPV only. Lanes 2 to 4-HighFive cells infected with bac-F at MOI of 1, 5 and 10 respectively. Lanes 6 to 8-HighFive cells infected with bac-GA at MOI of 1, 5 and 10 respectively. Lanes 1 to 4 were probed with anti-myc antibodies and lanes 5 to 8 were probed with anti-FLAG antibodies. The major species of F and GA proteins are shown by the arrows.

5.3.3 Determining the specificity of the antibodies

To verify if the antibodies in immunoblotting were specific for the F and GA protein, wild-type AcMNPV was used to infect HighFive cells together with bac-F and bac-GA and probed with anti-myc and anti-FLAG antibodies (Fig 5.16). From the blots, it was observed that the anti-myc antibodies and the anti-FLAG antibodies were specific for the F and GA proteins respectively. Neither of the antibodies cross-reacted with the wild-type virus or cell proteins.

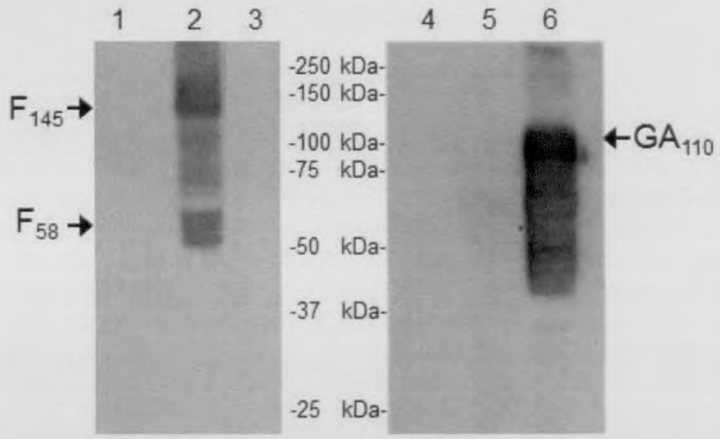

Figure 5.16. Infection of bac-F, bac-GA and wild-type AcMNPV in HighFive cells. Lanes 1 to 3 were probed with primary mouse anti-myc antibody and secondary goat anti-mouse HRP conjugated antibody. Lanes 4 to 6 were probed with primary rabbit anti-FLAG antibody and secondary goat anti-rabbit HRP conjugated antibody. Lanes 1 and 4 were harvested from AcMNPV infected cells. Lanes 2 and 5 were harvested from bac-F infected cells. Lanes 3 and 6 were harvested from bac-GA infected cells. The major species of F and GA proteins are shown by the arrows.

In the HighFive cell-line, bac-F and bac-GA produced the same protein species as noted in the earlier experiments (Fig 5.14 and 5.15). The F and GA proteins expressed in Sf9 cells were also similar in size (refer to Fig. 5.7).

5.3.4 Morphology of HighFive cells before and after infection

The morphology of the HighFive cells was studied after infection with bac-F, bac-GA and wild-type AcMNPV at an MOI of 1. This was compared with mock-infected cells. All the cells were observed at 1 day post-infection (Fig 5.17).

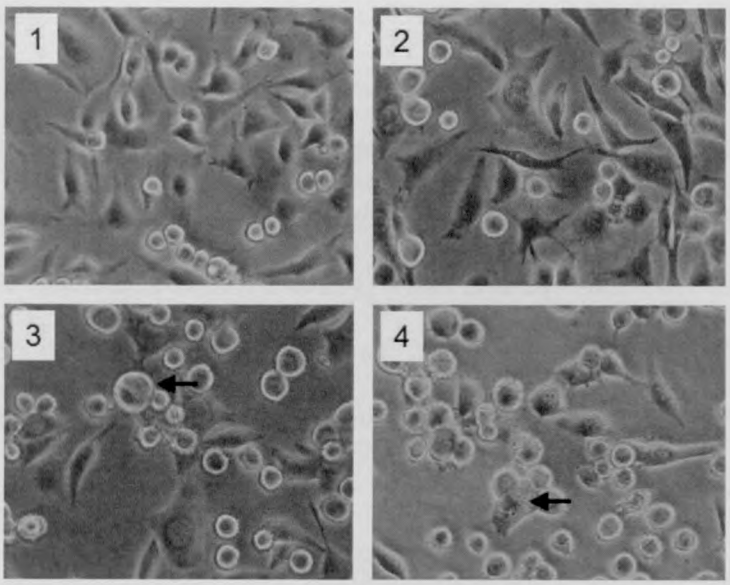

Figure 5.17. Morphology of HighFive cells after 1 day post-infection. Image 1 shows mock-infected cells. Image 2 shows wild-type AcMNPV-infected cells. Image 3 shows bac-F infected cells. Image 4 shows bac-GA infected cells. Cells were observed under an inverted light microscope at 20X magnification. The arrows indicate enlarged cells which have been infected with the bac-F or bac-GA viruses.

Similar to the Sf9 cells, the HighFive cells also exhibited the enlarged appearance when infected with both bac-F and bac-GA, with bac-GA infected cells showing a slightly greater degree of damage. The infected cells, including those infected with the wild-type AcMNPV, also had the tendency to fuse and clump. Cells infected with bac-F and bac-GA showed more extensive cell damage on days 2 and 3 post-infection (images not shown).

5.3.5 Immunofluorescence microscopy of infected HighFive cells

Expression of F and GA proteins in HighFive cells was studied using immunofluorescence microscopy (Fig 5.18). Cells mock-infected and infected with wild-type AcMNPV served as controls. After 1 day post-infection at an MOI of 1, the cells were fixed and permeabilised with methanol:acetone (1:1) prior to staining.

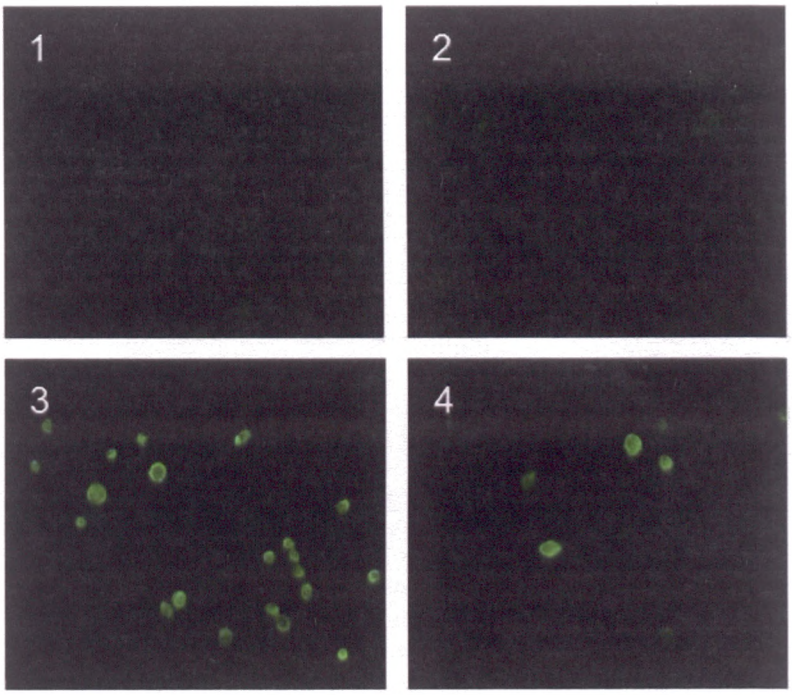

Figure 5.18. Immunofluorescence microscopy of HighFive cells expressing bac-F and bac-GA proteins. Image 1 shows mock-infected HighFive cells. Image 2 shows HighFive cells infected with wild-type AcMNPV. Image 3 and 4 shows HighFive cells infected with bac-F and bac-GA, respectively. Cells infected with bac-F were stained with primary anti-myc antibody and secondary anti-mouse FITC conjugated antibody. Cells infected with bac-GA were stained with primary anti-FLAG antibody and secondary anti-rabbit FITC conjugated antibody. The mock infected and AcMNPV infected cells were stained with both anti-myc and anti-FLAG antibodies followed by anti-mouse FITC and anti-rabbit FITC conjugated secondary antibodies. The cells were observed under a fluorescence microscope and pictures were taken at 200X magnification.

Intense fluorescence was observed in the cells infected with bac-F and bac-GA thus confirming the expression of recombinant F and GA protein in these cells. This was in contrast to the mock infected and AcMNPV infected cells which only showed background staining.

5.3.6 Comparison of the expression levels of Sf9 and HighFive cells

To verify which insect cell line has a higher level of protein expression, a comparative experiment was performed using bac-F and bac-GA in both cell lines. The same cell density of Sf9 and HighFive cells were infected with bac-F and bac-GA at MOI of 1. The cells were harvested after 2 days and analysed on SDS-PAGE (Fig 5.19, below).

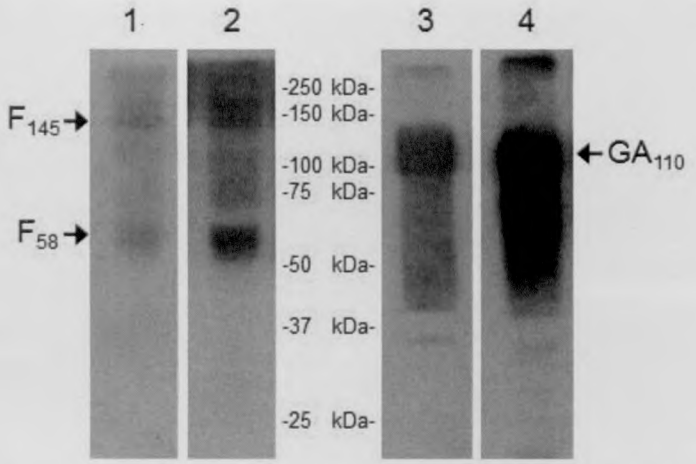

Figure 5.19. Western blot comparison of F and GA proteins expressed in Sf9 and HighFive cells. Cells from both cell lines were harvested at 2 days post-infection (MOI=1) and probed with the respective primary and secondary antibodies. The film used was exposed for 1 minute before developing. Lane 1- Sf9 cells infected with bac-F, lane 2- HighFive cells infected with bac-F, lane 3- Sf9 cells infected with bac-GA, lane 4- HighFive cells infected with bac-GA. The main F and GA protein species are shown with their respective sizes in kDa.

It was observed that even at 2 days post-infection, HighFive cells showed higher levels of protein expression compared to the Sf9 cells. This characteristic of HighFive cells would be exploited in subsequent experiments for HMPV protein expression in insect cells and for the generation of virus-like particles.

5.3.7 Study of F and GA glycosylation

Analysis of N-glycosylation in the expressed F and GA proteins from HighFive cells were carried out using PNGase F and Endo H (Fig 5.20). The actions of these two enzymes have been described previously. It was observed that both recombinant F and GA proteins were sensitive to PNGaseF treatment, as seen by appearance of a smear probably due to O-linked sugar chains. The reduction of the F protein bands to a faint smear by PNGaseF is unusual and was not noted in any other cell line. It may be possible that the removal of the N-linked sugars in F and GA resulted in degradation of the proteins but this requires further investigation. The GA proteins around 110 kDa were also reduced to a smear with a loss in total protein after treatment with PNGaseF. When both proteins were treated with Endo H, there was no significant alteration of the

sizes of F and GA, suggesting that the N-linked sugar modifications on F and GA proteins were mature.

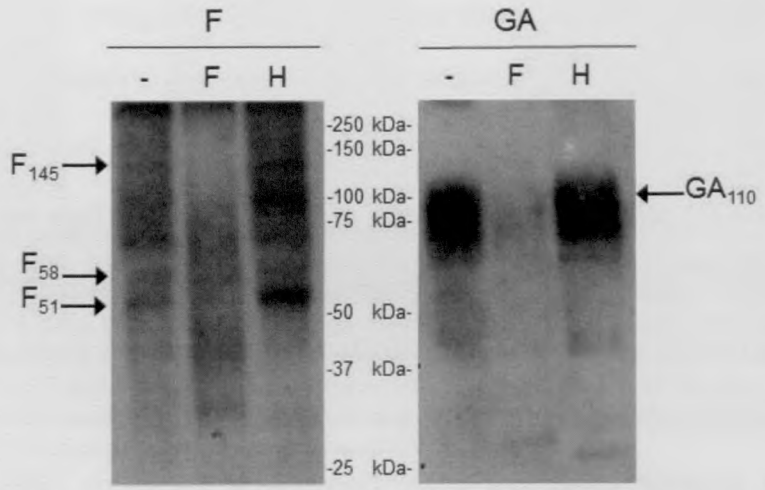

Figure 5.20. N-glycosylation analysis of total cell protein in HighFive cells. HighFive cells were infected with bac-F and bac-GA at an M.O.I of 1 and were harvested 3 days post-infection. Cells were then treated with either Endo H or PNGase F enzyme. Cells that were not treated with enzymes served as controls. (-)- Non-treated cells, F:-PNGase F treated cells, H:-EndoH treated cells. The major F and G protein species are shown together with their expected sizes in kDa.

After studying the total expressed proteins, the expression of F and GA proteins on the cell surface was studied (image not shown). However, as with expression in Sf9 cells, the antibodies were not very specific for the tagged recombinant proteins and there appeared to be some low level of cross-reaction between the anti-myc/anti-FLAG antibodies and the cellular proteins.

5.3.8 Summary of F and G expression in HighFive cells

The baculovirus-insect cell system has many advantages over mammalian and bacterial expression systems (Invitrogen). Having a limited host range, they are firstly non-pathogenic to mammals and plants, thus making it safe for humans use. It is also easy to scale-up with high levels of protein expression and, most importantly, the insect cell is able to carry out mammalian-like post-translational modifications like glycosylations. However, one drawback of this system could be the slight difference in

glycosylation. O-glycosylation in insects cells has been shown to be less diversified, resulting in shorter and less complex sugar chains (Lopez et al., 1999). Insect cell lines have also been shown to be unable to produce complex, terminally sialylated N-glycans but give rise to paucimannosidic N-glycans instead (Harrison and Jarvis, 2006; Kulakosky et al., 1998). However, to overcome this limitation, there have been efforts by various groups to engineer the insect cells such that they produce mammalianized recombinant glycoproteins (Harrison and Jarvis, 2006). Few studies have been done with HMPV proteins being expressed in a baculovirus system (Endo et al., 2008; Ishiguro et al., 2005; Liu et al., 2010). This is a unique study where expression and glycosylation studies of HMPV F and GA proteins have been performed and compared in two different insect cell lines, *Spodoptera frugiperda* (Sf9) and *Trichoplusia nii* (HighFive).

5.4 Expression of M, N and $F_{\Delta TM}$ proteins in Sf9 and HighFive cells

Three other baculovirus constructs were made in addition to bac-F and bac-GA. Bac-M and bac-N were designed to investigate the formation of HMPV virus-like particles in an insect cell system. Bac-$F_{\Delta TM}$ was used to study the possible production of secreted F protein for downstream applications like antibody production and molecular structural studies.

5.4.1 Time-course assays

Additional time-course assays were carried for bac-M, bac-N and bac-$F_{\Delta TM}$ infection in Sf9 (Fig 5.21) and HighFive (Fig 5.22) cells at intervals of one to three-days. Cells were infected at a MOI of 1 and were harvested after 1, 2 or 3 days. Western blot analysis was performed probing with the appropriate antibodies and the results are shown below.

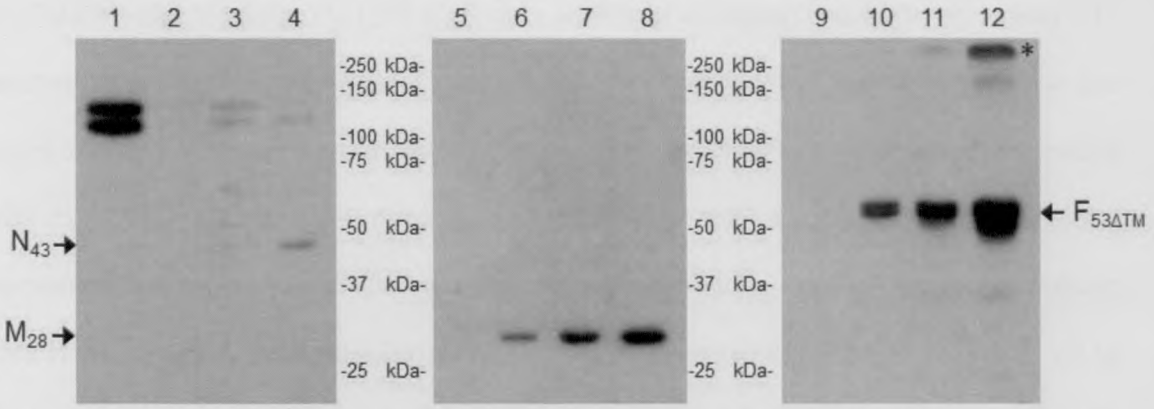

Figure 5.21. Time-course assay using Sf9 cells infected with bac-N, bac-M and bac-$F_{\Delta TM}$. Lanes 1,5,9-mock infected Sf9 cells. Lanes 2 to 4-Sf9 cells infected with bac-N which was harvested after 1, 2 and 3 days post-infection. Lane 6 to 8-Sf9 cells infected with bac-M which was harvested after 1,2 and 3 days post-infection. Lanes 10 to 12-Sf9 cells infected with bac-$F_{\Delta TM}$ which was harvested after 1, 2 and 3 days post-infection. Lanes 1 to 4 were probed with anti-6His antibodies, lanes 5 to 8 were probed with anti-M antibodies and lanes 9 to 12 were probed with anti-myc antibodies. The major species of M, N and $F_{\Delta TM}$ proteins are shown by the arrows with their sizes in kDa. (*) indicates high molecular weight $F_{\Delta TM}$ species.

Comparing the expression levels of the three proteins in Sf9 and HighFive cells, the HighFive cells consistently showed greater levels of protein expression than Sf9 cells. This confirms the earlier observation in 5.3.6 with bac-F and bac-GA. The most remarkable difference was found using bac-N in both cell lines. The presence of N protein in Sf9 was almost undetectable at 3 days post-infection, whereas in HighFive cells there was a large amount produced only after 2 days of incubation.

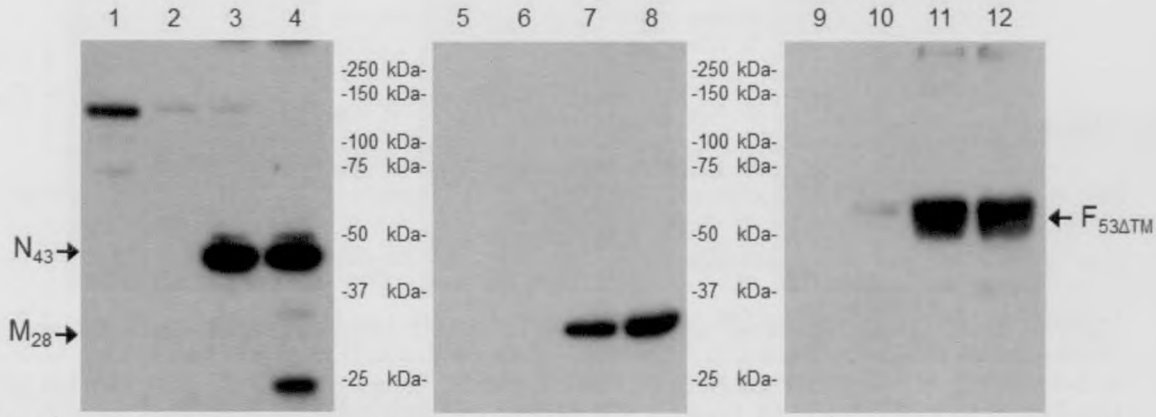

Figure 5.22. Time-course assay using HighFive cells infected with bac-N, bac-M and bac-$F_{\Delta TM}$. Lanes 1,5,9-mock infected HighFive cells. Lanes 2 to 4-HighFive cells infected with bac-N which was harvested after 1, 2 and 3 days post-infection. Lane 6 to 8-HighFive cells infected with bac-M which was harvested after 1,2 and 3 days post-infection. Lanes 10 to 12-HighFive cells infected with bac-$F_{\Delta TM}$ which was harvested after 1, 2 and 3 days post-infection. Lanes 1 to 4 were probed with anti-6His antibodies, lanes 5 to 8 were probed with anti-M antibodies and lanes 9 to 12 were probed with anti-myc antibodies. The major species of M, N and $F_{\Delta TM}$ proteins are shown by the arrows with their sizes in kDa.

The presence of a band (single in HighFive, double in Sf9) of protein of 130-140 kDa in the wild-type infected cells appeared to be a cross-reaction of some viral or cellular protein with the anti-6His antibody. A high molecular mass protein in the bac-$F_{\Delta TM}$-infected Sf9 cells (Fig 5.22, lane 12) is likely to be aggregated proteins. A small 25 kDa product (Fig 5.22, lane 4) in bac-N infected HighFive cells could be due to breakdown of the N protein due to cellular proteases release by cell lysis after 3 days. Bac-N also produced high molecular weight products which could be aggregates after 2 days post-infection.

5.4.2 Multiplicity of infection assays

Additional MOI assays were carried for bac-M, bac-N and bac-$F_{\Delta TM}$ infection in Sf9 (Fig 5.23) and HighFive (Fig 5.24) cells. Cells were incubated for 2 days for Sf9 cells or 3 days for HighFive cells. Western blot analysis was performed by probing with the appropriate antibodies and the results are shown below.

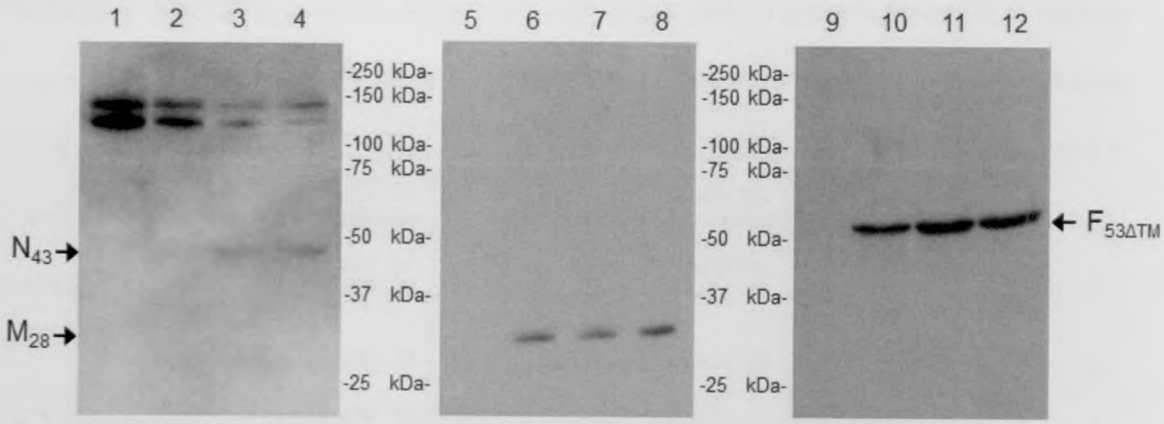

Figure 5.23. MOI assay using Sf9 cells infected with bac-N, bac-M and bac-$F_{\Delta TM}$. Lanes 1,5,9-mock-infected Sf9 cells. Lanes 2 to 4-Sf9 cells infected with bac-N at MOI of 1, 5 and 10. Lane 6 to 8-9 Sf9 cells infected with bac-M at MOI of 1, 5 and 10. Lanes 10 to 12-Sf9 cells infected with bac-$F_{\Delta TM}$ at MOI of 1, 5 and 10. Lanes 1 to 4 were probed with anti-6His antibodies, lanes 5 to 8 were probed with anti-M antibodies and lanes 9 to 12 were probed with anti-myc antibodies. Cells were harvested 2 days post-infection. The major species of M, N and $F_{\Delta TM}$ proteins are shown by the arrows with their sizes in kDa.

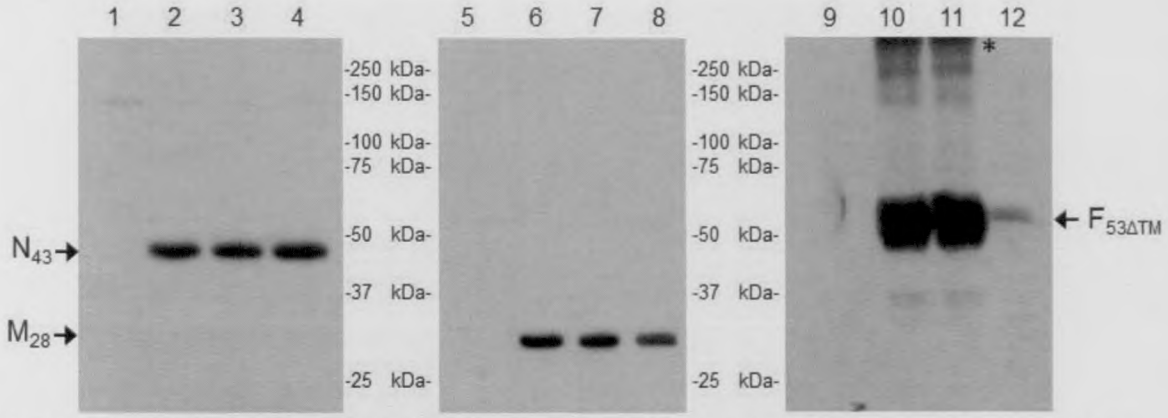

Figure 1.24. MOI assay using HighFive cells infected with bac-N, bac-M and bac-$F_{\Delta TM}$. Lanes 1,5,9-mock-infected HighFive cells. Lanes 2 to 4-HighFive cells infected with bac-N at MOI of 1, 5 and 10. Lane 6 to 8-HighFive cells infected with bac-M at MOI of 1, 5 and 10. Lanes 10 to 12-HighFive cells infected with bac-$F_{\Delta TM}$ at MOI of 1, 5 and 10. Lanes 1 to 4 were probed with anti-6His antibodies, lanes 5 to 8 were probed with anti-M antibodies and lanes 9 to 12 were probed with anti-myc antibodies. The major species of M, N and $F_{\Delta TM}$ proteins are shown by the arrows with their sizes in kDa. (*)- highlights the high molecular weight aggregates of $F_{\Delta TM}$ protein.

Results for the MOI assay were similar to those of bac-F and bac-GA expressed proteins. The increase in MOI beyond the value of 1 did not offer any advantage in terms of increased protein production. In the case of bac-$F_{\Delta TM}$, the increase of MOI to 10 in HighFive cells resulted in an entirely opposite effect where the level of protein was drastically reduced. This could be due to increased breakdown by intracellular proteases from excessive cell lysis.

5.4.3 Morphology of cells after infection

The morphology of the HighFive cells was studied after infection with bac-M, bac-N and bac-$F_{\Delta TM}$ at an MOI of 1 (Fig 5.25). This was compared with non-infected cells and those infected with wild-type AcMNPV. All the cells were observed 2 days post-infection. Sf9 cells were not studied.

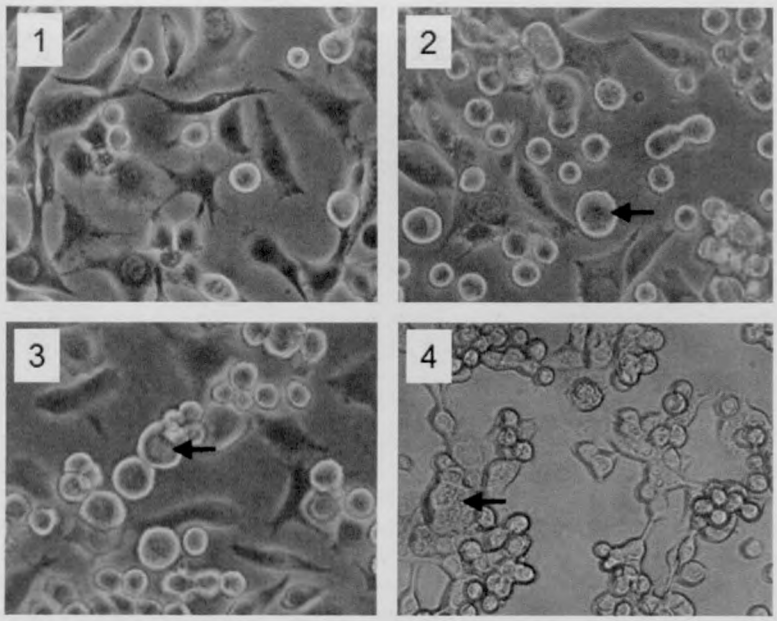

Figure 5.25. Morphology of HighFive cells after 1 day post-infection. Image 1 shows wild-type AcMNPV-infected cells. Image 2 shows bac-M infected cells. Image 3 shows bac-N infected cells. Image 4 shows bac-$F_{\Delta TM}$ infected cells. Cells were observed under an inverted light microscope at 20X magnification. The arrows indicate enlarged cells which have been infected with the bac-M, bac-N or bac-$F_{\Delta TM}$ viruses.

As with the bac-F and bac-GA infected HighFive cells, these cells also exhibited the enlarged appearance when infected with bac-M, bac-N and bac-$F_{\Delta TM}$. The infected cells were observed to fuse and clump together.

5.4.4 Immunofluorescence microscopy of infected cells

Expression of M, N and $F_{\Delta TM}$ proteins in HighFive cells was studied using immunofluorescence microscopy (Fig 5.26). Cells infected with wild-type AcMNPV served as a control. After 1 day post-infection at an MOI of 1, the cells were fixed and permeabilised with methanol:acetone (1:1) prior to staining. Intense fluorescence was observed in the cells infected with bac-M, bac-N and bac-$F_{\Delta TM,}$ thus confirming the expression of the three recombinant proteins in these cells. This was in comparison to the AcMNPV-infected cells which only showed background staining. The cells infected with bac-M showed the characteristic staining pattern similar to mammalian cells transfected with pCAGGS/M plasmid (refer to section 4.4.2) where the appearance of "web-like" strands were seen in the cell cytoplasm.

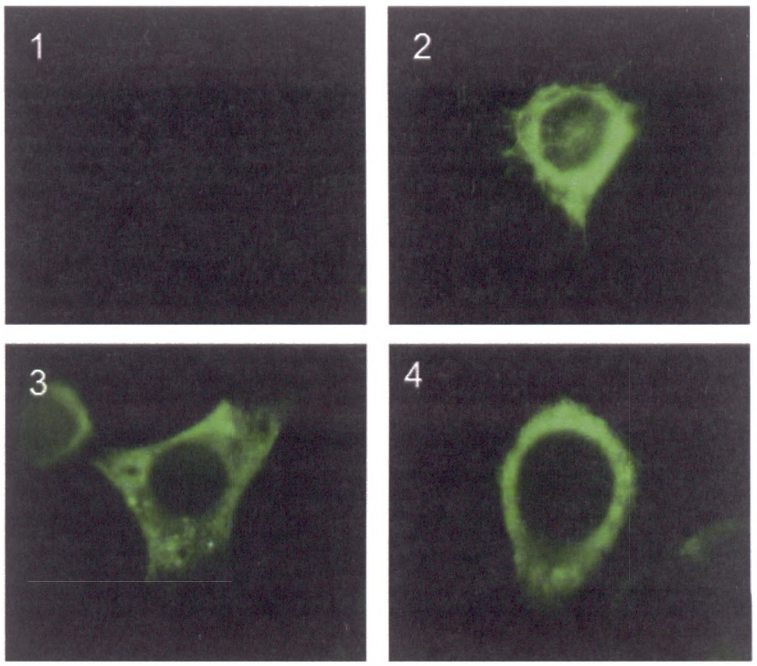

Figure 5.26. Immunofluorescence microscopy of HighFive cells expressing M, N and $F_{\Delta TM}$ proteins. Image 1 shows HighFive cells infected with wild-type AcMNPV. Image 2 shows HighFive cells infected with bac-M. Image 3 shows HighFive cells infected with bac-N. Image 4 shows HighFive cells infected with bac-$F_{\Delta TM}$. Cells infected with bac-$F_{\Delta TM}$ were stained with primary anti-myc antibody and secondary anti-mouse FITC conjugated antibody. Cells infected with bac-N were stained with primary anti-6His antibody and secondary anti-mouse FITC conjugated antibody. Cells infected with bac-M were stained with primary anti-M antibody and secondary anti-mouse FITC conjugated antibody. The mock infected and AcMNPV infected cells were stained with anti-myc, anti-6His and anti-M antibodies followed by anti-mouse FITC conjugated secondary antibodies. The cells were observed under a fluorescence microscope and pictures were taken at 100X magnification.

The staining pattern for bac-N was quite even throughout the cytoplasm but there were a few scattered inclusion bodies. When the HighFive cells were infected with bac-$F_{\Delta TM}$, the expressed protein was observed around the cell nucleus.

5.4.5 Summary of M, N and $F_{\Delta TM}$ expression in Sf9 and HighFive cells

The expression of HMPV M, HMPV N and HMPV $F_{\Delta TM}$ proteins in insect cells produced proteins of the expected sizes. HMPV M was observed as a single 28 kDa band indicating that the protein exists in the monomeric form. HMPV N was observed predominantly as a 43 kDa band but also formed smaller molecular mass products and large molecular mass aggregates as the infection time increased. The smaller products could be due to the breakdown of the N protein in the cells, whereas the large

aggregates could be the result of oligomerisation. HMPV $F_{\Delta TM}$ was observed as a 53 kDa band in both Sf9 and HighFive cells. However there was no evidence of a multimeric form of $F_{\Delta TM}$ in the insect cell systems but the $F_{\Delta TM}$ in HighFive cells did form high molecular mass aggregates (Fig. 5.24).

5.5 Chapter summary

The expression of HMPV F and GA proteins in Sf9 and HighFive cells differed from those expressed in mammalian systems in terms of their size and glycosylation patterns. The expression of F protein in Sf9 and HighFive cells was similar to that in mammalian cells, i.e. there were primarily two forms of the protein: a monomeric form and a multimeric form. However, a slight difference in protein sizes was observed. The pCAGGS expressed F monomer was about 60 kDa in cell lysates, compared to 58 kDa in insect cells. The GA protein is usually modified by O-glycosylation which can result in a more heterogeneous variety of protein sizes as seen in mammalian cells. GA protein in Sf9 and HighFive cells showed similar band sizes. Both cell lines produced a GA_{110} protein species with little trace of lower molecular mass species. HighFive cells showed good potential for the production of VLPs due to their naturally higher expression level.

The HMPV $F_{\Delta TM}$ protein expressed by HighFive cells is a potential candidate for the production of antibodies. The fact that the protein is soluble and secreted into the cell culture medium allows it to be easily purified for inoculation into animals. This avenue should be explored because of the possibility to generate antibodies for diagnostics and research.

Chapter 6 Assembling Human Metapneumovirus Virus-Like Particles in Both Mammalian and Insect Cells

Part of the work from the previous two chapters was in preparation for the attempt to produce and characterize VLPs in both the mammalian cell lines and the insect cell lines. The four HMPV proteins F, GA, M and N were selected for co-expression in HighFive and 293T cells. The selection was based on a previous publication by (Patch et al., 2007) who made VLPs from Nipah virus F, G, N and M proteins. The VLPs were analysed by immunofluorescence microscopy, continuous/discontinuous sucrose gradient centrifugation and electron microscopy. Similar to a hRSV infection, the HMPV VLPs produced by the mammalian and insect cells are not released from the cell surface. Therefore, we had to evaluate two methods for removing the viruses from the cell surface. One method is treatment of the cells by rapid freeze-thawing. The other is treatment of the cells by mechanical shearing. Vero E6 cells were used for microscopy work in place of 293T cells due to their flatter shape and better adhesion on glass coverslips.

The purpose of the work described in this chapter is to produce and characterize VLPs from mammalian and insect cell lines.

6.1 Immunofluorescence microscopy of cells expressing N, M, F and GA proteins

6.1.1 HighFive cells

HighFive cells on coverslips were infected with bac-F, bac-GA, bac-M and bac-N simultaneously and fixed after 24 hours with methanol:acetone (1:1). Another set of cells was infected with wild-type AcMNPV as negative controls. The cells were stained

with a combination of antibodies: anti-myc+anti-FLAG to stain the F and GA proteins (Fig 6.1); anti-M+antiFLAG to stain the M and GA proteins (Fig 6.2); anti-6His+anti-FLAG to stain the N and GA proteins (Fig 6.3).

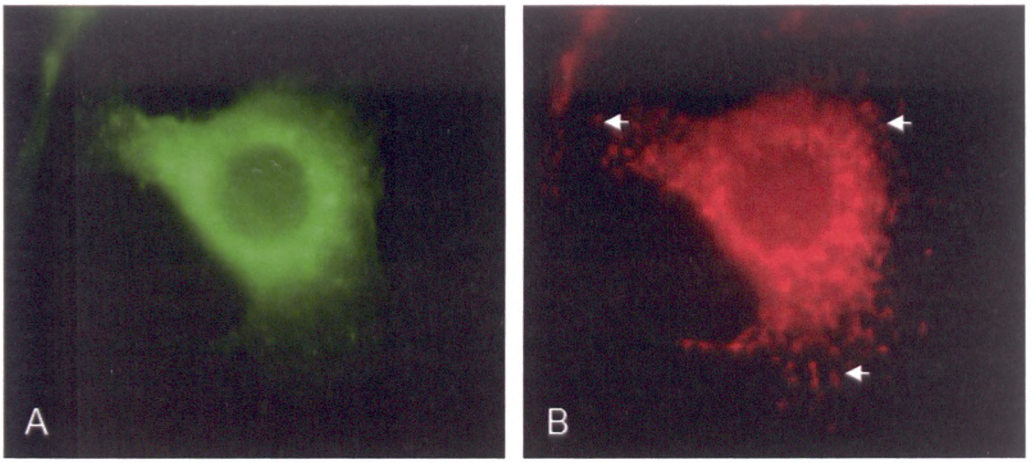

Figure 6.1. Immunofluorescence microscopy of HighFive cells infected with bac-F, bac-GA, bac-M, bac-N and stained with the appropriate antibodies to show the presence of (A) F protein and (B) GA protein viewed under a 100X objective. The presence of filament-like projections from the cell surface are highlighted by the white arrows.

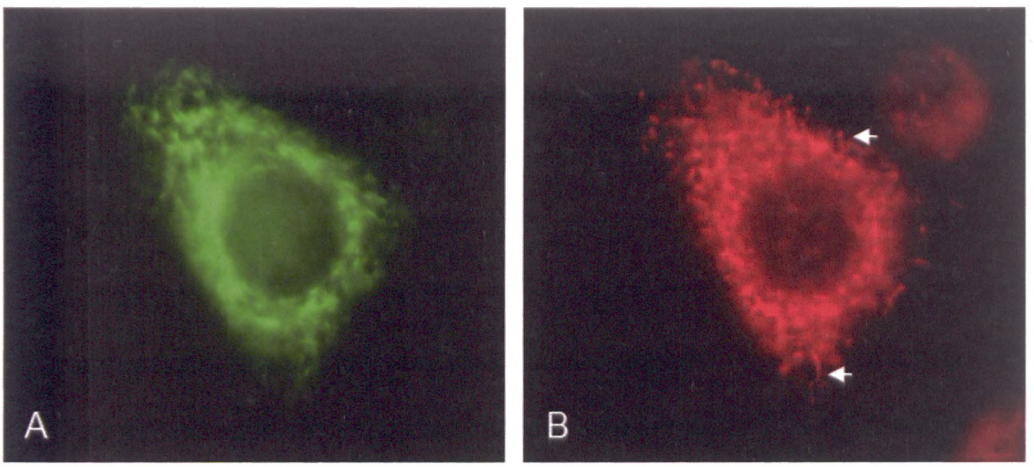

Figure 6.2. Immunofluorescence microscopy of HighFive cells infected with bac-F, bac-GA, bac-M, bac-N and stained with the appropriate antibodies to show the presence of (A) M protein and (B) GA protein viewed under a 100X objective. The presence of filament-like projections from the cell surface are highlighted by the white arrows.

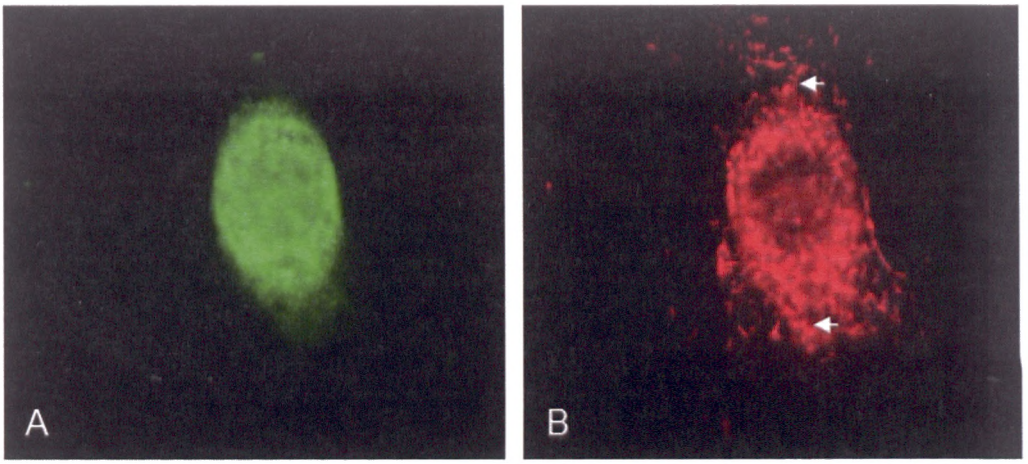

Figure 6.3. Immunofluorescence microscopy of HighFive cells infected with bac-F, bac-GA, bac-M, bac-N and stained with the appropriate antibodies to show the presence of (A) N protein and (B) GA protein viewed under a 100X objective. The presence of filament-like projections from the cell surface are highlighted by the white arrows.

The co-staining of F and GA proteins (Fig 6.1) showed similar staining distribution especially around the nucleus and near the cell surface. This was also observed in images of HEp-2 cells expressing the HMPV F and GA proteins (refer to 4.2.6). In the images of co-stained M and GA proteins (Fig 6.2), the staining locations of both proteins seemed to overlap around the cell nucleus. When both N and GA proteins were stained together (Fig 6.3), the two expressed proteins were not as closely located within the cell. In all three staining combinations, it was observed that the GA protein forms filament-like structures especially around the periphery of the cells. This may possibly be the formation of virus filaments as was observed by (Jeffree et al., 2003).

Confocal microscopy was performed on HighFive cells expressing all four proteins but stained for GA and M proteins (Fig 6.4). The cross-sectional views of the HighFive cell clearly show the location of the GA protein along the cell surface and forming filament-like structures. There is a small degree of colocalisation of the M and GA proteins. This was seen as the yellow regions of the cell due to the overlap of red (GA) and green (M) channels.

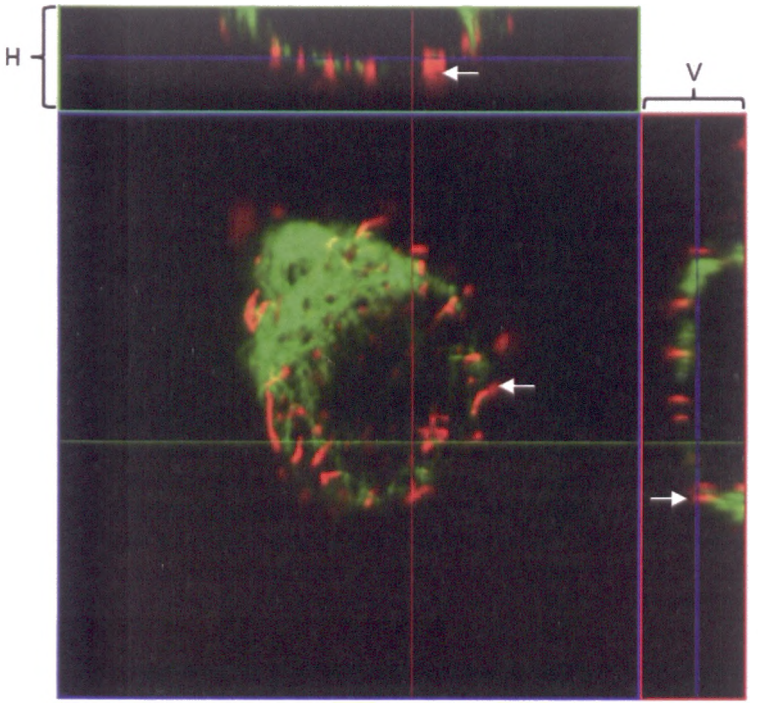

Figure 6.4. Confocal immunofluorescence microscopy of HighFive cell infected with bac-F, bac-GA, bac-M, bac-N and stained with the appropriate antibodies to show the presence of M protein (green channel) and GA (red channel) protein viewed under 100X objective. Horizontal (H) and vertical (V) cross-sectional images are shown at the top and right side of the main image respectively. The presence of filament-like projections from the cell surface are highlighted by the white arrows.

Taking into consideration the fact that the F and GA proteins colocalise in cells co-expressing both proteins, we can infer that there is a possible role for the F, GA and M proteins in VLP formation. This hypothesis would be further strengthened by electron microscopy images and sucrose gradient ultracentrifugation results presented subsequently.

6.1.2 Vero E6 cells

Vero E6 cells on coverslips were transfected with pCAGGS/F-myc, pCAGGS/GA-FLAG, pCAGGS/M and pCAGGS/N-myc simultaneously and fixed after 24 hours with methanol:acetone (1:1). Another set of cells was infected with wild-type pCAGGS plasmid as negative control. The cells were stained with a combination of antibodies: anti-myc+anti-FLAG to stain the F+N and GA proteins (Fig 6.5); anti-M+antiFLAG to stain the M and GA proteins (Fig 6.6).

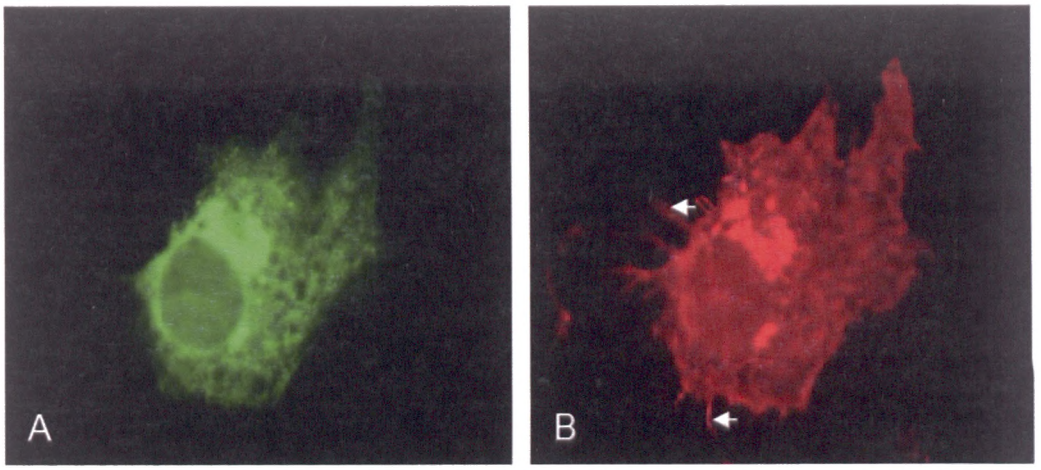

Figure 6.5. Immunofluorescence microscopy of Vero E6 cells transfected with pCAGGS/F-myc, pCAGGS/GA-FLAG, pCAGGS/M, pCAGGS/N-myc and stained with the appropriate antibodies to show the presence of (A) F+N proteins and (B) GA protein. The presence of filament-like projections from the cell surface are highlighted by the white arrows.

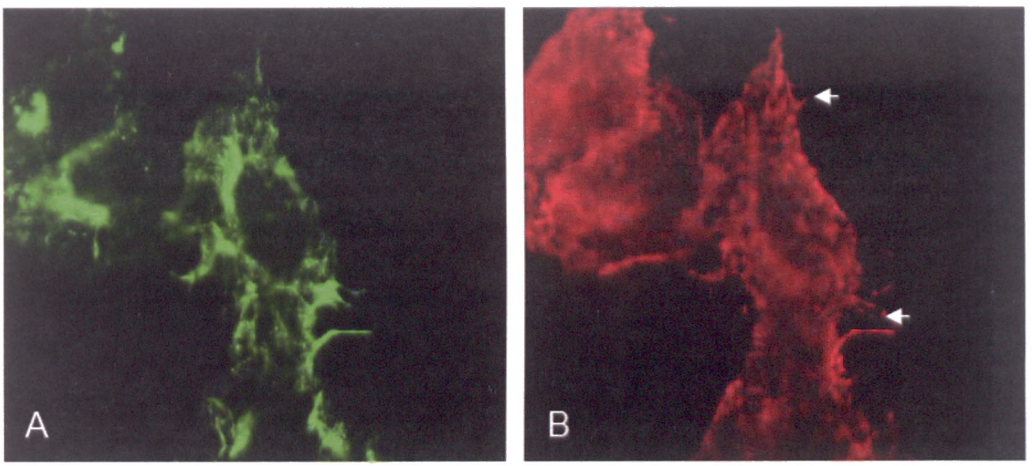

Figure 6.6. Immunofluorescence microscopy of Vero E6 cells infected with pCAGGS/F-myc, pCAGGS/GA-FLAG, pCAGGS/M, pCAGGS/N-myc and stained with the appropriate antibodies to show the presence of (A) M protein and (B) GA protein. The presence of filament-like projections from the cell surface are highlighted by the white arrows.

The cells co-stained to visualize F+N and GA proteins (Fig 6.5) showed similar patterns around the nucleus which suggest protein accumulation and processing in the endoplasmic reticulum. This pattern is similar to that observed in HighFive cells stained to visualize the HMPV F and HMPV GA proteins (Fig 6.1). In the images of co-stained M and GA proteins (Fig 6.6), both proteins were located around the perinuclear region. Again, this pattern was previously observed in HighFive cells stained for the HMPV M and HMPV GA proteins (Fig 6.2). As with the HighFive cells expressing the four proteins, the formation of filament-like structures was noted in the Vero E6 cells. After

analyzing this set of results, it was decided that VLPs could be generated by expressing all four proteins in HighFive or Vero E6 cells.

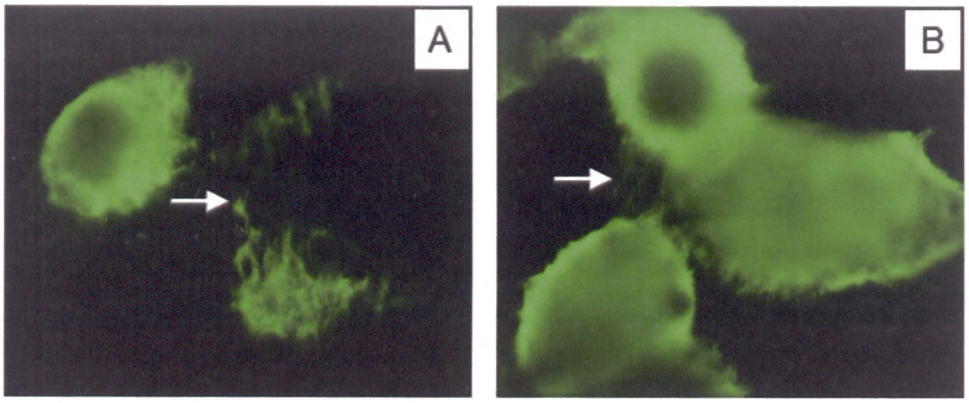

Figure 6.7. Comparison of cells infected by HMPV and hRSV. Immunofluorescence microscopy images of (A) LLC-MK2 cells infected with HMPV after 7 days, (B) HEp-2 cells infected with hRSV after 2 days. HMPV was probed with primary anti-F58 antibody and hRSV was probed with primary anti-F antibody. Anti-mouse FITC was used for both viruses. The arrows show the location of filaments from the cell surface.

In order to comfirm the appearance of the filament-like projections in infected cells, a simple experiment staining HMPV and hRSV infected cells was performed (Fig. 6.7). LLC-MK2 cells were infected with clinical HMPV strain A174 for 7 days. HEp-2 cells were infected with hRSV strain A2 for 2 days. Both sets of cells were stained for their respective viral F proteins. The presence of viral filaments was clearly visible further suggesting that VLPs could be present in the filaments. As another control experiment, a batch of Vero E6 cells was co-transfected with pCAGGS/F-myc, pCAGGS/$GA_{\Delta CT}$-FLAG (truncated GA protein without cytoplasmic tail) and pCAGGS/M. The cells were fixed and stained after overnight incubation as described above. The results (Fig. 6.8 and 6.9) show that the lack of the cytoplasmic tail region in the GA protein has severely affected the ability to produce filament-like structures. The N protein was omitted from this experiment when it was confirmed that it was not involved in VLP formation (see 6.2.2).

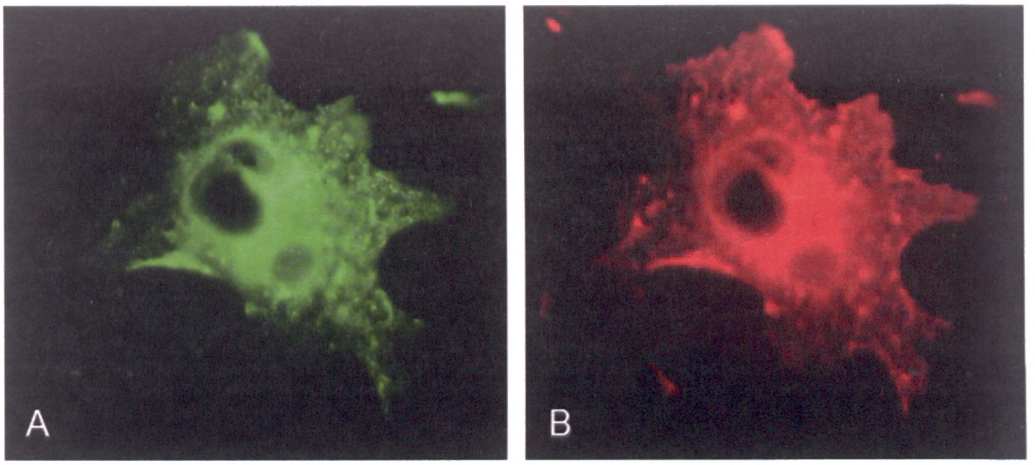

Figure 6.8. Immunofluorescence microscopy of Vero cells transfected with pCAGGS/F-myc, pCAGGS/$GA_{\Delta CT}$-FLAG, pCAGGS/M, and stained with the appropriate antibodies to show the presence of (A) F proteins and (B) $GA_{\Delta CT}$ protein. No filament-like projections from the cell surface were observed.

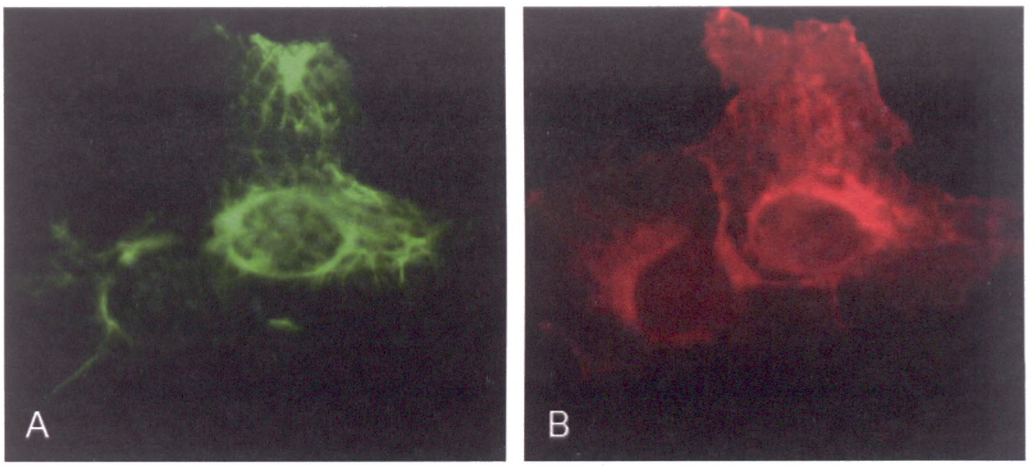

Figure 6.9. Immunofluorescence microscopy of Vero cells infected with pCAGGS/F-myc, pCAGGS/$GA_{\Delta CT}$-FLAG, pCAGGS/M and stained with the appropriate antibodies to show the presence of (A) M protein and (B) $GA_{\Delta CT}$ protein. No filament-like projections from the cell surface were observed.

6.2 Expression of N, M, F and GA proteins in HighFive cells

6.2.1 Determining the optimal method of harvesting virus-like particles

The four proteins from HMPV were selected for co-expression in HighFive cells based on the work by (Patch et al., 2007). They had found that cells expressing F, G, M and N proteins from Nipah virus were able to generate virus-like particles (VLPs). For the HMPV proteins; bac-F, bac-GA, bac-M and bac-N were already expressed singly in Sf9 and HighFive cells (refer to Chapter 5). Since the expression levels in HighFive cells

were found to be superior to Sf9 cells (Refer to 5.3.6), HighFive cells were chosen for this follow-up study and infected with all four baculovirus constructs at MOI of 1. At 3 days post-infection, cells were harvested together with the culture media and treated by freeze-thawing 3 times using dry ice-ethanol and 37°C waterbath or mixing with a dounce homogenizer (refer to Methods 2.9.3). The two treatment methods were used to shear off the viral-like filaments from cell surface. After low speed centrifugation (2,500 g, 10 min) the cell pellet was put aside and the supernatant was centrifuged at high speed (200,000 g, 1 hour). The resulting pellet and supernatant were analysed by SDS-PAGE (Fig 6.10) and probed with anti-FLAG and anti-M to determine the presence of the GA and M proteins respectively in the various fractions.

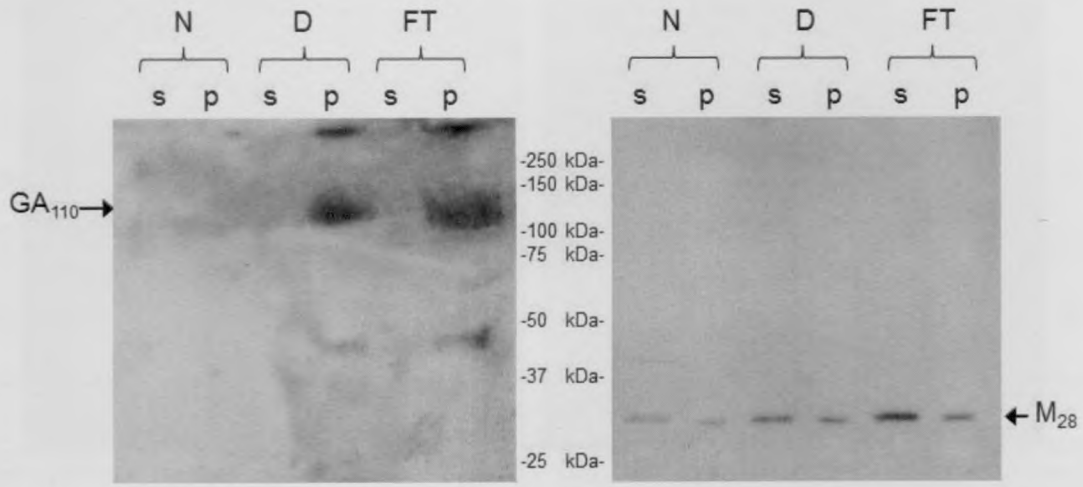

Figure 6.10. HighFive cells infected with bac-F, bac-GA, bac-M and bac-N. Cells and media were harvested 3 days post-infection. After treatment, cells were centrifuged at low speed (2,500 g) and the supernatant was removed and centrifuged at high speed (200,000 g). The resulting pellet (p) was run on SDS-PAGE with the supernatant (s) to determine the presence of the GA and M proteins. The protein species are shown with their sizes in kDa. N- non-treated cells and media, D-cells and media dounced 40 times in a homogenizer, FT-cells and media freeze-thawed 3 times.

Based on the immunoblotting results, the GA protein was detected in the pelleted fraction after freeze-thaw treatment and douncing but not in the supernatant fractions. When the cells were untreated, there was no GA protein either in the supernatant or pellet confirming that the protein was still part of the cells. The M protein, on the other hand, was detected in every pellet and supernatant fraction including the non-treated cells. This seems to indicate that the M protein is not only secreted into the media but is also present in the pellet. Both douncing and freeze-thaw methods can effectively

remove virus-like filaments from the cell surface but the freeze-thawing method was selected for its slightly better yield.

6.2.2 Preliminary analysis of virus-like particles

A follow-up experiment was performed with HighFive cells infected with the four baculovirus constructs. The cells were prepared in a similar way as above and freeze-thawed to obtain virus-like filaments. This time, the initial cell pellet from the low speed centrifugation was included in the SDS-PAGE analysis (Fig 6.11).

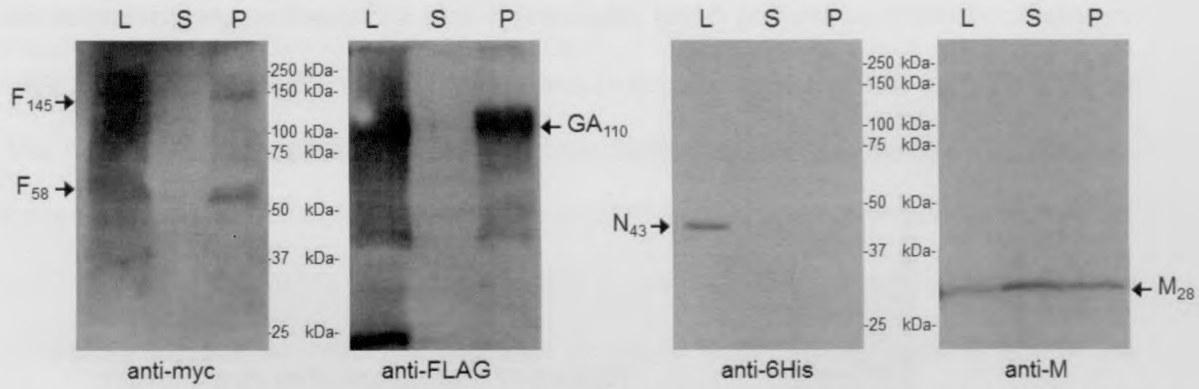

Figure 6.11. Western blot analysis of HighFive cells infected with bac-F, bac-GA, bac-M and bac-N. The cells were harvested 3 days post-infection and treated as the previous experiment in Fig 6.10. The 3 fractions analysed were L-cell material after low speed centrifugation. S-media supernatant after high speed centrifugation. P-virus pellet obtained after high speed centrifugation. Each of the four proteins was detected by their respective antibody. The major protein species are shown with their sizes in kDa.

Looking at the immunoblotting results, it is clear that all four proteins were detected in the cellular material. This was not unexpected since the proteins were shown to be expressed in the cells previously (refer to 5.3 and 5.4). However, the N protein was not detected in any other fraction than the cellular fraction. This strongly suggests that the N protein is perhaps not essential for VLP formation in HMPV. The other three proteins F, GA and M were detected in the high-speed centrifuge pellet and thus would most likely be involved in VLP formation. The F_{58} and GA_{110} proteins were of the expected sizes in HighFive cells. Another interesting point is that the M protein was found in the supernatant fraction after high-speed centrifugation. This provided additional evidence

(also refer to Fig 6.10) that the M protein might be secreted into the media under normal conditions.

6.2.3 Concentration of virus-like particles by ultracentrifugation

In order to concentrate the VLPs from HighFive cells, the technique of ultracentrifugation was employed. Firstly, the four proteins were expressed in HighFive cells, harvested and treated by the freeze-thaw method. The cell suspension was then centrifuged at low speed (refer 6.2.1). The supernatant was purified through a 10% sucrose cushion, the resulting pellet was loaded onto a discontinuous gradient of 20-50-60% sucrose (refer to Methods 2.9.4) and centrifuged for 1 hour at 200,000g. After centrifugation, three fractions were collected at the density interfaces (Fig 6.12).

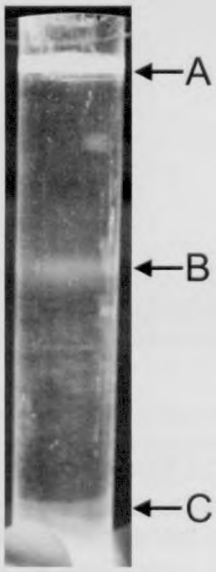

Figure 6.12. Photograph of an ultracentrifuge tube containing the VLPs from HighFive cells in a discontinuous sucrose gradient after spinning at 200,000g for 1 hour at 4°C. The fractions collected were: A-the top of the gradient, B-the interface between 20% and 50% sucrose, C-the interface between 50% and 60% sucrose. Approximately 500 µl was collected from each fraction.

The three fractions were run on SDS-PAGE and probed with each of the respective antibodies to detect each of the four proteins (Fig 6.13). There was no protein detected in the last fraction. There were smaller proportions of GA and M proteins detected in the top fraction which could be due to the free proteins in the solution. The F, GA and M proteins were detected in the middle fraction.

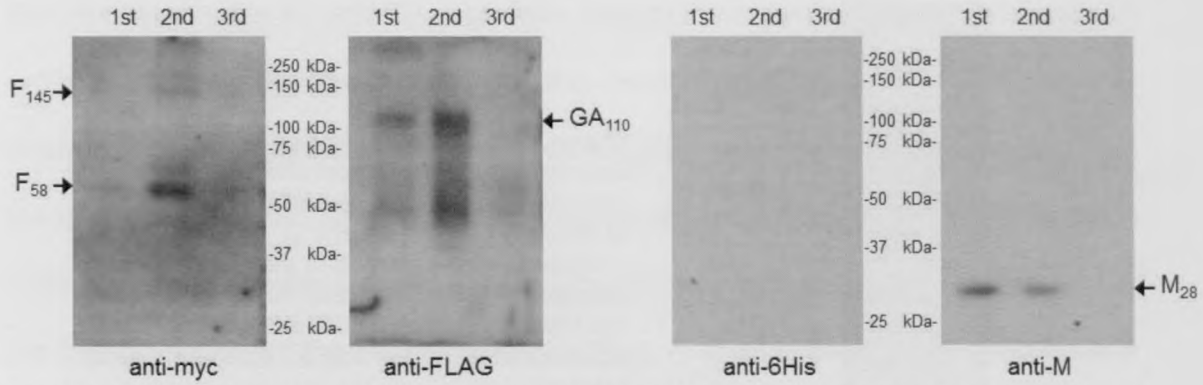

Figure 6.13. Western blot analysis of HighFive cells infected with bac-F, bac-GA, bac-M and bac-N after ultracentrifugation. The cells were harvested 3 days post-infection and treated with the freeze-thaw method (refer 6.2.1). After low-speed centrifugation, the supernatant was centrifuged through a 10% sucrose cushion and the resulting pellet was centrifuged through a discontinuous 20-50-60% sucrose gradient. Three fractions were harvested and analysed on SDS-PAGE: 1st-fraction (A) at the top of the gradient, 2nd-fraction (B) at the 20-50% interface, 3rd-fraction (C) at the 50-60% interface. Each of the four proteins was detected by their respective antibody (anti-myc for F, anti-FLAG for GA, anti-6His for N, anti-M for M). The major protein species are shown with their sizes in kDa.

The middle fraction, which is at the interface of the 20% and 50% sucrose solutions, corresponds to the expected density of virus particles (Pantua et al., 2006; Patch et al., 2007; Weng et al., 2011). This confirms the earlier experiments that F, GA and M are necessary for VLP formation. There was no signal from the N protein in any of the fractions, demonstrating that it was most likely not a component of HMPV VLPs.

6.3 Expression of N, M, F and GA proteins in 293T cells

6.3.1 Concentration of virus-like particles by ultracentrifugation

As with the expression of HMPV N, M, F, and GA in HighFive cells; the presence of VLPs was also investigated in mammalian cells. For this phase of experiments, 293T cells were used. These cells were co-tranfected with the four plasmid constructs: pCAGGS/F-myc, pCAGGS/GA-FLAG, pCAGGS/M and pCAGGS/N-myc. The cells were harvested 2 days post-transfection and treated the same way as the HighFive cells (refer to 6.2.3).

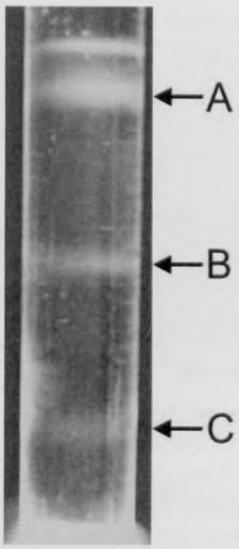

Figure 6.14. Photograph of an ultracentrifuge tube containing VLPs from 293T cells in a discontinuous sucrose gradient after spinning at 200,000g for 1 hour at 4°C. The fractions collected were: A-the top of the gradient, B-the interface between 20% and 50% sucrose, C-the interface between 50% and 60% sucrose. Approximately 500 µl was collected from each fraction.

The same three fractions from the discontinuous sucrose gradient (Fig 6.14) were subjected to SDS-PAGE and probed with each of the respective antibodies to detect the four proteins (Fig 6.15). There were no significant amounts of the proteins detected in the first and last fractions of the sucrose gradient. As seen previously in HighFive cells (Fig 6.10), the N protein was not detected in any of the gradient fractions but in the cell lysate.

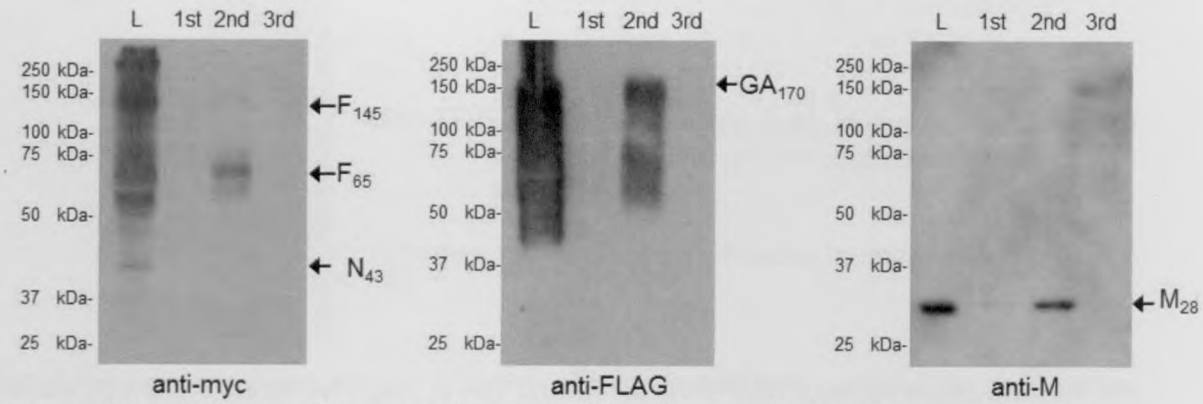

Figure 6.15. Western blot analysis of 293T cells transfected with pCAGGS/F-myc, pCAGGS/GA-FLAG, pCAGGS/M and pCAGGS/N-myc after ultracentrifugation. The cells were harvested 2 days post-transfection and treated with the freeze-thaw method. After low speed centrifugation, the supernatant was spun through a 10% sucrose cushion and the resulting pellet was spun through a discontinuous 20-50-60% sucrose gradient. Three fractions were harvested and analysed on SDS-PAGE: 1st-fraction at the top of the gradient, 2nd-fraction at the 20-50% interface, 3rd-fraction at the 50-60% interface. L- lysate of the cell pellet after low speed centrifugation. Each of the four proteins was detected by their respective antibody (anti-myc for F and N, anti-FLAG for GA, anti-M for M). The major protein species are shown with their sizes in kDa.

The F, GA and M proteins were all concentrated within the 20-50% sucrose interface. This result is in agreement with the HighFive cell expression system. The only

differences were the F_{65} and GA_{170} proteins were of the expected sizes in 293T cells. In order to further refine the results from the discontinuous sucrose gradient, another analysis was performed using a continuous sucrose gradient instead. The results from the continuous sucrose gradient analysis are shown in Fig 6.16. A total of 12 fractions were harvested and they ranged from the lowest density at the top of the gradient to the highest density at the bottom of the gradient. A small aliquot of each fraction was analysed by SDS-PAGE. Three sets of gels were run and each was probed with a different antibody (anti-cmyc, anti-FLAG, anti-M). Both the F protein and GA protein were detected mainly in fractions 5 to 7. On the other hand, the M protein was mainly detected in fractions 6 to 8.

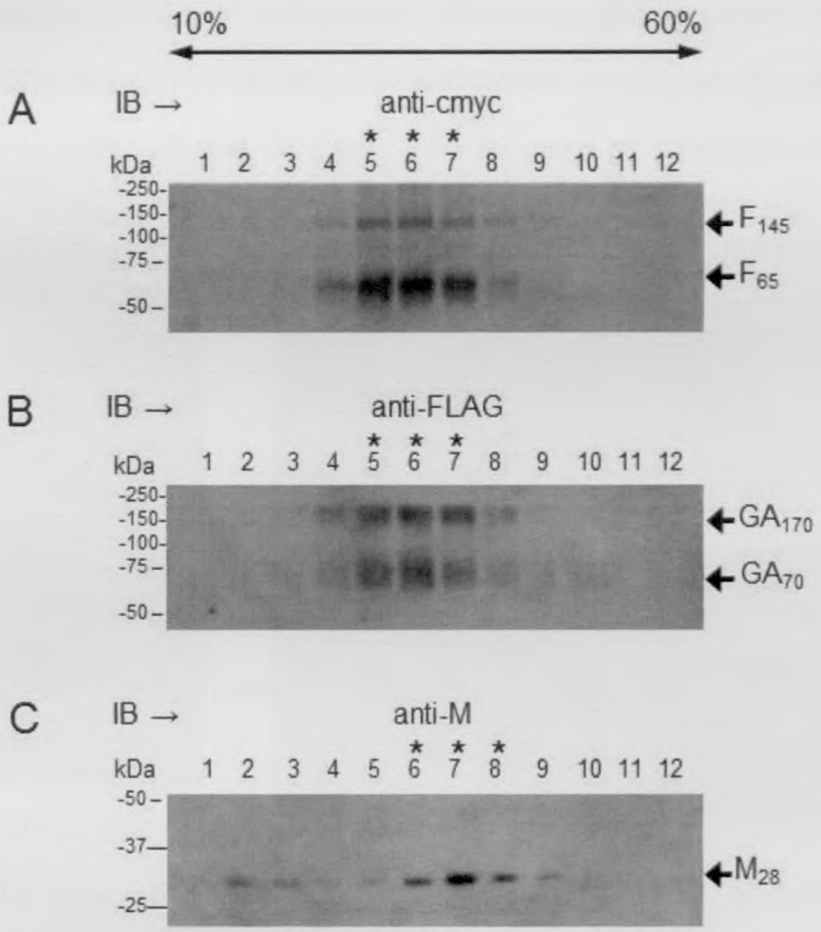

Figure 6.16. Western blot analysis of continuous sucrose gradient fractions from 293T expressed HMPV proteins. 293T cells were transfected with pCAGGS/F-myc, pCAGGS/GA-FLAG and pCAGGS/M and harvested 2 days post-transfection. (A) Fractions probed with anti-myc antibodies, (B) fractions probed with anti-FLAG antibodies, (C) fractions probed with anti-M antibodies. Fractions 1 to 12 are from the lowest (10%) to highest (60%) density.

In addition to the peak fractions, the M protein was also detected in smaller quantities from fractions 2 to 10. This is unlike the F and GA proteins which were also observed in small amounts in fractions 4 to 10. A possible explanation could be that the non-VLP-associated form of M protein has a lower density compared to non-VLP-associated forms of the F and GA proteins.

6.4 Analysis of virus-like particles by electron microscopy

In order to investigate the formation of filaments and their possible role in VLP production, we utilized a method previously published by (Jeffree et al., 2003) involving field emission scanning electron microscope (FE-SEM). Vero E6 cells were mock-transfected and co-transfected with pCAGGS/F-myc, pCAGGS/GA-FLAG and pCAGGS/M.

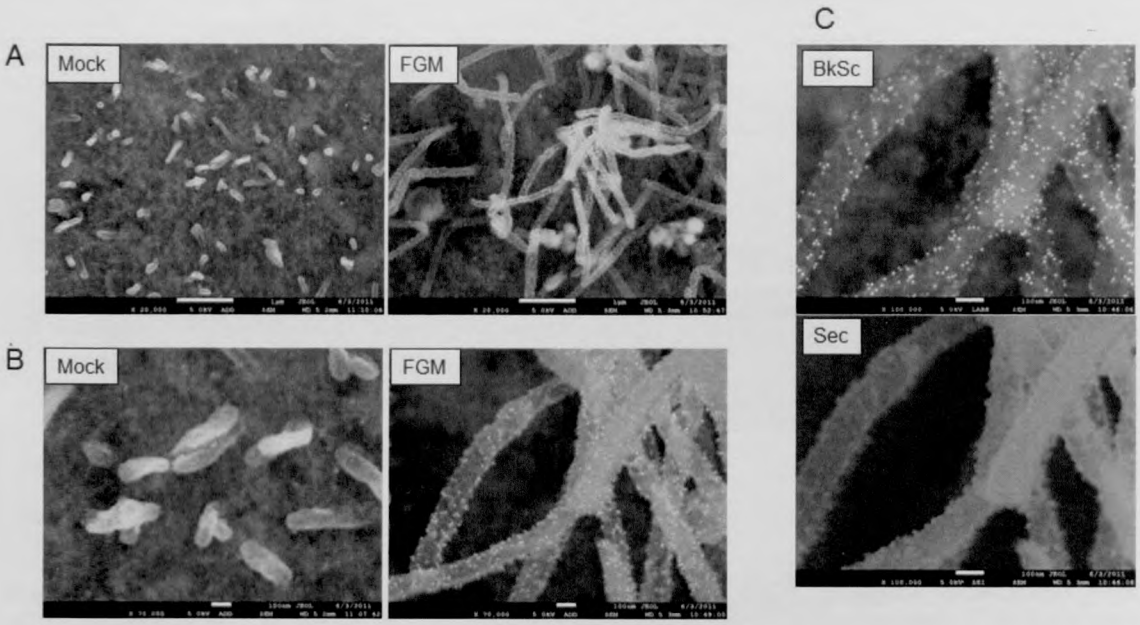

Mock	0.8 ± 0.6 gold particles per 100nm
Transfected	11.4 ± 2.8 gold particles per 100nm

Figure 6.17. Images of Vero E6 cells mock-transfected (mock) and transfected with F+GA+M (FGM) viewed under field emission scanning electron microscope (FE-SEM) using a combination of secondary electron imaging and backscatter electron imaging at 5 kV. Cells were viewed under (A) 20,000X and (B) 70,000X magnification. (C) A magnified view of the F+GA+M transfected cells at 100,000X shows the presence of gold particles (white spots) in the filaments protruding from the cell surface. The backscatter (BkSc) image shows the location of the gold particles. The secondary image (Sec) shows the general morphology of the filaments with spherical projections along the surface. An approximate gold particle density calculation is shown.

After overnight transfection, both sets of cells were immunostained with anti-FLAG primary antibodies and anti-rabbit secondary antibodies conjugated with colloidal gold as described in Methods 2.9.1. The cells were viewed under FE-SEM at magnifications from 20,000X to 100,000X using both secondary electron images and backscatter electron images to distinguish the presence of the gold particles on the surface of the cell (Fig. 6.17A, B, C). We found a significantly ($p<0.001$) higher concentration of gold particles present in filaments protruding from the triple plasmid transfected cells compared to the mock-transfected cells. In addition, the position of the gold particles in the triple transfected cells appeared to co-localise with the spherical protrusions on the filament surface. This observation is similar to the work by (Jeffree et al., 2003) who were able to observe the presence and distribution of hRSV G protein in viral filaments produced from hRSV-infected Vero cells. The presence of G proteins within the filaments of F+GA+M co-transfected cells confirmed the role of GA in VLP formation.

6.5 Chapter summary

The formation of HMPV VLPs in mammalian cells requires the presence of F, G and M proteins and occurs concurrently with filament formation similar to observations in hRSV infection. These filaments are likely to be involved in the cell-to-cell spread of HMPV. Comparing the VLPs produced by HighFive and 293T cells, the HighFive-produced VLPs appear to be good candidates for vaccines since the production can be scaled-up to large quantities in a relatively short period of time. Even though baculoviruses can successfully infect a wide range of host cells, they do not replicate in mammalian cells because most of the regulatory genes cannot be transcribed in these cells (Ghosh et al., 2002). Therefore, baculovirus vectors avoid potential pitfalls due to possible pre-existing immunity against the vector. Another advantage of baculovirus vectors is their natural ability to stimulate the adaptive immune response such that the

use of adjuvants may not be necessary (Hervas-Stubbs et al., 2007), hence simplifying the process of vaccine development. Baculovirus vectors can be designed to contain multiple genes for co-expression, thus giving them an edge over other vaccine delivery systems. However, noting the difference between the GA and GB proteins of HMPV, there would be a need to study the protectiveness of using a GA protein-based VLP vaccine against a GB virus infection and vice versa. Perhaps a combination vaccine using both GA and GB-based VLPs could be considered.

Conclusions

The human metapneumovirus is a significant cause of childhood respiratory infection and its worldwide prevalence has sparked interest in research on this pathogen. In Singapore, it has been established that HMPV is responsible for about 5% of respiratory infections in children. Although there has not been any fatality attributed to HMPV infection locally, there have been reports elsewhere of deaths due to HMPV primarily among immunocompromised individuals. Thus, the virus remains one of the important pathogens that should be diagnosed in a medical laboratory. Apart from HMPV, the emergence of newer viruses, for example, HBoV remind us that there are more undiscovered viruses which may pose a threat in the future. Recently, there have been reports of new strains of HBoV which cause gastroenteritis (Chow et al., 2010). Combined with this threat, there are also a number of previously ignored respiratory viruses which have proven to have greater impact on human population health than expected. A good example of this is rhinovirus which is now being accepted as the main cause of asthma exacerbation (Proud, 2011). Another genus of lesser known respiratory viruses is HCoV which comprise a mix of "old" species (HCoV-229E, HCoV-OC43) and "new" species (HCoV-NL63, HCoV-HKU-1, SARS-CoV) (Wevers and van der Hoek, 2009). The SARS-CoV outbreak in 2003 changed the previously held perception of HCoV infections as being associated with low mortality rates and of little significance. In order to better understand the pattern of respiratory virus infections in children in Singapore, a long-term study spanning at least a year should be initiated to screen a statistically significant cohort of clinical specimens. Such a study can provide information on any seasonal variation of HMPV genogroups and other respiratory viruses. It can also increase the likelihood of identifying previously undiscovered viruses in the local population. Other than screening samples from sick children, additional screening of samples from asymptomatic and/or adult populations may yield clues as to the existence of HMPV during the "low" virus seasons.

The key strategy for virus entry among Paramyxoviruses is the combined action of the fusion and attachment glycoproteins (Lamb et al., 2006). In this study, the F and G glycoproteins of HMPV have been shown to be associated on the surface of transfected cells. The two proteins were found to form high molecular weight protein complexes, via crosslinking methods, which resemble similar structures in other Paramyxoviruses responsible for membrane fusion. The exact mechanism of F and G protein interaction in HMPV is still unknown. A similar interaction between hRSV F and G proteins was elucidated by (Low et al., 2008). Newcastle disease virus (Gravel and Morrison, 2003) and parainfluenza virus (Yao et al., 1997) F and HN proteins have also been demonstrated to interact with each other. Further study is needed to understand this phenomenon better. The role of the small hydrophobic protein in the virus life-cycle is poorly understood and deserves more research work. Alternatively, the interaction of the HMPV surface glycoproteins with host cell surface receptors could also be determined. Additional knowledge in this area will have implications in antiviral therapy, e.g. designing fusion protein inhibitors or attachment protein inhibitors. A soluble, truncated and secreted fusion protein produced in HighFive cells shows promise as an antigen. This protein can be purified before inoculating into animals for antibody generation. Antibodies against the soluble F protein have potential applications in diagnostic kits.

There is strong suggestion that the role of the F protein cytoplasmic tail domain is involved in the processing and maturation of the F protein. Subsequent work could be carried out with the truncated cytoplasmic tail fusion proteins to find out why the amino acid residues in the cytoplasmic region of the fusion protein that are close to the transmembrane region seem to affect the processing of the protein more severely than the other residues. The cytoplasmic tail domain of the hRSV F protein was found to be important in intracellular localization (Oomens et al., 2006). Other studies using simian virus 5 (Waning et al., 2004) have shown that the cytoplasmic tail domain is involved in the signaling process in F protein action. In measles virus, the truncation of the H protein was found to reduce the F-mediated cell fusion (Moll et al., 2002). Initial

mutation experiments using the G protein of HMPV appear to suggest that this protein is the driving force behind the formation of virus filaments which facilitate cell-to-cell transmission of virus. The loss of the cytoplasmic region of the attachment protein hampers the formation of filaments produced from the surface of transfected cells. This research angle should be pursued in the future.

Virus-like particles were created by co-expressing HMPV F, G and M proteins in HighFive insect cells and human 293T cells. The presence of virus-like particles was confirmed by various experimental methods including Western blotting, sucrose gradient ultracentrifugation, confocal and electron microscopy. Unexpectedly, the N protein was found to be non-essential for the formation of VLPs unlike some other Paramyxoviruses. Some examples include parainfluenza 1 virus (Coronel et al., 1999), simian virus 5 (Schmitt et al., 2002), Newcastle disease virus (Pantua et al., 2006) and avian pneumovirus (Weng et al., 2011); all of which require the N protein for VLP formation. However, there are examples of Paramyxoviruses that do not require the N protein for VLP formation e.g. Nipah virus (Patch et al., 2007) and measles virus (Pohl et al., 2007). Cells expressing F, G, and M proteins were observed to form filaments protruding from the cell surface. This is similar to the filaments occurring in HMPV and hRSV infected cells. These filaments are thought to be involved in the cell-to-cell spread of hRSV and HMPV. As a follow up, various methods for purifying the virus-like particles (e.g. chromatography or centrifugation) should be evaluated. Obtaining purified VLPs would be the first step in the process of testing the VLPs as a vaccine candidate. Although both HighFive and 293T cells can effectively produce VLPs, the HighFive-produced VLPs would be a better candidate for vaccines due to a number of factors: (i) Insect cells can be grown in suspension and serum-free media which allows VLP production to be scaled-up to large quantities in a relatively short period of time. (ii) Even though baculoviruses can successfully infect a wide range of mammalian host cells, they do not replicate in mammalian cells because most of the virus regulatory genes are cannot be transcribed in these cells (Ghosh et al., 2002). This allows baculovirus vectors to avoid potential problems due to pre-existing immunity against

the vector. (iii) Another advantage of baculovirus vectors is their natural ability to stimulate the adaptive immune response, such that the use of adjuvants may not be necessary (Hervas-Stubbs et al., 2007), hence simplifying the process of vaccine development. (iv) Baculovirus vectors can be designed to contain multiple genes for co-expression and thus providing them an edge over other vaccine delivery systems. Whatever VLP vaccine is produced, there will be a need to have a rigorous testing program in the pre-clinical phase. Of main concern will be the previous experiences with the testing of formalin-inactivated virus vaccines using animal models for hRSV (De Swart et al., 2002; Kim et al., 1969) and HMPV (de Swart et al., 2007; Yim et al., 2007). Given the success of the HPV vaccine Cervarix based on baculovirus-generated VLPs, there is a very good potential for the development of a similar vaccine for HMPV in the future.

References:

Aberle, J.H., Aberle, S.W., Redlberger-Fritz, M., Sandhofer, M.J., Popow-Kraupp, T., 2010. Human metapneumovirus subgroup changes and seasonality during epidemics. Pediatr Infect Dis J 29, 1016-1018.

Al-Sonboli, N., Hart, C.A., Al-Aghbari, N., Al-Ansi, A., Ashoor, O., Cuevas, L.E., 2006. Human metapneumovirus and respiratory syncytial virus disease in children, Yemen. Emerg Infect Dis 12, 1437-1439.

Allander, T., Tammi, M.T., Eriksson, M., Bjerkner, A., Tiveljung-Lindell, A., Andersson, B., 2005. Cloning of a human parvovirus by molecular screening of respiratory tract samples. Proc Natl Acad Sci U S A 102, 12891-12896.

Alvarez, R., Jones, L.P., Seal, B.S., Kapczynski, D.R., Tripp, R.A., 2004a. Serological cross-reactivity of members of the Metapneumovirus genus. Virus Res 105, 67-73.

Alvarez, R., Harrod, K.S., Shieh, W.J., Zaki, S., Tripp, R.A., 2004b. Human metapneumovirus persists in BALB/c mice despite the presence of neutralizing antibodies. J Virol 78, 14003-14011.

Ansari, S.A., Springthorpe, V.S., Sattar, S.A., Rivard, S., Rahman, M., 1991. Potential role of hands in the spread of respiratory viral infections: studies with human parainfluenza virus 3 and rhinovirus 14. J Clin Microbiol 29, 2115-2119.

Aramburo, A., van Schaik, S., Louie, J., Boston, E., Messenger, S., Wright, C., Lawrence Drew, W., 2011. Role of real-time reverse transcription polymerase chain reaction for detection of respiratory viruses in critically ill children with respiratory disease: Is it time for a change in algorithm? Pediatr Crit Care Med 12, e160-165.

Arnold, J.C., Singh, K.K., Milder, E., Spector, S.A., Sawyer, M.H., Gavali, S., Glaser, C., 2009. Human metapneumovirus associated with central nervous system infection in children. Pediatr Infect Dis J 28, 1057-1060.

Arnott, A., Vong, S., Sek, M., Naughtin, M., Beaute, J., Rith, S., Guillard, B., Deubel, V., Buchy, P., 2011. Genetic variability of human metapneumovirus amongst an all ages population in Cambodia between 2007 and 2009. Infect Genet Evol.epub

Arthur, J.L., Higgins, G.D., Davidson, G.P., Givney, R.C., Ratcliff, R.M., 2009. A novel bocavirus associated with acute gastroenteritis in Australian children. PLoS Pathog 5, e1000391.

Aslanzadeh, J., Zheng, X., Li, H., Tetreault, J., Ratkiewicz, I., Meng, S., Hamilton, P., Tang, Y.W., 2008. Prospective evaluation of rapid antigen tests for diagnosis of respiratory syncytial virus and human metapneumovirus infections. J Clin Microbiol 46, 1682-1685.

Bao, X., Kolli, D., Liu, T., Shan, Y., Garofalo, R.P., Casola, A., 2008a. Human metapneumovirus small hydrophobic protein inhibits NF-kappaB transcriptional activity. J Virol 82, 8224-8229.

Bao, X., Liu, T., Shan, Y., Li, K., Garofalo, R.P., Casola, A., 2008b. Human metapneumovirus glycoprotein G inhibits innate immune responses. PLoS Pathog 4, e1000077.

Bastien, N., Liu, L., Ward, D., Taylor, T., Li, Y., 2004. Genetic variability of the G glycoprotein gene of human metapneumovirus. J Clin Microbiol 42, 3532-3537.

Bastien, N., Normand, S., Taylor, T., Ward, D., Peret, T.C., Boivin, G., Anderson, L.J., Li, Y., 2003a. Sequence analysis of the N, P, M and F genes of Canadian human metapneumovirus strains. Virus Res 93, 51-62.

Bastien, N., Ward, D., Van Caeseele, P., Brandt, K., Lee, S.H., McNabb, G., Klisko, B., Chan, E., Li, Y., 2003b. Human metapneumovirus infection in the Canadian population. J Clin Microbiol 41, 4642-4646.

Berkley, J.A., Munywoki, P., Ngama, M., Kazungu, S., Abwao, J., Bett, A., Lassauniere, R., Kresfelder, T., Cane, P.A., Venter, M., Scott, J.A., Nokes, D.J., 2010. Viral etiology of severe pneumonia among Kenyan infants and children. JAMA 303, 2051-2057.

Biacchesi, S., Pham, Q.N., Skiadopoulos, M.H., Murphy, B.R., Collins, P.L., Buchholz, U.J., 2005. Infection of nonhuman primates with recombinant human metapneumovirus lacking the SH, G, or M2-2 protein categorizes each as a nonessential accessory protein and identifies vaccine candidates. J Virol 79, 12608-12613.

Biacchesi, S., Pham, Q.N., Skiadopoulos, M.H., Murphy, B.R., Collins, P.L., Buchholz, U.J., 2006. Modification of the trypsin-dependent cleavage activation site of the human metapneumovirus fusion protein to be trypsin independent does not increase replication or spread in rodents or nonhuman primates. J Virol 80, 5798-5806.

Biacchesi, S., Skiadopoulos, M.H., Boivin, G., Hanson, C.T., Murphy, B.R., Collins, P.L., Buchholz, U.J., 2003. Genetic diversity between human metapneumovirus subgroups. Virology 315, 1-9.

Biacchesi, S., Skiadopoulos, M.H., Yang, L., Lamirande, E.W., Tran, K.C., Murphy, B.R., Collins, P.L., Buchholz, U.J., 2004. Recombinant human Metapneumovirus lacking the small hydrophobic SH and/or attachment G glycoprotein: deletion of G yields a promising vaccine candidate. J Virol 78, 12877-12887.

Bissonnette, M.L., Donald, J.E., DeGrado, W.F., Jardetzky, T.S., Lamb, R.A., 2009. Functional analysis of the transmembrane domain in paramyxovirus F protein-mediated membrane fusion. J Mol Biol 386, 14-36.

Boivin, G., De Serres, G., Cote, S., Gilca, R., Abed, Y., Rochette, L., Bergeron, M.G., Dery, P., 2003. Human metapneumovirus infections in hospitalized children. Emerg Infect Dis 9, 634-640.

Boivin, G., Abed, Y., Pelletier, G., Ruel, L., Moisan, D., Cote, S., Peret, T.C., Erdman, D.D., Anderson, L.J., 2002. Virological features and clinical manifestations associated with human metapneumovirus: a new paramyxovirus responsible for acute respiratory-tract infections in all age groups. J Infect Dis 186, 1330-1334.

Boivin, G., Mackay, I., Sloots, T.P., Madhi, S., Freymuth, F., Wolf, D., Shemer-Avni, Y., Ludewick, H., Gray, G.C., LeBlanc, E., 2004. Global genetic diversity of human metapneumovirus fusion gene. Emerg Infect Dis 10, 1154-1157.

Boivin, G., De Serres, G., Hamelin, M.E., Cote, S., Argouin, M., Tremblay, G., Maranda-Aubut, R., Sauvageau, C., Ouakki, M., Boulianne, N., Couture, C., 2007. An outbreak of severe respiratory tract infection due to human metapneumovirus in a long-term care facility. Clin Infect Dis 44, 1152-1158.

Bosis, S., Esposito, S., Niesters, H.G., Crovari, P., Osterhaus, A.D., Principi, N., 2005. Impact of human metapneumovirus in childhood: comparison with respiratory syncytial virus and influenza viruses. J Med Virol 75, 101-104.

Bosis, S., Esposito, S., Osterhaus, A.D., Tremolati, E., Begliatti, E., Tagliabue, C., Corti, F., Principi, N., Niesters, H.G., 2008. Association between high nasopharyngeal viral load and disease severity in children with human metapneumovirus infection. J Clin Virol 42, 286-290.

Bruno, R., Marsico, S., Minini, C., Apostoli, P., Fiorentini, S., Caruso, A., 2009. Human metapneumovirus infection in a cohort of young asymptomatic subjects. New Microbiol 32, 297-301.

Buchholz, U.J., Nagashima, K., Murphy, B.R., Collins, P.L., 2006. Live vaccines for human metapneumovirus designed by reverse genetics. Expert Rev Vaccines 5, 695-706.

Buchholz, U.J., Biacchesi, S., Pham, Q.N., Tran, K.C., Yang, L., Luongo, C.L., Skiadopoulos, M.H., Murphy, B.R., Collins, P.L., 2005. Deletion of M2 gene open reading frames 1 and 2 of human metapneumovirus: effects on RNA synthesis, attenuation, and immunogenicity. J Virol 79, 6588-6597.

Cane, P.A., van den Hoogen, B.G., Chakrabarti, S., Fegan, C.D., Osterhaus, A.D., 2003. Human metapneumovirus in a haematopoietic stem cell transplant recipient with fatal lower respiratory tract disease. Bone Marrow Transplant 31, 309-310.

Carr, M.J., McCormack, G.P., Crowley, B., 2005. Human metapneumovirus-associated respiratory tract infections in the Republic of Ireland during the influenza season of 2003-2004. Clin Microbiol Infect 11, 366-371.

Chan, P.K., Tam, J.S., Lam, C.W., Chan, E., Wu, A., Li, C.K., Buckley, T.A., Ng, K.C., Joynt, G.M., Cheng, F.W., To, K.F., Lee, N., Hui, D.S., Cheung, J.L., Chu, I., Liu, E., Chung, S.S., Sung, J.J., 2003. Human metapneumovirus detection in patients with severe acute respiratory syndrome. Emerg Infect Dis 9, 1058-1063.

Chen, L., Gorman, J.J., McKimm-Breschkin, J., Lawrence, L.J., Tulloch, P.A., Smith, B.J., Colman, P.M., Lawrence, M.C., 2001. The structure of the fusion glycoprotein of Newcastle disease virus suggests a novel paradigm for the molecular mechanism of membrane fusion. Structure 9, 255-266.

Chow, B.D., Ou, Z., Esper, F.P., 2010. Newly recognized bocaviruses (HBoV, HBoV2) in children and adults with gastrointestinal illness in the United States. J Clin Virol 47, 143-147.

Chung, J.Y., Han, T.H., Kim, B.E., Kim, C.K., Kim, S.W., Hwang, E.S., 2006. Human metapneumovirus infection in hospitalized children with acute respiratory disease in Korea. J Korean Med Sci 21, 838-842.

Colman, P.M., Lawrence, M.C., 2003. The structural biology of type I viral membrane fusion. Nat Rev Mol Cell Biol 4, 309-319.

Condreay, J.P., Kost, T.A., 2007. Baculovirus expression vectors for insect and mammalian cells. Curr Drug Targets 8, 1126-1131.

Coronel, E.C., Murti, K.G., Takimoto, T., Portner, A., 1999. Human parainfluenza virus type 1 matrix and nucleoprotein genes transiently expressed in mammalian cells induce the release of virus-like particles containing nucleocapsid-like structures. J Virol 73, 7035-7038.

Cote, S., Abed, Y., Boivin, G., 2003. Comparative evaluation of real-time PCR assays for detection of the human metapneumovirus. J Clin Microbiol 41, 3631-3635.

Cseke, G., Maginnis, M.S., Cox, R.G., Tollefson, S.J., Podsiad, A.B., Wright, D.W., Dermody, T.S., Williams, J.V., 2009. Integrin alphavbeta1 promotes infection by human metapneumovirus. Proc Natl Acad Sci U S A 106, 1566-1571.

da Silva, L.H., Spilki, F.R., Riccetto, A.G., de Almeida, R.S., Baracat, E.C., Arns, C.W., 2008. Variant isolates of human metapneumovirus subgroup B genotype 1 in Campinas, Brazil. J Clin Virol 42, 78-81.

Darniot, M., Pitoiset, C., Petrella, T., Aho, S., Pothier, P., Manoha, C., 2009. Age-associated aggravation of clinical disease after primary metapneumovirus infection of BALB/c mice. J Virol 83, 3323-3332.

de Graaf, M., Osterhaus, A.D., Fouchier, R.A., Holmes, E.C., 2008. Evolutionary dynamics of human and avian metapneumoviruses. J Gen Virol 89, 2933-2942.

de Swart, R.L., van den Hoogen, B.G., Kuiken, T., Herfst, S., van Amerongen, G., Yuksel, S., Sprong, L., Osterhaus, A.D., 2007. Immunization of macaques with formalin-inactivated human metapneumovirus induces hypersensitivity to hMPV infection. Vaccine 25, 8518-8528.

De Swart, R.L., Kuiken, T., Timmerman, H.H., van Amerongen, G., Van Den Hoogen, B.G., Vos, H.W., Neijens, H.J., Andeweg, A.C., Osterhaus, A.D., 2002. Immunization of macaques with formalin-inactivated respiratory syncytial virus (RSV) induces interleukin-13-associated hypersensitivity to subsequent RSV infection. J Virol 76, 11561-11569.

Debur, M.C., Vidal, L.R., Stroparo, E., Nogueira, M.B., Almeida, S.M., Takahashi, G.A., Rotta, I., Pereira, L.A., Silveira, C.S., Delfraro, A., Nakatani, S.M., Skraba, I., Raboni, S.M., 2010. Impact of human metapneumovirus infection on in and outpatients for the years 2006-2008 in Southern Brazil. Mem Inst Oswaldo Cruz 105, 1010-1018.

Deffrasnes, C., Cote, S., Boivin, G., 2005. Analysis of replication kinetics of the human metapneumovirus in different cell lines by real-time PCR. J Clin Microbiol 43, 488-490.

Deffrasnes, C., Hamelin, M.E., Prince, G.A., Boivin, G., 2008a. Identification and evaluation of a highly effective fusion inhibitor for human metapneumovirus. Antimicrob Agents Chemother 52, 279-287.

Deffrasnes, C., Cavanagh, M.H., Goyette, N., Cui, K., Ge, Q., Seth, S., Templin, M.V., Quay, S.C., Johnson, P.H., Boivin, G., 2008b. Inhibition of human metapneumovirus replication by small interfering RNA. Antivir Ther 13, 821-832.

Dinwiddie, D.L., Harrod, K.S., 2008. Human metapneumovirus inhibits IFN-alpha signaling through inhibition of STAT1 phosphorylation. Am J Respir Cell Mol Biol 38, 661-670.

Dollner, H., Risnes, K., Radtke, A., Nordbo, S.A., 2004. Outbreak of human metapneumovirus infection in norwegian children. Pediatr Infect Dis J 23, 436-440.

Dutch, R.E., Jardetzky, T.S., Lamb, R.A., 2000. Virus membrane fusion proteins: biological machines that undergo a metamorphosis. Biosci Rep 20, 597-612.

Easton, A.J., Domachowske, J.B., Rosenberg, H.F., 2004. Animal pneumoviruses: molecular genetics and pathogenesis. Clin Microbiol Rev 17, 390-412.

Ebihara, T., Endo, R., Ma, X., Ishiguro, N., Kikuta, H., 2005. Detection of human metapneumovirus antigens in nasopharyngeal secretions by an immunofluorescent-antibody test. J Clin Microbiol 43, 1138-1141.

Ebihara, T., Endo, R., Ishiguro, N., Nakayama, T., Sawada, H., Kikuta, H., 2004a. Early reinfection with human metapneumovirus in an infant. J Clin Microbiol 42, 5944-5946.

Ebihara, T., Endo, R., Kikuta, H., Ishiguro, N., Ishiko, H., Kobayashi, K., 2004b. Comparison of the seroprevalence of human metapneumovirus and human respiratory syncytial virus. J Med Virol 72, 304-306.

Ebihara, T., Endo, R., Kikuta, H., Ishiguro, N., Yoshioka, M., Ma, X., Kobayashi, K., 2003. Seroprevalence of human metapneumovirus in Japan. J Med Virol 70, 281-283.

Ebihara, T., Endo, R., Kikuta, H., Ishiguro, N., Ishiko, H., Hara, M., Takahashi, Y., Kobayashi, K., 2004c. Human metapneumovirus infection in Japanese children. J Clin Microbiol 42, 126-132.

Egelman, E.H., Wu, S.S., Amrein, M., Portner, A., Murti, G., 1989. The Sendai virus nucleocapsid exists in at least four different helical states. J Virol 63, 2233-2243.

El Sayed Zaki, M., Raafat, D., El-Metaal, A.A., Ismail, M., 2009. Study of human metapneumovirus-associated lower respiratory tract infections in Egyptian adults. Microbiol Immunol 53, 603-608.

Elbein, A.D., 1991. The role of N-linked oligosaccharides in glycoprotein function. Trends Biotechnol 9, 346-352.

Endo, R., Ebihara, T., Ishiguro, N., Teramoto, S., Ariga, T., Sakata, C., Hayashi, A., Ishiko, H., Kikuta, H., 2008. Detection of four genetic subgroup-specific antibodies to human metapneumovirus attachment (G) protein in human serum. J Gen Virol 89, 1970-1977.

Escobar, C., Luchsinger, V., de Oliveira, D.B., Durigon, E., Chnaiderman, J., Avendano, L.F., 2009. Genetic variability of human metapneumovirus isolated from Chilean children, 2003-2004. J Med Virol 81, 340-344.

Escutenaire, S., Mohamed, N., Isaksson, M., Thoren, P., Klingeborn, B., Belak, S., Berg, M., Blomberg, J., 2007. SYBR Green real-time reverse transcription-polymerase chain reaction assay for the generic detection of coronaviruses. Arch Virol 152, 41-58.

Esper, F., Boucher, D., Weibel, C., Martinello, R.A., Kahn, J.S., 2003. Human metapneumovirus infection in the United States: clinical manifestations associated with a newly emerging respiratory infection in children. Pediatrics 111, 1407-1410.

Falsey, A.R., Criddle, M.C., Walsh, E.E., 2006. Detection of respiratory syncytial virus and human metapneumovirus by reverse transcription polymerase chain reaction in adults with and without respiratory illness. J Clin Virol 35, 46-50.

Fearns, R., Collins, P.L., 1999. Role of the M2-1 transcription antitermination protein of respiratory syncytial virus in sequential transcription. J Virol 73, 5852-5864.

Feldman, S.A., Hendry, R.M., Beeler, J.A., 1999. Identification of a linear heparin binding domain for human respiratory syncytial virus attachment glycoprotein G. J Virol 73, 6610-6617.

Feldman, S.A., Crim, R.L., Audet, S.A., Beeler, J.A., 2001. Human respiratory syncytial virus surface glycoproteins F, G and SH form an oligomeric complex. Arch Virol 146, 2369-2383.

Fields, B.N., Knipe, D.M., Howley, P.M., 2007. Fields virology. Wolters Kluwer Health/Lippincott Williams & Wilkins, Philadelphia.

Freymouth, F., Vabret, A., Legrand, L., Eterradossi, N., Lafay-Delaire, F., Brouard, J., Guillois, B., 2003. Presence of the new human metapneumovirus in French children with bronchiolitis. Pediatr Infect Dis J 22, 92-94.

Freymuth, F., Vabret, A., Cuvillon-Nimal, D., Simon, S., Dina, J., Legrand, L., Gouarin, S., Petitjean, J., Eckart, P., Brouard, J., 2006. Comparison of multiplex PCR assays and conventional techniques for the diagnostic of respiratory virus infections in children admitted to hospital with an acute respiratory illness. J Med Virol 78, 1498-1504.

Fulginiti, V.A., Eller, J.J., Downie, A.W., Kempe, C.H., 1967. Altered reactivity to measles virus. Atypical measles in children previously immunized with inactivated measles virus vaccines. JAMA 202, 1075-1080.

Furuse, Y., Suzuki, A., Kishi, M., Galang, H.O., Lupisan, S.P., Olveda, R.M., Oshitani, H., 2010. Detection of novel respiratory viruses from influenza-like illness in the Philippines. J Med Virol 82, 1071-1074.

Galiano, M., Trento, A., Ver, L., Carballal, G., Videla, C., 2006. Genetic heterogeneity of G and F protein genes from Argentinean human metapneumovirus strains. J Med Virol 78, 631-637.

Garcia-Barreno, B., Delgado, T., Melero, J.A., 1996. Identification of protein regions involved in the interaction of human respiratory syncytial virus phosphoprotein and nucleoprotein: significance for nucleocapsid assembly and formation of cytoplasmic inclusions. J Virol 70, 801-808.

Garcia-Garcia, M.L., Calvo, C., Pozo, F., Perez-Brena, P., Quevedo, S., Bracamonte, T., Casas, I., 2008. Human bocavirus detection in nasopharyngeal aspirates of children without clinical symptoms of respiratory infection. Pediatr Infect Dis J 27, 358-360.

Ghosh, S., Parvez, M.K., Banerjee, K., Sarin, S.K., Hasnain, S.E., 2002. Baculovirus as mammalian cell expression vector for gene therapy: an emerging strategy. Mol Ther 6, 5-11.

Gioula, G., Chatzidimitriou, D., Melidou, A., Exindari, M., Kyriazopoulou-Dalaina, V., 2010. Contribution of human metapneumovirus to influenza-like infections in North Greece, 2005-2008. Euro Surveill 15.

Goh, A., 2002. Asthma study, unpublished.

Goutagny, N., Jiang, Z., Tian, J., Parroche, P., Schickli, J., Monks, B.G., Ulbrandt, N., Ji, H., Kiener, P.A., Coyle, A.J., Fitzgerald, K.A., 2010. Cell type-specific recognition of human metapneumoviruses (HMPVs) by retinoic acid-inducible gene I (RIG-I) and TLR7 and viral interference of RIG-I ligand recognition by HMPV-B1 phosphoprotein. J Immunol 184, 1168-1179.

Gravel, K.A., Morrison, T.G., 2003. Interacting domains of the HN and F proteins of newcastle disease virus. J Virol 77, 11040-11049.

Gray, G.C., Capuano, A.W., Setterquist, S.F., Erdman, D.D., Nobbs, N.D., Abed, Y., Doern, G.V., Starks, S.E., Boivin, G., 2006a. Multi-year study of human

metapneumovirus infection at a large US Midwestern Medical Referral Center. J Clin Virol 37, 269-276.

Gray, G.C., Capuano, A.W., Setterquist, S.F., Sanchez, J.L., Neville, J.S., Olson, J., Lebeck, M.G., McCarthy, T., Abed, Y., Boivin, G., 2006b. Human metapneumovirus, Peru. Emerg Infect Dis 12, 347-350.

Greensill, J., McNamara, P.S., Dove, W., Flanagan, B., Smyth, R.L., Hart, C.A., 2003. Human metapneumovirus in severe respiratory syncytial virus bronchiolitis. Emerg Infect Dis 9, 372-375.

Gupta, C.K., Leszczynski, J., Gupta, R.K., Siber, G.R., 1996. Stabilization of respiratory syncytial virus (RSV) against thermal inactivation and freeze-thaw cycles for development and control of RSV vaccines and immune globulin. Vaccine 14, 1417-1420.

Gutierrez-Ortega, A., Sanchez-Hernandez, C., Gomez-Garcia, B., 2008. Respiratory syncytial virus glycoproteins uptake occurs through clathrin-mediated endocytosis in a human epithelial cell line. Virol J 5, 127.

Hall, C.B., Douglas, R.G., Jr., Geiman, J.M., 1980. Possible transmission by fomites of respiratory syncytial virus. J Infect Dis 141, 98-102.

Hall, T.A., 1999. BioEdit: a user-friendly biological sequence alignment editor and analysis program for Windows 95/98/NT. Nucl. Acids Symp. Ser. 41, 95-98.

Hamelin, M.E., Prince, G.A., Boivin, G., 2006. Effect of ribavirin and glucocorticoid treatment in a mouse model of human metapneumovirus infection. Antimicrob Agents Chemother 50, 774-777.

Hamelin, M.E., Yim, K., Kuhn, K.H., Cragin, R.P., Boukhvalova, M., Blanco, J.C., Prince, G.A., Boivin, G., 2005. Pathogenesis of human metapneumovirus lung infection in BALB/c mice and cotton rats. J Virol 79, 8894-8903.

Han, T.H., Chung, J.Y., Kim, S.W., Hwang, E.S., 2007. Human Coronavirus-NL63 infections in Korean children, 2004-2006. J Clin Virol 38, 27-31.

Handforth, J., Friedland, J.S., Sharland, M., 2000. Basic epidemiology and immunopathology of RSV in children. Paediatr Respir Rev 1, 210-214.

Harrison, R.L., Jarvis, D.L., 2006. Protein N-glycosylation in the baculovirus-insect cell expression system and engineering of insect cells to produce "mammalianized" recombinant glycoproteins. Adv Virus Res 68, 159-191.

Harro, C.D., Pang, Y.Y., Roden, R.B., Hildesheim, A., Wang, Z., Reynolds, M.J., Mast, T.C., Robinson, R., Murphy, B.R., Karron, R.A., Dillner, J., Schiller, J.T., Lowy, D.R., 2001. Safety and immunogenicity trial in adult volunteers of a human papillomavirus 16 L1 virus-like particle vaccine. J Natl Cancer Inst 93, 284-292.

Hayden, F.G., Turner, R.B., Gwaltney, J.M., Chi-Burris, K., Gersten, M., Hsyu, P., Patick, A.K., Smith, G.J., 3rd, Zalman, L.S., 2003. Phase II, randomized, double-blind, placebo-controlled studies of ruprintrivir nasal spray 2-percent suspension for prevention and treatment of experimentally induced rhinovirus colds in healthy volunteers. Antimicrob Agents Chemother 47, 3907-3916.

Heikkinen, T., Thint, M., Chonmaitree, T., 1999. Prevalence of various respiratory viruses in the middle ear during acute otitis media. N Engl J Med 340, 260-264.

Heminway, B.R., Yu, Y., Tanaka, Y., Perrine, K.G., Gustafson, E., Bernstein, J.M., Galinski, M.S., 1994. Analysis of respiratory syncytial virus F, G, and SH proteins in cell fusion. Virology 200, 801-805.

Herfst, S., Mas, V., Ver, L.S., Wierda, R.J., Osterhaus, A.D., Fouchier, R.A., Melero, J.A., 2008. Low-pH-induced membrane fusion mediated by human metapneumovirus F protein is a rare, strain-dependent phenomenon. J Virol 82, 8891-8895.

Hervas-Stubbs, S., Rueda, P., Lopez, L., Leclerc, C., 2007. Insect baculoviruses strongly potentiate adaptive immune responses by inducing type I IFN. J Immunol 178, 2361-2369.

Honda, H., Iwahashi, J., Kashiwagi, T., Imamura, Y., Hamada, N., Anraku, T., Ueda, S., Kanda, T., Takahashi, T., Morimoto, S., 2006. Outbreak of human metapneumovirus infection in elderly inpatients in Japan. J Am Geriatr Soc 54, 177-180.

Horikami, S.M., Curran, J., Kolakofsky, D., Moyer, S.A., 1992. Complexes of Sendai virus NP-P and P-L proteins are required for defective interfering particle genome replication in vitro. J Virol 66, 4901-4908.

Hornung, V., Ellegast, J., Kim, S., Brzozka, K., Jung, A., Kato, H., Poeck, H., Akira, S., Conzelmann, K.K., Schlee, M., Endres, S., Hartmann, G., 2006. 5'-Triphosphate RNA is the ligand for RIG-I. Science 314, 994-997.

Huang, C.G., Tsao, K.C., Lin, T.Y., Huang, Y.C., Lee, L.A., Chen, T.H., Huang, Y.L., Shih, S.R., 2010. Estimates of individuals exposed to human metapneumovirus in a community-based Taiwanese population in 1999. Arch Virol 155, 343-350.

Huck, B., Scharf, G., Neumann-Haefelin, D., Puppe, W., Weigl, J., Falcone, V., 2006a. Novel human metapneumovirus sublineage. Emerg Infect Dis 12, 147-150.

Huck, B., Egger, M., Bertz, H., Peyerl-Hoffman, G., Kern, W.V., Neumann-Haefelin, D., Falcone, V., 2006b. Human metapneumovirus infection in a hematopoietic stem cell transplant recipient with relapsed multiple myeloma and rapidly progressing lung cancer. J Clin Microbiol 44, 2300-2303.

Ingram, R.E., Fenwick, F., McGuckin, R., Tefari, A., Taylor, C., Toms, G.L., 2006. Detection of human metapneumovirus in respiratory secretions by reverse-transcriptase polymerase chain reaction, indirect immunofluorescence, and virus isolation in human bronchial epithelial cells. J Med Virol 78, 1223-1231.

International Committee on Taxonomy of Viruses., Fauquet, C., International Union of Microbiological Societies. Virology Division., 2006. Virus taxonomy : classification and nomenclature of viruses: eighth report of the International Committee on Taxonomy of Viruses
Elsevier/Academic Press, Oxford, UK.

Invitrogen, Bac-to-Bac® Baculovirus Expression System. In: Technologies, I.L. (Ed.).

Ishiguro, N., Ebihara, T., Endo, R., Ma, X., Kikuta, H., Ishiko, H., Kobayashi, K., 2004. High genetic diversity of the attachment (G) protein of human metapneumovirus. J Clin Microbiol 42, 3406-3414.

Ishiguro, N., Ebihara, T., Endo, R., Ma, X., Shirotsuki, R., Ochiai, S., Ishiko, H., Kikuta, H., 2005. Immunofluorescence assay for detection of human metapneumovirus-specific antibodies by use of baculovirus-expressed fusion protein. Clin Diagn Lab Immunol 12, 202-205.

Jardetzky, T.S., Lamb, R.A., 2004. Virology: a class act. Nature 427, 307-308.

Jartti, T., van den Hoogen, B., Garofalo, R.P., Osterhaus, A.D., Ruuskanen, O., 2002. Metapneumovirus and acute wheezing in children. Lancet 360, 1393-1394.

Jeffree, C.E., Rixon, H.W., Brown, G., Aitken, J., Sugrue, R.J., 2003. Distribution of the attachment (G) glycoprotein and GM1 within the envelope of mature respiratory syncytial virus filaments revealed using field emission scanning electron microscopy. Virology 306, 254-267.

Jensen, P.H., Kolarich, D., Packer, N.H., 2010. Mucin-type O-glycosylation--putting the pieces together. FEBS J 277, 81-94.

Kaplan, N.M., Dove, W., Abu-Zeid, A.F., Shamoon, H.E., Abd-Eldayem, S.A., Hart, C.A., 2006. Evidence of human metapneumovirus infection in Jordanian children. Saudi Med J 27, 1081-1083.

Kapoor, A., Simmonds, P., Slikas, E., Li, L., Bodhidatta, L., Sethabutr, O., Triki, H., Bahri, O., Oderinde, B.S., Baba, M.M., Bukbuk, D.N., Besser, J., Bartkus, J., Delwart, E., 2010. Human bocaviruses are highly diverse, dispersed, recombination prone, and prevalent in enteric infections. J Infect Dis 201, 1633-1643.

Kaverin, N., 2010. Postreassortment amino acid substitutions in influenza A viruses. Future Microbiol 5, 705-715.

Kawai, T., Akira, S., 2008. Toll-like receptor and RIG-I-like receptor signaling. Ann N Y Acad Sci 1143, 1-20.

Kim, H.W., Canchola, J.G., Brandt, C.D., Pyles, G., Chanock, R.M., Jensen, K., Parrott, R.H., 1969. Respiratory syncytial virus disease in infants despite prior administration of antigenic inactivated vaccine. Am J Epidemiol 89, 422-434.

Kimura, K., Mori, S., Tomita, K., Ohno, K., Takahashi, K., Shigeta, S., Terada, M., 2000. Antiviral activity of NMSO3 against respiratory syncytial virus infection in vitro and in vivo. Antiviral Res 47, 41-51.

Kimura, K., Ishioka, K., Hashimoto, K., Mori, S., Suzutani, T., Bowlin, T.L., Shigeta, S., 2004. Isolation and characterization of NMSO3-resistant mutants of respiratory syncytial virus. Antiviral Res 61, 165-171.

Kitagawa, Y., Zhou, M., Yamaguchi, M., Komatsu, T., Takeuchi, K., Itoh, M., Gotoh, B., 2010. Human metapneumovirus M2-2 protein inhibits viral transcription and replication. Microbes Infect 12, 135-145.

Klein, M.B., Yang, H., DelBalso, L., Carbonneau, J., Frost, E., Boivin, G., 2010. Viral pathogens including human metapneumovirus are the primary cause of febrile respiratory illness in HIV-infected adults receiving antiretroviral therapy. J Infect Dis 201, 297-301.

Koch, W.H., 2004. Technology platforms for pharmacogenomic diagnostic assays. Nat Rev Drug Discov 3, 749-761.

Kolli, D., Bataki, E.L., Spetch, L., Guerrero-Plata, A., Jewell, A.M., Piedra, P.A., Milligan, G.N., Garofalo, R.P., Casola, A., 2008. T lymphocytes contribute to antiviral immunity and pathogenesis in experimental human metapneumovirus infection. J Virol 82, 8560-8569.

Kolokoltsov, A.A., Deniger, D., Fleming, E.H., Roberts, N.J., Jr., Karpilow, J.M., Davey, R.A., 2007. Small interfering RNA profiling reveals key role of clathrin-mediated endocytosis and early endosome formation for infection by respiratory syncytial virus. J Virol 81, 7786-7800.

Kuiken, T., van den Hoogen, B.G., van Riel, D.A., Laman, J.D., van Amerongen, G., Sprong, L., Fouchier, R.A., Osterhaus, A.D., 2004. Experimental human metapneumovirus infection of cynomolgus macaques (Macaca fascicularis) results in virus replication in ciliated epithelial cells and pneumocytes with associated lesions throughout the respiratory tract. Am J Pathol 164, 1893-1900.

Kulakosky, P.C., Shuler, M.L., Wood, H.A., 1998. N-glycosylation of a baculovirus-expressed recombinant glycoprotein in three insect cell lines. In Vitro Cell Dev Biol Anim 34, 101-108.

Kumar, D., Husain, S., Chen, M.H., Moussa, G., Himsworth, D., Manuel, O., Studer, S., Pakstis, D., McCurry, K., Doucette, K., Pilewski, J., Janeczko, R., Humar, A., 2010. A prospective molecular surveillance study evaluating the clinical impact of community-acquired respiratory viruses in lung transplant recipients. Transplantation 89, 1028-1033.

Kuypers, J., Wright, N., Ferrenberg, J., Huang, M.L., Cent, A., Corey, L., Morrow, R., 2006. Comparison of real-time PCR assays with fluorescent-antibody assays for diagnosis of respiratory virus infections in children. J Clin Microbiol 44, 2382-2388.

Kyte, J., Doolittle, R.F., 1982. A simple method for displaying the hydropathic character of a protein. J Mol Biol 157, 105-132.

Laham, F.R., Israele, V., Casellas, J.M., Garcia, A.M., Lac Prugent, C.M., Hoffman, S.J., Hauer, D., Thumar, B., Name, M.I., Pascual, A., Taratutto, N., Ishida, M.T., Balduzzi, M., Maccarone, M., Jackli, S., Passarino, R., Gaivironsky, R.A., Karron, R.A., Polack, N.R., Polack, F.P., 2004. Differential production of inflammatory cytokines in primary infection with human metapneumovirus and with other common respiratory viruses of infancy. J Infect Dis 189, 2047-2056.

Lamb, R.A., Paterson, R.G., Jardetzky, T.S., 2006. Paramyxovirus membrane fusion: lessons from the F and HN atomic structures. Virology 344, 30-37.

Lamson, D., Renwick, N., Kapoor, V., Liu, Z., Palacios, G., Ju, J., Dean, A., St George, K., Briese, T., Lipkin, W.I., 2006. MassTag polymerase-chain-reaction detection of respiratory pathogens, including a new rhinovirus genotype, that caused influenza-like illness in New York State during 2004-2005. J Infect Dis 194, 1398-1402.

Larkin, M.A., Blackshields, G., Brown, N.P., Chenna, R., McGettigan, P.A., McWilliam, H., Valentin, F., Wallace, I.M., Wilm, A., Lopez, R., Thompson, J.D., Gibson, T.J., Higgins, D.G., 2007. Clustal W and Clustal X version 2.0. Bioinformatics 23, 2947-2948.

Lau, S.K., Yip, C.C., Tsoi, H.W., Lee, R.A., So, L.Y., Lau, Y.L., Chan, K.H., Woo, P.C., Yuen, K.Y., 2007. Clinical features and complete genome characterization of a distinct human rhinovirus (HRV) genetic cluster, probably representing a previously undetected HRV species, HRV-C, associated with acute respiratory illness in children. J Clin Microbiol 45, 3655-3664.

Lee, W.M., Grindle, K., Pappas, T., Marshall, D.J., Moser, M.J., Beaty, E.L., Shult, P.A., Prudent, J.R., Gern, J.E., 2007a. High-throughput, sensitive, and accurate multiplex PCR-microsphere flow cytometry system for large-scale comprehensive detection of respiratory viruses. J Clin Microbiol 45, 2626-2634.

Lee, W.M., Kiesner, C., Pappas, T., Lee, I., Grindle, K., Jartti, T., Jakiela, B., Lemanske, R.F., Jr., Shult, P.A., Gern, J.E., 2007b. A diverse group of previously unrecognized human rhinoviruses are common causes of respiratory illnesses in infants. PLoS One 2, e966.

Leung, J., Esper, F., Weibel, C., Kahn, J.S., 2005. Seroepidemiology of human metapneumovirus (hMPV) on the basis of a novel enzyme-linked immunosorbent assay utilizing hMPV fusion protein expressed in recombinant vesicular stomatitis virus. J Clin Microbiol 43, 1213-1219.

Levine, S., Klaiber-Franco, R., Paradiso, P.R., 1987. Demonstration that glycoprotein G is the attachment protein of respiratory syncytial virus. J Gen Virol 68 (Pt 9), 2521-2524.

Liao, R.S., Appelgate, D.M., Pelz, R.K., 2012. An outbreak of severe respiratory tract infection due to human metapneumovirus in a long-term care facility for the elderly in Oregon. J Clin Virol 53, 171-173.

Liao, S., Bao, X., Liu, T., Lai, S., Li, K., Garofalo, R.P., Casola, A., 2008. Role of retinoic acid inducible gene-I in human metapneumovirus-induced cellular signalling. J Gen Virol 89, 1978-1986.

Lichtenstein, D.L., Roberts, S.R., Wertz, G.W., Ball, L.A., 1996. Definition and functional analysis of the signal/anchor domain of the human respiratory syncytial virus glycoprotein G. J Gen Virol 77 (Pt 1), 109-118.

Linsuwanon, P., Payungporn, S., Samransamruajkit, R., Posuwan, N., Makkoch, J., Theanboonlers, A., Poovorawan, Y., 2009. High prevalence of human rhinovirus C infection in Thai children with acute lower respiratory tract disease. J Infect 59, 115-121.

Liu, L., Bastien, N., Li, Y., 2007. Intracellular processing, glycosylation, and cell surface expression of human metapneumovirus attachment glycoprotein. J Virol 81, 13435-13443.

Liu, L., Qian, Y., Zhu, R., Zhao, L., Deng, J., 2010. Generation of recombinant nucleocapsid protein of human metapneumovirus in baculovirus for detecting antibodies in the Beijing population. Arch Virol 155, 47-54.

Liu, Y., Haas, D.L., Poore, S., Isakovic, S., Gahan, M., Mahalingam, S., Fu, Z.F., Tripp, R.A., 2009. Human metapneumovirus establishes persistent infection in the lungs of mice and is reactivated by glucocorticoid treatment. J Virol 83, 6837-6848.

Ljubin Sternak, S., Vilibic Cavlek, T., Falsey, A.R., Walsh, E.E., Mlinaric Galinovic, G., 2006. Serosurvey of human metapneumovirus infection in Croatia. Croat Med J 47, 878-881.

Loo, L.H., Tan, B.H., Ng, L.M., Tee, N.W., Lin, R.T., Sugrue, R.J., 2007. Human metapneumovirus in children, Singapore. Emerg Infect Dis 13, 1396-1398.

Lopez, M., Tetaert, D., Juliant, S., Gazon, M., Cerutti, M., Verbert, A., Delannoy, P., 1999. O-glycosylation potential of lepidopteran insect cell lines. Biochim Biophys Acta 1427, 49-61.

Louie, J.K., Schnurr, D.P., Pan, C.Y., Kiang, D., Carter, C., Tougaw, S., Ventura, J., Norman, A., Belmusto, V., Rosenberg, J., Trochet, G., 2007. A summer outbreak of human metapneumovirus infection in a long-term-care facility. J Infect Dis 196, 705-708.

Low, K.W., Tan, T., Ng, K., Tan, B.H., Sugrue, R.J., 2008. The RSV F and G glycoproteins interact to form a complex on the surface of infected cells. Biochem Biophys Res Commun 366, 308-313.

Ludewick, H.P., Abed, Y., van Niekerk, N., Boivin, G., Klugman, K.P., Madhi, S.A., 2005. Human metapneumovirus genetic variability, South Africa. Emerg Infect Dis 11, 1074-1078.

Lwamba, H.C., Alvarez, R., Wise, M.G., Yu, Q., Halvorson, D., Njenga, M.K., Seal, B.S., 2005. Comparison of the full-length genome sequence of avian metapneumovirus subtype C with other paramyxoviruses. Virus Res 107, 83-92.

Mackay, I.M., Bialasiewicz, S., Jacob, K.C., McQueen, E., Arden, K.E., Nissen, M.D., Sloots, T.P., 2006. Genetic diversity of human metapneumovirus over 4 consecutive years in Australia. J Infect Dis 193, 1630-1633.

Mackay, I.M., Jacob, K.C., Woolhouse, D., Waller, K., Syrmis, M.W., Whiley, D.M., Siebert, D.J., Nissen, M., Sloots, T.P., 2003. Molecular assays for detection of human metapneumovirus. J Clin Microbiol 41, 100-105.

Mackay, I.M., Bialasiewicz, S., Waliuzzaman, Z., Chidlow, G.R., Fegredo, D.C., Laingam, S., Adamson, P., Harnett, G.B., Rawlinson, W., Nissen, M.D., Sloots, T.P., 2004. Use of the P gene to genotype human metapneumovirus identifies 4 viral subtypes. J Infect Dis 190, 1913-1918.

MacPhail, M., Schickli, J.H., Tang, R.S., Kaur, J., Robinson, C., Fouchier, R.A., Osterhaus, A.D., Spaete, R.R., Haller, A.A., 2004. Identification of small-animal and primate models for evaluation of vaccine candidates for human metapneumovirus (hMPV) and implications for hMPV vaccine design. J Gen Virol 85, 1655-1663.

Madhan, S., Prabakaran, M., Kwang, J., 2010. Baculovirus as vaccine vectors. Curr Gene Ther 10, 201-213.

Maertzdorf, J., Wang, C.K., Brown, J.B., Quinto, J.D., Chu, M., de Graaf, M., van den Hoogen, B.G., Spaete, R., Osterhaus, A.D., Fouchier, R.A., 2004. Real-time reverse transcriptase PCR assay for detection of human metapneumoviruses from all known genetic lineages. J Clin Microbiol 42, 981-986.

Maggi, F., Pifferi, M., Vatteroni, M., Fornai, C., Tempestini, E., Anzilotti, S., Lanini, L., Andreoli, E., Ragazzo, V., Pistello, M., Specter, S., Bendinelli, M., 2003. Human metapneumovirus associated with respiratory tract infections in a 3-year study of nasal swabs from infants in Italy. J Clin Microbiol 41, 2987-2991.

Martin, E.T., Fairchok, M.P., Kuypers, J., Magaret, A., Zerr, D.M., Wald, A., Englund, J.A., 2010. Frequent and prolonged shedding of bocavirus in young children attending daycare. J Infect Dis 201, 1625-1632.

McAdam, A.J., Hasenbein, M.E., Feldman, H.A., Cole, S.E., Offermann, J.T., Riley, A.M., Lieu, T.A., 2004. Human metapneumovirus in children tested at a tertiary-care hospital. J Infect Dis 190, 20-26.

Melendi, G.A., Laham, F.R., Monsalvo, A.C., Casellas, J.M., Israele, V., Polack, N.R., Kleeberger, S.R., Polack, F.P., 2007. Cytokine profiles in the respiratory tract during primary infection with human metapneumovirus, respiratory syncytial virus, or influenza virus in infants. Pediatrics 120, e410-415.

Miller, S.A., Tollefson, S., Crowe, J.E., Jr., Williams, J.V., Wright, D.W., 2007. Examination of a fusogenic hexameric core from human metapneumovirus and

identification of a potent synthetic peptide inhibitor from the heptad repeat 1 region. J Virol 81, 141-149.

Moll, M., Klenk, H.D., Maisner, A., 2002. Importance of the cytoplasmic tails of the measles virus glycoproteins for fusogenic activity and the generation of recombinant measles viruses. J Virol 76, 7174-7186.

Monsma, S.A., Oomens, A.G., Blissard, G.W., 1996. The GP64 envelope fusion protein is an essential baculovirus protein required for cell-to-cell transmission of infection. J Virol 70, 4607-4616.

Moore, E.C., Barber, J., Tripp, R.A., 2008. Respiratory syncytial virus (RSV) attachment and nonstructural proteins modify the type I interferon response associated with suppressor of cytokine signaling (SOCS) proteins and IFN-stimulated gene-15 (ISG15). Virol J 5, 116.

Morrow, B.M., Hatherill, M., Smuts, H.E., Yeats, J., Pitcher, R., Argent, A.C., 2006. Clinical course of hospitalised children infected with human metapneumovirus and respiratory syncytial virus. J Paediatr Child Health 42, 174-178.

Murphy, L.B., Loney, C., Murray, J., Bhella, D., Ashton, P., Yeo, R.P., 2003. Investigations into the amino-terminal domain of the respiratory syncytial virus nucleocapsid protein reveal elements important for nucleocapsid formation and interaction with the phosphoprotein. Virology 307, 143-153.

Nissen, M.D., Siebert, D.J., Mackay, I.M., Sloots, T.P., Withers, S.J., 2002. Evidence of human metapneumovirus in Australian children. Med J Aust 176, 188.

Njenga, M.K., Lwamba, H.M., Seal, B.S., 2003. Metapneumoviruses in birds and humans. Virus Res 91, 163-169.

NLM, 2010. Ribavirin. American Society of Health-System Pharmacists.

Noad, R., Roy, P., 2003. Virus-like particles as immunogens. Trends Microbiol 11, 438-444.

Noyola, D.E., Alpuche-Solis, A.G., Herrera-Diaz, A., Soria-Guerra, R.E., Sanchez-Alvarado, J., Lopez-Revilla, R., 2005. Human metapneumovirus infections in Mexico: epidemiological and clinical characteristics. J Med Microbiol 54, 969-974.

Ong, B.H., Gao, Q., Phoon, M.C., Chow, V.T., Tan, W.C., Van Bever, H.P., 2007. Identification of human metapneumovirus and Chlamydophila pneumoniae in children with asthma and wheeze in Singapore. Singapore Med J 48, 291-293.

Oomens, A.G., Bevis, K.P., Wertz, G.W., 2006. The cytoplasmic tail of the human respiratory syncytial virus F protein plays critical roles in cellular localization of the F protein and infectious progeny production. J Virol 80, 10465-10477.

Ordas, J., Boga, J.A., Alvarez-Arguelles, M., Villa, L., Rodriguez-Dehli, C., de Ona, M., Rodriguez, J., Melon, S., 2006. Role of metapneumovirus in viral respiratory infections in young children. J Clin Microbiol 44, 2739-2742.

Osbourn, M., McPhie, K.A., Ratnamohan, V.M., Dwyer, D.E., Durrheim, D.N., 2009. Outbreak of human metapneumovirus infection in a residential aged care facility. Commun Dis Intell 33, 38-40.

Ottolini, M.G., Porter, D.D., Hemming, V.G., Prince, G.A., 2000. Enhanced pulmonary pathology in cotton rats upon challenge after immunization with inactivated parainfluenza virus 3 vaccines. Viral Immunol 13, 231-236.

Pantua, H.D., McGinnes, L.W., Peeples, M.E., Morrison, T.G., 2006. Requirements for the assembly and release of Newcastle disease virus-like particles. J Virol 80, 11062-11073.

Parodi, A.J., 2000. Protein glucosylation and its role in protein folding. Annu Rev Biochem 69, 69-93.

Patch, J.R., Crameri, G., Wang, L.F., Eaton, B.T., Broder, C.C., 2007. Quantitative analysis of Nipah virus proteins released as virus-like particles reveals central role for the matrix protein. Virol J 4, 1.

Peiris, J.S., Tang, W.H., Chan, K.H., Khong, P.L., Guan, Y., Lau, Y.L., Chiu, S.S., 2003. Children with respiratory disease associated with metapneumovirus in Hong Kong. Emerg Infect Dis 9, 628-633.

Pelletier, G., Dery, P., Abed, Y., Boivin, G., 2002. Respiratory tract reinfections by the new human Metapneumovirus in an immunocompromised child. Emerg Infect Dis 8, 976-978.

Peret, T.C., Abed, Y., Anderson, L.J., Erdman, D.D., Boivin, G., 2004. Sequence polymorphism of the predicted human metapneumovirus G glycoprotein. J Gen Virol 85, 679-686.

Peret, T.C., Boivin, G., Li, Y., Couillard, M., Humphrey, C., Osterhaus, A.D., Erdman, D.D., Anderson, L.J., 2002. Characterization of human metapneumoviruses isolated from patients in North America. J Infect Dis 185, 1660-1663.

Pichlmair, A., Schulz, O., Tan, C.P., Naslund, T.I., Liljestrom, P., Weber, F., Reis e Sousa, C., 2006. RIG-I-mediated antiviral responses to single-stranded RNA bearing 5'-phosphates. Science 314, 997-1001.

Pitoiset, C., Darniot, M., Huet, F., Aho, S.L., Pothier, P., Manoha, C., 2010. Human metapneumovirus genotypes and severity of disease in young children (n = 100) during a 7-year study in Dijon hospital, France. J Med Virol 82, 1782-1789.

Pizzorno, A., Masner, M., Medici, C., Sarachaga, M.J., Rubio, I., Mirazo, S., Frabasile, S., Arbiza, J., 2010. Molecular detection and genetic variability of human metapneumovirus in Uruguay. J Med Virol 82, 861-865.

Poch, O., Blumberg, B.M., Bougueleret, L., Tordo, N., 1990. Sequence comparison of five polymerases (L proteins) of unsegmented negative-strand RNA viruses: theoretical assignment of functional domains. J Gen Virol 71 (Pt 5), 1153-1162.

Pohl, C., Duprex, W.P., Krohne, G., Rima, B.K., Schneider-Schaulies, S., 2007. Measles virus M and F proteins associate with detergent-resistant membrane fractions and promote formation of virus-like particles. J Gen Virol 88, 1243-1250.

Pozo, F., Garcia-Garcia, M.L., Calvo, C., Cuesta, I., Perez-Brena, P., Casas, I., 2007. High incidence of human bocavirus infection in children in Spain. J Clin Virol 40, 224-228.

Proud, D., 2011. Role of rhinovirus infections in asthma. Asian Pac J Allergy Immunol 29, 201-208.

Rafiefard, F., Yun, Z., Orvell, C., 2008. Epidemiologic characteristics and seasonal distribution of human metapneumovirus infections in five epidemic seasons in Stockholm, Sweden, 2002-2006. J Med Virol 80, 1631-1638.

Rawling, J., Melero, J.A., 2007. The use of monoclonal antibodies and lectins to identify changes in viral glycoproteins that are influenced by glycosylation: the case of human respiratory syncytial virus attachment (G) glycoprotein. Methods Mol Biol 379, 109-125.

Regev, L., Hindiyeh, M., Shulman, L.M., Barak, A., Levy, V., Azar, R., Shalev, Y., Grossman, Z., Mendelson, E., 2006. Characterization of human metapneumovirus infections in Israel. J Clin Microbiol 44, 1484-1489.

Roberts, S.R., Lichtenstein, D., Ball, L.A., Wertz, G.W., 1994. The membrane-associated and secreted forms of the respiratory syncytial virus attachment glycoprotein G are synthesized from alternative initiation codons. J Virol 68, 4538-4546.

Russell, C.J., Luque, L.E., 2006. The structural basis of paramyxovirus invasion. Trends Microbiol 14, 243-246.

Russell, C.J., Kantor, K.L., Jardetzky, T.S., Lamb, R.A., 2003. A dual-functional paramyxovirus F protein regulatory switch segment: activation and membrane fusion. J Cell Biol 163, 363-374.

Ryder, A.B., Tollefson, S.J., Podsiad, A.B., Johnson, J.E., Williams, J.V., 2010. Soluble recombinant human metapneumovirus G protein is immunogenic but not protective. Vaccine 28, 4145-4152.

Sanderson, C.M., McQueen, N.L., Nayak, D.P., 1993. Sendai virus assembly: M protein binds to viral glycoproteins in transit through the secretory pathway. J Virol 67, 651-663.

Sanderson, C.M., Wu, H.H., Nayak, D.P., 1994. Sendai virus M protein binds independently to either the F or the HN glycoprotein in vivo. J Virol 68, 69-76.

Schickli, J.H., Kaur, J., Ulbrandt, N., Spaete, R.R., Tang, R.S., 2005. An S101P substitution in the putative cleavage motif of the human metapneumovirus fusion protein is a major determinant for trypsin-independent growth in vero cells and does not alter tissue tropism in hamsters. J Virol 79, 10678-10689.

Schickli, J.H., Kaur, J., Macphail, M., Guzzetta, J.M., Spaete, R.R., Tang, R.S., 2008. Deletion of human metapneumovirus M2-2 increases mutation frequency and attenuates growth in hamsters. Virol J 5, 69.

Schildgen, O., Glatzel, T., Geikowski, T., Scheibner, B., Matz, B., Bindl, L., Born, M., Viazov, S., Wilkesmann, A., Knopfle, G., Roggendorf, M., Simon, A., 2005. Human metapneumovirus RNA in encephalitis patient. Emerg Infect Dis 11, 467-470.

Schmitt, A.P., Leser, G.P., Waning, D.L., Lamb, R.A., 2002. Requirements for budding of paramyxovirus simian virus 5 virus-like particles. J Virol 76, 3952-3964.

Schowalter, R.M., Smith, S.E., Dutch, R.E., 2006a. Characterization of Human Metapneumovirus F Protein-Promoted Membrane Fusion: Critical Roles for Proteolytic Processing and Low pH▽. J Virol 80, 10931-10941.

Schowalter, R.M., Smith, S.E., Dutch, R.E., 2006b. Characterization of human metapneumovirus F protein-promoted membrane fusion: critical roles for proteolytic processing and low pH. J Virol 80, 10931-10941.

Schowalter, R.M., Chang, A., Robach, J.G., Buchholz, U.J., Dutch, R.E., 2009. Low-pH triggering of human metapneumovirus fusion: essential residues and importance in entry. J Virol 83, 1511-1522.

Seal, B.S., 2000. Avian pneumoviruses and emergence of a new type in the United States of America. Anim Health Res Rev 1, 67-72.

Semple, M.G., Cowell, A., Dove, W., Greensill, J., McNamara, P.S., Halfhide, C., Shears, P., Smyth, R.L., Hart, C.A., 2005. Dual infection of infants by human metapneumovirus and human respiratory syncytial virus is strongly associated with severe bronchiolitis. J Infect Dis 191, 382-386.

Shi, X., Jarvis, D.L., 2007. Protein N-glycosylation in the baculovirus-insect cell system. Curr Drug Targets 8, 1116-1125.

Shields, B., Mills, J., Ghildyal, R., Gooley, P., Meanger, J., 2003. Multiple heparin binding domains of respiratory syncytial virus G mediate binding to mammalian cells. Arch Virol 148, 1987-2003.

Shirogane, Y., Takeda, M., Iwasaki, M., Ishiguro, N., Takeuchi, H., Nakatsu, Y., Tahara, M., Kikuta, H., Yanagi, Y., 2008. Efficient multiplication of human metapneumovirus in Vero cells expressing the transmembrane serine protease TMPRSS2. J Virol 82, 8942-8946.

Sidhu, M.S., Menonna, J.P., Cook, S.D., Dowling, P.C., Udem, S.A., 1993. Canine distemper virus L gene: sequence and comparison with related viruses. Virology 193, 50-65.

Sloots, T.P., McErlean, P., Speicher, D.J., Arden, K.E., Nissen, M.D., Mackay, I.M., 2006a. Evidence of human coronavirus HKU1 and human bocavirus in Australian children. J Clin Virol 35, 99-102.

Sloots, T.P., Mackay, I.M., Bialasiewicz, S., Jacob, K.C., McQueen, E., Harnett, G.B., Siebert, D.J., Masters, B.I., Young, P.R., Nissen, M.D., 2006b. Human metapneumovirus, Australia, 2001-2004. Emerg Infect Dis 12, 1263-1266.

Smith, G.E., Summers, M.D., Fraser, M.J., 1983. Production of human beta interferon in insect cells infected with a baculovirus expression vector. Mol Cell Biol 3, 2156-2165.

Sugrue, R.J., 2007. Viruses and glycosylation: an overview. Methods Mol Biol 379, 1-13.

Sugrue, R.J., Tan, B.H., Loo, L.H., 2008. The emergence of human metapneumovirus. Future Virology 3, 363-371.

Tacket, C.O., Sztein, M.B., Losonsky, G.A., Wasserman, S.S., Estes, M.K., 2003. Humoral, mucosal, and cellular immune responses to oral Norwalk virus-like particles in volunteers. Clin Immunol 108, 241-247.

Tamminen, K., Huhti, L., Koho, T., Lappalainen, S., Hytonen, V.P., Vesikari, T., Blazevic, V., 2012. A comparison of immunogenicity of norovirus GII-4 virus-like particles and P-particles. Immunology 135, 89-99.

Tamura, K., Dudley, J., Nei, M., Kumar, S., 2007. MEGA4: Molecular Evolutionary Genetics Analysis (MEGA) software version 4.0. Mol Biol Evol 24, 1596-1599.

Tan, B.H., Loo, L.H., Lim, E.A., Kheng Seah, S.L., Lin, R.T., Tee, N.W., Sugrue, R.J., 2009a. Human rhinovirus group C in hospitalized children, Singapore. Emerg Infect Dis 15, 1318-1320.

Tan, B.H., Lim, E.A., Seah, S.G., Loo, L.H., Tee, N.W., Lin, R.T., Sugrue, R.J., 2009b. The incidence of human bocavirus infection among children admitted to hospital in Singapore. J Med Virol 81, 82-89.

Tang, R.S., Mahmood, K., Macphail, M., Guzzetta, J.M., Haller, A.A., Liu, H., Kaur, J., Lawlor, H.A., Stillman, E.A., Schickli, J.H., Fouchier, R.A., Osterhaus, A.D., Spaete, R.R., 2005. A host-range restricted parainfluenza virus type 3 (PIV3) expressing the human metapneumovirus (hMPV) fusion protein elicits protective immunity in African green monkeys. Vaccine 23, 1657-1667.

Tarbouriech, N., Curran, J., Ebel, C., Ruigrok, R.W., Burmeister, W.P., 2000. On the domain structure and the polymerization state of the sendai virus P protein. Virology 266, 99-109.

Templeton, K.E., Scheltinga, S.A., Beersma, M.F., Kroes, A.C., Claas, E.C., 2004. Rapid and sensitive method using multiplex real-time PCR for diagnosis of infections by influenza a and influenza B viruses, respiratory syncytial virus, and parainfluenza viruses 1, 2, 3, and 4. J Clin Microbiol 42, 1564-1569.

Thammawat, S., Sadlon, T.A., Hallsworth, P.G., Gordon, D.L., 2008. Role of cellular glycosaminoglycans and charged regions of viral G protein in human metapneumovirus infection. J Virol 82, 11767-11774.

Thanasugarn, W., Samransamruajkit, R., Vanapongtipagorn, P., Prapphal, N., Van den Hoogen, B., Osterhaus, A.D., Poovorawan, Y., 2003. Human metapneumovirus infection in Thai children. Scand J Infect Dis 35, 754-756.

Tollefson, S.J., Cox, R.G., Williams, J.V., 2010. Studies of culture conditions and environmental stability of human metapneumovirus. Virus Res 151, 54-59.

Toquin, D., de Boisseson, C., Beven, V., Senne, D.A., Eterradossi, N., 2003. Subgroup C avian metapneumovirus (MPV) and the recently isolated human MPV exhibit a common organization but have extensive sequence divergence in their putative SH and G genes. J Gen Virol 84, 2169-2178.

van den Hoogen, B.G., Bestebroer, T.M., Osterhaus, A.D., Fouchier, R.A., 2002. Analysis of the genomic sequence of a human metapneumovirus. Virology 295, 119-132.

van den Hoogen, B.G., de Jong, J.C., Groen, J., Kuiken, T., de Groot, R., Fouchier, R.A., Osterhaus, A.D., 2001. A newly discovered human pneumovirus isolated from young children with respiratory tract disease. Nat Med 7, 719-724.

van den Hoogen, B.G., Herfst, S., Sprong, L., Cane, P.A., Forleo-Neto, E., de Swart, R.L., Osterhaus, A.D., Fouchier, R.A., 2004. Antigenic and genetic variability of human metapneumoviruses. Emerg Infect Dis 10, 658-666.

Van den Steen, P., Rudd, P.M., Dwek, R.A., Opdenakker, G., 1998. Concepts and principles of O-linked glycosylation. Crit Rev Biochem Mol Biol 33, 151-208.

van der Hoek, L., Sure, K., Ihorst, G., Stang, A., Pyrc, K., Jebbink, M.F., Petersen, G., Forster, J., Berkhout, B., Uberla, K., 2005. Croup is associated with the novel coronavirus NL63. PLoS Med 2, e240.

Velayudhan, B.T., Nagaraja, K.V., Thachil, A.J., Shaw, D.P., Gray, G.C., Halvorson, D.A., 2006. Human metapneumovirus in turkey poults. Emerg Infect Dis 12, 1853-1859.

Vicente, D., Montes, M., Cilla, G., Perez-Yarza, E.G., Perez-Trallero, E., 2006. Differences in clinical severity between genotype A and genotype B human metapneumovirus infection in children. Clin Infect Dis 42, e111-113.

von Linstow, M.L., Larsen, H.H., Eugen-Olsen, J., Koch, A., Nordmann Winther, T., Meyer, A.M., Westh, H., Lundgren, B., Melbye, M., Hogh, B., 2004. Human metapneumovirus and respiratory syncytial virus in hospitalized danish children with acute respiratory tract infection. Scand J Infect Dis 36, 578-584.

Wang, S.M., Liu, C.C., Wang, H.C., Su, I.J., Wang, J.R., 2006. Human metapneumovirus infection among children in Taiwan: a comparison of clinical manifestations with other virus-associated respiratory tract infections. Clin Microbiol Infect 12, 1221-1224.

Waning, D.L., Russell, C.J., Jardetzky, T.S., Lamb, R.A., 2004. Activation of a paramyxovirus fusion protein is modulated by inside-out signaling from the cytoplasmic tail. Proc Natl Acad Sci U S A 101, 9217-9222.

Weigl, J.A., Puppe, W., Meyer, C.U., Berner, R., Forster, J., Schmitt, H.J., Zepp, F., 2007. Ten years' experience with year-round active surveillance of up to 19 respiratory pathogens in children. Eur J Pediatr 166, 957-966.

Weng, Y., Lu, W., Harmon, A., Xiang, X., Deng, Q., Song, M., Wang, D., Yu, Q., Li, F., 2011. The cellular endosomal sorting complex required for transport pathway is not involved in avian metapneumovirus budding in a virus-like-particle expression system. J Gen Virol 92, 1205-1213.

Wemo, A.M., Anderson, T.P., Jennings, L.C., Jackson, P.M., Murdoch, D.R., 2004. Human metapneumovirus in children with bronchiolitis or pneumonia in New Zealand. J Paediatr Child Health 40, 549-551.

Wertz, G.W., Krieger, M., Ball, L.A., 1989. Structure and cell surface maturation of the attachment glycoprotein of human respiratory syncytial virus in a cell line deficient in O glycosylation. J Virol 63, 4767-4776.

Westenberg, M., Uijtdewilligen, P., Vlak, J.M., 2007. Baculovirus envelope fusion proteins F and GP64 exploit distinct receptors to gain entry into cultured insect cells. J Gen Virol 88, 3302-3306.

Wevers, B.A., van der Hoek, L., 2009. Recently discovered human coronaviruses. Clin Lab Med 29, 715-724.

Williams, J.V., Tollefson, S.J., Nair, S., Chonmaitree, T., 2006a. Association of human metapneumovirus with acute otitis media. Int J Pediatr Otorhinolaryngol 70, 1189-1193.

Williams, J.V., Harris, P.A., Tollefson, S.J., Halburnt-Rush, L.L., Pingsterhaus, J.M., Edwards, K.M., Wright, P.F., Crowe, J.E., Jr., 2004. Human metapneumovirus and lower respiratory tract disease in otherwise healthy infants and children. N Engl J Med 350, 443-450.

Williams, J.V., Crowe, J.E., Jr., Enriquez, R., Minton, P., Peebles, R.S., Jr., Hamilton, R.G., Higgins, S., Griffin, M., Hartert, T.V., 2005. Human metapneumovirus infection plays an etiologic role in acute asthma exacerbations requiring hospitalization in adults. J Infect Dis 192, 1149-1153.

Williams, J.V., Wang, C.K., Yang, C.F., Tollefson, S.J., House, F.S., Heck, J.M., Chu, M., Brown, J.B., Lintao, L.D., Quinto, J.D., Chu, D., Spaete, R.R., Edwards, K.M., Wright, P.F., Crowe, J.E., Jr., 2006b. The role of human metapneumovirus in upper respiratory tract infections in children: a 20-year experience. J Infect Dis 193, 387-395.

Wu, P.S., Chang, L.Y., Berkhout, B., van der Hoek, L., Lu, C.Y., Kao, C.L., Lee, P.I., Shao, P.L., Lee, C.Y., Huang, F.Y., Huang, L.M., 2008. Clinical manifestations of human coronavirus NL63 infection in children in Taiwan. Eur J Pediatr 167, 75-80.

Wyatt, L.S., Moss, B., Rozenblatt, S., 1995. Replication-deficient vaccinia virus encoding bacteriophage T7 RNA polymerase for transient gene expression in mammalian cells. Virology 210, 202-205.

Wyde, P.R., Chetty, S.N., Jewell, A.M., Boivin, G., Piedra, P.A., 2003. Comparison of the inhibition of human metapneumovirus and respiratory syncytial virus by ribavirin and immune serum globulin in vitro. Antiviral Res 60, 51-59.

Wyde, P.R., Moylett, E.H., Chetty, S.N., Jewell, A., Bowlin, T.L., Piedra, P.A., 2004. Comparison of the inhibition of human metapneumovirus and respiratory syncytial virus by NMSO3 in tissue culture assays. Antiviral Res 63, 51-59.

Xiao, N.G., Xie, Z.P., Zhang, B., Yuan, X.H., Song, J.R., Gao, H.C., Zhang, R.F., Hou, Y.D., Duan, Z.J., 2010. Prevalence and clinical and molecular characterization of human metapneumovirus in children with acute respiratory infection in China. Pediatr Infect Dis J 29, 131-134.

Yang, C.F., Wang, C.K., Tollefson, S.J., Piyaratna, R., Lintao, L.D., Chu, M., Liem, A., Mark, M., Spaete, R.R., Crowe, J.E., Jr., Williams, J.V., 2009. Genetic diversity and evolution of human metapneumovirus fusion protein over twenty years. Virol J 6, 138.

Yao, Q., Hu, X., Compans, R.W., 1997. Association of the parainfluenza virus fusion and hemagglutinin-neuraminidase glycoproteins on cell surfaces. J Virol 71, 650-656.

Yim, K.C., Cragin, R.P., Boukhvalova, M.S., Blanco, J.C., Hamlin, M.E., Boivin, G., Porter, D.D., Prince, G.A., 2007. Human metapneumovirus: enhanced pulmonary disease in cotton rats immunized with formalin-inactivated virus vaccine and challenged. Vaccine 25, 5034-5040.

Yin, H.S., Paterson, R.G., Wen, X., Lamb, R.A., Jardetzky, T.S., 2005. Structure of the uncleaved ectodomain of the paramyxovirus (hPIV3) fusion protein. Proc Natl Acad Sci U S A 102, 9288-9293.

Yin, H.S., Wen, X., Paterson, R.G., Lamb, R.A., Jardetzky, T.S., 2006. Structure of the parainfluenza virus 5 F protein in its metastable, prefusion conformation. Nature 439, 38-44.

Yuan, P., Thompson, T.B., Wurzburg, B.A., Paterson, R.G., Lamb, R.A., Jardetzky, T.S., 2005. Structural studies of the parainfluenza virus 5 hemagglutinin-neuraminidase tetramer in complex with its receptor, sialyllactose. Structure 13, 803-815.

Appendix A

Screening results for clinical nasopharyngeal samples

Specimen number	Age group	Diagnosis indicated	Year tested	Antigen detection	HMPV RT-PCR (Ct)	HCoV RT-PCR	HBoV PCR	HRV RT-PCR
1	1-3	fever	2005					
2	<1	bronchiolitis	2005	hRSV				
3	3-10	pneumonia	2005					
4	<1	pneumonia	2005					
5	<1	bronchiolitis	2005					
6	3-10	URTI	2005					
7	<1	NNP	2005					
8	<1	fever	2005	hRSV				
9	<1	NNP	2005					
10	<1	poor feeding	2005					
11	1-3	Kawasaki disease	2005					
12	1-3	URTI	2005				pos	
13	1-3	bronchiolitis	2005					
14	1-3	bronchiolitis	2005		Pos (24.6)			
15	3-10	rhinitis	2005					
16	>10	?	2005					
17	3-10	bronchiolitis	2005					
18	3-10	infection	2005					
19	1-3	viral fever	2005	PIV3				
20	<1	poor feeding	2005					

Specimen number	Age group	Diagnosis indicated	Year tested	Antigen detection	HMPV RT-PCR (Ct)	HCoV RT-PCR	HBoV PCR	HRV RT-PCR
21	1-3	febrile fit	2005					
22	<1	febrile fit	2005				pos	
23	3-10	URTI	2005					
24	<1	bronchiolitis	2005	hRSV				
25	1-3	prolonged fever	2005					
26	<1	URTI	2005					
27	<1	infantile pyrexia	2005					
28	1-3	fever	2005					
29	1-3	febrile fit	2005		Pos (34.8)			
30	<1	infantile pyrexia	2005					
31	3-10	bronchiolitis	2005					
32	3-10	URTI	2005	FA				
33	3-10	NNP	2005					
34	1-3	CLD	2005	hRSV				
35	1-3	bronchiolitis	2005					pos
36	<1	bronchiolitis	2005					
37	1-3	pneumonia	2005					
38	3-10	asthma	2005					
39	1-3	bronchiolitis	2005					
40	1-3	acute bronchiolitis	2005					
41	3-10	URTI	2005					
42	<1	URTI	2005	hRSV				
43	1-3	chest infection	2005					
44	<1	?chickenpox	2005					
45	<1	bronchiolitis	2005					

Specimen number	Age group	Diagnosis indicated	Year tested	Antigen detection	HMPV RT-PCR (Ct)	HCoV RT-PCR	HBoV PCR	HRV RT-PCR
46	<1	bronchiolitis	2005				pos	
47	1-3	pneumonia	2005					
48	>10	?	2005					
49	1-3	febrile fit	2005	FA				
50	<1	URTI	2005		Pos (26.6)			
51	1-3	bronchiolitis	2005		Pos (34.9)			
52	1-3	pharyngitis	2005		Pos (24.3)			
53	3-10	seizure	2005					
54	<1	URTI	2005	hRSV				
55	<1	infantile pyrexia	2005	hRSV				
56	<1	NNP	2005					
57	1-3	ALTB	2005	PIV1				
58	3-10	URTI	2005					pos
59	1-1	febrile fit	2005	FB				
60	3-10	fever	2005					
61	<1	febrile fit	2005					
62	3-10	?aspergillosis	2005					pos
63	1-3	seizure	2005					
64	1-3	?dengue	2005					
65	1-3	Kawasaki disease	2005					
66	1-3	bronchiolitis	2005					
67	1-3	URTI	2005					
68	1-3	bronchitis	2005					

Specimen number	Age group	Diagnosis indicated	Year tested	Antigen detection	HMPV RT-PCR (Ct)	HCoV RT-PCR	HBoV PCR	HRV RT-PCR
69	3-10	bronchitis	2005					
70	<1	infantile pyrexia	2005		Pos (18.4)			
71	1-3	acute gastritis	2005					
72	3-10	gastritis	2005					
73	<1	bronchiolitis	2005	hRSV				
74	3-10	asthma	2005					pos
75	<1	pharyngitis	2005					
76	1-3	bronchitis	2005					
77	1-3	URTI	2005					
78	<1	fever	2005					
79	1-3	herpangina	2005				pos	
80	3-10	pneumonia	2005					
81	1-3	pneumonia	2005					
82	3-10	bronchiolitis	2005	hRSV				
83	1-3	fever	2005					
84	<1	URTI	2005		Pos (28.7)			
85	3-10	pneumonia	2005					
86	3-10	asthma	2005				pos	
87	1-3	bronchiolitis	2005					
88	>10	fever	2005					
89	1-3	bronchitis	2005					
90	1-3	seizure	2005					
91	1-3	infection	2005					pos
92	<1	herpangina	2005					

Specimen number	Age group	Diagnosis indicated	Year tested	Antigen detection	HMPV RT-PCR (Ct)	HCoV RT-PCR	HBoV PCR	HRV RT-PCR
93	<1	URTI	2005					
94	<1	bronchiolitis	2005					
95	3-10	?dengue	2005					
96	3-10	bronchitis	2005	hRSV				
97	1-3	fever	2005					
98	1-3	?	2005					
99	1-3	pneumonia	2005					
100	1-3	SCID	2005	PIV1				
101	1-3	bronchiolitis	2005		Pos (31.9)			
102	1-3	pneumonia	2005		Pos (31.5)			
103	<1	Kawasaki disease	2005					
104	<1	pneumonia	2005				pos	
105	1-3	chest infection	2005					
106	1-3	ALTB	2005	PIV1				
107	1-3	acute bronchiolitis	2005					pos
108	3-10	pneumonia	2005					
109	<1	URTI	2005					
110	3-10	bronchitis	2005					
111	1-3	bronchitis	2005					
112	1-3	febrile fit	2005					
113	>10	seizure	2005					
114	1-3	Broncho pneumonia	2005					
115	3-10	URTI	2005					

Specimen number	Age group	Diagnosis indicated	Year tested	Antigen detection	HMPV RT-PCR (Ct)	HCoV RT-PCR	HBoV PCR	HRV RT-PCR
116	1-3	infection	2005					
117	1-3	URTI	2005					
118	<1	poor feeding	2005					
119	3-10	gastritis	2005					
120	1-3	fever	2005					
121	3-10	?	2005					pos
122	1-3	URTI	2005					
123	<1	choking	2005					
124	<1	pharyngitis	2005					
125	1-3	asthma	2005					
126	1-3	bronchitis	2005					
127	<1	NNP	2005					
128	<1	febrile fit	2005					
129	1-3	bronchiolitis	2005					pos
130	3-10	asthma	2005					
131	<1	fever	2005					
132	<1	infantile pyrexia	2005					
133	3-10	fever	2005					
134	3-10	asthma	2005					
135	1-3	URTI	2005		Pos (21.3)			
136	1-3	Fever	2005					
137	3-10	Kawasaki disease	2005					
138	1-3	Bronchiolitis	2005					
139	<1	Meningitis	2005					
140	<1	URTI	2005					

Specimen number	Age group	Diagnosis indicated	Year tested	Antigen detection	HMPV RT-PCR (Ct)	HCoV RT-PCR	HBoV PCR	HRV RT-PCR
141	<1	?	2005					
142	3-10	URTI	2005					
143	<1	Gastritis	2005					
144	<1	Bronchiolitis	2005					pos
145	<1	URTI	2005					
146	3-10	URTI	2005					
147	<1	febrile fit	2005					
148	1-3	Broncho pneumonia	2005					
149	3-10	?	2005					
150	1-3	?	2005				pos	
151	<1	fever	2006					
152	<1	fever	2006					
153	<1	RSV exposure	2006					
154	<1	RSV exposure	2006					
155	<1	fever	2006					
156	<1	RSV exposure	2006					
157	<1	URTI	2006					
158	<1	gastritis	2006					
159	1-3	Bronchiolitis	2006	hRSV			pos	
160	<1	CLD	2006					
161	3-10	Gastritis	2006					
162	3-10	Fever	2006					
163	1-3	Pneumonia	2006	hRSV				
164	3-10	Kawasaki disease	2006					
165	1-3	CLD	2006	hRSV			pos	

Specimen number	Age group	Diagnosis indicated	Year tested	Antigen detection	HMPV RT-PCR (Ct)	HCoV RT-PCR	HBoV PCR	HRV RT-PCR
166	1-3	wheezing	2006					
167	1-3	URTI	2006				pos	
168	1-3	asthma	2006					
169	<1	NNP	2006					
170	3-10	URTI	2006					
171	<1	bronchiolitis	2006	hRSV				
172	3-10	febrile fit	2006					
173	3-10	bronchitis	2006					pos
174	<1	gastritis	2006					
175	<1	bronchiolitis	2006					
176	<1	fever	2006					
177	<1	bronchitis	2006	hRSV				pos
178	3-10	cerebral abscess	2006					
179	1-3	URTI	2006					pos
180	<1	URTI	2006					
181	1-3	bronchitis	2006	hRSV				
182	<1	URTI	2006					
183	1-3	bronchiolitis	2006					
184	>10	gastritis	2006					
185	3-10	URTI	2006	hRSV				
186	3-10	seizure	2006					
187	<1	wheezing	2006		Pos (24.1)			
188	<1	URTI	2006					pos
189	3-10	gastritis	2006	hRSV				
190	3-10	seizure	2006	hRSV				

Specimen number	Age group	Diagnosis indicated	Year tested	Antigen detection	HMPV RT-PCR (Ct)	HCoV RT-PCR	HBoV PCR	HRV RT-PCR
191	3-10	?	2006					
192	3-10	URTI	2006					
193	3-10	asthma	2006				pos	
194	<1	URTI	2006	hRSV			pos	
195	1-3	acute bronchiolitis	2006				pos	
196	<1	vomitting	2006					pos
197	3-10	Broncho pneumonia	2006	hRSV				
198	<1	pneumonia	2006					
199	1-3	URTI	2006					
200	<1	gastritis	2006					
201	<1	URTI	2006					pos
202	<1	poor feeding	2006					
203	<1	infantile pyrexia	2006					
204	<1	NNP	2006	hRSV				
205	1-3	chest infection	2006					pos
206	3-10	bronchitis	2006	hRSV				
207	<1	fever	2006					
208	3-10	gastritis	2006					
209	1-3	fever	2006					
210	<1	bronchiolitis	2006					
211	<1	ALTB	2006			pos		
212	1-3	asthma	2006	hRSV				
213	1-3	afebrile fit	2006					pos
214	<1	bronchiolitis	2006	hRSV				
215	<1	bronchitis	2006	hRSV				

Specimen number	Age group	Diagnosis indicated	Year tested	Antigen detection	HMPV RT-PCR (Ct)	HCoV RT-PCR	HBoV PCR	HRV RT-PCR
216	<1	bronchiolitis	2006					
217	<1	asthma	2006		Pos (26.0)			
218	1-3	bronchiolitis	2006				pos	pos
219	3-10	asthma	2006					
220	1-3	pneumonia	2006	hRSV				pos
221	3-10	asthma	2006					
222	<1	URTI	2006	hRSV				
223	3-10	asthma	2006					
224	1-3	URTI	2006		Pos (29.9)			
225	3-10	URTI	2006					
226	1-3	URTI	2006					
227	<1	bronchiolitis	2006					
228	3-10	febrile fit	2006					
229	1-3	bronchiolitis	2006					
230	1-3	pneumonia	2006					
231	<1	?	2006					
232	1-3	acute bronchitis	2006		Pos (23.8)			
233	<1	NNP	2006					
234	<1	URTI	2006				pos	pos
235	1-3	bronchiolitis	2006					
236	<1	pneumonia	2006	PIV3				
237	1-3	gastritis	2006	hRSV				
238	3-10	URTI	2006					

Specimen number	Age group	Diagnosis indicated	Year tested	Antigen detection	HMPV RT-PCR (Ct)	HCoV RT-PCR	HBoV PCR	HRV RT-PCR
239	3-10	?	2006	hRSV				
240	1-3	gastritis	2006	hRSV				
241	>10	asthma	2006					Pos
242	<1	URTI	2006					
243	<1	croup	2006				pos	
244	3-10	asthma	2006					
245	<1	bronchiolitis	2006					Pos
246	3-10	pneumonia	2006				pos	
247	>10	fever	2006					
248	1-3	eczema	2006					
249	3-10	fever	2006					
250	<1	infantile pyrexia	2006				pos	
251	<1	premature	2006					
252	3-10	URTI	2006					Pos
253	3-10	wheezing	2006	hRSV				
254	3-10	chest infection	2006					
255	1-3	chest infection	2006					
256	<1	bronchiolitis	2006					
257	>10	asthma	2006					Pos
258	<1	URTI	2006	hRSV			pos	
259	3-10	febrile fit	2006					
260	<1	URTI	2006					Pos
261	3-10	?	2006					
262	<1	NNP	2006					
263	>10	asthma	2006				pos	Pos
264	<1	URTI	2006	hRSV				

Specimen number	Age group	Diagnosis indicated	Year tested	Antigen detection	HMPV RT-PCR (Ct)	HCoV RT-PCR	HBoV PCR	HRV RT-PCR
265	>10	sarcoma	2006					
266	1-3	URTI	2006	PIV3				
267	<1	bronchiolitis	2006	hRSV				
268	1-3	pneumonia	2006	PIV3			pos	
269	1-3	acute bronchiolitis	2006	hRSV				
270	1-3	wheezing	2006	hRSV				
271	>10	chest infection	2006		Pos (19.4)			
272	3-10	URTI	2006		Pos (21.9)			
273	1-3	URTI	2006		Pos (22.0)			
274	<1	URTI	2006					
275	3-10	asthma	2006				pos	
276	1-3	acute bronchiolitis	2006	PIV3				
277	3-10	URTI	2006		Pos (23.8)			
278	<1	fever	2006					Pos
279	<1	bronchiolitis	2006					
280	<1	chest infection	2006					
281	3-10	gastritis	2006					Pos
282	3-10	?	2006					
283	1-3	Kawasaki disease	2006					
284	3-10	bronchitis	2006					
285	1-3	gastritis	2006					
286	<1	?	2006					

Specimen number	Age group	Diagnosis indicated	Year tested	Antigen detection	HMPV RT-PCR (Ct)	HCoV RT-PCR	HBoV PCR	HRV RT-PCR
287	<1	URTI	2006					
288	1-3	gastritis	2006					
289	1-3	bronchitis	2006		Pos (26.4)			
290	1-3	bronchitis	2006	PIV3			pos	
291	<1	URTI	2006					
292	3-10	asthma	2006					
293	3-10	bronchitis	2006					
294	3-10	?	2006					
295	1-3	bronchitis	2006			pos		
296	<1	?	2006	hRSV				
297	<1	bronchiolitis	2006	hRSV				
298	3-10	fever	2006	PIV3				
299	1-3	tonsillitis	2006					
300	3-10	asthma	2006					
301	<1	whooping cough	2006					Pos
302	1-3	bronchiolitis	2006					Pos
303	1-3	URTI	2006					
304	1-3	asthma	2006					Pos
305	<1	HFMD	2006	hRSV				
306	<1	ALTB	2006					
307	1-3	URTI	2006					
308	1-3	febrile fit	2006					Pos
309	1-3	Kawasaki disease	2006					
310	1-3	URTI	2006					
311	<1	NNP	2006					

Specimen number	Age group	Diagnosis indicated	Year tested	Antigen detection	HMPV RT-PCR (Ct)	HCoV RT-PCR	HBoV PCR	HRV RT-PCR
312	<1	infantile pyrexia	2006					
313	<1	URTI	2006					
314	3-10	bronchiolitis	2006					
315	3-10	asthma	2006					
316	1-3	URTI	2006					pos
317	1-3	seizure	2006					
318	3-10	hypoventilation	2006					
319	<1	URTI	2006					
320	1-3	acute bronchiolitis	2006					
321	3-10	asthma	2006					
322	3-10	fever	2006					
323	<1	URTI	2006	PIV3				
324	3-10	?	2006					pos
325	1-3	ALTB	2006	PIV1			pos	
326	1-3	pneumonia	2006					
327	<1	bronchiolitis	2006	hRSV				
328	<1	URTI	2006				pos	
329	<1	fever	2006					
330	3-10	?	2006					
331	3-10	pneumonia	2006	AdV				
332	<1	NNP	2006					
333	<1	febrile fit	2006					
334	<1	URTI	2006					pos
335	<1	bronchiolitis	2006					
336	<1	URTI	2006					pos
337	<1	bronchiolitis	2006					

Specimen number	Age group	Diagnosis indicated	Year tested	Antigen detection	HMPV RT-PCR (Ct)	HCoV RT-PCR	HBoV PCR	HRV RT-PCR
338	1-3	URTI	2006					
339	1-3	SCID	2006					
340	3-10	URTI	2006					
341	3-10	asthma	2006					pos
342	3-10	gastritis	2006					
343	<1	chest infection	2006					
344	<1	wheezing	2006					
345	1-3	URTI	2006					
346	<1	wheezing	2006					
347	3-10	asthma	2006					
348	1-3	URTI	2006					pos
349	<1	bronchiolitis	2006	hRSV				
350	3-10	bronchiolitis	2006					
351	3-10	fever	2006					
352	3-10	URTI	2006					pos
353	1-3	URTI	2006	hRSV			pos	
354	3-10	URTI	2006					pos
355	<1	poor feeding	2006					
356	3-10	?	2006					
357	1-3	bronchiolitis	2006					
358	3-10	?	2006					
359	1-3	febrile fit	2006					
360	3-10	asthma	2006					
361	1-3	febrile fit	2006					
362	<1	infantile pyrexia	2006					
363	<1	NNP	2006					

Specimen number	Age group	Diagnosis indicated	Year tested	Antigen detection	HMPV RT-PCR (Ct)	HCoV RT-PCR	HBoV PCR	HRV RT-PCR
364	<1	pneumonia	2006					
365	3-10	?	2006					
366	<1	bronchiolitis	2006	hRSV				
367	3-10	?	2006					
368	1-3	pneumonia	2006					
369	1-3	pneumonia	2006					
370	1-3	gastritis	2006					
371	3-10	bronchitis	2006				pos	
372	<1	URTI	2006					pos
373	<1	bronchiolitis	2006					
374	>10	URTI	2006				pos	
375	1-3	asthma	2006				pos	
376	>10	seizure	2006					
377	1-3	bronchitis	2006	hRSV				
378	3-10	?	2006					
379	1-3	URTI	2006					
380	<1	overfeeding	2006					pos
381	<1	gastritis	2006					pos
382	<1	infantile pyrexia	2006					pos
383	3-10	URTI	2006					
384	1-3	chest infection	2006		Pos (20.4)			
385	3-10	febrile fit	2006	FA				
386	<1	bronchiolitis	2006	hRSV				
387	1-3	seizure	2006					
388	<1	persistent crying	2006					

Specimen number	Age group	Diagnosis indicated	Year tested	Antigen detection	HMPV RT-PCR (Ct)	HCoV RT-PCR	HBoV PCR	HRV RT-PCR
389	3-10	asthma	2006					
390	3-10	pneumonia	2006					
391	<1	bronchiolitis	2006					pos
392	1-3	prolonged fever	2006					
393	1-3	?	2006					
394	<1	?	2006					
395	<1	ALTB	2006			pos		
396	<1	NNP	2006					
397	<1	bronchiolitis	2006					pos
398	3-10	asthma	2006		Pos (19.6)			
399	1-3	bronchiolitis	2006				pos	
400	<1	pneumonia	2006					
401	3-10	acute bronchitis	2007		Pos (31.5)			
402	<1	NNP	2007					
403	<1	?	2007					
404	<1	bronchiolitis	2007					pos
405	1-3	bronchitis	2007					pos
406	3-10	pharyngitis	2007					
407	1-3	bronchiolitis	2007					
408	1-3	tonsillitis	2007					
409	1-3	seizure	2007					
410	3-10	fever	2007					
411	1-3	bronchiolitis	2007					
412	<1	NNP	2007					pos

Specimen number	Age group	Diagnosis indicated	Year tested	Antigen detection	HMPV RT-PCR (Ct)	HCoV RT-PCR	HBoV PCR	HRV RT-PCR
413	<1	bronchiolitis	2007					
414	3-10	wheezing	2007					
415	<1	bronchiolitis	2007					
416	3-10	URTI	2007					pos
417	<1	infantile pyrexia	2007					
418	1-3	gastritis	2007	hRSV				
419	1-3	URTI	2007	hRSV				
420	<1	bronchiolitis	2007					
421	<1	URTI	2007				pos	pos
422	>10	URTI	2007					
423	3-10	URTI	2007		Pos (19.9)			
424	1-3	bronchiolitis	2007	hRSV				
425	3-10	bronchiolitis	2007					pos
426	1-3	pneumonia	2007	hRSV				
427	1-3	croup	2007				pos	
428	1-3	?	2007					
429	1-3	croup	2007					
430	3-10	?	2007	hRSV			pos	
431	3-10	asthma	2007					
432	<1	bronchiolitis	2007				pos	
433	>10	fever	2007					
434	<1	bronchiolitis	2007					
435	<1	NNP	2007					
436	3-10	asthma	2007					pos
437	>10	pneumonia	2007					

Specimen number	Age group	Diagnosis indicated	Year tested	Antigen detection	HMPV RT-PCR (Ct)	HCoV RT-PCR	HBoV PCR	HRV RT-PCR
438	<1	bronchiolitis	2007	hRSV				
439	1-3	asthma	2007					pos
440	3-10	acute bronchitis	2007					
441	3-10	ALL	2007				pos	pos
442	3-10	asthma	2007		Pos (29.0)			
443	3-10	chest infection	2007					
444	1-3	gastritis	2007					
445	1-3	asthma	2007					
446	<1	bronchiolitis	2007	hRSV				
447	1-3	gastritis	2007					
448	3-10	cellulitis	2007					
449	1-3	URTI	2007					
450	<1	anaemia	2007					
451	<1	viral fever	2007					
452	<1	hypertension	2007					
453	>10	seizure	2007					
454	<1	NNP	2007					pos
455	<1	bronchiolitis	2007					
456	3-10	bronchiolitis	2007					
457	3-10	meningitis	2007	FB				
458	1-3	bronchitis	2007					pos
459	<1	URTI	2007	hRSV				
460	3-10	bronchitis	2007					
461	3-10	URTI	2007		Pos (20.9)			

Specimen number	Age group	Diagnosis indicated	Year tested	Antigen detection	HMPV RT-PCR (Ct)	HCoV RT-PCR	HBoV PCR	HRV RT-PCR
462	>10	?	2007					
463	1-3	Kawasaki disease	2007					pos
464	3-10	pneumonia	2007					
465	1-3	seizure	2007	hRSV				
466	<1	URTI	2007					
467	3-10	URTI	2007					
468	3-10	URTI	2007	hRSV				
469	1-3	URTI	2007	FA				
470	3-10	asthma	2007				pos	pos
471	3-10	asthma	2007					pos
472	1-3	chest infection	2007					
473	<1	URTI	2007					
474	<1	infantile pyrexia	2007					
475	1<1	URTI	2007					
476	3-10	URTI	2007					
477	3-10	URTI	2007					
478	1-3	fever	2007					pos
479	>10	seizure	2007					
480	3-10	fever	2007		Pos (24.6)			
481	3-10	URTI	2007		Pos (32.6)			
482	3-10	asthma	2007					
483	1-3	bronchiolitis	2007					
484	<1	bronchiolitis	2007	hRSV				
485	1-3	URTI	2007	hRSV				

Specimen number	Age group	Diagnosis indicated	Year tested	Antigen detection	HMPV RT-PCR (Ct)	HCoV RT-PCR	HBoV PCR	HRV RT-PCR
486	3-10	asthma	2007					pos
487	3-10	URTI	2007					
488	3-10	asthma	2007					
489	3-10	febrile fit	2007		Pos (35.0)			
490	1-3	URTI	2007					
491	1-3	bronchitis	2007					
492	<1	bronchiolitis	2007	hRSV				
493	3-10	pneumonia	2007					
494	1-3	URTI	2007				pos	
495	3-10	asthma	2007		Pos (24.1)			
496	>10	bronchitis	2007				pos	
497	>10	pneumonia	2007				pos	pos
498	1-3	URTI	2007					
499	<1	URTI	2007					
500	3-10	gastritis	2007				pos	pos

Legend: FA – influenza A virus
FB – influenza B virus
PIV1 – parainfluenza 1 virus
PIV3 – parainfluenza 3 virus
Adv – adenovirus
hRSV – human respiratory syncytial virus
HMPV - human metapneumovirus
HCoV - human coronavirus
HBoV – human bocavirus
HRV-human rhinovirus

pos - postive for virus (number in brackets represents the Ct value for real-time RT-PCR)

blank space – no virus detected

Age group classification:
less than 1 year old (<1),
1 to less than 3 years old (1-3),
3 to less than 10 years old (3-10) and
10 years and older (>10).

Appendix B

Virus gene sequences submitted to GenBank

Description	Accession number
HMPV isolate SIN05-NTU14 fusion protein gene, partial	EF397618
HMPV isolate SIN05-NTU50 fusion protein gene, partial	EF397619
HMPV isolate SIN05-NTU70 fusion protein gene, partial	EF397620
HMPV isolate SIN05-NTU84 fusion protein gene, partial	EF397621
HMPV isolate SIN05-NTU135 fusion protein gene, partial	EF397622
HMPV isolate SIN06-NTU187 fusion protein gene, partial	EF397623
HMPV isolate SIN06-NTU217 fusion protein gene, partial	EF397624
HMPV isolate SIN06-NTU224 fusion protein gene, partial	EF397625
HMPV isolate SIN06-NTU232 fusion protein gene, partial	EF397626
HMPV isolate SIN06-NTU271 fusion protein gene, complete	EF397627
HMPV isolate SIN06-NTU272 fusion protein gene, partial	EF397628
HMPV isolate SIN06-NTU273 fusion protein gene, partial	EF397629
HMPV isolate SIN06-NTU277 fusion protein gene, partial	EF397630
HMPV isolate SIN06-NTU289 fusion protein gene, partial	EF397631
HMPV isolate SIN06-NTU384 fusion protein gene, partial	EF397632
HMPV isolate SIN06-NTU398 fusion protein gene, partial	EF397633
HMPV isolate SIN05-NTU135 attachment protein gene, partial	JQ309673
HMPV isolate SIN06-NTU187 attachment protein gene, partial	JQ309674
HMPV isolate SIN06-NTU224 attachment protein gene, partial	JQ309675
HMPV isolate SIN06-NTU232 attachment protein gene, partial	JQ309676
HMPV isolate SIN06-NTU271 attachment protein gene, complete	JQ309677
HMPV isolate SIN06-NTU272 attachment protein gene, complete	JQ309678
HMPV isolate SIN06-NTU273 attachment protein gene, partial	JQ309679
HMPV isolate SIN06-NTU277 attachment protein gene, partial	JQ309680
HMPV isolate SIN06-NTU384 attachment protein gene, partial	JQ309681
HMPV isolate SIN06-NTU398 attachment protein gene, partial	JQ309682
HMPV isolate SIN05-NTU14 matrix protein gene, partial	JQ309643
HMPV isolate SIN05-NTU29 matrix protein gene, partial	JQ309644
HMPV isolate SIN05-NTU50 matrix protein gene, partial	JQ309645
HMPV isolate SIN05-NTU51 matrix protein gene, partial	JQ309646
HMPV isolate SIN05-NTU52 matrix protein gene, partial	JQ309647
HMPV isolate SIN05-NTU70 matrix protein gene, partial	JQ309648
HMPV isolate SIN05-NTU84 matrix protein gene, complete	JQ309649
HMPV isolate SIN05-NTU101 matrix protein gene, partial	JQ309650
HMPV isolate SIN05-NTU102 matrix protein gene, partial	JQ309651
HMPV isolate SIN05-NTU135 matrix protein gene, partial	JQ309652
HMPV isolate SIN06-NTU187 matrix protein gene, partial	JQ309653
HMPV isolate SIN06-NTU217 matrix protein gene, partial	JQ309654
HMPV isolate SIN06-NTU224 matrix protein gene, partial	JQ309655
HMPV isolate SIN06-NTU232 matrix protein gene, partial	JQ309656
HMPV isolate SIN06-NTU271 matrix protein gene, partial	JQ309657
HMPV isolate SIN06-NTU272 matrix protein gene, partial	JQ309658
HMPV isolate SIN06-NTU273 matrix protein gene, partial	JQ309659
HMPV isolate SIN06-NTU277 matrix protein gene, partial	JQ309660

HMPV isolate SIN06-NTU289 matrix protein gene, partial	JQ309661
HMPV isolate SIN06-NTU384 matrix protein gene, partial	JQ309662
HMPV isolate SIN06-NTU398 matrix protein gene, partial	JQ309663
HMPV isolate SIN07-NTU423 matrix protein gene, partial	JQ309664
HMPV isolate SIN07-NTU442 matrix protein gene, partial	JQ309665
HMPV isolate SIN05-NTU70 nucleoprotein gene, complete	JQ309641
HMPV isolate SIN05-NTU84 nucleoprotein gene, partial	JQ309642
HMPV isolate SIN05-NTU14 phosphoprotein gene, partial	EF409364
HMPV isolate SIN05-NTU29 phosphoprotein gene, partial	EF409353
HMPV isolate SIN05-NTU50 phosphoprotein gene, partial	EF409358
HMPV isolate SIN05-NTU51 phosphoprotein gene, partial	EF409355
HMPV isolate SIN05-NTU52 phosphoprotein gene, partial	EF409354
HMPV isolate SIN05-NTU70 phosphoprotein gene, partial	EF409351
HMPV isolate SIN05-NTU84 phosphoprotein gene, partial	EF409357
HMPV isolate SIN05-NTU101 phosphoprotein gene, partial	EF409359
HMPV isolate SIN05-NTU102 phosphoprotein gene, partial	EF409352
HMPV isolate SIN05-NTU135 phosphoprotein gene, partial	EF409371
HMPV isolate SIN06-NTU187 phosphoprotein gene, partial	EF409360
HMPV isolate SIN06-NTU217 phosphoprotein gene, partial	EF409365
HMPV isolate SIN06-NTU224 phosphoprotein gene, partial	EF409366
HMPV isolate SIN06-NTU232 phosphoprotein gene, partial	EF409362
HMPV isolate SIN06-NTU271 phosphoprotein gene, partial	EF409361
HMPV isolate SIN06-NTU272 phosphoprotein gene, partial	EF409368
HMPV isolate SIN06-NTU273 phosphoprotein gene, partial	EF409369
HMPV isolate SIN06-NTU277 phosphoprotein gene, partial	EF409370
HMPV isolate SIN06-NTU289 phosphoprotein gene, partial	EF409356
HMPV isolate SIN06-NTU384 phosphoprotein gene, partial	EF409363
HMPV isolate SIN06-NTU398 phosphoprotein gene, partial	EF409367
HMPV isolate SIN07-NTU401 phosphoprotein gene, partial	JQ309666
HMPV isolate SIN07-NTU423 phosphoprotein gene, partial	JQ309667
HMPV isolate SIN07-NTU442 phosphoprotein gene, partial	JQ309668
HMPV isolate SIN07-NTU461 phosphoprotein gene, partial	JQ309669
HMPV isolate SIN07-NTU480 phosphoprotein gene, partial	JQ309670
HMPV isolate SIN07-NTU481 phosphoprotein gene, partial	JQ309671
HMPV isolate SIN07-NTU495 phosphoprotein gene, partial	JQ309672

HBoV sequences submitted to GenBank

Description	Accession number
HBoV isolate SIN05-NTU12 NS1 gene, partial	EU014167
HBoV isolate SIN05-NTU22 NS1 gene, partial	EU014168
HBoV isolate SIN05-NTU46 NS1 gene, partial	EU014169
HBoV isolate SIN05-NTU79 NS1 gene, partial	EU014170
HBoV isolate SIN05-NTU86 NS1 gene, partial	EU014171
HBoV isolate SIN05-NTU104 NS1 gene, partial	EU014172
HBoV isolate SIN05-NTU150 NS1 gene, partial	EU014173
HBoV isolate SIN06-NTU159 NS1 gene, partial	EU014174
HBoV isolate SIN06-NTU165 NS1 gene, partial	EU014175
HBoV isolate SIN06-NTU167 NS1 gene, partial	EU014176

HBoV isolate SIN06-NTU193 NS1 gene, partial	EU014177
HBoV isolate SIN06-NTU194 NS1 gene, partial	EU014178
HBoV isolate SIN06-NTU195 NS1 gene, partial	EU014179
HBoV isolate SIN06-NTU218 NS1 gene, partial	EU014180
HBoV isolate SIN06-NTU234 NS1 gene, partial	EU014181
HBoV isolate SIN06-NTU243 NS1 gene, partial	EU014182
HBoV isolate SIN06-NTU246 NS1 gene, partial	EU014183
HBoV isolate SIN06-NTU250 NS1 gene, partial	EU014184
HBoV isolate SIN06-NTU258 NS1 gene, partial	EU014185
HBoV isolate SIN06-NTU263 NS1 gene, partial	EU014186
HBoV isolate SIN06-NTU268 NS1 gene, partial	EU014187
HBoV isolate SIN06-NTU275 NS1 gene, partial	EU014188
HBoV isolate SIN06-NTU290 NS1 gene, partial	EU014189
HBoV isolate SIN06-NTU325 NS1 gene, partial	EU014190
HBoV isolate SIN06-NTU328 NS1 gene, partial	EU014191
HBoV isolate SIN06-NTU353 NS1 gene, partial	EU014192
HBoV isolate SIN06-NTU371 NS1 gene, partial	EU014193
HBoV isolate SIN06-NTU374 NS1 gene, partial	EU014194
HBoV isolate SIN06-NTU375 NS1 gene, partial	EU014195
HBoV isolate SIN06-NTU399 NS1 gene, partial	EU014196
HBoV isolate SIN07-NTU421 NS1 gene, partial	EU014197
HBoV isolate SIN07-NTU427 NS1 gene, partial	EU014198
HBoV isolate SIN07-NTU430 NS1 gene, partial	EU014199
HBoV isolate SIN07-NTU432 NS1 gene, partial	EU014200
HBoV isolate SIN07-NTU441 NS1 gene, partial	EU014201
HBoV isolate SIN07-NTU470 NS1 gene, partial	EU014202
HBoV isolate SIN07-NTU494 NS1 gene, partial	EU014203
HBoV isolate SIN07-NTU496 NS1 gene, partial	EU014204
HBoV isolate SIN07-NTU497 NS1 gene, partial	EU014205
HBoV isolate SIN07-NTU500 NS1 gene, partial	EU014206

HCoV sequences submitted to GenBank

Description	Accession number
HCoV isolate SIN06-NTU211 replicase polyprotein gene, partial	EU370700
HCoV isolate SIN06-NTU295 replicase polyprotein gene, partial	EU370702
HCoV isolate SIN06-NTU395 replicase polyprotein gene, partial	EU370701

HRV sequences submitted to GenBank

Description	Accession number
HRV isolate SIN05-NTU35 5' untranslated region	FJ645773
HRV isolate SIN05-NTU58 5' untranslated region	FJ645805
HRV isolate SIN05-NTU62 5' untranslated region	FJ645806
HRV isolate SIN05-NTU74 5' untranslated region	FJ645790

HRV isolate SIN05-NTU91 5' untranslated region	FJ645779
HRV isolate SIN05-NTU107 5' untranslated region	FJ645783
HRV isolate SIN05-NTU129 5' untranslated region	FJ645771
HRV isolate SIN05-NTU144 5' untranslated region	FJ645782
HRV isolate SIN05-NTU173 5' untranslated region	FJ645774
HRV isolate SIN05-NTU177 5' untranslated region	FJ645809
HRV isolate SIN05-NTU179 5' untranslated region	FJ645808
HRV isolate SIN05-NTU188 5' untranslated region	FJ645812
HRV isolate SIN05-NTU196 5' untranslated region	FJ645826
HRV isolate SIN05-NTU201 5' untranslated region	FJ645803
HRV isolate SIN05-NTU205 5' untranslated region	FJ645804
HRV isolate SIN05-NTU213 5' untranslated region	FJ645798
HRV isolate SIN05-NTU218 5' untranslated region	FJ645828
HRV isolate SIN05-NTU220 5' untranslated region	FJ645781
HRV isolate SIN05-NTU234 5' untranslated region	FJ645796
HRV isolate SIN05-NTU241 5' untranslated region	FJ645820
HRV isolate SIN05-NTU245 5' untranslated region	FJ645801
HRV isolate SIN05-NTU252 5' untranslated region	FJ645807
HRV isolate SIN05-NTU257 5' untranslated region	FJ645789
HRV isolate SIN05-NTU260 5' untranslated region	FJ645819
HRV isolate SIN05-NTU263 5' untranslated region	FJ645813
HRV isolate SIN05-NTU278 5' untranslated region	FJ645785
HRV isolate SIN05-NTU281 5' untranslated region	FJ645823
HRV isolate SIN05-NTU301 5' untranslated region	FJ645802
HRV isolate SIN05-NTU302 5' untranslated region	FJ645778
HRV isolate SIN05-NTU304 5' untranslated region	FJ645788
HRV isolate SIN05-NTU308 5' untranslated region	FJ645786
HRV isolate SIN05-NTU324 5' untranslated region	FJ645818
HRV isolate SIN05-NTU334 5' untranslated region	FJ645787
HRV isolate SIN05-NTU336 5' untranslated region	FJ645784
HRV isolate SIN05-NTU341 5' untranslated region	FJ645824
HRV isolate SIN05-NTU348 5' untranslated region	FJ645815
HRV isolate SIN06-NTU352 5' untranslated region	FJ645817
HRV isolate SIN05-NTU354 5' untranslated region	FJ645780
HRV isolate SIN05-NTU380 5' untranslated region	FJ645792
HRV isolate SIN05-NTU381 5' untranslated region	FJ645791
HRV isolate SIN05-NTU391 5' untranslated region	FJ645814
HRV isolate SIN05-NTU397 5' untranslated region	FJ645799
HRV isolate SIN05-NTU404 5' untranslated region	FJ645772
HRV isolate SIN05-NTU405 5' untranslated region	FJ645800
HRV isolate SIN05-NTU412 5' untranslated region	FJ645776
HRV isolate SIN05-NTU416 5' untranslated region	FJ645816
HRV isolate SIN05-NTU421 5' untranslated region	FJ645777
HRV isolate SIN05-NTU425 5' untranslated region	FJ645825
HRV isolate SIN05-NTU436 5' untranslated region	FJ645811
HRV isolate SIN05-NTU441 5' untranslated region	FJ645797
HRV isolate SIN05-NTU454 5' untranslated region	FJ645795
HRV isolate SIN05-NTU458 5' untranslated region	FJ645793
HRV isolate SIN05-NTU463 5' untranslated region	FJ645821
HRV isolate SIN05-NTU470 5' untranslated region	FJ645794
HRV isolate SIN05-NTU471 5' untranslated region	FJ645827
HRV isolate SIN05-NTU478 5' untranslated region	FJ645810
HRV isolate SIN05-NTU486 5' untranslated region	FJ645775
HRV isolate SIN05-NTU497 5' untranslated region	FJ645822

Appendix C

Published work related to this PhD project

Loo, L.H., Fu, Y., Ayi, T.C., Tan, B.H., Sugrue, R.J. 2012. The expression of recombinant attachment protein of human metapneumovirus in mammalian cells is sufficient to produce virus-like particles. *Manuscript in preparation*.

Loo, L.H., Tan, B.H., Ng, L.M., Tee, N.W., Lin, R.T., Sugrue, R.J., 2007. Human metapneumovirus in children, Singapore. Emerg Infect Dis 13, 1396-1398.

Sugrue, R.J., Tan, B.H., **Loo, L.H.**, 2008. The emergence of human metapneumovirus. Future Virology 3, 363-371.

Tan, B.H., **Loo, L.H.**, Lim, E.A., Kheng Seah, S.L., Lin, R.T., Tee, N.W., Sugrue, R.J., 2009a. Human rhinovirus group C in hospitalized children, Singapore. Emerg Infect Dis 15, 1318-1320.

Tan, B.H., Lim, E.A., Seah, S.G., **Loo, L.H.**, Tee, N.W., Lin, R.T., Sugrue, R.J., 2009b. The incidence of human bocavirus infection among children admitted to hospital in Singapore. J Med Virol 81, 82-89.

Human Metapneumovirus in Children, Singapore

Liat Hui Loo,*† Boon Huan Tan,‡ Ley Moy Ng,* Nancy W.S. Tee,† Raymond T.P. Lin,§ and Richard J. Sugrue*

Four hundred specimens were collected from pediatric patients hospitalized in Singapore; 21 of these specimens tested positive for human metapneumovirus (HMPV), with the A2 genotype predominating. A 5% infection rate was estimated, suggesting that HMPV is a significant cause of morbidity among the pediatric population of Singapore.

Human metapneumovirus (HMPV) is a new member of the family *Paramyxoviridae*. It was first identified in children with respiratory diseases in the Netherlands and is now recognized as a substantial cause of acute respiratory infection in pediatric patients (*1*). The clinical symptoms in children are similar to those observed during respiratory syncytial virus (RSV) infections and vary from upper respiratory tract infection (URTI) to bronchiolitis and pneumonia. HMPV infections have been detected in young children 5 years of age (*2*) as well as in adults of all age groups (*3*). Sequence analysis of HMPV isolates has identified 2 main lineages, A and B; each group is further subdivided into 2 more lineages, A1 and A2, and B1 and B2 (*4,5*). Both virus genotypes were reported in various countries in the Americas, Europe, and Asia. This study aims to assess the importance of HMPV infection among hospitalized pediatric patients in Singapore.

The Study

Kandang Kerbau Women's and Children's hospital is one of the major centers in Singapore for the admission of sick children, including those showing respiratory illness. After obtaining prior approval from the Hospital's ethics committee (approval number EC/043/2004), we collected nasopharyngeal swabs from 400 pediatric patients between October 2005 and January 2007. When admitted to the hospital, these patients exhibited symptoms of acute lower respiratory tract infections (LRTI) (bronchiolitis, bronchitis, pneumonia, asthma, and wheezing) and URTI (pharnygitis). Specimens were sent to the hospital's microbiologic laboratory for routine testing for influenza A and B viruses, RSV, adenovirus, and parainfluenza virus (serotypes 1–3) by immunofluorescence assay (LIGHTDIAGNOSTICS, Chemicon, Tamacula, CA, USA). The clinical specimens were stored at –80°C until further analysis for HMPV was performed (not longer than a week after collection). Viral RNA (vRNA) was extracted from each of the thawed nasopharyngeal swabs with the QIAamp viral RNA minikit (QIAGEN Inc., Valencia, CA, USA) according to the manufacturer's instructions. Of the total RNA extracted from the clinical specimens, 5 μL was subjected to real-time reverse transcription–PCR (RT-PCR) testing by using the N gene specific primer set NL–N (*6*). This was performed with the OneStep RT–PCR kit (QIAGEN) on a Corbett Research Rotorgene 3000 (Corbett Life Science, Sydney, NSW, Australia). The PCR cycling conditions were 50°C for 30 min, 95°C for 15 min, and 45 cycles (95°C for 20 s and 60°C for 60 s). Specimens that tested positive by real-time RT-PCR analysis were confirmed by conventional RT–PCR by using the NL–N primer set. The amplified products (163 bp) were detected by using agarose gel electrophoresis, and their identity was confirmed by DNA sequencing.

Of the 400 samples collected, 21 tested positive for HMPV infection, which suggests an incidence rate of ≈5.3%, compared with an 11.5% incidence rate for RSV (Table 1). Previous reports have suggested that in some cases severe symptoms exhibited by RSV-infected patients are associated with dual infections involving HMPV (*7*). Although we detected the presence of HMPV and RSV in the patients screened, no evidence for co-infections was observed, which suggests a low occurrence for these viruses in Singapore. In a recent study in Australia, only 8 of 10,000 screened hospitalized patients showed evidence of co-infection with HMPV and RSV (*8*). In contrast, several recent studies suggest that co-infections may account for a substantial number of instances in which HMPV has been detected. For example, a recent study in Brazil, which used a lower sample size than in our study, reported an 8% incidence rate for pediatric patients who had RSV and HMPV co-infections (*9*). Therefore, environmental factors may be a key feature in the development of co-infections.

Table 1. Positive test results for respiratory viruses from clinical specimens (n = 400)

Virus	No. positive (%)
Respiratory syncytial virus	46 (11.5)
Influenza A virus	3 (0.8)
Influenza B virus	1 (0.3)
Parainfluenza 1 virus	4 (1.0)
Parainfluenza 2 virus	0 (0)
Parainfluenza 3 virus	8 (2.0)
Adenovirus	1 (0.3)
Human metapneumovirus	21 (5.3)
Total	84 (21.0)

*Nanyang Technological University, Singapore; †Kandang Kerbau Women's and Children's Hospital, Singapore; ‡DSO National Laboratories, Singapore; and §National University Hospital, Singapore

The entire P gene sequences were amplified directly from the specimens by RT–PCR using the primers hmptPF 5′-ATGTCGTTCCCTGAAGGAAAAGATATTC-3′ and hmptPR 5′-TTAAACTACATAATTAAGTGGTAAAT-3′. Amplicons 884 bp in size were generated and corresponded to 1209 nt–2093 nt of the HMPV genome (strain JPS03-240, AY530095). PCR cycling was performed on a conventional thermal cycler by using a "touch-down" procedure; conditions were 94°C for 5 min followed by 30 cycles of 94°C for 15 s, 62°C (reducing by 0.5°C/cycle) for 30 s, 72°C for 1 min, and a final extension step of 72°C for 7 min. The sizes of the respective PCR-amplified products were examined by using agarose gel electrophoresis, gel-purified, and confirmed by DNA sequencing. The sequences were submitted to GenBank under accession nos. EF409351–EF409371. The genetic relationship between the Singapore HMPV isolates and those HMPV isolates described previously was analyzed by comparing the P gene sequences (*10*). Alignments of nucleic acid sequences were created by using ClustalX version 1.83 (bips.u-strasbg.fr/fr/documentation/clustalx). Phylogenetic trees were constructed by using the neighbor-joining method (1,000 bootstrap replicates) and edited with MEGA 3.1 (*11*). Comparisons were made with representatives of the 4 genetic lineages (Figure). This analysis shows that although isolates representing both A and B genotypes were detected, the Singapore isolates clustered more predominantly with representative HMPV strains in lineage A, in particular the sublineage A2. In this study HMPV was detected throughout the year, which suggests that in Singapore, HPMV is present in the pediatric community throughout the year. We also noted a slight increase in the incidence of B genotypes (B1 and B2) during the last quarter of 2006, but the implications of this finding are unclear.

The age and clinical characteristics of the HMPV patients were next compared with the different HMPV lineages (Table 2). Children with HMPV infection were 1 month to 12 years in age; 67% were ≤1 year of age compared with 63% of RSV-infected children. Of the HMPV-infected patients, 52% exhibited LRTI; of these, 82% were infected with the HMPV sublineage A2. In contrast, ≈43% of the patients exhibited URTI caused by the sublineages A2 and B2. In comparison, 61% and 20% of the RSV patients had a clinical diagnosis of LRTI or URTI, respectively. Our data suggested an increased association of sublineage A2 with LRTI in the HMPV-infected patients. The implications of this are unclear, but several reports note a correlation between severity of infection and the presence of the A genotype (*12,13*). Unfortunately, we were not able to make a strict comparison of our data with data from recent studies in Southeast Asia (*14,15*); these studies used significantly smaller sample sizes and a different selection criterion for

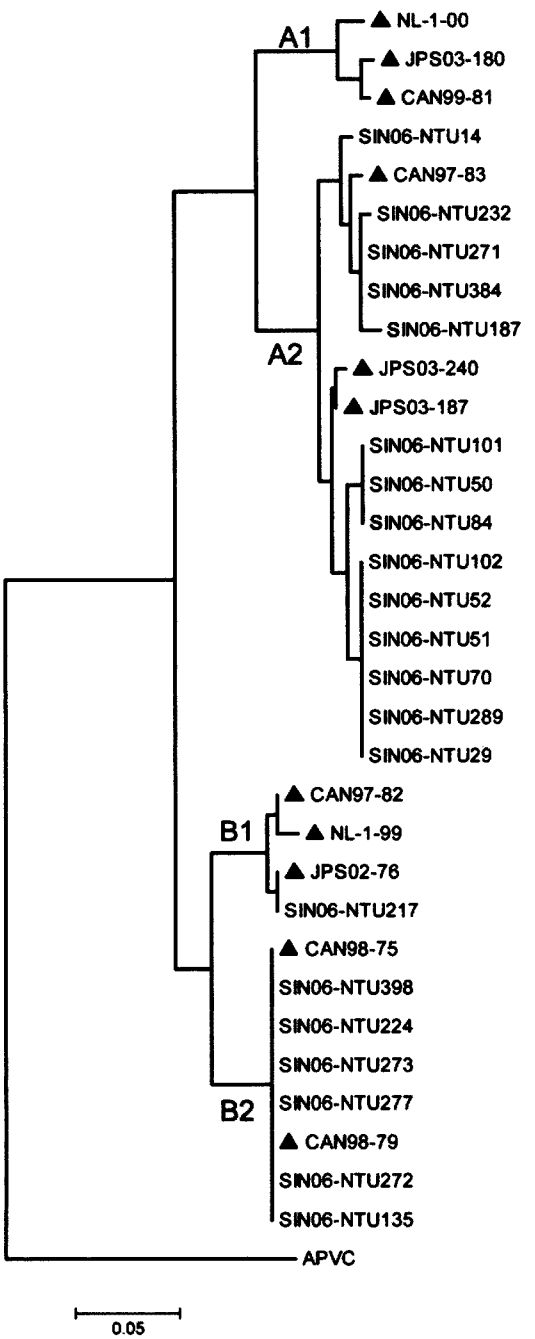

Figure. Phylogenetic analyses of nucleotide sequences of HMPV phosphoprotein showing comparisons with Singapore-Nanyang Technological University (SIN06-NTU*) sequences. The specimen number acquired during the course of the investigation (e.g., SIN06-NTU14) was made with known strains (highlighted ▲) from Canada [CAN99-81 (AY145294, AY145249), CAN97-83 (AY297749), CAN97-82 (AY145295, AY145250), CAN98-75 (AY297748), CAN98-79 (AY145293, AY145248)], Japan [JPS03-180 (AY530092), JPS03-240 (AY530095), JPS03-187 (AY530093), JPS02-76 (AY530089)], and the Netherlands [NL-1-00 (AF371337), NL-17-00 (AY304360), NL-1-99 (AY525843), NL-1-94 (AY304362)]. Avian pneumovirus type C (APVC AY590688) was used as the outgroup.

Table 2. Characteristics of pediatric patients with human metapneumovirus (HMPV) infection

Patient no.	Age	Clinical diagnosis*	Lineage of HMPV
14	2 y	L	A2
29	1 y	O	A2
50	6 mo	U	A2
51	1 y	L	A2
52	1 y	U	A2
70	11 mo	U	A2
84	6 mo	U	A2
101	1 y	L	A2
102	2 y	L	A2
135	1 y	U	B2
187	3 mo	L	A2
217	1 mo	L	B1
224	1 y	U	B2
232	1 y	L	A2
271	12 y	L	A2
272	4 y	U	B2
273	1 y	U	B2
277	5 y	U	B2
289	1 y	L	A2
384	2 y	L	A2
398	7 y	L	B2

*L, lower respiratory infections including bronchiolitis, bronchitis, pneumonia, asthma, wheezing or chest infection; U, upper respiratory infections including infantile pyrexia and pharyngitis; O, febrile fit.

the patients screened (i.e., LRTI [*14*] and wheezing and asthma [*15*]).

Conclusions

Our study is the first, to our knowledge, that has attempted to assess the importance of HMPV among the pediatric population in Singapore. We analyzed 400 samples that were collected from pediatric patients who were admitted to a hospital over a 16-month period. An infection rate of 5.3% was observed, which is consistent with the reported infection rates of several other industrialized countries. We also noted that of the viruses detected, ≈67% were of the A subtype and 33% were of the B subtype, which suggests that the former was the predominant HMPV subtype causing illness in these patients. Furthermore, a significant proportion of the HMPV-infected patients had LRTI. Our findings suggest that HMPV is a substantial cause of illness among the pediatric population of Singapore.

This work was funded by the National Medical Research Council of Singapore (NMRC/0956/2005). L.H.L. is supported by Kandang Kerbau Women's and Children's Hospital (KKH) and a Medical Research Scientist Award from the NMRC-Lee Foundation.

Mr Loo is a graduate student in the School of Biological Sciences at Nanyang Technological University.

References

1. Van den Hoogen BG, de Jong JC, Groen J, Kuiken T, de Groot R, Fouchier RA, et al. A newly discovered human pneumovirus isolated from young children with respiratory tract disease. Nat Med. 2001;7:719–24.
2. Principi N, Bosis S, Esposito S. Human metapneumovirus in paediatric patients. Clin Microbiol Infect. 2006;12:301–8.
3. Falsey AR, Erdman D, Anderson J, Walsh EE. Human metapneumovirus infections in young and elderly adults. J Infect Dis. 2003;187:785–90.
4. Van den Hoogen BG, Herfst S, Sprong L, Cane PA, Forleo-Neto E, de Swart RL, et al. Antigenic and genetic variability of human metapneumoviruses. Emerg Infect Dis. 2004;10:658–66.
5. Biacchesi S, Skiadopoulos MH, Boivin G, Hanson CT, Murphy BR, Collins PL, et al. Genetic diversity between metapneumovirus subgroups. Virology. 2003;315:1–9.
6. Maertzdorf J, Wang CK, Brown JB, Quinto JD, Chu M, de Graaf M, et al. Real-time reverse transcriptase PCR assay for detection of human metapneumoviruses from all known genetic lineages. J Clin Microbiol. 2004;42:981–6.
7. Greensill J, McNamara PS, Dove W, Flanagan B, Smyth RL, Hart CA. Human metapneumovirus in severe respiratory syncytial virus bronchiolitis. Emerg Infect Dis. 2003;9:372–5.
8. Sloots TP, Mackay IM, Bialasiewicz S, Jacob KC, McQueen E, Harnett GB et al. Human metapneumovirus, Australia, 2001–2004. Emerg Infect Dis. 2006;12:1263–6.
9. Cuevas LE, Nasser AM, Dove W, Gurgel RQ, Greensill J, Hart CA. Human metapneumovirus and respiratory syncytial virus, Brazil. Emerg Infect Dis. 2003;9:1626–8.
10. Mackay IM, Bialasiewicz S, Waliuzzaman Z, Chidlow GR, Fegredo DC, Laingam S, et al. Use of the P gene to genotype human metapneumovirus identifies 4 viral subtypes. J Infect Dis. 2004;190:1913–8.
11. Kumar S, Tamura K, Nei M. MEGA3: Integrated software for Molecular Evolutionary Genetics Analysis and sequence alignment. Brief Bioinform. 2004;5:150–63.
12. Esper F, Martinello RA, Boucher D, Weibel C, Ferguson D, Landry ML, et al. A 1-year experience with human metapneumovirus in children aged <5 years. J Infect Dis. 2004;189:1388–96.
13. Schildgen O, Glatzel T, Geikowski T, Scheibner B, Matz B, Bindl L, et al. Human metapneumovirus RNA in encephalitis patient. Emerg Infect Dis. 2005;11:467–70.
14. Samransamruajkit R, Thanasugarn W, Prapphal N, Theamboonlers A, Poovorawan Y. Human metapneumovirus in infants and young children in Thailand with lower respiratory tract infections; molecular characteristics and clinical presentations. J Infect. 2006;52:254–63.
15. Ong BH, Gao Q, Phoon MC, Chow VT, Tan WC, Van Bever HP. Identification of human metapneumovirus and *Chlamydophila pneumoniae* in children with asthma and wheeze in Singapore. Singapore Med J. 2007;48:291–3.

Address for correspondence: Richard J. Sugrue, Nanyang Technological University, School of Biological Sciences, 60 Nanyang Dr, Singapore 637551; email: rjsugrue@ntu.edu.sg

The emergence of human metapneumovirus

Richard J Sugrue†, Boon-Huan Tan & Liat-Hui Loo

†Author for correspondence
Division of Molecular & Cell Biology, School of Biological Sciences, Nanyang Technological University, 60 Nanyang Drive, 637551, Singapore
Tel.: +65 6316 2889;
Fax: +65 6791 3856;
rjsugrue@ntu.edu.sg

Until relatively recently there had been episodes when children had been admitted into hospitals with symptoms that were similar to those expected for human respiratory syncytial virus (HRSV), but the available diagnostic procedures failed to detect the presence of HRSV, and the causative disease agent remained unidentified. Dutch scientists examined nasopharyngeal aspirates from similar patients in Holland using advanced molecular biology and imaging techniques. The conclusions of this study were published in 2001, revealing that a previously unidentified paramyxovirus was responsible for these infections. This agent was grouped within the subfamily *Pneumovirinae*, genus *metapneumovirus*, and given the name human metapneumovirus (HMPV) to distinguish it from other members of the genus *Metapneumovirus* that are of avian origin. Although HMPV is associated with upper respiratory tract infection, it is now recognized as a major cause of lower respiratory infection (LRTI) in children in a variety of different geographical regions. Furthermore, retrospective studies have detected the presence of HMPV in archived clinical material dating from the 1950s, suggesting that this was not a new virus, but it had remained undetected for several decades until its 'emergence' in 2001. This review will discuss the increasing global importance of HMPV as a cause of LRTI among young children.

The classification of human metapneumovirus

Human metapneumovirus (HMPV) has been visualized by electron microscopy, revealing a pleiomorphic morphology that is similar in appearance to that observed in other paramyxoviruses [1]. Although HMPV is difficult to cultivate in tissue culture, some tissue culture-adapted isolates have been obtained (e.g., the Canadian isolate CAN97-83) [2], and have been used to examine the properties of some of the virus proteins. However, partly because of the difficulty in studying HMPV infection using standard laboratory experimental systems, much of the current understanding of the structure of the HMPV has been inferred from other closely related viruses, for example, respiratory syncytial virus (RSV) and avian pneumovirus (APV).

HMPV is thought to express nine proteins and, by analogy with other paramyxoviruses, they can be classified as either integral membrane proteins, which are embedded in the virus envelope, or internal proteins, which associate with the virus polymerase beneath the virus envelope [3]. The viral genome interacts with the nucleo (N) protein, phospho (P) protein and RNA-dependant RNA polymerase (L protein) to form the virus ribonucleoparticle (RNP), a characteristic structure found in all paramyxoviruses [4]. The M2-1 protein is a transcription factor that interacts with the RNP, and the M2-2 protein plays a role in virus genome replication [5]. By analogy with human RSV (HRSV), the matrix (M) protein surrounds the RNP beneath the virus envelope, and it is a major determinant of virus morphology. The virus also expresses three integral membrane proteins: the fusion (F) protein, attachment (G) protein and small hydrophobic (SH) protein. The F protein mediates the fusion of the host cell membrane and virus envelope during the initial stages of virus entry. It is initially expressed as a single polypeptide chain, which subsequently undergoes cleavage by a trypsin-like protease to create the mature form of the protein [6]. The G protein is expressed as a polypeptide chain, which subsequently undergoes extensive *N*- and *O*-linked glycosylation [7], and by analogy with HRSV, it is thought to play a role in virus attachment. As in the case of HRSV, the role that the SH protein plays during the HMPV replication cycle is currently unclear.

The first complete genome sequence of HMPV was published in 2002 [3], and revealed a single-stranded 13.3 kb RNA genome of negative polarity (**Figure 1**). A detailed examination of the HMPV genome [2,8] confirmed it was a paramyxovirus belonging to the subfamily *Pneumovirinae*, which contains the human and animal RSV [9]. Eight genes were identified in the HMPV genome, and comparison of the HMPV and the HRSV genomes revealed significant differences [3]. The

Keywords: emerging viruses, human metapneumovirus, human respiratory syncytial virus, molecular diagnostics, paramyxovirus, virus epidemiology

future medicine part of fsg

Figure 1. Organization of the human metapneumovirus genome.

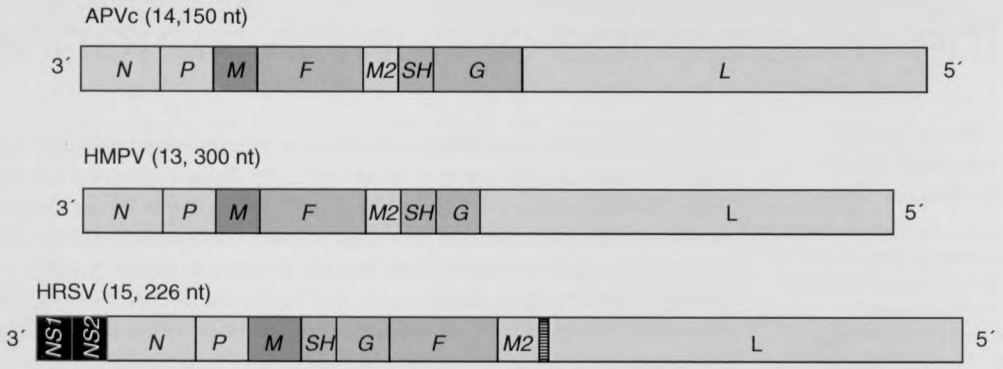

The genome organization of HMPV compared with that of APVc and HRSV. Genes encoding nonstructural proteins (black), polymerase-associated proteins (light gray), glycoproteins (gray) and matrix protein (dark gray) are shown. The overlap between the HRSV *M2* and *L* genes is also shown (hatch). The relative gene sizes are approximately drawn to scale with the keys representing viral genes.
APVc: Avian pneumovirus C; F: Fusion protein; G: Attachment protein; HMPV: Human metapneumovirus; HRSV: Human respiratory syncytial virus; L: Large polymerase subunit; M: Matrix protein; N: Nucleoprotein; NS: Nonstructural; P: Phophoprotein; SH: Small hydrophobic protein.

HMPV genome is significantly smaller and, although the gene order of the *N*, *P* and *M* genes was similar in both HMPV and HRSV, the gene order between the *M* and *L* genes differed. In HMPV the *F* and *M2* genes are located before the *SH* and *G* genes compared with the corresponding genes in HRSV. Furthermore, the HMPV genome lacked the *NS1* and *NS2* genes, whose presence are characteristic of members of the genus *Pneumovirus*. A comparison of the HMPV genome with other viruses revealed that it was most closely related to the APV [3], which formed the basis of its classification as a new addition to the genus *Metapneumovirus* (**Figure 2**). Further detailed genetic analysis revealed a relatively high degree of sequence variability between different HMPV virus isolates. Two major subgroups, A and B, were initially identified, and subsequent genetic analysis led to a further subdivision of the HMPV A and B subgroups into the subtypes 1A, 2A, 1B and 2B [2,10]. Although several APV isolates share similar genetic characteristics to HMPV, HRSV is currently the closest genetically related virus that is known to cause significant disease in humans.

HMPV detection & epidemiology

Although HMPV was first identified in 2001 in children in the Netherlands [1], examination of sera taken from patients in the late 1950s showed the presence of HMPV-specific antibodies. This retrospective study suggested that HMPV was not a new virus, but had been circulating in the human population for at least 50 years prior to its isolation in the Netherlands. Furthermore, owing to its genetic relatedness to APV, it was speculated that HMPV may have originally been a zoonotic infection that had crossed over from birds to humans [1]. Although its source of entry into the human population is still unclear, this speculation is supported by serologic analysis that has demonstrated some cross-reactivity between APV and HMPV antigens [11,12].

HRSV isolated from infected patients has been successfully cultivated using the human laryngeal carcinoma cell line HEp-2. This causes a clearly visible cytopathic effect (i.e., syncytial formation) in this cell line. By contrast, HMPV isolates replicate relatively poorly in HEp-2 cells and remains largely undetectable. This underlines a major problem in the detection of HMPV; relatively few cell lines efficiently support HMPV replication. This was a major factor in the inability to detect the presence of HMPV in clinical samples. Primary isolation of HMPV in tissue culture was first achieved using tMK cells [1], HEp-2 cells [13] and Vero cells [2], but more recently the LLC-MK2 cell line has been successfully used. Cultivation in LLC-MK2 cells can require up to 14 days incubation before cytopathic effects are visible [14]. The addition of

trypsin to the culture medium is also required to allow processing of the HMPV F protein into its mature form, a prerequisite for virus infectivity. More recently, cultivation of HMPV in the human bronchiolar cell line 16HBE140 has been described, which gave superior results when compared with LLC-MK2 cells, and additionally did not require the presence of trypsin [15].

As early as 2003, diagnostic protocols were developed for the detection of HMPV from clinical specimens, a development that has facilitated the more recent epidemiological studies. These protocols range from conventional gel-based reverse-transcription PCR (RT-PCR) tests targeting the *N* [16], *M* and *L* genes [17,18] to more sophisticated real-time RT-PCR methods using SYBR® green targeting the *N* and *L* genes [19], and sequence-specific probes targeting the *N* [20,21], *L* [14,22] and *F* gene [23] (**Figure 3, Table 1**). In many diagnostic laboratories the detection of HRSV, together with a variety of other respiratory viruses, is routinely performed using immunofluorescence-based assays. Monoclonal antibodies prepared from infected HMPV viral lysates have been used to detect the virus in clinical samples [24–26]. The seroprevalence of HMPV has also been successfully determined in human sera from patients using HMPV antigens produced from infected cell lysates [1,27–32]. HMPV antibodies have also been produced using *Escherichia coli*-expressed N and M proteins [33,34], baculovirus-expressed N and F proteins [35,36] and vesicular stomatis virus expressing the F protein [37]. These immunologic reagents are currently undergoing evaluation in several diagnostic laboratories. There are two rapid antigen detection assays that are commercially available from Oxoid Ltd (Basingstoke, Hampshire, UK) and Diagnostic Hybrids Inc. (Athens, OH, USA). These reagents were recently evaluated with 515 nasopharygenal specimens using direct fluorescence assays and yielded promising results [38].

The development and widespread use of PCR-based diagnostic reagents for the detection of HMPV has allowed several recent epidemiological studies to examine the importance of HMPV infection in different geographical regions. These studies have demonstrated the presence of HMPV in humans from every geographical region in which these studies have been performed. The virus has been detected in children with respiratory diseases in Europe [1,39–45], the Americas [30,46–49], Australia, [50], New Zealand [51] and Asia [28,52–57]. Recently, HMPV has also been reported in countries in the Middle East [32,58–60] and Africa [61].

These studies have also shown a clear correlation between the presence of the virus in patients and respiratory infection, with significant numbers of cases of lower respiratory infection (LRTI) being recorded in these patients. Although HMPV has been reported to infect patients in different age groups, several epidemiological studies have shown that the highest incidence of HMPV infection is within the first 6 months of life [62,63]. By the age of 5–10 years old, almost all children have been infected by HMPV [28,32,37]. HMPV has also been reported to cause severe infections in the elderly [31]. Some studies have attempted to

Figure 2. The classification of human metapneumovirus and other paramyxovirus members within the *Paramyxoviridae* family.

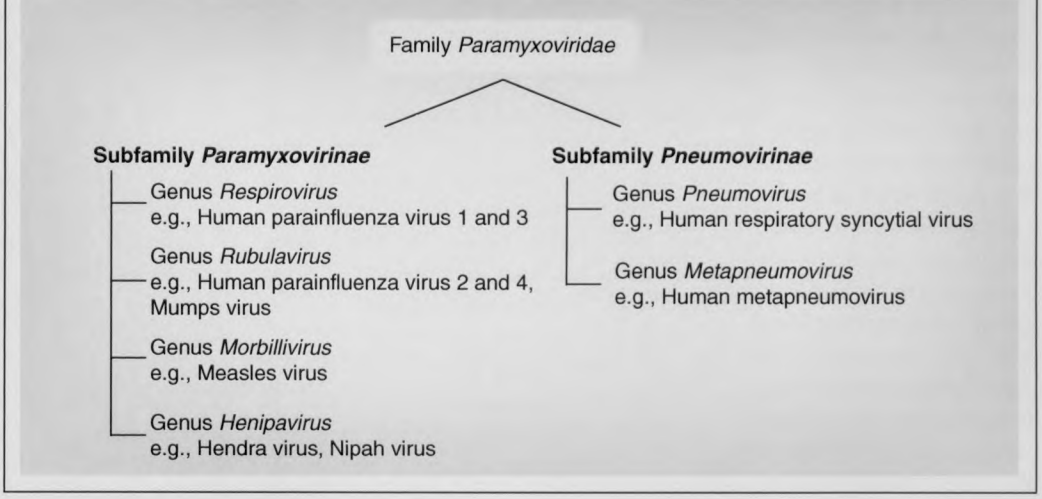

Table 1. List of primer sets used in both conventional and real-time reverse transcription-PCR assays.

	Sequences (5′ to 3′)		Ref.
	Forward primer (probe)	***Reverse primer***	
Conventional RT-PCR			
N gene*	ATGTCTCTTCAAGGGATTCACCT	TCTGCAGCATATTTGTAATCAG	[16]
M gene‡	GAGTCCTACCTAGTAGACAC	TTGTYCCTTGRTGRCTCCA	[17]
L gene	CATGCCCACTATAAAAGGTCAG (CTGTTAATATCCCACACCA)	CACCCCAGTCTTTCTTGAAA	[18]
F gene	Outer primer: AGCTGTTCCATTGGCAGC Inner primer: GAGTAGGGATCATCAAGCA	Outer primer: ATGCTGTTCRCCYTCAACTTT Inner primer: GCTTAGCTGRTATACAGTGTT	[13]
Real-time RT-PCR			
N gene	ATGGGACAAGTGAAAATGTC	GAGTCTCAGTACACAATAA	[19]
L gene	GTTGCCATAGAGAATCCTGTTA	CATTCAGACTGTTGCTTACCCA	[19]
N gene	AACCGTGTACTAAGTGATGCACTC (CTTTGCCATACTCAATGAACAAAC)	CATTGTTTGACCGGCCCCATAA	[20]
N gene	CATATAAGCATGCTATATTAAAAGAGTCTC (TGYAATGATGAGGGTGTCACTGCGGTTG)	CCTATTTCTGCAGCATATTTGTAATCAG	[21]
L gene	GTTGCCATAGAGAATCCTGTTA (CGAGCATGTTAGACTCAAAAATGCA)	CCAATTACTAAACCAATTGCTTACCCA	[14]
L gene	CATGCCCACTATAAAAGGTCAG (GCTGCGGCATGYCAYTGGTGTGGGATATTCGCAGC)	CACCCCAGTCTTTCTTGAAA	[22]
F gene	Subtype A : GCCGTTAGCTTCAGTCAATTCAA (CAACATTTAGAAACCTTCT) Subtype B: GCT GTCAGCTTCAGTCAATTCAA (CGCACAACATTTAGGAATCTTCT)	TCCAGCATTGTCTGAAAATTGC GTTATCCCTGCATTGTCTGAAAACT	[23]

Note: Sequences in parenthesis represent probe sequence used in real-time PCR.

**This RT-PCR assay was performed with the primer sets as described but in *, another round of hemi-nested PCR amplification was performed with a different forward primer (CATGCTATATTAAAAGAGTCTCA) but the same reverse primer.*

‡This RT-PCR assay with the primer set was followed by another round of hemi-nested PCR amplification with the same forward primer but a new reverse primer (TCTTGCAKATYYTRCTKATGCT).

RT-PCR: Reverse transcription PCR.

examine the importance of HMPV genotype and disease symptoms, and a recent study has suggested that the HMPV A subtype may elicit more severe symptoms [64]. There are some reports that HMPV infection is associated with encephalitis [65,66], and there is at least one example where HMPV was detected in a patient who died of complications associated with encephalitis [65]. In this case, viral RNA was detected in both the brain and lung tissues, suggesting that under certain circumstances, the virus can leave the confines of the respiratory airway and infect other tissues. In some cases, severe infection has been documented as being associated with immunocompromised patients [67,68], which has also been reported for HRSV.

Although several studies have reported the isolation of HMPV from patients in many parts of the world, there have been very few long-term studies on HMPV infection [69–72]. In a recent epidemiological study in Australia, over 10,000 patients were screened for the presence of HMPV over a 4-year period [71]. An average incidence rate of approximately 7.0% was recorded for HMPV over the 4 years. The study clearly demonstrated a seasonal variation in the incidence of HMPV infections, with the winter and spring months showing the highest levels of virus detection. In this study, all four subtypes were detected during each year of the study, providing evidence that co-circulation of the subtypes can occur. Furthermore, this study suggested a seasonal variation in the predominant circulating HMPV subtypes.

Although these epidemiological studies have focused on HMPV detection, many have also tested for the presence of other respiratory pathogens in these patients. In most cases HMPV was the sole agent detected in patients exhibiting LRTI, but in some cases the presence of other viruses in HMPV-infected patients was observed. The presence of coinfections involving HMPV and other viruses that can cause acute

Figure 3. Real-time reverse transcription-PCR detection of the human metapneumovirus *N* gene in clinical specimens using Taqman probes.

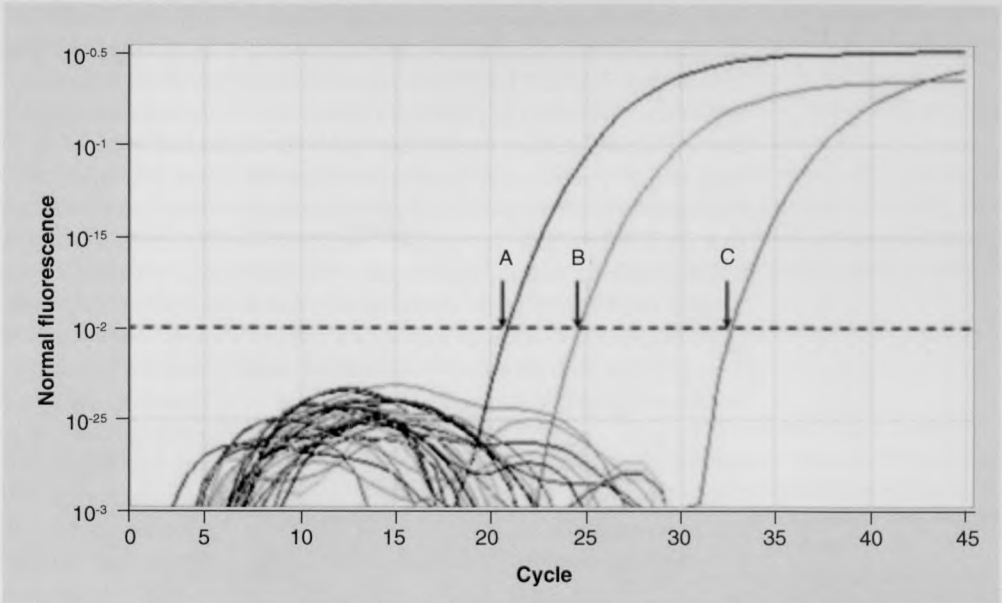

The graph shows the fluorescence, represented by log, versus cycle number for the real-time reverse transcription-PCR assays over the entire reaction run of 45 cycles. Human metapneumovirus-positive specimens show an increase in fluorescence above the threshold value (dotted line). Three clinical specimens A, B and C are shown, which have cycle threshold values of approximately 21, 24 and 32 cycles, respectively (highlighted by black arrows). All the other specimens did not show any fluorescence increase and would be considered negative (see [57]).

respiratory infections serves to further complicate the clinical scenario. This has led to the proposal that these coinfections may have a significant impact on the clinical symptoms. For example, studies in young children infected with HRSV have suggested a correlation between severity of infection and the presence of HMPV [73], indicating a possible role for coinfections in exacerbating the symptoms associated with HRSV infection. In an early study by Greensill and colleagues [74], HMPV was found to be present in 70% of infants exhibiting severe symptoms. Although these reports showed a correlation between the presence of HMPV and severity of symptoms in HRSV-infected patients, other studies have failed to establish this correlation [75]. Furthermore, in the Australian study by Mackay and colleagues [62], coinfection with HMPV and HRSV only accounted for approximately 1.0% of HRSV infections, suggesting that coinfection with HMPV and HRSV may normally be rare in most populations. More recent studies have highlighted coinfection with HMPV and other respiratory pathogens, for example SARS corona virus [13,76] and human bocavirus [77]. Collectively, these reports have been inconclusive in correlating an increased severity of infection with coinfections. The reason for these differences is still uncertain, but suggests that environmental and genetic factors may also play an important role in clinical outcome in patients coinfected with HMPV and other viruses.

Conclusion

Many clinical samples are sent to hospital diagnostic laboratories where pathogens may be successfully identified, and a case successfully diagnosed. However, in a significant number of cases the available diagnostic tests fail to detect a specific pathogen. In many of these cases, the causative agent remains undetected. As diagnostic techniques are improved and developed, it is likely that new previously unidentified viruses will be identified during syndromic surveillance of hospitalized patients. HMPV is an example of a virus that causes significant infection among humans, but had gone undetected until very recently. Similarly to HMPV, several new viruses have recently been identified that are associated with acute respiratory tract infection in children, although their role as causative disease agents will

need to be carefully assessed. These agents include human bocavirus [78], the human coronavirus NL63 [79] and HKU1 [80], and two polyomaviruses, named KI [81] and WU [82]. As more epidemiological studies are performed it is becoming clear that HMPV is responsible for a significant proportion of respiratory disease burden in children in many parts of the world. However, several questions still need to be addressed. Pathogen–host interactions need to be identified that are likely to give rise to LRTI in HMPV-infected patients, and the significance of coinfections in relation to HMPV disease severity needs to be examined. This could lead to the development of new strategies for the prevention and treatment of HMPV infection.

Future perspective

There have been few systematic and long-term studies to assess the real importance of HMPV as a community-acquired infection. Furthermore, the effect of virus infection on the long-term health of infected individuals is unknown. However, the current body of literature supports the view that HMPV is an important cause of LRTI in children, and suggests that HMPV should be included in the routine testing for respiratory viral pathogens in diagnostic laboratories. The routine surveillance for HMPV will allow several important aspects of HMPV infection to be ascertained, including the molecular basis of virus pathogenicity. Several laboratories have reported that coinfection with HMPV and other respiratory pathogens can influence the severity of infection, while many other laboratories have found no correlation between severity of infection and coinfection. Therefore, the role that coinfections play in disease progression in patients still needs to be clarified. In addition, it is still unclear if the severity of infection is genotype specific, and this important question needs to be examined. Although some reports have indicated that HMPV A subtypes

Executive summary

Discovery of human metapneumovirus

- First reported in children from the Netherlands in 2001.
- Retrospective studies have shown the presence of human metapneumovirus (HMPV) in the human population from as early as the 1950s.

Classification of HMPV

- Belongs to paramyxovirus family.
- Classified in the genus *Pneumovirus*, family *Metapneumovirus*.
- Closely related to avian *Pneumovirus*.
- Eight genes have been identified, which encode nine proteins.
- Virus strains can be subdivided into subtypes A1, A2, B1 and B2 on the basis of sequence variation in some genes, for example, the *N*, *P*, *F* and *G* genes.

Detection in clinical samples

- Difficult to culture in most cell lines.
- Several PCR protocols are available for HMPV detection.
- Immunologic methods are a good alternative for rapid detection and are undergoing evaluation.

Epidemiology

- HMPV has been found worldwide.
- Symptoms exhibited by patients are similar to those in respiratory syncytial virus-infected patients.
- Clinical symptoms vary, but it is a significant cause of lower respiratory tract infection in children.
- In addition to children, the elderly and immunocompromised individuals are most vulnerable to severe forms of infection.
- HMPV accounts for between 5 and 7% of children admitted to hospital with respiratory infection.
- Few long-term studies have been performed, but they suggest seasonality in the incidence of HMPV infections.
- A recent study has found that subytpe A may cause more severe symptoms.
- Coinfection with other respiratory viruses is uncommon and its effect on severity of infection is uncertain.

Conclusions

- Our current knowledge of the biology of HMPV is still relatively poor, and needs to be improved.
- HMPV infection will become increasingly important as its routine detection is performed in more diagnostic laboratories.
- There are no vaccines or specific drugs in use in the prevention or treatment of HMPV infection.

can cause more severe infection in patients, this suggestion is based on isolated reports in the literature, and is thus more anecdotal than proven. Characterization of HMPV pathogenicity will require the large-scale sequencing of clinical isolates in long-term studies, and matching the sequence variation in the virus isolates with clinical data. This will be facilitated by the use of high-throughput molecular diagnostics, and the development of immunologic agents for HMPV detection. HMPV surveillance will improve our knowledge of the interactions between HMPV and the host, which in turn should facilitate the development of novel strategies for the prevention and treatment of HMPV infection.

Financial & competing interests disclosure

We acknowledge the National Medical Research Council of Singapore and Nanyang Technological University of Singapore for research support. L-H Loo is a graduate student in the School of Biological Sciences at the Nanyang Technological University. He is supported by KK Women's and Children's Hospital, Singapore and a Medical Research Scientist Award from the NMRC-Lee Foundation.

The authors have no other relevant affiliations or financial involvement with any organization or entity with a financial interest in or financial conflict with the subject matter or materials discussed in the manuscript apart from those disclosed.

No writing assistance was utilized in the production of this manuscript.

Bibliography

1. van den Hoogen BG, de Jong J, Groen J *et al.*: A newly discovered human pneumovirus isolated from young children with respiratory tract disease. *Nat. Med.* 7(6), 719–724 (2001).
2. Biacchesi S, Skiadopoulos MH, Boivin G *et al.*: Genetic diversity between human metapneumovirus subgroups. *Virology* 315, 1–9 (2003).
3. van den Hoogen BG, Bestebroer TM, Osterhaus ADME *et al.*: Analysis of the genomic sequence of a human metapneumovirus. *Virology* 295, 119–132 (2002).
4. Garcia-Barreno B, Delgado T, Melero JA: Identification of protein regions involved in the interaction of human respiratory syncytial virus phosphoprotein and nucleoprotein: significance for nucleocapsid assembly and formation of cytoplasmic inclusions. *J. Virol.* 70, 801–808 (1996).
5. Buchholz UJ, Biacchesi S, Pham QN *et al.*: Deletion of M2 gene open reading frames 1 and 2 of human metapneumovirus: effects on RNA synthesis, attenuation and immunogenicity. *J. Virol.* 79(11), 6588–6597 (2005).
6. Schowalter RM, Smith SE, Dutch RE: Characterisation of human metapneumovirus F protein-promoted membrane fusion: critical roles for proteolytic processing and low pH. *J. Virol.* 80(22), 10931–10941 (2006).
7. Liu L, Bastien N, Li Y: Intracellular processing, glycosylation and cell surface expression of human metapneumovirus attachment glycoprotein. *J. Virol.* 81(24), 13435–13443 (2007).
8. Herfst S, de Graaf M, Schickli JH *et al.*: Recovery of human metapneumovirus genetic lineages A and B from cloned cDNA. *J. Virol.* 78(15), 8264–8270 (2004).
9. Fauquet CM *et al.*: Virus taxonomy: classification and nomenclature of viruses. In: *Eighth Report of the International Committee on Taxonomy of Viruses.* Elsevier/Academic Press, Oxford, UK (2006).
10. van den Hoogen BG, Herfst S, Sprong L *et al.*: Antigenic and genetic variability of human metapneumoviruses. *Emerg. Infect. Dis.* 10(4), 658–666 (2004).
11. Alvarez R, Jones LP, Seal BS *et al.*: Serological cross-reactivity of members of the *Metapneumovirus* genus. *Virus Res.* 105(1), 67–73 (2004).
12. Govindarajan D, Buchholz UJ, Samal SK: Recovery of avian metapneumovirus subgroup C from cDNA: cross-recognition of avian and human metapneumovirus support proteins. *J. Virol.* 80(12), 5790–5797 (2006).
13. Chan PKS, Tam JS, Lam C *et al.*: Human metapneumovirus detection in patients with severe acute respiratory syndrome. *Emerg. Infect. Dis.* 9(9), 1058–1063 (2003).
14. Deffrasnes C, Côté S, Boivin G: Analysis of replication kinetics of the human metapneumovirus in different cell lines by real-time PCR. *J. Clin. Microbiol.* 43(1), 488–490 (2005).
15. Ingram RE, Fenwick F, McGuckin R *et al.*: Detection of human metapneumovirus in respiratory secretions by reverse-transcriptase polymerase chain reaction, indirect immunofluorescence and virus isolation in human bronchial epithelial cells. *J. Med. Virol.* 78, 1223–1231 (2006).
16. Falsey AR, Criddle MC, Walsh EE: Detection of respiratory syncytial virus and human metapneumovirus by reverse transcription polymerase chain reaction in adults with and without respiratory illness. *J. Clin. Virol.* 35(1), 46–50 (2006).
17. López-Huertas MR, Casas I, Acosta-Herrera B *et al.*: Two RT-PCR based assays to detect human metapneumovirus in nasopharyngeal aspirates. *J. Virol. Methods* 129(1), 1–7 (2005).
18. van den Hoogen BG, van Doornum GJJ, Fockens JC *et al.*: Prevalence and clinical symptoms of human metapneumovirus infection in hospitalized patients. *J. Infect. Dis.* 188, 1571–1577 (2003).
19. Côté S, Abed Y, Boivin G: Comparative evaluation of real-time PCR assays for detection of the human metapneumovirus. *J. Clin. Microbiol.* 41(8), 3631–3635 (2003).
20. Mackay IM, Jacob KC, Woolhouse D *et al.*: Molecular assays for detection of human metapneumovirus. *J. Clin. Microbiol.* 41(1), 100–105 (2003).
21. Maertzdorf J, Wang CK, Brown JB *et al.*: Real-time reverse transcriptase PCR assay for detection of human metapneumoviruses from all known genetic lineages. *J. Clin. Microbiol.* 42(3), 981–986 (2004).
22. Scheltinga SA, Templeton KE, Beersma MF *et al.*: Diagnosis of human metapneumovirus and rhinovirus in patients with respiratory tract infections by an internally controlled multiplex real-time RNA PCR. *J. Clin. Virol.* 33(4), 306–311 (2005).
23. Kuypers J, Wright N, Corey L *et al.*: Detection and quantification of human metapneumovirus in pediatric specimens by real-time RT-PCR. *J. Clin. Virol.* 33(4), 299–305 (2005).
24. Ma X, Endo R, Ebihara T *et al.*: Production and characterization of neutralizing monoclonal antibodies against human metapneumovirus F protein. *Hybridoma* 24(4), 201–205 (2005).

25. Percivalle E, Sarasini A, Visai L *et al.*: Rapid detection of human metapneumovirus strains in nasopharyngeal aspirates and shell vial cultures by monoclonal antibodies. *J. Clin. Microbiol.* 43(7), 3443–3446 (2005).
26. Gerna G, Sarasini A, Percivalle E *et al.*: Simultaneous detection and typing of human metapneumovirus strains in nasopharyngeal secretions and cell cultures by monoclonal antibodies. *J. Clin. Virol.* 35(1), 113–116 (2006).
27. Boivin G, Abed Y, Pelletier G *et al.*: Virological features and clinical manifestations associated with human metapneumovirus: a new paramyxovirus responsible for acute respiratory-tract infections in all age groups. *J. Infect. Dis.* 186(9), 1330–1334 (2002).
28. Ebihara T, Endo R, Kikuta H *et al.*: Seroprevalence of human metapneumovirus in Japan. *J. Med. Virol.* 70(2), 281–283 (2003).
29. Ebihara T, Endo R, Kikuta H *et al.*: Comparison of the seroprevalence of human metapneumovirus and human respiratory syncytial virus. *J. Med. Virol.* 72(2), 304–306 (2004).
30. Esper F, Boucher D, Weibel C *et al.*: Human metapneumovirus infection in the United States: clinical manifestations associated with a newly emerging respiratory infection in children. *Pediatrics* 111(6 Pt 1), 1407–1410 (2003).
31. Falsey AR, Erdman D, Anderson LJ *et al.*: Human metapneumovirus infections in young and elderly adults. *J. Infect. Dis.* 187(5), 785–790 (2003).
32. Wolf DG, Zakay-Rones Z, Fadeela A *et al.*: High seroprevalence of human metapneumovirus among young children in Israel. *J. Infect. Dis.* 188(12), 1865–1867 (2003).
33. Hamelin ME, Boivin G: Development and validation of an enzyme-linked immunosorbent assay for human metapneumovirus serology based on a recombinant viral protein. *Clin. Diagn. Lab. Immunol.* 12(2), 249–253 (2005).
34. Ishiguro N, Ebihara T, Endo R *et al.*: Detection of antibodies against human metapneumovirus by Western blot using recombinant nucleocapsid and matrix proteins. *J. Med. Virol.* 78(8), 1091–1095 (2006).
35. Liu L, Bastien N, Sidaway F *et al.*: Seroprevalence of human metapneumovirus (hMPV) in the Canadian province of Saskatchewan analyzed by a recombinant nucleocapsid protein-based enzyme-linked immunosorbent assay. *J. Med. Virol.* 79(3), 308–313 (2007).
36. Ishiguro N, Ebihara T, Endo R *et al.*: Immunofluorescence assay for detection of human metapneumovirus-specific antibodies by use of baculovirus-expressed fusion protein. *Clin. Diagn. Lab. Immunol.* 12(1), 202–205 (2005).
37. Leung J, Esper F, Weibel C *et al.*: Seroepidemiology of human metapneumovirus (hMPV) on the basis of a novel enzyme-linked immunosorbent assay utilizing hMPV fusion protein expressed in recombinant vesicular stomatitis virus. *J. Clin. Microbiol.* 43(3), 1213–1219 (2005).
38. Aslanzadeh J, Zheng X, Li H *et al.*: Prospective evaluation of rapid antigen tests for diagnosis of respiratory syncytial virus and human metapneumovirus infections. *J. Clin. Microbiol.* 46(5), 1682–1685 (2008).
39. Freymouth F, Vabret L, Legrand N *et al.*: Presence of the new human metapneumovirus in French children with bronchiolitis. *Pediatr. Infect. Dis. J.* 22, 92–94 (2003).
40. Maggi F, Pifferi M, Vatteroni M *et al.*: Human metapneumovirus associated with respiratory tract infections in a 3-year study of nasal swabs from infants in Italy. *J. Clin. Microbiol.* 41(7), 2987–2991 (2003).
41. Dollner H, Risnes K, Radtke A *et al.*: Outbreak of human metapneumovirus infection in Norwegian children. *Pediatr. Infect. Dis. J.* 23(5), 436–440 (2004).
42. von Linstow ML, Larsen HH, Eugen-Olsen J *et al.*: Human metapnuemovirus and respiratory syncytial virus in hospitalised Danish children with acute respiratory tract infection. *Scan. J. Infect. Dis.* 36(8), 578–584 (2004).
43. Carr MJ, McCormack GP, Crowley B: Human metapneumovirus-associated respiratory tract infections in the Republic of Ireland during the influenza season of 2003–2004. *Clin. Microbiol. Infect.* 11(5), 366–371 (2005).
44. Ordás J, Boga JA, Alvarez-Argüelles M *et al.*: Role of metapneumovirus in viral respiratory infections in young children. *J. Clin. Microbiol.* 44(8), 2739–2742 (2006).
45. Heikkinen T, Osterback R, Peltola V *et al.*: Human metapneumovirus infections in children. *Emerg. Infect. Dis.* 14(1), 101–106 (2008).
46. Peret TC, Boivin G, Li Y *et al.*: Characterization of human metapneumoviruses isolated from patients in North America. *J. Infect. Dis.* 185(11), 1660–1663 (2002).
47. Bastien N, Ward D, Van Caeseele P *et al.*: Human metapneumovirus infection in the Canadian population. *J. Clin. Microbiol.* 41(10), 4642–4646 (2003).
48. Noyola DE, Alpuche-Solís AG, Herrera-Díaz A *et al.*: Human metapneumovirus infections in Mexico: epidemiological and clinical characteristics. *J. Med. Microbiol.* 54(Pt 10), 969–974 (2005).
49. da Silva LH, Spilki FR, Riccetto AG *et al.*: Variant isolates of human metapneumovirus subgroup B genotype 1 in Campinas, Brazil. *J. Clin. Virol.* 42(1), 78–81 (2008).
50. Nissen MD, Siebert DJ, Mackay IM *et al.*: Evidence of human metapneumovirus in Australian children. *Med. J. Aust.* 176(4), 188 (2002).
51. Werno AM, Anderson TP, Jennings LC *et al.*: Human metapneumovirus in children with bronchiolitis or pneumonia in New Zealand. *J. Paediatr. Child Health* 40(9–10), 549–551 (2004).
52. Peiris JSM, Tang W, Chan K *et al.*: Children with respiratory disease associated with metapneumovirus in Hong Kong. *Emerg. Infect. Dis.* 9, 628–633 (2003).
53. Thanasugarn W, Samransamruajkit R, Vanapongtipagorn P *et al.*: Human metapneumovirus infection in Thai children. *Scand. J. Infect. Dis.* 35(10), 754–756 (2003).
54. Rao BL, Gandhe SS, Pawar SD *et al.*: First detection of human metapneumovirus in children with acute respiratory infection in India: a preliminary report. *J. Clin. Microbiol.* 42(12), 5961–5962 (2004).
55. Chung JY, Han TH, Kim BE *et al.*: Human metapneumovirus infection in hospitalized children with acute respiratory disease in Korea. *J. Korean Med. Sci.* 21(5), 838–842 (2006).
56. Wang SM, Liu CC, Wang HC *et al.*: Human metapneumovirus infection among children in Taiwan: a comparison of clinical manifestations with other virus-associated respiratory tract infections. *Clin. Microbiol. Infect.* 12(12), 1221–1224 (2006).
57. Loo LH, Tan BH, Ng LM *et al.*: Human metapneumovirus in children, Singapore. *Emerg. Infect. Dis.* 13(9), 1396–1398 (2007).
58. Al-Sonboli N, Hart CA, Al-Aeryani A *et al.*: Respiratory syncytial virus and human metapneumovirus in children with acute respiratory infections in Yemen. *Pediatr. Infect. Dis. J.* 24(8), 734–736 (2005).
59. Regev L, Hindiyeh M, Shulman LM *et al.*: Characterization of human metapneumovirus infections in Israel. *J. Clin. Microbiol.* 44(4), 1484–1489 (2006).

60. Kaplan NM, Dove W, Abd-Eldayem SA *et al.*: Molecular epidemiology and disease severity of respiratory syncytial virus in relation to other potential pathogens in children hospitalized with acute respiratory infection in Jordan. *J. Med. Virol.* 80(1), 168–174 (2008).
61. IJpma FF, Beekhuis D, Cotton MF *et al.*: Human metapneumovirus infection in hospital-referred South African children. *J. Med. Virol.* 73(3), 486–493 (2004).
62. Mackay IM, Bialasiewicz S, Jacob KC *et al.*: Genetic diversity of human metapneumovirus over 4 consecutive years in Australia. *J. Infect. Dis.* 193(12), 1630–1633 (2006).
63. Manoha C, Espinosa S, Aho SL *et al.*: Epidemiological and clinical features of hMPV, RSV and RVs infections in young children. *J. Clin. Virol.* 38(3), 221–226 (2007).
64. Vicente D, Montes M, Cilla G *et al.*: Differences in clinical severity between genotype A and genotype B human metapneumovirus infection in children. *Clin. Infect. Dis.* 42(12), e111–e113 (2006).
65. Schildgen O, Glatzel T, Geikowski T *et al.*: A human metapneumovirus RNA in encephalitis patient. *Emerg. Infect. Dis.* 11(3), 467–470 (2005).
66. Hata M, Ito M, Kiyosawa S *et al.*: A fatal case of encephalopathy possibly associated with human metapneumovirus infection. *Jpn J. Infect. Dis.* 60, 328–329 (2007).
67. Pelletier G, Dery P, Abed Y *et al.*: Respiratory tract reinfections by the new human metapneumovirus in an immunocompromised child. *Emerg. Infect. Dis.* 8, 976–978 (2002).
68. Cane PA, van den Hoogen BG, Chakrabarti S *et al.*: Human metapneumovirus in a haematopoietic stem cell transplant recipient with fatal lower respiratory tract disease. *Bone Marrow Transplant.* 31, 309–310 (2003).
69. Williams JV, Wang CK, Yang CF *et al.*: The role of human metapneumovirus in upper respiratory tract infections in children: a 20 year experience. *J. Infect. Dis.* 193, 387–395 (2006).
70. Weigl JA, Puppe W, Meyer CU *et al.*: Ten year's experience with year-round active surveillance of up to 19 respiratory pathogens in children. *Eur. J. Pediatr.* 166(9), 957–966 (2007).
71. Sloots TP, Mackay IM, Bialasiewicz S *et al.*: Human metapneumovirus, Australia, 2001–2004. *Emerg. Infect. Dis.* 12(8), 1263–1266 (2006).
72. Gerna G, Campanini G, Rovida F *et al.*: Changing circulation rate of human metapneumovirus strains and types among hospitalized pediatric patients during three consecutive winter–spring seasons. *Arch. Virol.* 150, 2365–2375 (2005).
73. Semple MG, Cowell A, Dove W *et al.*: Dual infection of infants by human metapneumovirus and human respiratory syncytial virus is strongly associated with severe bronchiolitis. *J. Infect. Dis.* 191(3), 382–386 (2005).
74. Greensill J, McNamara PS, Dove W *et al.*: Human metapneumovirus in severe respiratory syncytial virus bronchiolitis. *Emerg. Infect. Dis.* 9, 372–375 (2003).
75. Al-Sonboli N, Hart CA, Al-Aghbari N *et al.*: Human metapneumovirus and respiratory syncytial virus disease in children, Yemen. *Emerg. Infect. Dis.* 12(9), 1437–1439 (2006).
76. Lee N, Chan PK, Yu IT *et al.*: Co-circulation of human metapneumovirus and SARS-associated coronavirus during a major nosocomial SARS outbreak in Hong Kong. *J. Clin. Virol.* 40(4), 333–337 (2007).
77. Choi EH, Lee HJ, Kim SJ *et al.*: The association of newly identified respiratory viruses with lower respiratory tract infections in Korean children, 2000–2005. *Clin. Infect. Dis.* 43(5), 585–592 (2006).
78. Allander T, Tammi MT, Eriksson M *et al.*: Cloning of a human parvovirus by molecular screening of respiratory tract samples. *Proc. Natl Acad. Sci. USA* 102(36), 12891–12896 (2005).
79. van der Hoek L, Pyrc K, Jebbink MF *et al.*: Identification of a new human coronavirus. *Nat. Med.* 10(4), 368–373 (2004).
80. Woo PC, Lau SK, Chu CM *et al.*: Characterization and complete genome sequence of a novel coronavirus, coronavirus HKU1, from patients with pneumonia. *J. Virol.* 79(2), 884–895 (2005).
81. Allander T, Andreasson K, Gupta S *et al.*: Identification of a third human polyomavirus. *J. Virol.* 81(8), 4130–4136 (2007).
82. Gaynor AM, Nissen MD, Whiley DM *et al.*: Identification of a novel polyomavirus from patients with acute respiratory tract infections. *PLoS Pathog.* 3(5), e64 (2007).

Affiliations

- *Richard J Sugrue*
  Division of Molecular & Cell Biology, School of Biological Sciences, Nanyang Technological University, 60 Nanyang Drive, 637551, Singapore
  Tel.: +65 6316 2889;
  Fax: +65 6791 3856;
  rjsugrue@ntu.edu.sg
- *Boon-Huan Tan*
  Detection & Diagnostics Laboratory, Defence Medical & Environmental Research Institute, DSO National Laboratories, 27 Medical Drive, #13–00, 117510, Singapore
  Tel.: +65 6485 7240;
  Fax: +65 6485 7262;
  tboonhua@dso.org.sg
- *Liat-Hui Loo*
  Division of Molecular & Cell Biology, School of Biological Sciences, Nanyang Technological University, 60 Nanyang Drive, 637551, Singapore
  Tel.: +65 6316 2928;
  Fax: +65 6791 3856;
  lool0002@ntu.edu.sg

Province enjoy eating frog meat, particularly from wild frogs, many frogs have been sold in the market, including a substantial number of wild frogs. The results of our survey show that infection of wild frogs with spargana reached 27.3% in western Guangdong Province; hence, consumption of wild frogs (and use as poultices) poses a high risk for sparganum infection. Therefore, public health officials, epidemiologists, medical practitioners, parasitologists, veterinarians, and the general public should be aware of such risks and should implement strategies to reduce or eliminate them.

This study was supported in part by grants from Guangdong Scientific and Technological Program (no. 8452408801000010), Guangdong Ocean University (no. 0612117, to M.-W.L.), and the Program for Changjiang Scholars and Innovative Research Team in University (no. IRT0723, to X.-Q.Z.).

Ming-Wei Li, Hong-Ying Lin, Wei-Tian Xie, Ming-Jian Gao, Zhi-Wei Huang, Jun-Ping Wu, Chun Li, Rui-Qing Lin, and Xing-Quan Zhu

Author affiliations: Guangdong Ocean University, Zhanjiang, People's Republic of China (M.-W. Li, H.-Y. Lin, W.-T. Xie, M.-J. Gao, Z.-W. Huang, J.-P. Wu); and South China Agricultural University, Guangzhou, People's Republic of China (C. Li, R.-Q. Lin, X.-Q. Zhu).

DOI: 10.3201/eid1508.090099

References

1. Wiwanitkit V. A review of human sparganosis in Thailand. Int J Infect Dis. 2005;9:312–6. DOI: 10.1016/j.ijid.2004.08.003
2. Pampiglione S, Fioravanti ML, Rivasi F. Human sparganosis in Italy. Case report and review of the European cases. APMIS. 2003;111:349–54. DOI: 10.1034/j.1600-0463.2003.1110208.x
3. Gray ML, Rogers F, Little S, Puette M, Ambrose D, Hoberg EP. Sparganosis in feral hogs (*Sus scrofa*) from Florida. J Am Vet Med Assoc. 1999;215:204–8.
4. Yoon KC, Seo MS, Park SW, Park YG. Eyelid sparganosis. Am J Ophthalmol. 2004;138:873–5. DOI: 10.1016/j.ajo.2004.05.055
5. Cho JH, Lee KB, Yong TS, Kim BS, Park HB, Ryu KN, et al. Subcutaneous and musculoskeletal sparganosis: imaging characteristics and pathologic correlation. Skeletal Radiol. 2000;29:402–8. DOI: 10.1007/s002560000206
6. Zhou P, Chen N, Zhang RL, Lin RQ, Zhu XQ. Food-borne parasitic zoonoses in China: perspective for control. Trends Parasitol. 2008;24:190–6. DOI: 10.1016/j.pt.2008.01.001
7. Ooi HK, Chang SL, Huang CC, Kawakami Y, Uchida A. Survey of *Spirometra erinaceieuropaei* in frogs in Taiwan and its experimental infection in cats. J Helminthol. 2000;74:173–6.
8. Fukushima T, Yamane Y. How does the sparganosis occur? Parasitol Today. 1999;15:124. DOI: 10.1016/S0169-4758(99)01405-2
9. Nithiuthai S, Anantaphruti MT, Waikagul J, Gajadhar A. Waterborne zoonotic helminthiases. Vet Parasitol. 2004;126:167–93. DOI: 10.1016/j.vetpar.2004.09.018

Address for correspondence: Xing-Quan Zhu, Laboratory of Parasitology, College of Veterinary Medicine, South China Agricultural University, 483 Wushan St, Tianhe District, Guangzhou, Guangdong Province 510642, People's Republic of China; email: xingquanzh@scau.edu.cn

Letters

Letters commenting on recent articles as well as letters reporting cases, outbreaks, or original research are welcome. Letters commenting on articles should contain no more than 300 words and 5 references; they are more likely to be published if submitted within 4 weeks of the original article's publication. Letters reporting cases, outbreaks, or original research should contain no more than 800 words and 10 references. They may have 1 Figure or Table and should not be divided into sections. All letters should contain material not previously published and include a word count.

Human Rhinovirus Group C in Hospitalized Children, Singapore

To the Editor: Human rhinovirus (HRV) is a common etiologic agent of upper respiratory tract infections and is associated with symptoms such as asthma and wheezing. HRV has >100 serotypes, and recently, several groups reported a new HRV group C (HRV-C) in children that is associated with more severe respiratory infections (*1–5*). We examined the incidence of respiratory viruses in children hospitalized in Kandang Kerbau Women's and Children's Hospital, Singapore (*6,7*). These studies also identified human metapneumovirus and human bocavirus (HBoV) among children in Singapore. We recently performed a retrospective study by using PCR-based testing (*8*) to identify HRV, in particular HRV-C, in these patients. From October 2005 through March 2007, a total of 500 nasopharyngeal swab specimens from pediatric patients (age range 1 month through 12 years) were collected and tested for HRVs.

PCR-based testing identified HRV with an incidence rate of 12.8% (64/500), the highest incidence rate in Singapore, compared with incidence rates of other respiratory viruses reported in the same study (*7*). Of the HRV-positive patients, 31 (48.4%) of 64 had symptoms of lower respiratory tract infections (LRTIs) and 16 (25%) of 64 had symptoms of upper respiratory tract infections. Ten patients infected with HRV were co-infected with a second respiratory virus, HBoV (8/10) or respiratory syncytial virus (RSV) (2/10).

HRV-C was detected by molecular serotyping as described (*3*). Briefly, the first PCR was performed with the forward primer P1–1 (5′-CAA GCA CTT CTG TYW CCC C-3′) and the reverse primer P3–1 (5′-ACG GAC ACC CAA AGT AG-3′). A second

heminested PCR was performed with forward primer P1–1 but with 3 different reverse primers, P2–1 (5′-TTA GCC ACA TTC AGG GGC-3′), P2–2 (5′-TTA GCC ACA TTC AGG AGC C-3′), and P2–3 (5′-TTA GCC GCA TTC AGG GG-3′). PCR amplicons were sequenced by using the P1–1 primer. DNA sequences were blasted by using the National Center for Biotechnology Information database (Bethesda, MD, USA) and aligned with available sequences by using Clustal X version 1.83 software (www.bips.u-strasbg.fr/fr/documentation/clustalx). All protocols are available on request.

A phylogenetic tree (GenBank accession nos. FJ645828–FJ645771) was constructed by using neighbor-joining method with 1,000 bootstrap replicates and MEGA version 4 software (*9*). The tree showed similar branching of known HRVs into serogroups (HRV-A, HRV-B, and HRV-C) as described (*3*). Forty-seven (73%) of the 64 HRV specimens from Singapore were grouped into HRV-A, 9 (14%) into HRV-B, and 2 (3%) into HRV-C. We also found a cluster of 10 HRV-A strains (Figure) diverging from the reference HRV-A strains. This finding suggests that these strains could be new strains of the HRV-A, as reported (*3*). We could not determine virus subtype for 6 specimens, possibly because of low virus load.

Our results confirm that HRV infections in Singapore are caused mainly by HRV-A. An increase in HRV-C infections with the onset of winter has been reported in the People's Republic of China (26%) (*5*) and the Hong Kong Special Administrative Region of China (80%) (*2*). These findings indicate that the incidence of HRV-C infections is seasonal, which may account for the apparent low rates of HRV infection in Singapore. However, the incidence rate for HRV-C infections in Singapore was higher than that for HRV-C infections in Australia (1.4%) (*4*), which has a clearly defined winter season.

The 2 patients in which HRV-C was detected had asthma (virus strain SING-06–263) and bronchiolitis (virus strain SING-06–291). These observations are consistent with reports of HRV-C in patients with severe wheezing (*2,4,10*). We also detected co-infection with another virus in 10 patients infected with HRV. Of these 10 co-infections, HRV-A was detect-

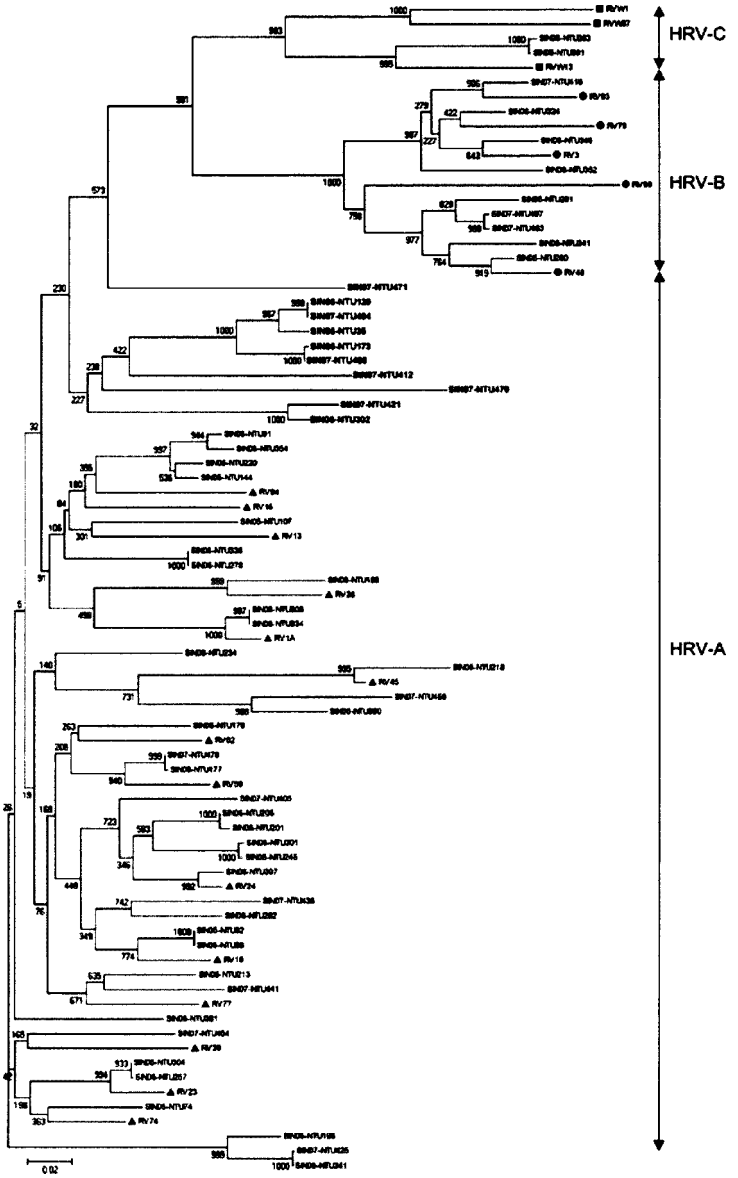

Figure. Phylogenetic analysis of human rhinoviruses (HRVs) from Singapore based on nucleotide sequences of the 5′ noncoding region. The tree was constructed by using the neighbor-joining method with 1,000 bootstrapped replicates generated by MEGA version 4 software (*9*). Sequences (GenBank accession nos. FJ645828–FJ645771) of viruses from Singapore (SIN) are indicated, where the 2 numbers represent the year the specimen was collected, and NTU (Nanyang Technological University) followed by 3 numbers represents the specimen number. Representative strains of HRV-C are indicated by squares, HRV-B by circles, and HRV-A by triangles. RV indicates rhinovirus strains, followed by the serotype no. These sequences were obtained from the report by Lee et al. (*3*). **Boldface** indicates a cluster of 10 HRV-A strains that diverged from reference HRV-A strains. Scale bar indicates nucleotide substitutions per site.

ed in 7 patients; 5 were co-infected with HBoV (2 patients had LRTIs, 2 had upper respiratory tract infections, and 1 had undefined symptoms), and 2 were co-infected with RSV (both patients had symptoms of LRTIs). Of the other 3 patients co-infected with HRV and HBoV, 1 was infected with HRV-B (had LRTI), 1 with HRV-C (had LRTI), and 1 with an untypeable HRV (had undefined symptoms). Co-infections with HRV and RSV (*4,5*) and HRV and HBoV (*4*) have been reported.

Although the clinical role of these co-infections needs to be clarified, these studies suggest that co-infections may result in more severe disease symptoms. The role of HRV-C in causing illness among the children of Singapore will require further study.

This study was supported by the National Medical Research Council of Singapore and the DSO National Laboratories, Singapore.

Boon-Huan Tan, Liat-Hui Loo, Elizabeth Ai-Sim Lim, Shirley Lay-Kheng Seah, Raymond T.P. Lin, Nancy W.S. Tee, and Richard J. Sugrue

Author affiliations: DSO National Laboratories, Singapore (B.-H. Tan, E.A.-S. Lim, S.L.-K. Seah); Nanyang Technological University, Singapore (L.-H. Loo, R.J. Sugrue); Kandang Kerbau Women's and Children's Hospital, Singapore (L.-H. Loo, N.W.S. Tee); and National University Hospital, Singapore (R.T.P. Lin)

DOI: 10.3201/eid1508.090321

References

1. Lamson D, Renwick N, Kapoor V, Liu Z, Palacios G, Ju J, et al. MassTag polymerase-chain-reaction detection of respiratory pathogens, including a new rhinovirus genotype, that caused influenza-like illness in New York State during 2004–2005. J Infect Dis. 2006;194:1398–402. DOI: 10.1086/508551
2. Lau SK, Yip CC, Tsoi HW, Lee RA, So LY, Lau YL, et al. Clinical features and complete genome characterization of a distinct human rhinovirus (HRV) genetic cluster, probably representing a previously undetected HRV species, HRV-C, associated with acute respiratory illness in children. J Clin Microbiol. 2007;45:3655–64. DOI: 10.1128/JCM.01254-07
3. Lee WM, Kiesner C, Pappas T, Lee I, Grindle K, Jartti T, et al. A diverse group of previously unrecognized human rhinoviruses are common causes of respiratory illnesses in infants. PLoS One. 2007;2:e966. DOI: 10.1371/journal.pone.0000966
4. McErlean P, Shackelton LA, Lambert SB, Nissen MD, Sloots TP, Mackay IM. Characterisation of a newly identified human rhinovirus, HRV-QPM, discovered in infants with bronchiolitis. J Clin Virol. 2007;39:67–75. DOI: 10.1016/j.jcv.2007.03.012
5. Xiang Z, Gonzalez R, Xie Z, Xiao Y, Chen L, Li Y, et al. Human rhinovirus group C infection in children with lower respiratory tract infection. Emerg Infect Dis. 2008;14:1665–7. DOI: 10.3201/eid1410.080545
6. Loo LH, Tan BH, Ng LM, Tee NW, Lin RT, Sugrue RJ. Human metapneumovirus in children, Singapore. Emerg Infect Dis. 2007;13:1396–8.
7. Tan BH, Lim EA, Seah SG, Loo LH, Tee NW, Lin RT, et al. The incidence of human bocavirus infection among children admitted to hospital in Singapore. J Med Virol. 2009;81:82–9. DOI: 10.1002/jmv.21361
8. Hayden FG, Turner RB, Gwaltney JM, Chi-Burris K, Gersten M, Hsyu P, et al. Phase II, randomized, double-blind, placebo-controlled studies of ruprintrivir nasal spray 2-percent suspension for prevention and treatment of experimentally induced rhinovirus colds in healthy volunteers. Antimicrob Agents Chemother. 2003;47:3907–16. DOI: 10.1128/AAC.47.12.3907-3916.2003
9. Tamura K, Dudley J, Nei M, Kumar S. MEGA4: Molecular Evolutionary Genetics Analysis (MEGA) software version 4.0. Mol Biol Evol. 2007;24:1596–9. DOI: 10.1093/molbev/msm092
10. Miller EK, Edwards KM, Weinberg GA, Iwane MK, Griffin MR, Hall CB, et al. New Vaccine Surveillance Network. A novel group of rhinoviruses is associated with asthma hospitalizations. J Allergy Clin Immunol. 2009;123:98–104. DOI: 10.1016/j.jaci.2008.10.007

Address for correspondence: Boon-Huan Tan, Detection and Diagnostics Laboratory, DSO National Laboratories, #13-00, 27 Medical Dr, Singapore 117510; email: tboonhua@dso.org.sg

Nondominant Hemisphere Encephalitis in Patient with Signs of Virai Meningitis, New York, USA

To the Editor: Herpes simplex virus (HSV) is the most common cause of sporadic fatal encephalitis across the globe and for all ages. HSV is the etiologic agent of 10%–20% of the 20,000 cases of encephalitis per year in the United States (*1*); >50% of untreated cases are fatal. Of the 2 types of HSV, HSV-1 and HSV-2, HSV-1 most commonly affects persons 20–40 years of age, whereas HSV-2 commonly affects neonates. This rapidly progressive disease is a common cause of fatal encephalitis in the United States. Signs and symptoms include fever and headache for a few days, followed by confusion, focal deficits, seizures or hemiparesis, hallucinations, and altered levels of consciousness (*2*). One third of all HSV encephalitis cases afflict children and adolescents. Lumbar puncture typically shows lymphocytic pleocytosis, increased erythrocytes, and elevated protein (*2*); glucose level is typically within normal limits. Serologic assays often show prior infection. Brain imaging frequently indicates unilateral frontal or temporal lobe abnormalities with edema or hematoma (*3,4*). The involvement of the nondominant brain hemisphere is associated with atypical signs and symptoms (*5*). Diagnosis is usually made by using PCR to examine viral DNA in cerebrospinal fluid (CSF) (*6*). This method of finding DNA in CSF is highly sensitive (98%) and specific (94%–100%). Without therapy, 70% of patients die; with therapy, 20%–30% die (*6*). Illness includes behavioral sequelae.

A 43-year-old female immigrant from China was admitted to Flushing

Journal of Medical Virology 81:82–89 (2009)

The Incidence of Human Bocavirus Infection Among Children Admitted to Hospital in Singapore

Boon-Huan Tan,[1]* Elizabeth Ai-Sim Lim,[1] Shirley Gek-Kheng Seah,[1] Liat-Hui Loo,[2,3] Nancy W.S. Tee,[3] Raymond T.P. Lin,[4] and Richard Joseph Sugrue[2]

[1]*Detection and Diagnostics Laboratory, Defence Medical and Environmental Research Institute, DSO National Laboratories, Singapore*
[2]*Division of Molecular and Cell Biology, School of Biological Sciences, Nanyang Technological University, Singapore*
[3]*Microbiology Laboratory, Kandang Kerbau Women's and Children's Hospital, Singapore*
[4]*Department of Laboratory Medicine, National University Hospital, Singapore*

Human bocavirus (HBoV) is a parvovirus, belonging to the genus *Bocavirus*. The virus was identified recently in Sweden, and has now been detected in several different countries. Although it is associated with lower respiratory tract infections in pediatric patients, the incidence of HBoV infection in a developed country in South East Asia, has not been examined. The objective of this study was to determine the importance of HBoV as a cause of lower respiratory tract infections among children admitted to hospital in Singapore. Five hundred nasopharyngeal swabs were collected from anonymized pediatric patients admitted to the Kandang Kerbau Women's and Children's Hospital for acute respiratory infections. The specimens were tested for the presence of HBoV using polymerase chain reactions. HBoV was detected in 8.0% of the patients tested, and a majority of these HBoV patients exhibited lower respiratory tract infections. A significant level of coinfection with respiratory syncytial viruses and rhinoviruses was also observed in these HBoV patients. The data suggest that HBoV is an important cause of lower respiratory tract infections among children admitted to hospital in Singapore, and is the first study examining the incidence of HBoV infection in a developed country in South East Asia. ***J. Med. Virol. 81:82–89, 2009.***

KEY WORDS: *Bocavirus*; coinfections; pediatric patients; lower respiratory tract infections; Singapore,

INTRODUCTION

Respiratory syncytial virus (RSV), parainfluenza viruses (PIV), adenovirus, rhinovirus (RHV), and influenza viruses are the most common etiological agents responsible for acute respiratory infections in children, causing either lower or upper respiratory tract infections. Recently, several new viruses have been discovered that are associated with respiratory infections in children [see reviews by Kahn, 2007; Sloots et al., 2008]. The human metapneumovirus was first discovered in Netherlands [Van der Hoogen et al., 2001], and is now reported to be an important global cause of lower respiratory tract infections in children. Similarly, human coronavirus (HCoV) NL63 and HKU1 were first isolated in the Netherlands [Van der Hoek et al., 2004], and Hong Kong [Woo et al., 2005], respectively, and have been reported to be associated with acute respiratory infections in children. Both strains have been detected subsequently in patients from other countries [see reviews by Van der Hoek et al., 2006; Pyrc et al., 2007].

A new parvovirus belonging to the genus *Bocavirus* was identified in Sweden [Allander et al., 2005], and its presence was associated with acute respiratory infections in pediatric patients [see reviews by Kahn, 2008; Schildgen et al., 2008]. This virus was referred to as human bocavirus (HBoV), and it was distinct genetically from the human parvovirus B19. Since its initial discovery, HBoV has been detected in children with lower respiratory tract infections in several different countries [see review by Allander, 2008]. In Asia, HBoV has been reported in Thailand [Fry et al., 2007], China [Qu et al., 2007], South Korea [Choi et al., 2006; Chung et al., 2006, 2007; Lee et al., 2007], Japan [Ma et al., 2006], and Hong Kong [Lau et al., 2007a]. In this study the incidence of HBoV was examined in pediatric

Grant sponsor: National Medical Research Council, Singapore.

*Correspondence to: Boon-Huan Tan, PhD, Head, Detection & Diagnostics Laboratory, DSO National Laboratories, #13-00, 27 Medical Drive, Singapore 117510, Singapore.
E-mail: tboonhua@dso.org.sg

Accepted 21 August 2008
DOI 10.1002/jmv.21361
Published online in Wiley InterScience (www.interscience.wiley.com)

patients admitted to hospital in Singapore. The data suggest that HBoV is a possible cause of lower respiratory tract infections among children admitted to hospital in Singapore.

MATERIALS AND METHODS

Specimen Collection

Between October 2005 and March 2007, nasopharyngeal swabs were obtained from pediatric patients admitted to Kandang Kerbau Women's and Children's Hospital for acute respiratory infections. The specimens were tested in the hospital's microbiology laboratory for the presence of influenza virus, RSV, adenovirus, HMPV and PIV as described previously [Loo et al., 2007]. In all cases, aliquots of the clinical specimens were stored at −80°C until they were tested for the presence of HBoV. This study was approved by the hospital's ethic committee, approval number EC/043/2004.

Extraction of Genetic Materials

The nasopharyngeal swabs were thawed and subjected to total nucleic acid extraction, using either the QIAamp viral RNA minikit or the QIAamp RNeasy minikit (Qiagen Inc., Valencia, CA), according to the manufacturer's instructions.

PCR Testing for HBoV, HCoV, and RHV

One to five microliters of the total extract were tested using PCR assays targeting HBoV [Sloots et al., 2006], HCoV [Escutenaire et al., 2007], and RHV [Hayden et al., 2003]. All primers were synthesized from ProOligo (Singapore). For the PCR testing of HBoV, the reaction was performed in a 50 μl reaction mixture containing 0.5 μM of each primer, 2.5 U Platinum Taq DNA polymerase (Invitrogen Corporation, Carlsbad, CA), 0.2 mM dNTPs, and 1.5 mM $MgCl_2$, in the conventional PCR machine. In the case of HCoV, the PCR reaction was carried out in a 25 μl reaction mixture containing SYBR Green RT-PCR reaction mix (Biorad, Hercules, CA) with 0.7 μM of each primer, and 0.5 μl of iScript reverse transcriptase (Biorad) in the I-Cycler (Biorad). At the end of the reaction, the products were subjected to a melting curve analysis by heating the products to 95°C for 1 min, and then cooling to 55°C for 45 sec, and heating back to 95°C at 0.5°C intervals. Positive products are represented by HCoV-specific melting peak as described [Escutenaire et al., 2007], and were confirmed by agarose gel analysis with visualisation in the presence of ethidium bromide staining. RHV identification was carried out with 0.5 μM of each forward and reverse primer, 0.1 μM of Taqman probe in Superscript reverse transcriptase/Platinum Taq enzyme reaction mix (Invitrogen Corporation) in the LightCycler machine (Roche Diagnostics, Mannheim, Germany). Positive products were represented by an exponential increase of fluorescence captured by the F2 channel of the LightCycler.

Sequencing Reactions

All amplified products were purified from agarose gel using the QIAquick gel extraction purification kit (Qiagen Inc.). The identity of the products were confirmed by DNA sequencing using the BigDye Terminator cycle sequencing kit (Applied Biosystems, Foster City, CA) with the same primers used for PCR testings.

Sequence and Phylogenetic Analyses

The DNA sequences were assembled using SeqMan (DNASTAR, Lasergene Version 7). The viral sequences were aligned using the algorithm CLUSTALW method in the program MEGALIGN (DNASTAR, Lasergene version 7). The percent sequence homology and phylogenetic trees were calculated and constructed using the neighbor-joining method at the nucleotide (nt) level, with bootstrap analysis performed on 1,000 replicates. The phylogenetic trees were viewed using TreeView version 1.6.6 [Page, 1996].

Nucleotide Accession Numbers

The partial sequences for both the Singapore HBoVs and HCoVs have been submitted to GenBank under the accession numbers EU014167 to 206, and EU370700 to 1.

RESULTS

Incident Rate of Respiratory Viruses in the Pediatric Patients

A total of 500 nasopharyngeal swabs were collected from pediatric patients admitted to Kandang Kerbau Women's and Children's Hospital with acute respiratory infections. The patients exhibited symptoms that were consistent with both lower respiratory tract infections (bronchiolitis, bronchitis, pneumonia, chronic lung disease, asthma, and wheezing) or upper respiratory tract infections (croup, infantile pyrexia, pharnygitis). The age group of the children ranged from 1 month to 12 years. Of the 500 specimens collected, 59 tested positive for RSV (11.8%), 4 for influenza A virus (0.8%), 2 for influenza B virus (0.4%), 4 for PIV1 (0.8%), 0 for PIV2; 8 for PIV3 (1.6%), 1 for adenovirus (0.2%) and 29 for HMPV (5.8%) (Table I). In addition, PCR analysis revealed that 40 patients were positive for HBoV (8.0%), and 3 tested positive for HCoV (0.6%).

Clinical Presentation and Age Distribution of Patients Infected With Respiratory Viruses

The clinical symptoms exhibited by the patients in which HBoV was detected were compared with patients in which RSV, HMPV and HCoV-NL63 were detected (Tables I and II). In the current study, 50% of the patients in which HBoV was detected presented symptoms that were consistent with lower respiratory tract infections, which compared with 57.6% and 48.3% for RSV and HMPV, respectively. These data placed HBoV

TABLE I. Number of Positives and Age Distribution of Patients Infected With RSV, HMPV, and HBoV

		Age distribution of patients[b] (%)					Respiratory infections[c]		
Viral agents tested	No. of positives[a] (%) (N = 500)	≤3 months (N = 85)	>3 to ≤6 months (N = 45)	>6 to ≤12 months (N = 141)	>12 to <24 months (N = 64)	>24 months (N = 165)	L (%)	U(%)	O (%)
Respiratory syncytial virus	59 (11.8)	12 (14.1)	11 (24.4)	18 (12.8)	7 (10.9)	11 (6.7)	34 (57.6)	13 (22.0)	12 (20.4)
Human metapneumovirus	29(5.8)	2 (2.4)	2 (4.4)	10 (7.1)	3 (4.7)	12 (7.3)	14 (48.3)	12 (41.4)	3 (10.3)
Human bocavirus	40 (8)	4 (4.8)	3 (6.7)	15 (10.6)	5 (7.8)	13 (7.9)	20 (50)	13 (32.5)	7 (17.5)
Influenza A virus	4(0.8)	0	0	0	2 (3.1)	2 (1.2)	0	2	2
Influenza B virus	2 (0.4)	0	0	1 (0.7)	0	1 (0.6)	0	0	2
Parainfluenza virus type 1	4(0.8)	0	0	3 (2.1)	1 (1.6)	0	3	0	1
Parainfluenza virus type 2	0	—	—	—	—	—	—	—	—
Parainfluenza virus type 3	8(1.6)	1 (1.2)	1 (2.2)	2 (1.4)	3 (4.7)	1 (0.6)	4	2	3
Adenovirus	1(0.2)	0	0	0	0	1 (0.6)	1	0	0
Coronavirus	3(0.6)	0	2 (4.4)	0	0	1 (0.6)	0	2	1

[a]The no. of positives refer to the samples that tested positive for each viral agent, relative to the total no. of samples collected for the study.
[b]The % age distribution of patients refer to the samples that tested positive for each viral agent, relative to N, representing the no. of samples collected for the respective age group.
[c]The respiratory infections are relative to the no. of samples that tested positive for each viral agent, and L refers to LRTI with symptoms for bronchiolitis, bronchitis, pneumonia, asthma, wheezing, and chronic lung disease; U to URTI with symptoms for croup or laryngotracheobronchilitis, and pharnygitis; and O to others with symptoms not defined as L or U.

J. Med. Virol. DOI 10.1002/jmv

TABLE II. Clinical Characteristics of Patients Infected With HBoV

Specimen	Age[a]	*L, U, O[b]	Co-infection
SIN05-NTU-12	1	U	
SIN05-NTU-22	10 months	O	
SIN05-NTU-46	9 months	L	
SIN05-NTU-79	1	O	
SIN05-NTU-86	5	L	
SIN05-NTU-104	10 months	L	
SIN05-NTU-150	2	O	
SIN06-NTU-159	1	L	RSV
SIN06-NTU-165	1	L	RSV
SIN06-NTU-167	1	U	
SIN06-NTU-193	4	L	
SIN06-NTU-194	6 months	U	RSV
SIN06-NTU-195	2	L	
SIN06-NTU-218	2	L	RHV
SIN06-NTU-234	2 months	U	RHV
SIN06-NTU-243	8 months	U	
SIN06-NTU-246	6	L	
SIN06-NTU-250	3 months	U	
SIN06-NTU-258	1 months	U	RSV
SIN06-NTU-263	11	L	RHV
SIN06-NTU-268	2	L	PIV3
SIN06-NTU-275	3	L	
SIN06-NTU-290	1	L	PIV3
SIN06-NTU-325	1	O	PIV1
SIN06-NTU-328	6 months	U	
SIN06-NTU-353	1	U	RSV
SIN06-NTU-371	5	L	
SIN06-NTU-374	13	U	
SIN06-NTU-375	2	L	
SIN06-NTU-399	1	L	
SIN07-NTU-421	3 months	U	RHV
SIN07-NTU-427	1	U	
SIN07-NTU-430	4	O	RSV
SIN07-NTU-432	4 months	L	
SIN07-NTU-441	3	O	RHV
SIN07-NTU-470	3	L	RHV
SIN07-NTU-494	1	U	
SIN07-NTU-496	12	L	
SIN07-NTU-497	10	L	RHV
SIN07-NTU-500	8	0	RHV

[a]refers to age of patients in years, unless otherwise stated.
[b]L refers to LRTI with symptoms for bronchiolitis, bronchitis, pneumonia, asthma, wheezing, and chronic lung disease; U to URTI with symptoms for croup or laryngotracheobronchilitis, and pharnygitis; and O to others with symptoms not defined as L or U. RSV, respiratory syncytial virus; PIV, parainfluenza virus; RHV, rhinovirus.

as the second most likely cause of lower respiratory tract infections. The incident rate for upper respiratory tract infections in patients in which HBoV was detected was 32.5%, which compared with 22.0% and 41.4% for RSV and HMPV, respectively.

The age distribution and clinical presentation of the patients infected with HBoV were examined and compared. Fifty-five percent of the HBoV-infected patients were 1 year old or younger, which compared with detection rates of 70% and 48% for RSV and HMPV respectively (Table I). Most reported studies on the detection of HBoV have been carried out in patients who exhibited respiratory symptoms, and there were few parallel studies on healthy children. Similarly, this current study did not examine the incidence of HBoV in healthy children, or other pediatric patients with non-respiratory symptoms. However, a recent report had clearly described the detection rate in healthy children to be less significant than that in children exhibiting clinical symptoms consistent with respiratory tract infections [Garcia-Garcia et al., 2008]. Several reports have also noted the presence of HBoV in fecal [Lau et al., 2007a; Lee et al., 2007; Vicente et al., 2007] and urine samples from children [Pozo et al., 2007], suggesting that the virus is associated with both enteric and respiratory infections. The current study did not find any symptoms of gastroenteritis presented by the HBoV patients. However, this does not exclude the possibility that the virus does not cause enteric infections as fecal samples were not collected.

Of the three patients in whom HCoV was detected, two tested positive for the HCoV-NL63, and one for HCoV-OC43. Both HCoV-NL63 patients exhibited croup, which is consistent with reports from Germany, Taiwan and South Korea [Van der Hoek et al., 2005; Han et al., 2007; Wu et al., 2008]. However, the small number of

patients in which HCoV was detected makes any clinical association with the presence of the virus and severity of infection impossible. It is possible that the assay used in the current study may not be sensitive enough to detect HCoV in some patients. This is unlikely to be the reason, since similar low rates of HCoV detection have been observed consistently elsewhere [Koetz et al., 2006; Chung et al., 2007; Kaplan et al., 2007; Pierangeli et al., 2007].

Coinfections of HBoV With Other Respiratory Viruses

Although HBoV can be the single cause of lower respiratory tract infection in children, several studies have reported that HBoV coinfections with other respiratory viruses resulted in an increased severity of infection [Allander et al., 2005; Choi et al., 2006; Chung et al., 2006; Foulongne et al., 2006; Manning et al., 2006; Sloots et al., 2006; Fry et al., 2007]. The 40 HBoV positive specimens were therefore examined for the presence of other respiratory viruses. In 23 of these HBoV patients, HBoV was the only virus detected, and lower respiratory tract infections was observed in 12 (52.1%) of single infections. Interestingly, in 17 (42.5%) of the patients infected with HBoV, the presence of RSV, PIV1 and 3, and RHV were also detected (Table II). The rate of HBoV coinfection was almost similar to the 40% coinfections reported in Thai pediatric patients [Chieochansin et al., 2008], but less than that reported elsewhere [Pozo et al., 2007; Hindiyeh et al., 2008]. In the current study, both RSV and RHV each accounted for 6 (35%) and 8 (47%) of the coinfections respectively, with PIV at 3 (17.6%). Of the 17 patients who showed evidence of coinfections with respiratory viruses, 47% exhibited lower respiratory tract infections, lower than that caused by single HBoV infections, while 29% of these exhibited upper respiratory tract infections. Four of the eight coinfected with RHV showed lower respiratory tract infections, compared to only two out of six patients coinfected with RSV. Coinfections with more than one of the other respiratory viruses were not detected.

Sequence and Phylogenetic Analyses of HBoV and HCoV

The HBoVs detected in this study were sequenced to determine the genetic relationship with other HBoVs reported elsewhere. A 245 bp region of the NS1 gene sequence was used to analyze the genetic relatedness of the Singapore isolates as described previously [Chung et al., 2006; Sloots et al., 2006]. The Singapore HBoV isolates showed nt identity ranging from 91% to 100% with published HBoV sequences. Approximately 60% of the Singapore HBoV isolates were identical at the nt sequence level, and the remaining HBoV isolates showed only minor nt differences. This highly conserved sequence identity is consistent with HBoV which has been isolated in other countries [Chung et al., 2006; Qu et al., 2007]. The HBoV sequences were aligned, and percent sequence homology was calculated and phylogenetic trees were constructed as described in Materials and Methods Section. The analysis showed that the majority of the Singapore HBoV strains clustered with the prototype virus, st1 strain, that was first detected in Sweden (Fig. 1). In addition, the Singapore HBoV strains appeared to be closely related to canine minute virus and bovine parvovirus than the human parvovirus

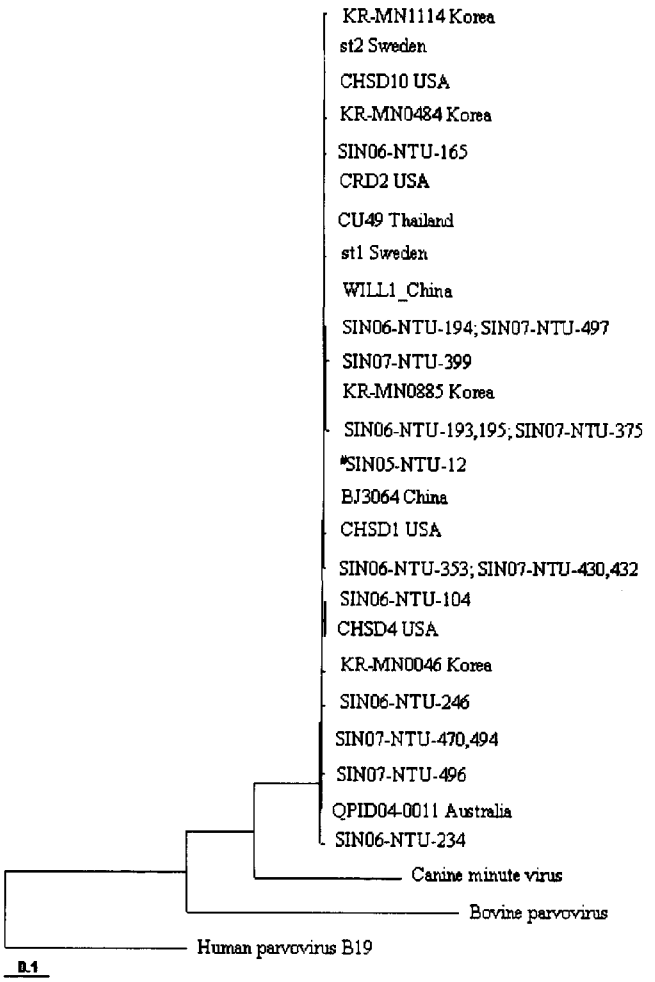

Fig. 1. Phylogenetic analysis of the partial NS1 gene region (245 bp) for HBoV detected from hospitalized pediatric patients. The phylogenetic tree was constructed using the neighbour-joining method and the bootstrap values were generated in 1,000 replicates. The viral sequences from the Singapore strains are represented by SIN05-NTU, followed by the specimen number. SIN represents Singapore and 05 represents the year the specimen was collected. *SIN05-NTU-12 is the representative strain for a cluster of 24 strains, comprising of specimen numbers SIN05-NTU-12, 22, 46, 79, 86, 150; SIN06-NTU-159, 167, 218, 243, 250, 258, 263, 268, 275, 290, 325, 328, 371, 374; and SIN07-NTU-421, 427, 441, and 500, with 100% sequence similarity at the nucleotide level. The Singapore HBoV sequences were analyzed with the two HBoV prototypes isolated in Sweden, st1_Sweden and st2_Sweden (DQ000495 and DQ000496), and published sequences from GenBank, whose strain names are reported next to their country of isolation. Their accession numbers are: QPID04-0011_Australia, DQ206702; WILL1_China, DQ778300; BJ3064_China, DQ988933; CU49_Thailand, EF203921; KR-MN0046_Korea, MN0484_Korea, KR-MN0885_Korea, KR-MN1114_Korea, DQ340225 to 8; CHSD1, 4 and 10_USA, DQ471812, DQ471814, and DQ471820; CRD2_USA, DQ340570; human parvovirus B19, DQ408301; canine minute virus, NC004442; and bovine parvovirus, NC001540.

B19, which is consistent with recent reports from other regions of the world [Chung et al., 2006; Foulongne et al., 2006; Sloots et al., 2006; Qu et al., 2007].

The main focus of this study was to detect the incidence rate of HBoV in the pediatric population in Singapore. As recent reports have indicated that HCoVs may have a possible role in respiratory infections, their presence was also assessed in the same cohort of patients. Only three HCoVs were detected from the 500 specimens. Their PCR amplicons was subjected to DNA sequencing to confirm their identities by blasting the sequences with published HCoV sequences. SIN06-NTU-259 was confirmed to be HCoV-OC43, whereas both SIN06-NTU-211 and SIN07-NTU-395 were HCoV-NL63. The Singapore HCoV-NL63 strains showed 100% nt identities with each other, and with the Dutch NL63 strains. Interestingly, the phylogenetic tree constructed at the partial orf 1b gene region showed that the Singapore HCoV-NL63 isolates, SIN06-NTU-211 and SIN07-NTU-395, clustered with the Dutch strains, away from the rest of the HCoVs including the recent strains of HCoV-NL63 from Australia and Japan (Fig. 2). SIN06-NTU-259, as expected, clustered with the HCoV-OC43. The clustering of the HCoVs was somewhat similar to that reported by Escutenaire et al. [2007].

DISCUSSION

The main focus of this study was to examine the incidence of HBoV infections among the pediatric patients in Singapore. Respiratory viruses were detected in 141 of the specimens, giving an incident rate of 28.2%. RSV was the most common virus detected in the current study (11.8%), followed by HBoV (8.0%), and HMPV (5.8%). The rate of HBoV detection in this study was similar to that reported in China [Qu et al., 2007] and South Korea [Chung et al., 2006], but was higher than the reported rates in Thailand [Fry et al., 2007], Japan [Ma et al., 2006], and in several non-Asian countries [Allander et al., 2005; Arnold et al., 2006; Bastien et al., 2006; Foulongne et al., 2006; Sloots et al., 2006]. One reason for the difference in incidence rates could be the criteria used in the sampling population. For example, in a report by Sloots et al. [2006] the study population included hospitalized and non-hospitalized patients exhibiting both lower respiratory tract infections and upper respiratory tract infections, with a wide age range from 7 days to 86 years. In contrast to the current study, and that reported from China and South Korea, the sampling population was confined to hospitalized children exhibiting respiratory tract infections.

Coinfections of HBoV with a range of respiratory viruses have been reported, with the highest rates at 69% and 60% in children admitted to hospital in Israel [Hindiyeh et al., 2008] and Spain, respectively [Pozo et al., 2007]. A high proportion of these HBoV coinfections have been associated with either RSV, HMPV, or PIV [Choi et al., 2006; Chung et al., 2006; Fry et al., 2007]. The Israeli study also reported a high rate of coinfection with adenoviruses [Hindiyeh et al., 2008]. Recent studies have also suggested a correlation between the severity of infection and the presence of coinfections involving HBoV [Allander et al., 2005; Choi et al., 2006; Chung et al., 2006; Foulongne et al., 2006; Manning et al., 2006; Sloots et al., 2006; Fry et al., 2007; see review by Schildgen et al., 2008]. For example, in a recent study in Thailand, wheezing was associated in patients infected with HBoV and coinfected with RSV, PIV, or RHV, compared to single infections with these viruses [Fry et al., 2007]. In the same study, a significant number of patients presented with lower respiratory tract infections in which HBoV was the only virus detected. This trend of coinfections with other respiratory viruses was also observed in the current study. In the current study, 50% of the coinfections with RHV caused lower respiratory tract infections in children, whereas in contrast, only 33% of the coinfections with RSV caused lower respiratory tract infections. Interestingly, a recent study described the association of HBoV coinfections with RHV-A, as well as a newly identified RHV species, designated as RHV-C by Lau et al. [2007b]. RHV is also an important cause of lower respiratory tract infections in children. Coinfections with HBoV may exacerbate the symptoms in children, giving rise to hospital admission with the requirement of intensive medical care. Coinfections with RSV and HMPV have also been associated with an increase severity in respiratory infections, although this correlation remains controversial. Some reports have described an increased severity in a high proportion of coinfections [Greensill et al., 2003; Semple et al., 2005], whereas in others, a low proportion of co-infections or no co-infections were found [Al-Sonboli et al., 2006; Mackay et al., 2006]. However, in the previous report [Loo et al., 2007] and the current study, only single HMPV infections were detected among the Singaporean children. The increased severity in coinfections with respiratory viruses remained to be challenged. A larger sampling population, and a longer duration for the study of coinfections will be required to confirm the correlation.

In conclusion, this report describes the first comprehensive study examining the prevalence of HBoV among the pediatric population in Singapore. Five hundred specimens were analyzed, and an infection rate for HBoV at 8% was reported, with 55% of these patients were 1 year old or younger. A significant level of coinfection was also detected in the patients with HBoV, with RSV and RHV being the most common viruses detected. 52% of the HBoV patients in which HBoV was the sole agent detected showed evidence of lower respiratory tract infection, which compared with 47% of the HBoV coinfections. This study, therefore, suggests that HBoV is a significant cause of lower respiratory tract infections among the pediatric population of Singapore. Furthermore, the current data suggest that single infection with HBoV is sufficient to cause severe respiratory infection, and the clinical significance of

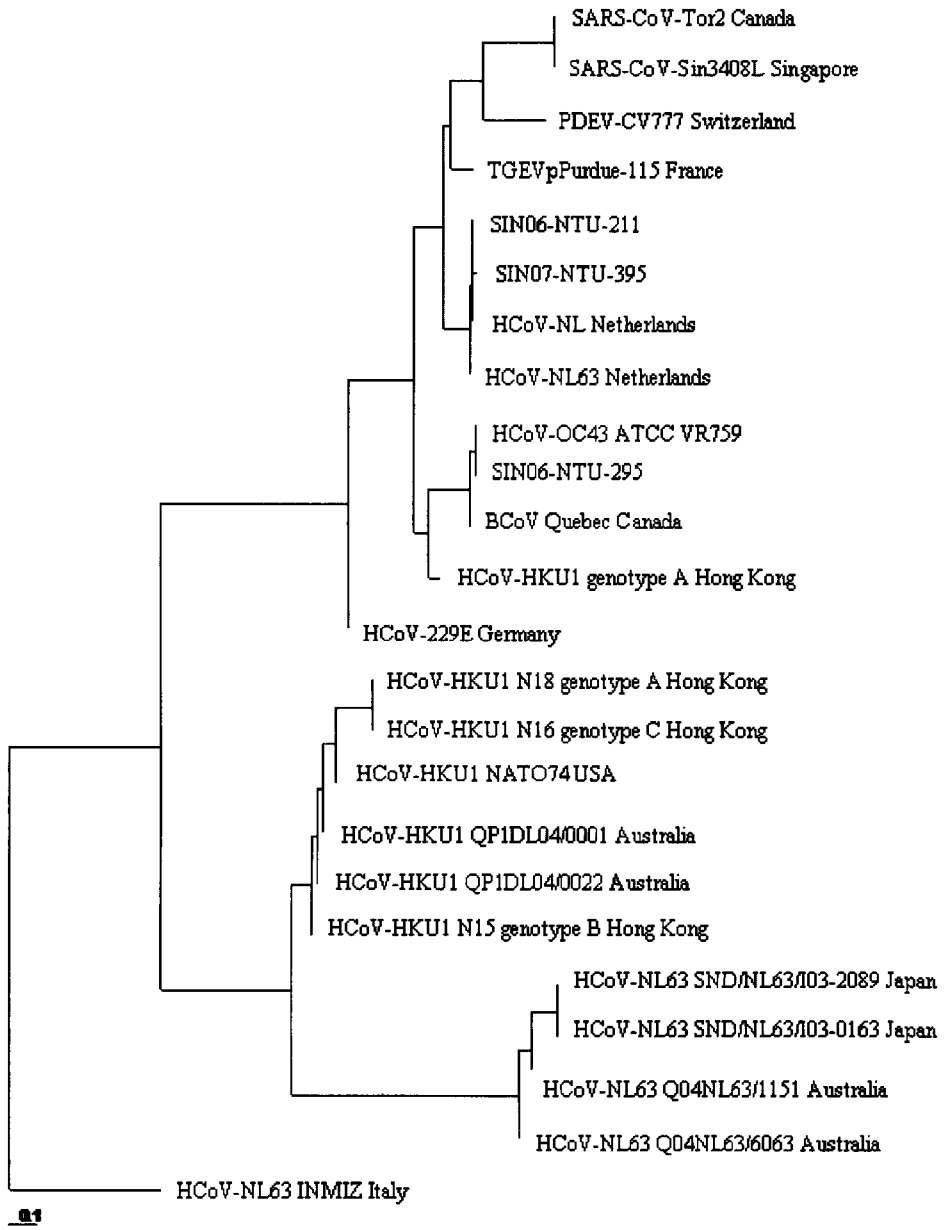

Fig. 2. Phylogenetic analysis of the partial orf 1b region (99 bp) for HCoV detected from hospitalized pediatric patients. The phylogenetic tree was constructed as described for Figure 1. The viral sequences from the Singapore strains are represented by SIN06-NTU, followed by the specimen number. SIN represents Singapore and 06 represents the year the specimen was collected. The Singapore sequences were analyzed with published sequences of coronviruses obtained from GenBank, whose strain names are reported next to their country or cities of isolation. Their accession numbers are: human coronavirus (HCoV)-NL63-004NL63/1151 Australia, AY600446; HCoV-NL63-Q04NL63/6063 Australia, AY600443; HCoV-HKU1 QP1D04\0001 Australia, DQ190472; HCoV-HKU1 QP1D04\0022 Australia, DQ206693; human coronavirus (HCoV)-229E Germany, AF304460; HCoV-HKU1 genotype A Hong Kong, AY597011; HCoV-HKU1 N18 genotype A Hong Kong, DQ415914; HCoV-HKU1 N15 genotype B Hong Kong, DQ415911; HCoV-HKU1 N16 genotype C Hong Kong, DQ415912; HCoV-NL63-INMIZ Italy, EU030685; HCoV-NL63-SND/NL63/I03-2089 Japan, AY662698; HCoV-NL63-SND/NL63/I03-0163 Japan, AY662694; HCoV-NL Netherlands, AY518894; HCoV-NL63 Netherlands, AY567487; HCoV-HKU1-NAT074 USA, EF077277; and HCoV-OC43 ATCC VR-759, AY391777; severe acute respiratory syndrome coronaviruses, (SARS-CoV)-Tor2 Canada, AY274119; SARS-CoV-SIN3408L Singapore, AY559097; bovine coronavirus (BCoV)-Quebec Canada, AF220295; porcine epidemic diarrhea virus (PEDV)-CV777 Switzerland, AF353511; transmissible gastroenteritis virus (TGEV)-Purdue-115 France, Z34093.

HBoV coinfections with other respiratory viruses in Singapore remains to be established.

REFERENCES

Allander T. 2008. Human bocavirus. J Clin Virol 41:29–33.

Allander T, Tammi MT, Eriksson M, Bjerkner A, Tiveljung-Lindell A, Andersson B. 2005. Cloning of a human parvovirus by molecular screening of respiratory tract samples. Proc Natl Acad Sci USA 102:12891–12896.

Al-Sonboli N, Hart CA, Al-Aghbari N, Al-Ansi A, Ashoor O, Cuevas LE. 2006. Human metapneumovirus and respiratory syncytial virus disease in children, Yemen. Emerg Infect Dis 12(9):1437–1439.

Arnold JC, Singh KK, Spector SA, Sawyer MH. 2006. Human bocavirus: Prevalence and clinical spectrum at a children's hospital. Clin Infect Dis 43:283–288.

Bastien N, Brandt K, Dust K, Ward D, Li Y. 2006. Human bocavirus infection, Canada. Emerg Infect Dis 12:8484–8500.

Chieochansin T, Samransamruajkit R, Chutinimitkul S, Payungporn S, Hiranras T, Theamboonlers A, Poovorawan Y. 2008. Human bocavirus (HBoV) in Thailand: Clinical manifestations in a hospitalized pediatric patient and molecular virus characterization. J Infect 56:137–142.

Choi EH, Lee HJ, Kim SJ, Eun BW, Kim NH, Lee JA, Lee JH, Song EK, Kim SH, Park JY, Sung JY. 2006. The association of newly identified respiratory viruses with lower respiratory tract infections in Korean Children, 2000–2005. Clin Infect Dis. 43:585–592.

Chung JY, Han TH, Kim CK, Kim SW. 2006. Bocavirus infection in hospitalized children, South Korea. Emerg Infect Dis 12:1254–1256.

Chung JY, Han TH, Kim SW, Kim CK, Hwang ES. 2007. Detection of viruses identified recently in children with acute wheezing. J Med Virol 79:1238–1243.

Escutenaire S, Mohamed N, Isaksson M, Thoren P, Klingeborn B, Belak S, Berg M, Blomberg J. 2007. SYBR green real-time reverse transcription-polymerase chain reaction assay for the generic detection of coronaviruses. Arch Virol 152:41–58.

Foulongne V, Olejnik Y, Perez V, Elaerts S, Rodiere M, Segondy M. 2006. Human bocavirus in French children. Emerg Infect Dis 12:1251–1253.

Fry AM, Lu X, Chittaganpitch M, Peret T, Fischer J, Dowell SF, Anderson LJ, Erdman D, Olsen SJ. 2007. Human bocavirus: A novel parvovirus epidemiologically associated with pneumonia requiring hospitalization in Thailand. J Infect Dis 195:1038–1045.

Garcia-Garcia ML, Calvo C, Pozo F, Perez-Brena P, Quevedo S, Bracamonte T, Casa I. 2008. Human bocavirus detection in nasopharyngeal aspirates of children without clinical symptoms of respiratory infection. Pediatr Infect Dis 27:358–360.

Greensill J, McNamara PS, Dove W, Flanagan B, Smyth RL, Hart CA. 2003. Human metapneumovirus in severe respiratory syncytial virus bronchiolitis. Emerg Infect Dis 9:372–375.

Han TH, Chung JY, Kim SW, Hwang ES. 2007. Human coronavirus-NL63 infections in Korean children, 2004–2006. J Clin Virol 38:27–31.

Hayden FG, Herrington DT, Coats TL, Kim K, Cooper EC, Villano SA, Liu S, Hudson S, Pevear DC, Collett M, McKinlay M, and the Pleconaril Respiratory Infection Study Group. 2003. Efficacy and safety of oral pleconaril for treatment of colds due to picornaviruses in adults: Results of 2 double-blind, randomized, placebo-controlled trials. Clin Infect Dis 35:1523–1532.

Hindiyeh M, Keller N, Mandelboim M, Ram D, Rubinov J, Regev L, Levy V, Orzitzer S, Shaharabani H, Azar R, Mendelson E, Grossman Z. 2008. High rate of human bocavirus and adenovirus coinfection in hospitalized Israeli children. J Clin Microbiol 46:334–337.

Kahn JS. 2007. Newly identified respiratory viruses. Pediatr Infect Dis J 26:745–746.

Kahn J. 2008. Human bocavirus: Clinical significance and implications. Curr Opin Pediatr 20:62–66.

Kaplan NM, Dove W, Abd-Eldayem SA, Abu-Zeid AF, Shamoon HE, Hart CA. 2007. Molecular epidemiology and disease severity of respiratory syncytial virus in relation to other potential pathogens in children hospitalized with acute respiratory infection in Jordan. J Med Virol 80:168–174.

Koetz A, Nilsson P, Linden M, Van der Hoek L, Ripa T. 2006. Detection of human coronavirus NL63, human metapneumovirus and respiratory syncytial virus in children with respiratory tract infections in south-west Sweden. Clin Microbiol Infect 12:1089–1096.

Lau SK, Yip CC, Que TL, Lee RA, Au-Yeung RK, Zhou B, So LY, Lau YL, Chan KH, Woo PC, Yuen KY. 2007a. Clinical and molecular epidemiology of human bocavirus in respiratory and fecal samples from children in Hong Kong. J Infect Dis 196:986–993.

Lau SK, Yip CC, Tsoi HW, Lee RA, So LY, Lau YL, Chan KH, Woo PC, Yuen KY. 2007b. Clinical features and complete genome characterization of a distinct human rhinovirus (HRV) genetic cluster, probably representing a previously undetected HRV species, HRV-C, associated with acute respiratory illness in children. J Clin Microbiol 45:3655–3664.

Lee JL, Chung JY, Han TH, Kim CK, Hwang ES. 2007. Detection of human bocavirus in children hospitalized because of acute gastroenteritis. J Infect Dis 196:994–997.

Loo LH, Tan BH, Ng LM, Tee NWS, Lin RTP, Sugrue RJ. 2007. Characterisation of human metapneumovirus isolated from paediatric patients in Singapore. Emerg Infect Dis 13:1396–1398.

Ma X, Endo R, Ishiguro N, Ebihara T, Ishiko H, Ariga T, Kikuta H. 2006. Detection of human bocavirus in Japanese children with lower respiratory tract infections. J Clin Microbiol 44:1132–1134.

Mackay IM, Bialasiewicz S, Jacob KC, McQueen E, Arden KE, Nissen MD, Sloots TP. 2006. Genetic diversity of human metapneumovirus over 4 consecutive years in Australia. J Infect Dis 193:1630–1633.

Manning A, Russell V, Eastick K, Leadbetter GH, Hallam N, Templeton K, Simmonds P. 2006. Epidemiological profile and clinical associations of human bocavirus and other human parvovirus. J Infect Dis 194:1283–1290.

Page RD. 1996. TreeView: An application to display phylogenetic trees on personal computers. Comput Appl Biosci 12:357–358.

Pierangeli A, Gentile M, Di Marco P, Pagnotti P, Scagnolari C, Trombetti S, Lo Russo L, Tromba V, Moretti C, Midulla F, Antonelli G. 2007. Detection and typing by molecular techniques of respiratory viruses in chlldren hospitalised for acute respiratory infections in Rome, Italy. J Med Virol 79:463–468.

Pozo F, Garcia-Garcia ML, Calvo C, Cuesta I, Perez-Brena P, Casa I. 2007. High incidence of human bocavirus infection in children in Spain. J Clin Virol 40:224–228.

Pyrc K, Berkhout B, van der Hock L. 2007. Identification of new human coronaviruses. Expert Rev Anti-Infect Ther 5:245–253.

Qu XW, Duan ZJ, Qi ZY, Xie ZP, Gao HC, Liu WP, Huang CP, Peng FW, Zheng LS, Hou YD. 2007. Human bocavirus infection, People's Republic of China. Emerg Infect Dis 13:165–168.

Schildgen O, Muller A, Allander T, Mackay IM, Volz S, Kupfer B, Simon A. 2008. Human bocavirus: Passenger or pathogen in acute respiratory tract infections? Clin Microbiol Rev 21:291–304.

Semple MG, Cowell A, Dove W, Greensill J, McNamara PS, Halfide C, Shears P, Smyth RL, Hart CA. 2005. Dual infection of infants by human metapneumovirus and human respiratory syncytial virus is strongly associated with severe bronchiolitis. J Infect Dis 191:382–386.

Sloots TP, McErlean P, Speicher DJ, Arden KE, Nissen MD, Mackay IA. 2006. Evidence of human coronavirus HKU1 and human bocavirus in Australian children. J Clin Virol 35:99–102.

Sloots TP, Whiley DM, Lambert SB, Nissen MD. 2008. Emerging respiratory agents: New viruses for old diseases? J Clin Virol 42:233–243.

Van der Hoek L, Pyrc K, Jebbink MF, Vermeulen-Oost W, Berhout RJ, Wolthers KC, Wertheim-van Dillen PM, Kaandorp J, Spaargaren J, Berkhout B. 2004. Identification of a new coronavirus. Nat Med 10:368–373.

Van der Hoek L, Suro K, Ihorst G, Stang A, Pyrc K, Jebbink MF, Petersen G, Forester J, Berkhout B, Uberla K. 2005. Croup is associated with the novel coronavirus NL63. PLoS Med 2:e240.

Van der Hoek L, Pyrc K, Berkhout B. 2006. Human coronavirus NL63, a new respiratory virus. FEMS Microbiol Rev 30:760–773.

Van den Hoogen BG, de Jong JC, Kuiken T, de Groot R, Fouchier RA, Osterhaus AD. 2001. A newly discovered human pneumovirus isolated from young children with respiratory tract disease. Nat Med 7:719–724.

Vicente D, Cilla G, Montes N, Perez-Yarza EG, Perez-Trallero E. 2007. Human bocavirus, a respiratory and enteric virus. Emerg Infect Dis 13:636–637.

Woo PC, Lau SKP, Chu CM, Chan KH, Tsoi HW, Huang Y, Wong BH, Poon RW, Cai JJ, Luk WK, Poon LL, Wong SS, Guan Y, Peiris JS, Yuen KY. 2005. Characterisation and complete genome sequence of a novel coronavirus, coronavirus HKU1, from patients with pneumonia. J Virol 79:884–895.

Wu PS, Chang LY, Berhout B, Van der Hoek L, Lu CY, Kao CL, Lee PI, Shao PL, Lee CY, Huang FY, Huang LM. 2008. Clinical manifestations of human coronaviruses NL63 infection in children in Taiwan. Eur J Pediatr 167:75–80.